Hazus Tsunami Model Technical Guidance

November 2017

This document is prepared for FEMA by:
NiyamIT, Inc.
2201 Cooperative Way #600
Herndon, VA 20171

Contract No. HSFE60-17-P-0004

Document History

Affected Section or Subsection	Date	Description
First Publication	November 2017	Initial version of new Hazus Tsunami Model Technical Guidance for Hazus version 4.0.

ACKNOWLEDGMENTS

The Hazus Tsunami Loss Model Software Development was supported by the FEMA Federal Insurance and Mitigation Administration and the DHS Science & Technology Flood Apex Program.

<u>FEMA Hazus Program Management</u>

Jesse Rozelle, FEMA HQ Hazus Program Manager
Scott McAfee, FEMA HQ Hazus Program Oversight

<u>Tsunami Model Development Team</u>

<u>Technical Manual Development</u>: Team NiyamIT: Lead→*Doug Bausch (Pacific Disaster Center), Daniel Horner: PM, Andrea Chatman, Sandeep Mehndiratta*

<u>User Guide Development</u>: *Team NiyamIT: Lead→Andrea Chatman (Pacific Disaster Center), Daniel Horner: PM, Doug Bausch*

<u>Software Development:</u> *IBM Customer and Data Services (Suhaib Khan, Andrea Jackman, Wei Zhang, Shanmugam Rajgopal, Swapan Mondal, Kavitha Paspuleti, David Sakoda); NiyamIT (Suman Biswas – Chief Architect, Nikolay Todorov, Ujvala Sharma, Sandeep Mehndiratta, Daniel Horner, Brad Klaus)*

<u>Design:</u> *Doug Bausch, Pacific Disaster Center*

<u>IV&V</u>: *Bill Bohn, Zack Baccala, Kevin Mickey*

<u>Hazus Tsunami Model Technical Committee Members</u>

Diego Arcas, NOAA / PMEL, Seattle, WA
John Bauer, Oregon Department of Geology and Mineral Industries
Doug Bausch, Pacific Disaster Center
Tamra Biasco, FEMA Region X
Jawhar Bouabid, Chubb Insurance
Gary Chock, Martin & Chock, Honolulu, HI
Edward Curtis, FEMA Region IX
Tim Frazier, Georgetown University
Gala Gulacsik, FEMA Region X
Michael Hornick, FEMA Region IX
Herbert (Gene) Longenecker, FEMA HQ Response Directorate
William Lehman, U.S. Army Corp of Engineers
Mike Mahoney, FEMA HQ Building Sciences
Cynthia McCoy, FEMA Region X
Kevin Miller, California Office of Emergency Management
Christopher Moore, NOAA / PMEL, Seattle, WA
Ian Robertson, University of Hawaii, Honolulu, HI
Jesse Rozelle, FEMA HQ Hazus Program Manager
Rick Wilson, California Geological Survey
Nate Wood, U.S. Geological Survey

Harry Yeh, Oregon State University

FEMA (2013) Tsunami Methodology Development

Tsunami Oversight Committee
Chairman, Eddie Bernard, NOAA / PMEL, Seattle, WA
Ian Robertson, University of Hawaii, Honolulu, HI
Gary Chock, Martin & Chock, Honolulu, HI
Thalia Anagnos, San Jose State University, San Jose, CA
William Johnstone, Spatial Vision Group, North Vancouver, BC
James D. Goltz, CEMA, Pasadena, CA
Diego Arcas, NOAA / PMEL / OERD, Seattle, WA
Solomon Yim, Oregon State University, Corvallis, OR
Yumei Wang, Oregon Department of Geology and Mineral Industries, Portland, OR
Nicky Hastings, Natural Resources Canada, Vancouver, BC
Michael Mahoney, FEMA, Washington, DC
Tamra Biasco, FEMA X, Bothell, WA

Tsunami Methodology Development Team
Project Manager, Mourad Bouhafs, Atkins North America, Atlanta, GA
Technical Manager, Jawhar Bouabid, Atkins North America, Atlanta, GA
Charles Kircher, Kircher & Associates, Palo Alto, CA
Harry Yeh, Oregon State University, Corvallis, OR
Ron Eguchi, ImageCat, Long Beach, CA
Bill Graf, ImageCat, Long Beach, CA
Peter Vickery, ARA, Raleigh, NC
David Mizzen, ARA, Raleigh, NC
Shunichi Koshimura, Tohoku University, Japan

Advisory Panel
Fredric Raichlen, Caltech, Pasadena, CA
Ron Riggs, University of Hawaii, Honolulu, HI
Chris Jones, Chris Jones Consulting, Raleigh, NC
Neil Blais, Blais & Associates, Dallas, TX
Mourad Zeghal, Rensselaer Polytechnic Institute, Troy, NY
Tim Hillier, CDM, Fairfax, VA

DHS, FEMA, Mitigation Division, Washington, D.C.
Program Manager, Eric Berman

National Institute of Building Sciences
Philip Schneider

Table of Contents

List of Figures

List of Tables

1.0 INTRODUCTION TO FEMA TSUNAMI LOSS ESTIMATION METHODOLOGY

The Hazus tsunami loss estimation methodology provides a state-of-the-art decision-support software for estimating potential losses from tsunami hazards. This loss estimation capability will enable users to anticipate the consequences of future tsunamis and to develop plans and strategies for reducing risk. The GIS-based software can be applied to study small or large geographic areas with a wide range of population characteristics and can be implemented by users with varying technical and subject expertise.

The Hazus methodology was originally developed for the Federal Emergency Management Agency (FEMA) by the National Institute of Building Sciences (NIBS) to provide a tool for developing earthquake loss estimates (FEMA, 2002). Since then, Hazus has been expanded to perform similar loss evaluations for hurricane wind, flood, and now tsunami, developed by a Tsunami Methodology Development Team (FEMA, 2013).

The Hazus Tsunami Model allows practitioners to estimate casualty and building economic losses from tsunamis. The information provided by the model will assist state and local officials in evaluating, planning for, and mitigating the effects of tsunamis. The Hazus Tsunami Model provides practitioners and policy makers with a tool to help reduce tsunami damage, reduce disaster payments, and make wise use of the nation's emergency management resources.

The Hazus Tsunami Model provides the capability to quantify potential building impacts and losses, as well as casualties. These are the first components of a planned tsunami model that, when fully implemented, will address essential facilities, lifelines, harbor facilities, debris, displaced households, and shelter needs. The model will analyze the potentially catastrophic tsunami scenarios associated with near-source by combining tsunami and earthquake losses, as well as distant-source tsunamis.

The current capability addresses Very High and High Tsunami Risk States and Territories as defined by the National Tsunami Hazard Mitigation Program (NTHMP). Estimates also will help guide the allocation of federal resources to stimulate risk mitigation efforts and to plan for federal tsunami response.

This ***Hazus Tsunami Model Technical Guidance*** document provides the background and technical methodology implemented in the Hazus Tsunami Model. It details the methodology developed and implemented from the *Tsunami Methodology Technical Manual* (FEMA, 2013), integrating the text, equations, tables, and figures, where possible, and incorporates updates to the methodology based on newer developments or where it was necessary to streamline for software implementation. Substantial sections are incorporated into this document from FEMA (2013) that were written by Dr. Harry Yeh, the primary author the Tsunami Hazard Analysis and Casualty Estimation chapters and from Charlie Kircher, the primary author of the Direct Physical Damage chapter.

The ***Hazus Tsunami Model User Guidance****,* a separate accompanying document, provides the instructions to complete a tsunami loss estimation study using Hazus. It also provides information on how to install and run the software, and how to interpret and report module outputs. Together, these documents provide a comprehensive overview of this nationally applicable loss estimation methodology.

1.1 Background

This technical guidance document describes the methodology implemented for the tsunami hazard and loss modeling capability for Hazus. These loss estimates would be used primarily by local, state, and regional officials to plan and stimulate efforts to reduce risks associated with tsunamis and to prepare for emergency response and recovery. The implemented methodology will also address the needs of emergency managers for a near real-time loss estimation capability during the immediate aftermath of a damaging tsunami (i.e., the first 3–6 hours).

The FEMA (2013) ***Hazus Tsunami Methodology Development Team*** of tsunami experts was composed of engineers, tsunami hazard modelers, emergency planners, economists, social scientists, geographic information systems analysts, and software developers.

The FEMA (2013) ***Hazus Tsunami Oversight Committee*** provided technical direction and review of the work. Members of both these teams are highlighted in the Acknowledgements section.

For the Hazus Tsunami 4.0 and 4.1 releases, software development was performed under the FEMA Customer and Data Services (CDS) Risk MAP program. The project was led by IBM and NiyamIT. The software design, case study development, and testing was developed and performed by the Pacific Disaster Center.

1.2 Scope

This methodology guide covers documentation of all approaches and data that are used by the tsunami methodology. This includes documentation of algorithms, identification of input data, and expected output which comprise the loss estimation methodology for tsunami hazards. Loss estimation methods and data are obtained from referenced sources tailored to fit the framework of the methodology, or from new methods and data developed when existing methods and data were lacking or not current.

This report is a comprehensive, highly technical collection of methods and data covering a broad range of topics and disciplines, structural engineering, tsunami hazard assessment, social science, and economics. Various sections of this report are written for readers who are expected to have some degree of expertise in the specific technical topics of interest. Users can be seen as composing two groups: those who perform the study and those who use the study results. For some studies these two groups will consist of the same people, but generally this will not be the case. However, the more interaction that occurs between these two groups, the better the study will be. End users of the loss estimation study need to be involved from the beginning to make results more usable.

Those who are using the Hazus Tsunami Model must, at a minimum, have a basic understanding of tsunamis and their consequences. In many cases, the results will be presented to audiences (i.e., city councils and other governing bodies) that have little technical knowledge of tsunami loss estimation.

1.3 Organization

This section has been written to help the Hazus Tsunami Model user navigate the guide and locate items of interest. Note that the portions of the FEMA (2013) methodology that have not yet been incorporated into software, such as essential and lifeline facility loss, debris, and shelter methods, are not included in this Technical Guidance for the Hazus software module.

Users interested in technical methodology for those areas need to refer to FEMA (2013). The chapters included here are as follows:

Chapter 1: Introduction to Hazus Tsunami Loss Estimation Methodology. This section introduces the reader to the methodology scope and organization.

Chapter 2: Provides an overview of the Hazus-approach and framework, the project vision, and the objectives. This chapter will provide the reader with an understanding of key concepts related to the Hazus Tsunami Model such as the levels of analysis.

Chapter 3: Summarizes the inventory components that are considered in this prototype. These include the general building stock, including the incorporation of the National Structure Inventory (NSI) developed by the U.S. Army Corps of Engineers (USACE) with FEMA, as well as the development of inventory data for the U.S. Territories.

Chapter 4: The Tsunami Hazard Analysis chapter contains descriptions of the integration of external hazard data. The model describes the hazard parameters used to characterize tsunami such as the depth, velocity, and momentum flux, as well as the levels of hazard data input. This chapter closely aligns with Chapter 4 of FEMA (2013) with the main exception related to integration of newer ASCE 7 methodologies.

Chapter 5: Addresses the damage assessment for buildings for the general building stock, as well as for user-defined facilities. It includes a discussion of the building damage functions and the application of these functions to the different categories of damage: structural, nonstructural, and contents. In addition, the methodology of combining the earthquake and tsunami damage-state probabilities is described. This chapter closely aligns with Chapter 5 of FEMA (2013).

Chapter 6: Describes the methodology for casualty estimation. The integration of the USGS Pedestrian Evacuation Analyst and levels of analysis are described. The discussion includes how the warning time and level of community preparedness are accounted for and how age, gender, and mobility may impact the casualty numbers. This chapter closely aligns with Chapter 8 of FEMA (2013) with the main exception related to integration of the newer USGS evacuation tool.

Chapter 7: Explains how the damage estimated for buildings and contents are translated into direct economic impacts such as building, content, and inventory losses for the general building stock and user-defined facilities.

Chapter 8: Provides an evaluation of building damage, based on sample curves, observed damages from recent tsunamis, and results from a FEMA benchmarking, validation, and calibration study.

2.0 Overall Approach and Framework of Methodology

2.1 Vision Statement

The overall objective of the Hazus project is to develop nationally applicable standardized multi-hazard methodologies for estimating potential wind, flood, tsunami, and earthquake losses on a regional basis. Hazus is intended to be used by local, state, and regional officials for planning and fostering mitigation efforts to reduce losses from natural disasters and preparing for emergency response and recovery following these events. The objective is also for the Hazus Tsunami methodology to provide, in a timely manner, some level of situational awareness for emergency managers during response.

The ultimate vision is to integrate the Hazus Tsunami Model fully with NOAA's rapid tsunami inundation modeling capability when a major tsunami occurs from a source anywhere in the world. NOAA could provide the hazard data and Hazus could return a near real-time damage assessment.

2.2 Project Objectives

The Hazus Tsunami Methodology is being developed to support decision makers in protecting coastal residents, visitors, and property from the damaging effects of tsunamis. It is an integrated approach for identifying and quantifying tsunami risks based on advanced science and engineering technology. The overall features and functionality envisioned for the Hazus Tsunami Model are illustrated and presented in Figures 2.1 and 2.2. Figure 2.1 highlights the methods associated with a local Near Source Earthquake where damage and impacts occur as the result of a combination of earthquake and tsunami hazards. Note that in the case of Distant Source Tsunami, earthquake effects are not considered, and the flowchart can be simplified into the schematic shown in Figure 2.2.

As shown in Figures 2.1 and 2.2, the tsunami methodology consists of three basic analytical processes: hazard analysis, damage assessment, and impact analysis. In the hazard analysis phase, source characteristics and bathymetry data are used to model the spatial variation in flood depth, velocity, and momentum flux. During the damage assessment phase, structural, nonstructural, and content damage is calculated based on the results of the hazard analysis using fragility curves. The impact phase translates the severity of tsunami and damage assessment into social and economic losses.

While the Hazus Tsunami Model supports a broad range of users, this methodology document is intended for technical experts, such as engineers and scientists, who have conducted previous tsunami loss studies.

2.3 Modularity

The methodology utilizes a modular approach with different modules addressing different user needs such as hazard analysis, damage assessment, and loss estimation. This approach avoids the need to decide on who is the designated user. The needs of most users are accommodated by the flexibility of this modular approach.

Figure 2.1: Tsunami Model Features – Near Source Earthquake

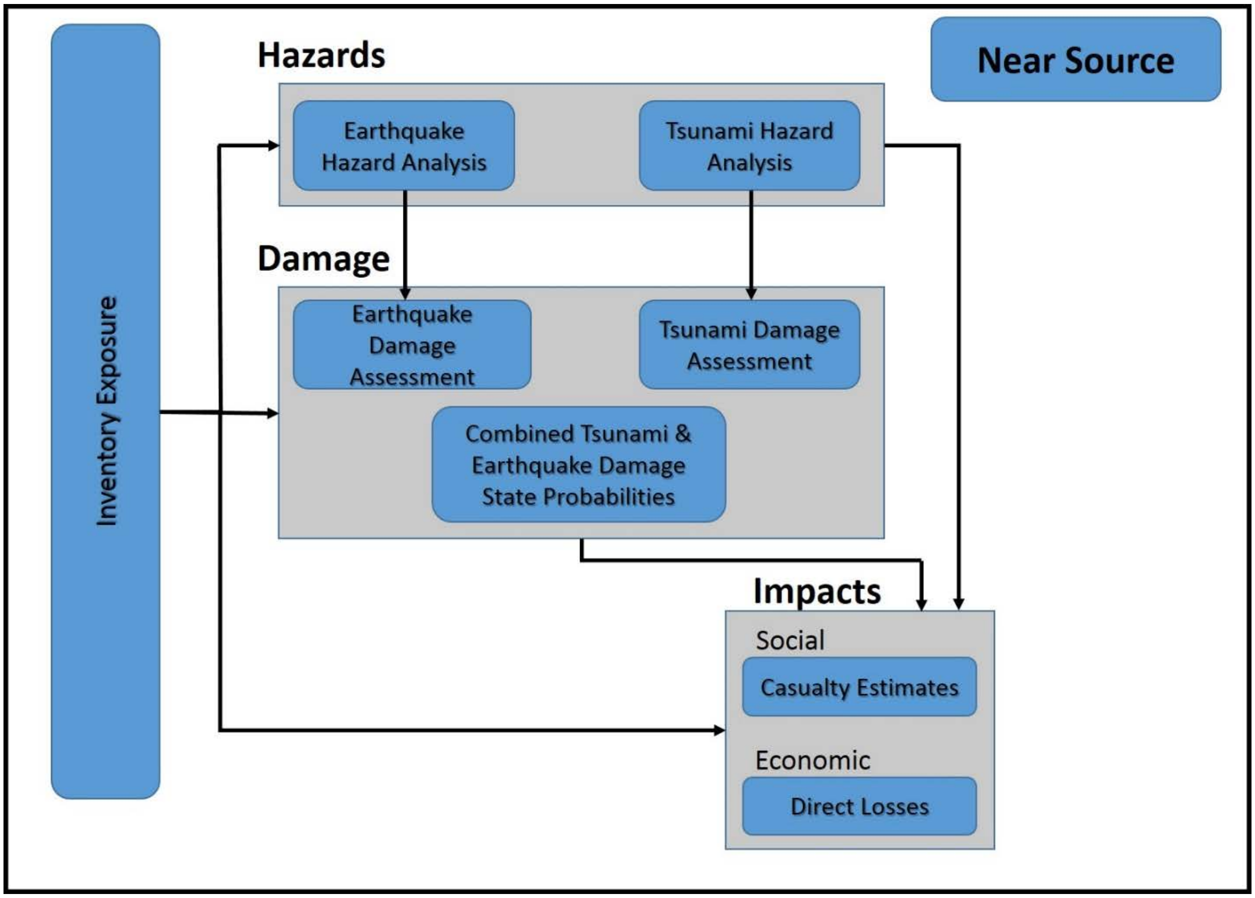

2.4 State-of-the-Art

To the practical extent possible, the methodology incorporates state-of-the-art models into the tsunami loss estimation methodology. In addition, the methodology allows users flexibility to utilize more current models and technology as they become available. For example, users can incorporate hazard depth grids, flow velocities, and momentum flux based on their own tsunami models and use customized damage functions. Modules include damage loss estimators that use a Performance-Based Tsunami Engineering (PBTE) approach. A nationally applicable scheme is applied for classifying buildings, largely based on the existing Hazus approach for earthquake and flood.

Figure 2.2 : Tsunami Model Features – Distant Source

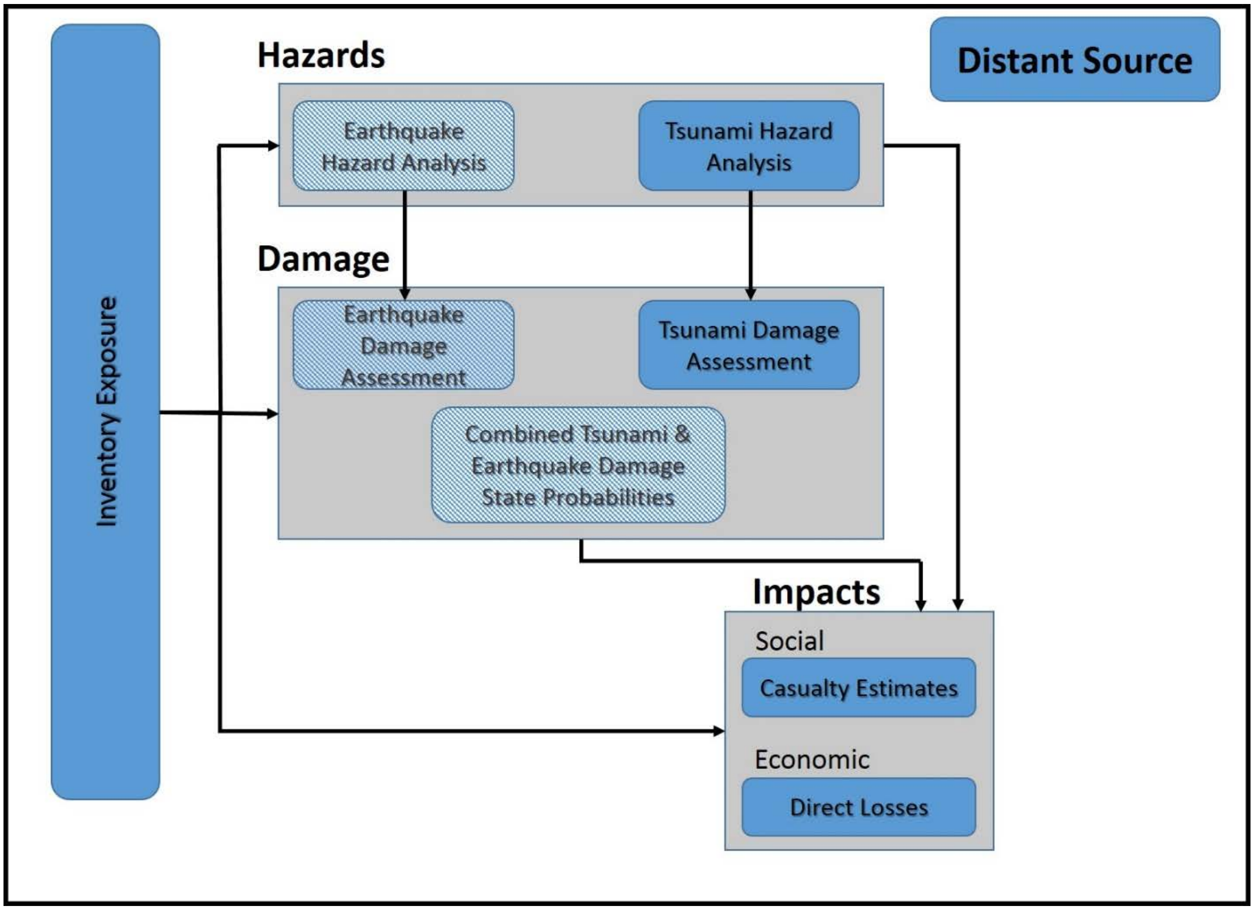

2.5 Standardization

The methodology includes streamlined methods for:

- Classifying occupancy of buildings and facilities
- Classifying building structure type
- Developing building damage functions
- Providing output

The methodology also defines a set of standard technical terms that provide a common basis for discussing tsunami hazards, risks, and consequences.

2.6 Level of Analysis

As illustrated in Figure 2.3, while the Hazus Tsunami Methodology permits three levels of analysis based primarily on the quality of hazard input, other inventory and engineering parameter enhancements also improve the analysis level. Note that the underlying methodology and the output, as would be implemented in Hazus, do not change from one level of analysis to another. Rather, it is the reliability of the data, used for modeling the input parameters, that increases.

Figure 2.3: Levels of Analysis for Tsunami Model

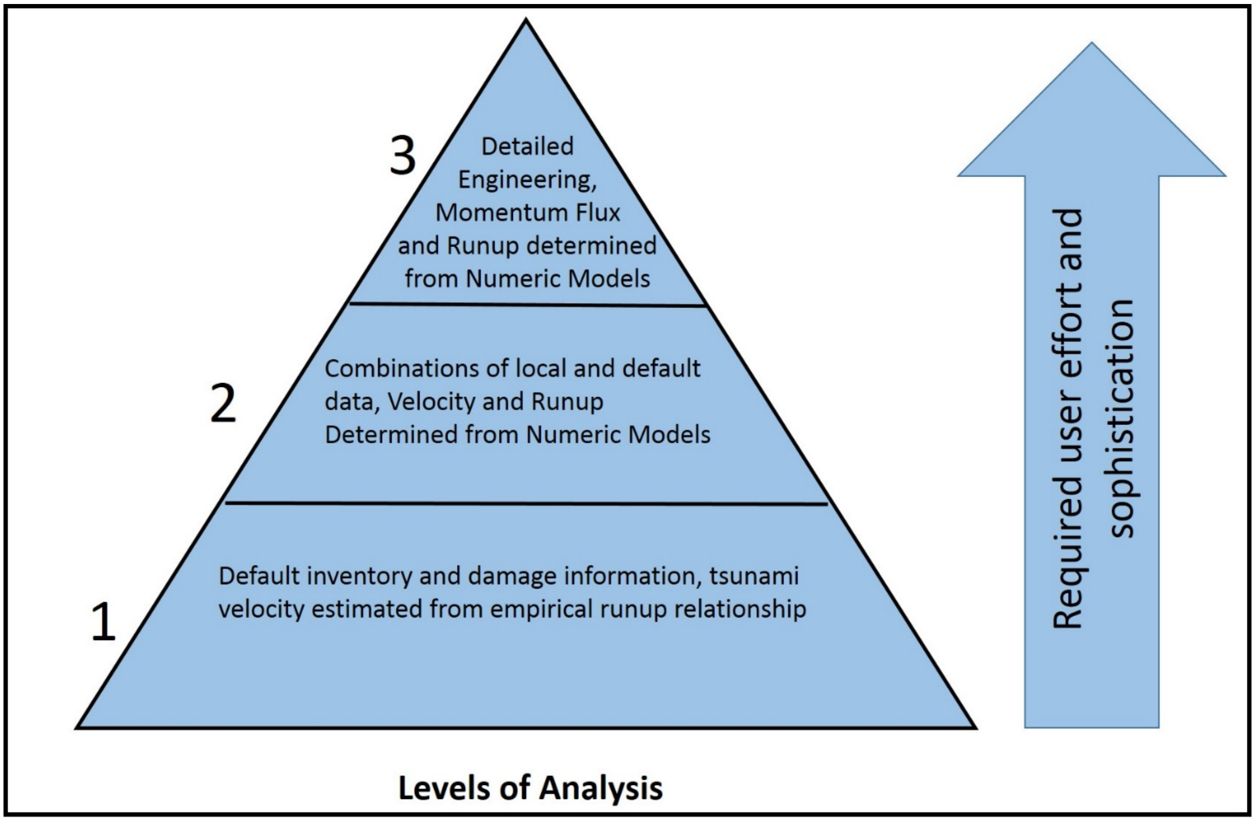

Level 1 (Basic Analysis) is the simplest type of analysis requiring minimum effort by the user as it uses primarily default input provided with the methodology (e.g., census information, semi-empirical-based approach for hazard quantification, default vulnerability modeling assumptions, etc.). The Level 1 tsunami hazard velocity grid data are developed using an empirical relationship and as little as a single observation of runup height may be used. The user is not expected to have extensive technical knowledge. While the methods require some user-supplied input to run, the type of input required could be gathered by referring to published information. At this level, estimates will have much greater uncertainty than Levels 2 or 3, and will likely be appropriate only as initial loss estimates to determine where more detailed analyses are warranted.

Level 2 (Advanced Analysis) is intended to improve the results from Level 1 by considering additional data that are readily available or can easily be converted or computed to meet the methodological requirements. In Level 2, the user may need to determine parameters from published reports or maps as input to the model. It requires more extensive inventory data and effort by the user than Default Data Analysis. The Level 2 tsunami hazard data includes velocity as well as runup grid information provided from an external hazard model. The purpose of this type of analysis is to provide the user with the best estimates of tsunami damage/loss that can be obtained using the methods included in the methodology.

All components of the methodology can be performed at this level and loss estimates are based on user-developed local inventories. As the user provides more complete data, the quality of the analysis and results improve. Depending on the size of the region and the level of detail desired by the user, as well as user experience, the required input for this type of analysis could take weeks to months to develop.

Level 3 (Advanced Data and Models Analysis) requires extensive effort by the user in developing information on the hazard and the measure of exposure, and may also necessitate incorporating results from engineering and economic studies carried out using methods and software not included within the methodology. The Level 3 tsunami hazard data includes momentum flux, as well as runup grid provided from an external numeric tsunami hazard model. At this level, one or more technical experts would be needed to acquire data, perform detailed analyses, assess damage/loss, and assist the user in gathering more extensive inventory. It is anticipated that at this level there will be extensive participation by local utilities and owners of special facilities.

There is no standardized Advanced Data and Models Analysis study. The quality and detail of the results depend upon the level of effort. An Advanced Data and Models Analysis Study could take six months to two years to complete. Each subsequent level builds on and adds to the data and analysis procedures available in previous levels.

3.0 Inventory Data

An important requirement for estimating losses from tsunamis is the identification, characterization, and valuation of the building stock, infrastructure, and population exposed to this hazard. Consequently, the Hazus model uses a comprehensive inventory in estimating damage, social, and economic losses. This inventory serves as the default when users of the model do not have better data available. The inventory consists of proxies for assumed types and proportions of building structural systems for the general building stock and national data for essential facilities, select lifeline systems, and demographics. This inventory data also could be interpreted as the best freely available, publicly accessible data that could be included in Hazus. The FEMA (2013) Tsunami Methodology leverages the existing earthquake and flood model-specific inventory attributes rather than requiring the development of new tsunami-specific vulnerability attributes. The tsunami building damage functions described in Chapter 5 are based entirely on specific earthquake building types and seismic design levels used by the Hazus Earthquake Model. The estimate of finished floor height required to estimate depth of tsunami within structures is based on the Hazus Flood Model foundation types and finished floor height relationships.

The general building stock for the Hazus Tsunami model utilizes the National Structure Inventory (NSI) developed by USACE in coordination with FEMA from Hazus General Building Stock (GBS) data described below. The NSI utilizes the Hazus GBS that was initially compiled at the census block level using U.S. Census Bureau data for the development of residential structures data while Dun & Bradstreet (D&B) provides the data for nonresidential structures. In addition, the NSI approach leverages the Hazus Flood Model Dasymetric Blocks distributing a point-based dataset within developed portions of census blocks. This helps prevent the location of buildings in undeveloped areas such as open space, wetlands, and beaches. This improves the accuracy when intersecting the inventory data with the tsunami hazard data. Figure 3.1 provides an illustration around the Diamond Head-Waikiki area where buildings are concentrated in high density developed area and removed in areas of open space. Since the NSI point data are notional rather than site-specific structure locations, Hazus Tsunami aggregates the inventory and results reporting of these structures at the Census Block for creating tables and thematic mapping. Furthermore, several post-processing steps to the NSI data described below allowed the incorporation of additional value-added attributes enhancing the accuracy of the NSI data for tsunami loss estimation. These included the addition of the earthquake building type and seismic design level required for the estimation of tsunami losses.

Figure 3.1: Example of the NSI building data

3.1 National Structure Inventory (NSI)

The National Structure Inventory Design and Development Plan (USACE, 2015) describes the overall design and development of the NSI for USACE systems. In addition the Hazus Release 3.0 FAQ for Homogeneous and Dasymetric Datasets provided an overview of the process and data. The USACE National Structure Inventory (NSI) and release notes documentation and data may be downloaded from: [National Structure Inventory Data Download](https://data.femadata.com/FIMA/NSI_2010/) (https://data.femadata.com/FIMA/NSI_2010/). The point data feature class *tsGbsNsi* was created and loaded into each Tsunami State Database. The required attributes for *tsGbsNsi* are summarized in Table 3.1 and it is the only inventory dataset required to produce Tsunami General Building Stock Losses and Casualties.

Table 3.1: Tsunami Model National Structure Inventory (SQL Table Name *tsNsiGbs*)

Column Name	Description	Data Type
NsiID	Unique ID	String Data. Max 24 characters
EqBldgTypeId	Index Value Based on Specific Earthquake Building Type	Small interger numeric
EqDesignLevelId	Index Value Based on Seismic Design Level	Small interger numeric
SOccTypeId	Index Value Based on Hazus Specific Occupancy Type	Small interger numeric
FoundTypeId	Index Value Based on Hazus Flood Foundation Type	Small interger numeric
CBFips	Census Block ID	String Data. Max 15 characters
NStories	Number of Stories	interger numerical
AreaSqft	Building Area (sqft)	Numeric (38, 8)
PerSqftAvgVal	Square footage Replacement Value ($/sqft)	Numeric (38, 20)
FirstFloorHt	Height of First Floor Relative to Ground Surface (feet)	Numeric (38, 8)
ValStruct	Replacement Value of Structure ($USD)	Numeric (38, 8)
ValCont	Replacement Value of Contents ($USD)	Numeric (38, 8)
ValOther	Replacement Value of Other ($USD)	Numeric (38, 8)
ValVehic	Replacement Value of Vehicles ($USD)	Numeric (38, 8)
MedYrBlt	Median Year Built	interger numerical
Pop2pmU65	Under Age 65 Daytime Population	interger numerical
Pop2pmO65	Age 65 and Older Daytime Population	interger numerical
Pop2amU65	Under Age 65 Nighttime Population	interger numerical
Pop2amO65	Age 65 and Older Nighttime Population	interger numerical
Latitude	Latitude (Decimal Degrees)	Numeric (38, 8)
Longitude	Longitude (Decimal Degrees)	Numeric (38, 8)

3.2 National Structure Inventory (NSI) Development

The NSI development assumes exposure only exists within areas which satellite and land-use data confirm as a built environment. The Hazus dasymetric data were developed by the U.S. Army Corps of Engineers, Hydrologic Engineering Center, Flood Impact Assessment Team (HEC-FIA Team) in partnership with the Federal Emergency Management Agency (FEMA), using the 2011 era National Land Cover Data (NLCD) (published in 2014) and used geospatial techniques to remove undeveloped areas. NLCD 2011 is a LULC classification scheme that has been applied consistently across the contiguous U.S. at a spatial resolution of 30 meters. The Developed and Cultivated classes were maintained in each census block, while the undeveloped, riparian, wetlands, and other classes were removed from the distribution of NSI data. The development of each field and its implementation in the Hazus Tsunami Model are described below:

NsiID: This is a unique ID for each structure. The ID is a concatenation of Specific Occupancy Type, County FIPS, and 7-digit ID created in sequence (e.g., AGR1 72005 00014207).

EqBldgTypeId: This is an ID representing the Hazus Earthquake Model Specific Building Type (EQ SBT). Table 3.2 lists the 36 model building types of the Hazus Tsunami Model, height ranges and typical heights, which are the same as those of the Hazus Earthquake Model (FEMA 2011a).

Table 3.2: Model Building Types, Height Ranges and Typical Heights

No.	Label	Description	Height Range: Name	Height Range: Stories	Typical Height in Stories	Typical Height in Feet
1	W1	Wood, Light Frame (≤ 5,000 sq. ft.)		All	1	14
2	W2	Wood, Greater than 5,000 sq. ft.		All	2	24
3	S1L	Steel Moment Frame	Low-Rise	1-3	2	24
4	S1M	Steel Moment Frame	Mid-Rise	4-7	5	60
5	S1H	Steel Moment Frame	High-Rise	8+	13	156
6	S2L	Steel Braced Frame	Low-Rise	1-3	2	24
7	S2M	Steel Braced Frame	Mid-Rise	4-7	5	60
8	S2H	Steel Braced Frame	High-Rise	8+	13	156
9	S3	Steel Light Frame		All	1	15
10	S4L	Steel Frame with Cast-in-Place Concrete Shear Walls	Low-Rise	1-3	2	24
11	S4M	Steel Frame with Cast-in-Place Concrete Shear Walls	Mid-Rise	4-7	5	60
12	S4H	Steel Frame with Cast-in-Place Concrete Shear Walls	High-Rise	8+	13	156
13	S5L	Steel Frame with Unreinforced Masonry Infill Walls	Low-Rise	1-3	2	24
14	S5M	Steel Frame with Unreinforced Masonry Infill Walls	Mid-Rise	4-7	5	60
15	S5H	Steel Frame with Unreinforced Masonry Infill Walls	High-Rise	8+	13	156
16	C1L	Concrete Moment Frame	Low-Rise	1-3	2	20
17	C1M	Concrete Moment Frame	Mid-Rise	4-7	5	50
18	C1H	Concrete Moment Frame	High-Rise	8+	12	120
19	C2L	Concrete Shear Walls	Low-Rise	1-3	2	20
19	C2M	Concrete Shear Walls	Mid-Rise	4-7	5	50
20	C2H	Concrete Shear Walls	High-Rise	8+	12	120
22	C3L	Concrete Frame with Unreinforced Masonry Infill Walls	Low-Rise	1-3	2	20
23	C3M	Concrete Frame with Unreinforced Masonry Infill Walls	Mid-Rise	4-7	5	50
24	C3H	Concrete Frame with Unreinforced Masonry Infill Walls	High-Rise	8+	12	120
25	PC1	Precast Concrete Tilt-Up Walls		All	1	15

No.	Label	Description	Height Range: Name	Height Range: Stories	Typical Height in Stories	Typical Height in Feet
26	PC2L	Precast Concrete Frames with Concrete Shear Walls	Low-Rise	1-3	2	20
27	PC2M	Precast Concrete Frames with Concrete Shear Walls	Mid-Rise	4-7	5	50
28	PC2H	Precast Concrete Frames with Concrete Shear Walls	High-Rise	8+	12	120
29	RM1L	Reinforced Masonry Bearing Walls with Wood or Metal Deck Diaphragms	Low-Rise	1-3	2	20
30	RM1M	Reinforced Masonry Bearing Walls with Wood or Metal Deck Diaphragms	Mid-Rise	4+	5	50
31	RM2L	Reinforced Masonry Bearing Walls with Precast Concrete Diaphragms	Low-Rise	1-3	2	20
32	RM2M	Reinforced Masonry Bearing Walls with Precast Concrete Diaphragms	Mid-Rise	4-7	5	50
33	RM2H	Reinforced Masonry Bearing Walls with Precast Concrete Diaphragms	High-Rise	8+	12	120
34	URML	Unreinforced Masonry Bearing Walls	Low-Rise	1-2	1	15
35	URM	Unreinforced Masonry Bearing Walls	Mid-Rise	3+	3	39
36	MH	Mobile Homes		All	1	12

The model building types of Table 3.2 were originally based on the classification system of FEMA 178, *NEHRP Handbook for the Seismic Evaluation of Existing Buildings (*FEMA, 1992) and may now be found in more recent ASCE publications including FEMA 310. The model building types of the Earthquake Model (and Tsunami Model) expand these building types to incorporate building height (e.g., low-rise, mid-rise, and high-rise building types), and to also include manufactured housing (mobile homes). General descriptions of the structural system of model building types are found in Chapter 5 of the Hazus Earthquake Model *Technical Manual.*

The EQ SBTs were assigned to the NSI points based on the percentages available in the existing Earthquake Model State Occupancy to Building Type Mapping Schemes. Since these do not exist for the new Tsunami Territories, Hawaii was used for the Pacific Territories, while Puerto Rico's schema was applied to estimate SBTs for the Virgin Islands. Note that all existing Hazus Earthquake Model schemes assign only low-rise building types (<4-5 stories). See Section 3.3 for NSI data enhancements. These distribution tables were added to each State Database as tsSOccupSbtPct. An example from Hawaii for COM1 building type distribution percentages are shown in Table 3.3.

Table 3.3: Hawaii Occupancy to Building Type Distribution for COM1 Example

SchemeID	Specific Occupancy	EQ SBT	Percent
HI2	COM1	C1L	5.92
HI2	COM1	C2L	9.99
HI2	COM1	C3L	1.11
HI2	COM1	PC1	15.17
HI2	COM1	PC2L	4.81
HI2	COM1	RM1L	16.08
HI2	COM1	RM2L	1.92
HI2	COM1	S1L	8.97
HI2	COM1	S2L	1.04
HI2	COM1	S3	1.95
HI2	COM1	S4L	1.04
HI2	COM1	URML	6
HI2	COM1	W2	26

EqDesignLevelId: This is an ID representing the Hazus Earthquake Model seismic design level of the structure (Table 3.4).

Table 3.4: Hazus Seismic Design Levels

DesignLevelID	DesignLevel	DesignLevelDesc
1	PC	Pre-Code
2	LC	Low Code
3	MC	Moderate Code
4	HC	High Code
5	LS	Low Code - Special
6	MS	Moderate Code - Special
7	HS	High Code - Special

The Hazus Earthquake model uses a statewide default mapping scheme to assign seismic design level. For the NSI, an approach utilizing Census Block level data with the estimated Median Year Built of the structure, and typical benchmark code adoption years for each State and Territory was used to assign a seismic design level for structures within the Census Block. The benchmark years are based on a review of online resources, including information from the International Code Council's Building Code Assessment Project (http://bcapcodes.org/code-status/state/), as well as the Earthquake Engineering Research Institute (www.eeri.org) and the Western States Seismic Policy Council (www.wsspc.org). Since benchmark years represent a combination of considerations regarding adoption, as well as implementation and enforcement was used in selecting the default design levels summarized in Table 3.5. This approach better distributes structures in older areas to lower seismic designs rather than randomly assigning seismic design levels across the State regardless of when the structures were built.

Table 3.5: Estimated Benchmark Year Seismic Design Levels for States and Territories

STATE	Pre-Code* (PC)	Low Code (LC)	Moderate Code (MC)	High Code (HC)	Special High-Code (HS)
Alaska	≤ 1964	1965-1994	1995-2000	≥ 2001	NA
California	≤ 1940	1941-1975	1976-1994	1995-2000	≥ 2001
Hawaii	≤ 1974	1975-1994	1995-2000	≥ 2001	NA
Oregon	≤ 1974	1975-1994	1995-2000	≥ 2001	NA
Washington	≤ 1955	1956-1974	1975-2003	≥ 2004	NA
Puerto Rico	≤ 1974	1975-1994	1995-2005	≥ 2006	NA
USVI	≤ 1974	1975-2005	≥ 2006	NA	NA
CNMI	≤ 1974	1975-2005	≥ 2006	NA	NA
Guam	≤ 1974	1975-2005	≥ 2006	NA	NA
American Samoa	≤ 1974	1975-2005	≥ 2006	NA	NA

* W1 in CA coastal counties will be at least MC (no PC or LC W1, per EQ *Technical Manual*) and LC (no PC W1) in other States

SOccType: This is an Index ID for the Hazus Specific Occupancy Type. This is Occupancy Type of the structure as defined in the Hazus General Building Stock (GBS) data aggregated by Census Block. NSI points are based on the number of a given occupancy type in a Census Block provided by the Hazus GBS. For example, if the Hazus GBS indicates there are 7 RES1 occupancy types in a particular Census Block, then 7 RES1 points are distributed within the developed portion of that block. This helps to define attributes of the structure like building and content value, day and night population distribution, number of stories, number of households, and other generic characteristics. A total of 33 specific occupancy classifications are used in the baseline inventory. The primary purpose of building classifications is to group buildings with similar valuation, damage, and loss characteristics into a set of pre-defined groups for analysis. Table 3.6 provides a complete list of all the building occupancies along with Standard (OSHA) Industrial Codes (https://www.osha.gov/pls/imis/sicsearch.html).

Table 3.6: Tables of Hazus Specific and General Occupancy Types

Occ Type ID	Specific Occupancy	Residential	Standard Industrial Codes (SIC)
1	RES1	Single Family Dwelling	
2	RES2	Mobile Home	
3	RES3A	Multi Family Dwelling - Duplex	
4	RES3B	Multi Family Dwelling – 3-4 Units	
5	RES3C	Multi Family Dwelling – 5-9 Units	
6	RES3D	Multi Family Dwelling – 10-19 Units	
7	RES3E	Multi Family Dwelling – 20-49 Units	
8	RES3F	Multi Family Dwelling – 50+ Units	
9	RES4	Temporary Lodging (e.g., hotels)	70
10	RES5	Institutional Dormitory (e.g., prisons)	
11	RES6	Nursing Home	8051, 8052, 8059

Occ Type ID	Specific Occupancy	Commercial	Standard Industrial Codes (SIC)
12	COM1	Retail Trade	52, 53, 54, 55, 56, 57, 59
13	COM2	Wholesale Trade	42, 50, 51
14	COM3	Personal and Repair Services	72, 75, 76, 83, 88
15	COM4	Business/Professional/Technical Services	40, 41, 44, 45, 46, 47, 49, 61, 62, 63, 64, 65, 67, 73, 78 (except 7832), 81, 87, 89
16	COM5	Depository Institutions	60
17	COM6	Hospital	8062, 8063, 8069
18	COM7	Medical Office/Clinic	80 (except 8051, 8052, 8059, 8062, 8063, 8069)
19	COM8	Entertainment & Recreation	48, 58, 79 (except 7911), 84
20	COM9	Theaters	7832, 7911
21	COM10	Parking	

Occ Type ID	Specific Occupancy	Industrial	Standard Industrial Codes (SIC)
22	IND1	Heavy	22, 24, 26, 32, 34, 35 (except 3571, 3572), 37
23	IND2	Light	23, 25, 27, 30, 31, 36 (except 3671, 3672, 3674), 38, 39
24	IND3	Food/Drugs/Chemicals	20, 21, 28, 29
25	IND4	Metals/Minerals Processing	10, 12, 13, 14, 33
26	IND5	High Technology	3571, 3572, 3671, 3672, 3674
27	IND6	Construction	15, 16, 17

Occ Type ID	Specific Occupancy	Agriculture	Standard Industrial Codes (SIC)
28	AGR1	Agriculture	01, 02, 07, 08, 09

Occ Type ID	Specific Occupancy	Religion/Nonprofit	Standard Industrial Codes (SIC)
29	REL1	Church/Membership Organizations	86

Occ Type ID	Specific Occupancy	Government	Standard Industrial Codes (SIC)
30	GOV1	General Services	43, 91, 92 (except 9221, 9224), 93, 94, 95, 96, 97
31	GOV2	Emergency Response	9221, 9224

Occ Type ID	Specific Occupancy	Education	Standard Industrial Codes (SIC)
32	EDU1	Schools/Libraries	82 (except 8221, 8222)
33	EDU2	Colleges/Universities	8221, 8222

FoundTypeId and FirstFloorHt: These attributes are interrelated since the First-Floor Height is directly related to the Flood Foundation Type. It includes a Foundation Type ID and the corresponding First-Floor Height based on the Hazus Flood Model for evaluation of tsunami inundation depth in the structure. As summarized in Table 3.7 these data provide estimates of first-floor heights as a function of foundation type, and building age. Median Year Built relative to the Flood Insurance Rate Map (FIRM) adoption for the community representing entry into the National Flood Insurance Program (NFIP) were used to establish pre-FIRM or post-FIRM construction. Table 3.8 provides the assumed default distribution of foundation types for coastal areas (see Hazus Flood *Technical Manual* for more details). Post-FIRM (feet)

Table 3.7: Default First-Floor Heights above Grade to Top of Finish (from Table 3.14, Flood *Technical Manual*, FEMA 2011b)

Foundation Type	Pre-FIRM (feet)	Post-FIRM (feet) A-Zone	Post-FIRM (feet) V-Zone
Pile (or column)	7	8	8
Pier (or post and beam)	5	6	8
Solid Wall	7	8	8
Basement	4	4	4
Crawl	3	4	4
Fill	2	2	2
Slab	1	1	1

Table 3.8: Distribution of Foundation Types for Coastal Areas (Heinz, 2000)

Foundation Types	Pile	Pier	Solid Wall	Basement	Crawl	Fill	Slab
Pre-Firm Construction – All	7%	7%	1%	2%	46%	0%	37%
Post-Firm Construction – A-Zone (Special Flood Hazard Area)	20%	5%	0%	0%	55%	0%	20%
Post-Firm Construction – V-Zone (Special Flood Hazard Area – High Hazard)	60%	25%	0%	0%	10%	0%	5%

CBFips: This is the census block that the structure exists in. This attribute is a string field with 15 numeric characters. In the case of data for the Territories, this is a 15-character ID of the 1 km grid cell with population. Views of Hazus GBS based on NSI points inventory and results tables as well as thematic mapping are based on the Census Block IDs and geometries.

N_Stories: This is the structure's number of stories provided for single and multi-family residences based on U.S. Census Region. This is an integer and is also used to classify Earthquake Specific Building Types into low, mid, and high-rise earthquake building types. Chapter 3 of the Hazus Flood *Technical Manual* provides the distribution by number of stories (1, 2, 3, and 5) for Residential Occupancies. Since no high-rises exist in the default Hazus mapping schemes, the maximum number of stories in the base NSI data is 5 stories. For new Tsunami Territories, the Puerto Rico multi-story residential distribution was used, however, number of stories was occasionally provided in the essential facility data for the Territories.

AreaSqft and PerSqftAvgVal: These are interrelated attributes since the base NSI data do not include building area (AreaSqft). Processing consisted of determining the average replacement value per square foot for each NSI structure (PerSqftAvgVal) by dividing the total $ value of a given specific occupancy by the total square footage of the occupancy for each Census Tract. As described in Chapter 3 of the Hazus Flood *Technical Manual*, square footage valuations are based on RSMeans[1] replacement costs by occupancy types that are then modified by County modification factors to reduce or increase replacement costs based on local costs of materials and services. In addition, the household income for each Census Tract relative to the national median is used to adjust the Single Family (RES1) replacement costs based on construction quality. Once PerSqftAvgValue is calculated, AreaSqft is estimated by dividing structural value (ValStruct) by PerSqftAvgValue.

ValStruct, ValCont, ValOther, and ValVehic: These are provided by the NSI data based on the Hazus GBS building and content replacement values by occupancy type, as well as the vehicle replacement value disaggregated from the block to the NSI point. These are the valuation attributes in dollars for Structure, Content, Other, and Vehicles, respectively. Other is a placeholder field and not currently used. These are directly obtained from Hazus GBS valuations for each occupancy type. The aggregated specific occupancy value within each Census Block is equally distributed to each NSI point in that Block based on specific occupancy.

MedYrBlt: Median year built is provided by the U.S. Census and applied within the Hazus Demographic Data attributes at the Census Block level. These values are contained in the

[1] RSMeans data from Gordian, https://www.rsmeans.com/

hzDemographicsB table in each State database and were joined with NSI structure data points based on Census Block ID.

POP_2AM_U65: This is the population at night for the structure, people under the age of 65 based on Census Bureau's Longitudinal Employer-Household Dynamics (LEHD) data. This is an integer.

POP_2AM_O65: This is the population at night for the structure, people over the age of 65 based on Census Bureau's Longitudinal Employer-Household Dynamics (LEHD) data. This is an integer.

POP_2PM_U65: This is the population at day for the structure, people under the age of 65 based on Census Bureau's Longitudinal Employer-Household Dynamics (LEHD) data. This is an integer.

POP_2PM_O65: This is the population at day for the structure, people over the age of 65 based on Census Bureau's Longitudinal Employer-Household Dynamics (LEHD) data. This is an integer.

The population estimates for each NSI structure are developed by USACE from the Census Bureau's Longitudinal Employer-Household Dynamics (LEHD) data (Will Lehman, USACE Economist, personal communication). The LEHD program produces several datasets, including Quarterly Workforce Indicators (QWI) and the LEHD Origin-Destination Employment Statistics (LODES). LODES, which can be useful for consequence modeling, provides employment statistics, including worker counts, linking residence and work locations at the Census Block-level. The LEHD/LODES method of population assignment uses four population pools; working population and residential population, day, and night. Census 2010 population data are used to approximate the total residential population of a census block. The LEHD dataset is then used to identify the nonresidential population of the block, as well as model the movement of population from residential structures into nonresidential.

3.3 National Structure Inventory (NSI) Enhancements

In addition to the enhancements completed above, several additional steps have been taken to further improve the capability of the NSI data to support tsunami building loss estimation and casualty assessment.

The default distribution and data associated with each educational (EDU) NSI point has been replaced by a site-specific dataset of school locations, including Colleges and Universities, Private Schools, and Public Schools. The data include numbers of students, teachers, and staff. The data provide national coverage, ensure more accurate locations of school facilities in relation to the tsunami hazard, and provide important daytime population exposure estimates for evacuation and casualty modeling. This dataset is available from the U.S. EPA's Environmental Dataset Gateway https://edg.epa.gov, and available for download from: https://edg.epa.gov/data/Public/OEI/ORNL_Education/ORNL_Education.zip.

Since the current default earthquake mapping schemes lack both mid- and high-rise structures, thresholds based on building size for the NSI structures were utilized to reclassify low-rise into mid- (4–7 stories), and high-rises(8+ stories) (see Model Building Type table below) for the Honolulu region. This is a critical requirement for implementation of the tsunami loss methodology in coastal urban areas. The continued classification of these buildings into low-rise categories will substantially inflate losses in urban areas when erroneously applying low-rise tsunami damage-state parameters (see Chapter 5) to high-rise buildings.

Based on the numbers of high and midrise buildings in the Honolulu region, the largest NSI buildings based on building area, were assigned high and low rise building types. For example, if 100 high rise and 200 midrise were identified in the region, the largest 100 NSI points were assigned high rise types and the next 200 largest were assigned to midrise earthquake specific building types, based on their low rise earthquake specific building type. The assumption is that large square footage buildings in coastal urban environments indicate taller, rather than wider buildings. Available data sources were used for calibrations, including The Skyscraper Page (http://skyscraperpage.com/cities/maps/?cityID=421) to ensure that counts of high-rise types in the urban area are in rough alignment. Remaining 4 story buildings in the NSI structure database were assigned to mid-rise building types. This may be feasible for other urban areas and can benefit earthquake model building mapping schemes that currently include low-rise only.

3.4 User-Defined Facilities

The quality of tsunami loss results may be further enhanced by developing User-Defined Facility (UDF) inventory datasets. The tsunami UDF capability utilizes the UDF inventory attribute table data already available for earthquake and flood loss modeling. This also allows the combination of tsunami and earthquake loss potential in the case of near-source earthquakes (where the region is impacted by both earthquake ground shaking and the earthquake generated tsunami). Users can use the existing Comprehensive Data Management System (CDMS) tool provided with Hazus to integrate site-specific structure data into their State Databases.

No new UDF table for tsunami will be required in the State Databases. On aggregation, the tsunami UDF Inventory table in the study region database will be populated with the attributes values available in the State Databases (Table 3.9).

Table 3.9: State Database User-Defined Facility Tables and Required Attributes

User Defined Facility General Table (hzUserDefinedFlty)	Note	Required for Tsunami Losses
[UserDefinedFltyId]	A unique ID	Yes
[Occupancy]	Specific Occupancy Type	Yes
[Tract]		No
[Name]		No
[Address]		No
[City]		No
[Statea]		No
[Zipcode]		No
[Contact]		No
[PhoneNumber]		No
[YearBuilt]		No
[Cost]	Structural Replacement Cost ($USD)	Yes
[BackupPower]		No
[NumStories]		No

User Defined Facility General Table (hzUserDefinedFlty)	Note	Required for Tsunami Losses
[Area]	Building Area (sqft)	Yes
[ContentCost]	Content Replacement Cost ($USD)	Yes
[ShelterCapacity]		No
[Latitude]		Yes
[Longitude]		Yes
[Comment]		No
[Shape]		No

User Defined Facility Earthquake Specific Table (eqUserDefinedFlty)	Note	Required for Tsunami Losses
[eqBldgType]	Specific Earthquake Building Type	Yes
[DesignLevel]	Seismic Design Level	Yes
[eqUdsClass]		No, but required for EQ model functionality loss

User Defined Facility Flood Specific Table (flUserDefinedFlty)	Note	Required for Tsunami Losses
[FirstFloorHt]	Top of Finished Floor Relative to Adjacent Grade (feet)	Yes
[foundationtype]		No, but useful in estimating FirstFloorHt

3.5 U.S. Territory Data Development

Data were developed to support tsunami loss modeling for five High Risk U.S. Territories. Enhancements were made to Puerto Rico's Essential Facility inventory based on the Puerto Rico 2.1 data available for download from FEMA's Map Service Center http://msc.fema.gov/portal/resources/hazus, however, a Hazus State Database for Puerto Rico already existed and NSI data were developed by USACE and enhanced as described in Sections 3.2 and 3.3, above. New State Databases were developed for Guam, American Samoa, Commonwealth of Northern Mariana Islands, and the U.S. Virgin Islands. These new datasets include the following layers:

- ***State:*** administrative boundary for Territory, based on Global Administrative Boundaries (GADM) www.gadm.org
- ***County:*** administrative boundaries for Counties (Districts), based on GADM

- ***Census Tract:*** Tract boundaries and demographic data based on U.S. Census 2010 https://www.census.gov/2010census/news/press-kits/island-areas/island-areas.html
- ***Census Block:*** based on 1 km grids provided by Landscan 2014 and demographic data based on U.S. Census 2010
- ***Essential Facilities:*** (Schools, Hospitals, Police, Fire, and EOCs): Developed by the Pacific Disaster Center (PDC) from public sources. Since multiple data sources were used for each Territory, searching by Territory name in the Global Hazards Information Network (GHIN) provides the metadata pages for each data layer: http://ghin.pdc.org

The NSI methodology described in Sections 3.2. and 3.3 above, provided the capability to provide a baseline General Building Stock inventory for the 44 (of 78 total) Puerto Rico counties that are located along the coast. However, the remaining U.S. Territories generally lack the detailed U.S. Census and other data available for U.S. States: http://www.census.gov/2010census/news/press-kits/island-areas/island-areas.html. In addition, no equivalent Census Block-level demographic data are available for the territories. Data from the Pacific Disaster Center (PDC) was utilized to develop an NSI for the remaining territories.

The first step was to develop building point data layer based on available points of interest from PDC (2010), essential facility data developed by PDC (2014-2016), parcel (Guam only, PDC 2000), land use, and building footprint data (American Samoa only, PDC, 2001), as well as imagery (ESRI World Imagery, 2016). Within lower-lying coastal regions, special care was taken to ensure that data in those high-risk areas were comprehensive and well located.

Assigning Hazus Specific Occupancy Types (Table 3.6) was the next step and were also based on available points of interest data (e.g., restaurants, hotels, etc.), essential facilities (e.g., schools, hospitals, fire and police stations), parcel data (e.g., multi-family, religious), land use (e.g., residential, commercial, and recreation zoning), as well as imagery. However, it was necessary to assign default-specific occupancies to many of the structure data points that could not be identified. The default-specific occupancies used were RES1 for Residential, COM1 for Commercial, and IND1 for Industrial. The default specific occupancy types were used for up to 50% of the total occupancy type assignments. These types produce reasonable valuations, however, reporting results for General, rather than Specific Occupancies should be considered more reliable.

Seismic Design Levels for the four new Territories were assigned based on the benchmark years summarized in Table 3.5 and the Median Year Built data provided by U.S. Census 2010 at the Tract level. The vertical Occupancy to EQ Specific Building Type mapping scheme was adopted from Puerto Rico and provided as a new State Database table (*tsSOccupSBTPct*) for each Territory.

Building areas were developed from Building Footprint data for American Samoa. Average building area by specific occupancy type were developed from the relationships between specific occupancy types and building area (Table 3.10) that were used when area was not available using footprints. In addition, structural replacement cost valuations were developed based on RS Means adjusted to 2016 using the Consumer Price Index (CPI) approach and application of Hawaii cost-modification factors (Table 3.10)

Table 3.10: Default Building Area and Replacement Costs for Territories

Specific Occupancy	Hazus Definition	Territory Default Building Area (sqft) *	Territory Replacement (sqft) +
AGR1	Agriculture	3,000	$124.52
COM1	Retail Trade	3,000	$128.23
COM10	Parking	5,500	$89.17
COM2	Wholesale Trade	3,700	$124.52
COM3	Personal and Repair Services	3,800	$151.22
COM4	Professional/Technical Service	4,600	$205.03
COM5	Banks	5,000	$297.11
COM6	Hospital	5,000	$392.73
COM7	Medical Office/Clinic	3,000	$282.33
COM8	Entertainment & Recreation	2,900	$262.06
COM9	Theaters	7,000	$196.54
EDU1	Schools/Libraries	2,700	$203.44
EDU2	Colleges/Universities	9,200	$226.54
GOV1	General Services	3,300	$160.88
GOV2	Emergency Response	5,000	$273.55
IND1	Heavy	2,200	$152.53
IND2	Light	3,700	$124.52
IND3	Food/Drugs/Chemicals	4,900	$241.89
IND4	Metals/Minerals Processing	4,900	$241.89
IND5	High Technology	4,900	$241.89
IND6	Construction	4,900	$124.52
REL1	Church	6,300	$209.84
RES1	Single Family Dwelling	1,500	*Table 3.11*
RES2	Mobile Home	1,000	$49.10
RES3A	Multi Family Dwelling - Duplex	2,700	$133.02
RES3B	Multi Family Dwelling – 3-4 Units	5,400	$116.94
RES3C	Multi Family Dwelling – 5-9 Units	7,300	$209.99
RES3D	Multi Family Dwelling – 10-19 Units	10,000	$197.50
RES3E	Multi Family Dwelling – 20-49 Units	31,000	$215.96
RES3F	Multi Family Dwelling – 50+ Units	50,000	$203.38
RES4	Temporary Lodging (e.g., hotels)	9,300	$221.62
RES5	Institutional Dormitory (e.g., prisons)	30,000	$238.52
RES6	Nursing Home	20,000	$242.21

** assigned based on occupancy averages determined from available building footprints and parcel data for U.S. Territories, rather than U.S. averages (MeansModelDesc), institutions such as schools, hospitals, etc. are represented by multiple points on structure and therefore each building footprint is typically far less than institutional averages*
+Territory replacement costs are estimated using RS Means adjusted to 2016 based on CPI and using HI location factor adjustment (1.17)

Single Family (RES1) replacement costs are further adjusted by the average household income in each Census Tract based on U.S. Census 2010 demographics relative to the U.S. Median Household income. This approach utilizes the income ratios and average RES1 replacement costs summarized in Table 3.11.

Table 3.11: Single Family (RES1) Replacement Base Cost for Territories

Income Ratio (IR)	RES1 Replacement
IR < 0.5	$107.39
0.5 ≤ IR < 0.85	$114.03
0.85 ≤ IR < 1.25	$142.63
1.25 ≤ IR < 2.0	$168.63
IR ≥ 2.0	$201.18

Most American Samoa and Marianas tracts were assigned relatively low income ratios, while Guam and the Virgin Islands were largely comparable to U.S. median income averages.

U.S. Census 2010 data contain general foundation type information (D401_S079 through D402_S082) that provided the percentage distribution of foundation types at the Tract level for RES1 only. Since no other data were available, all other Territory occupancy types were mapped to FoundationID 7 (slab), and FirstFloorHt = 1' with the exception of RES2 (FoundationID 5 (crawl), FirstFloorHt = 3').

U.S. Census 2010 demographic data were utilized to provide the population distribution by age and general occupancy types that were used to populate the Hazus Demographic table at the Tract level (*hzDemographicsT*) as shown in Table 3.12.

Table 3.12: Example of Tract Level Demographics Data for Guam Used for Population Distribution

6601004650	3,808	313	732	313	3,332	1,598	160	29	3	200	936	200
6601007250	4,917	436	1,294	436	4,313	1,631	163	48	5	215	1,293	215
6601013100	2,137	181	440	181	1,867	864	86	24	2	121	507	121
6601017650	8,875	717	1,722	717	7,787	3,639	364	68	7	524	2,205	524
6601026100	6,822	445	1,419	445	6,094	2,762	276	66	7	389	1,741	389
6601028050	44,943	3,252	9,737	3,252	39,880	17,648	1,765	459	46	2,229	11,618	2,229
6601034800	1,051	56	383	56	955	387	39	17	2	34	174	34
6601036500	2,273	145	531	145	2,041	844	84	25	3	103	625	103
6601046250	15,191	789	3,549	789	13,808	5,797	580	139	14	1,130	3,787	1,130
6601050150	1,850	138	510	138	1,654	572	57	5	1	63	562	63
6601051450	6,825	427	1,701	427	6,128	2,584	258	116	12	286	1,711	286
6601059250	1,454	115	283	115	1,279	591	59	12	1	99	354	99
6601062500	6,084	370	2,157	370	5,626	1,710	86	43	2	396	1,408	396
6601065750	2,592	245	558	245	2,240	1,052	105	20	2	128	589	128
6601069650	3,050	198	685	198	2,733	1,185	119	9	1	160	813	160
6601071600	19,685	1,374	3,956	1,374	17,351	9,408	941	192	19	930	3,825	930
6601078750	782	33	249	33	722	264	26	7	1	27	202	27
6601083300	20,539	1,123	5,338	1,123	18,674	7,213	721	205	21	1,232	5,428	1,232
6601084600	6,480	390	1,552	390	5,846	2,404	240	21	4	335	1,758	335
Total	**159,358**	**10,747**	**36,796**	**10,747**	**142,331**	**62,153**	**6,130**	**1,525**	**150**	**8,601**	**39,536**	**8,601**

working night is estimated based on 5 percent of day time working population. Res – Residential. Com – Commercial. Ind – Industrial.

The Census Block level demographic data are not directly provided by the U.S. Census, however, the U.S. Census 2010 Tract level demographics were distributed to the 1 km blocks using a population ratio determined from the Landscan 2014 total ambient (24-hour average) population.

Distribution of the population by age and general occupancy type was performed by first calculating a population distribution ratio for each NSI point. The ratio is the NSI point building area divided by the total square footage for the general occupancy type for the Census Tract and provided the basis for the Census 2010 population distribution to the NSI points (Table 3.13) with few exceptions described below.

Table 3.13: Distribution of Census 2010 Population to NSI for Territories

Census 2010	National Structure Inventory
O65ResidDay	Distribute to Residential (all res except RES4 & RES6) Pop2pmO65
U65ResDay	Distribute to Residential (all res except RES4 & RES6) Pop2pmU65
O65ResNight	Distribute to Residential (all res except RES4 & RES6) Pop2amO65
U65ResNight	Distribute to Residential (all res except RES4 & RES6) Pop2amU65
WorkingCom	Distribute to Commercial (and GOV1, exclude COM6 & COM10) Pop2pmU65
WorkComNight	Distribute to Commercial (and GOV1, exclude COM6 & COM10) Pop2amU65
WorkingInd	Distribute to Industrial Pop2pmU65
WorkIndNight	Distribute to Industrial Pop2amU65
SchoolEnrollmentKto12	Distribute to EDU1 Pop2pmU65
SchoolEnrollmentCollege	Distribute to EDU2***** Pop2pmU65

based on a ratio determined by the total EDU2 building area for the State, based on the assumption that college students come from all surrounding tracts

The use of population by square footage estimates from FEMA P-58 (Seismic Performance Assessment of Buildings, Table 3-1), and the Hazus Earthquake *Technical Manual* were utilized to increase accuracy when assigning population to essential and high occupancy facilities.

These estimates provide the peak day and peak night defaults utilized by the Hazus CDMS tool for preparing inventories for the Advanced Earthquake Building Model (AEBM) (Table 3.14). Table 3.14 was used to provide a quality check of the results of distributing populations from U.S. Census aggregated data to the NSI points. Rounding the NSI point populations to integers resulted in some loss of fractions. Some manual editing was required and checks were made to ensure that the night and day populations were balanced and did not exceed State level populations. For example, a check was made to ensure day time populations did not exceed night time for the entire Territory.

Table 3.14: Estimated Peak Day and Night Occupancy Loads

Occupancy	Description	Peak Day (~2:00 pm) (sqft/person)	Peak Night (~2:00 am) (sqft/person)	Sources for Estimate
AGR1	Agriculture	250	12,500	Table 14.8 (Flood) for employees; Table 13.2 (Earthquake) provides day and night ratios
COM1	Retail Trade	167	8,333	Table 3-1 (FEMA P-58); Table 13.2 (Earthquake) provides day and night ratios
COM10	Parking	-	-	Not applicable
COM2	Wholesale Trade	900	45,000	Table 14.8 (Flood) for employees; Table 13.2 (Earthquake) provides day and night ratios
COM3	Personal and Repair Services	590	5,900	Similar to IND2, Table 13.2 (Earthquake) provides day and night ratios
COM4	Professional/Technical Services	250	12,500	Table 3-1 (FEMA P-58); Table 13.2 (Earthquake) provides day and night ratios
COM5	Banks	250	12,500	Table 3-1 (FEMA P-58); Table 13.2 (Earthquake) provides day and night ratios
COM6	Hospital	200	667	Table 3-1 (FEMA P-58); Table 13.2 (Earthquake) provides day and night ratios
COM7	Medical Office/Clinic	200	-	Table 3-1 (FEMA P-58); Table 13.2 (Earthquake) provides day and night ratios
COM8	Entertainment & Recreation	75	-	Engineering ToolBox
COM9	Theaters	75	-	Engineering ToolBox
EDU1	Grade Schools	71	3,571	Table 3-1 (FEMA P-58); Table 13.2 (Earthquake) provides day and night ratios
EDU2	Colleges/Universities	83	4,167	Table 3-1 (FEMA P-58); Table 13.2 (Earthquake) provides day and night ratios
GOV1	General Services	250	12,500	Table 3-1 (FEMA P-58); Table 13.2 (Earthquake) provides day and night ratios
GOV2	Emergency Response	300	300	Engineering ToolBox

Occupancy	Description	Peak Day (~2:00 pm) (sqft/person)	Peak Night (~2:00 am) (sqft/person)	Sources for Estimate
IND1	Heavy	550	5,500	Table 14.8 (Flood) for employees; Table 13.2 (Earthquake) provides day and night ratios
IND2	Light	590	5,900	Table 14.8 (Flood) for employees; Table 13.2 (Earthquake) provides day and night ratios
IND3	Food/Drugs/Chemicals	540	5,400	Table 14.8 (Flood) for employees; Table 13.2 (Earthquake) provides day and night ratios
IND4	Metals/Minerals Processing	730	7,300	Table 14.8 (Flood) for employees; Table 13.2 (Earthquake) provides day and night ratios
IND5	High Technology	300	3,000	Table 14.8 (Flood) for employees; Table 13.2 (Earthquake) provides day and night ratios
IND6	Construction	250	2,500	Table 14.8 (Flood) for employees; Table 13.2 (Earthquake) provides day and night ratios
REL1	Churches and Other Nonprofit	20	-	Engineering ToolBox
RES1	Single Family Dwelling	1,201	841	Based on National median area (2,169 sqft) and average household (2.58) size from U.S. Census. Table 13.2 (Earthquake) provides day and night ratios
RES2	Manuf. Housing	461	323	Table 3-1 (FEMA P-58); Table 13.2 (Earthquake) provides day and night ratios
RES3A	Duplex	461	323	Table 3-1 (FEMA P-58); Table 13.2 (Earthquake) provides day and night ratios
RES3B	Triplex / Quads	461	323	Table 3-1 (FEMA P-58); Table 13.2 (Earthquake) provides day and night ratios
RES3C	Multi-dwellings (5 to 9 units)	461	323	Table 3-1 (FEMA P-58); Table 13.2 (Earthquake) provides day and night ratios
RES3D	Multi-dwellings (10 to 19 units)	461	323	Table 3-1 (FEMA P-58); Table 13.2 (Earthquake) provides day and night ratios
RES3E	Multi-dwellings (20 to 49 units)	461	323	Table 3-1 (FEMA P-58); Table 13.2 (Earthquake) provides day and night ratios
RES3F	Multi-dwellings (50+ units)	461	323	Table 3-1 (FEMA P-58); Table 13.2 (Earthquake) provides day and night ratios
RES4	Temporary Lodging - Hotel	2,105	400	Table 3-1 (FEMA P-58); Table 13.2 (Earthquake) provides day and night ratios
RES5	Institutional Dormitory	2,105	400	Table 3-1 (FEMA P-58); Table 13.2 (Earthquake) provides day and night ratios
RES6	Nursing Home	115	115	Engineering ToolBox

Note: general guidance only, peak loads provide worst case estimates of casualties, actual occupants may vary substantially by geography, season, time of day, day of week, holidays, etc.

Population distribution to essential and high occupancy facilities for the Territories was done separately to ensure peak day and night values were reasonable. Table 3.15 summarizes the day and night, as well as the under and over 65 population distribution for these occupancy types based on building area.

Table 3.15: Population Distributions for Special Occupancy Cases for Territories (Area=sqft)

Specific Occupancy	Pop2pmU65	Pop2pmO65	Pop2amU65	Pop2amO65
Hospitals (COM6)	0.95 * Area/200	0.05 * Area/200	0.95 * Area/667	0.05 * Area/667
Emergency Services (GOV2)	Area/300	NA	Area/300	NA
Hotels (RES 4)	0.95 * Area/2,105	0.05 * Area/2,105	0.95 * Area/400	0.05 * Area/400
Nursing Homes (RES 6)	0.05 * Area/115	0.95 * Area/115	0.05 * Area/115	0.95 * Area/115

It is also important to note that the Hazus Tsunami Casualty interface includes a processing step where the user is presented with the day and night, under and over 65 exposed populations that can be edited to include any transient or visitor populations common in tsunami risk areas such as beach populations and cruise ships.

4.0 Tsunami Hazard Analysis

4.1 Introduction

Mega tsunamis are rare but induce high impacts. The 2004 Indian Ocean Tsunami took almost 230,000 lives (USAID, 2005) in Indonesia, Thailand, Malaysia, Myanmar, Bangladesh, India, Sri Lanka, Maldives, and eastern Africa. This mega tsunami was created by an M_w 9.1 earthquake that ruptured the subduction fault for more than 1,000 km (USGS, 2005). The 2011 Tohoku Tsunami that was triggered by a M_w 9.0 earthquake rupturing 500 km length of a subduction fault, killing 15,893 people; 2,556 people were still categorized as missing as of December 9, 2016 (National Police Agency, 2016). This Tohoku tsunami propagated across the Pacific Ocean causing over $48 million in damage to nearly two-dozen harbors in California (Ewing, 2011). The largest earthquake measured in the 20th century was the 1960 Chile Earthquake with a moment magnitude (M_w) 9.5. Approximately 15 hours after the earthquake, tsunami waves inundated Hawaii, 10,000 km from Chile, causing $75 million in damage and 61 fatalities[2]. In 1964, the M_w 9.2 Great Alaskan Earthquake generated tsunamis that killed 122 people and caused approximately $300 to $400 million in damage to Alaska alone[3].

Smaller but significant tsunamis are more common. Even in the relatively short duration between the 2004 Indian Ocean Tsunami and the 2011 Tohoku Tsunami, there were at least seven significant events: namely tsunamis that affected Northern Sumatra in 2005 (M_w 8.7, 10 dead[4]), South Java in 2006 (M_w 7.7, 802 dead), Kuril Islands in 2006 (M_w 8.3), Solomon Island in 2007 (M_w 8.1, 52 dead), Samoa in 2009 (M_w 8.0, 192 dead), Chile in 2010 (M_w 8.8, 156 dead), and Mentawai in 2010 (M_w 7.8, 431 dead).

There is potential that a locally generated mega tsunami could strike the Pacific Northwest. Such a tsunami could be generated by a rupture of the 800 km long fault along the Cascadia subduction zone from British Columbia to Northern California (e.g., Atwater et al. 2005; Priest et al. 1997). In Southern California, there is a tsunami threat that could be triggered by a large submarine landslide off Santa Barbara or Los Angeles Basin (Borerro et al. 2004). A similar tsunami threat is also present in Puerto Rico, where in 1918 six-meter high tsunami waves killed 116 people (ten Brink et al., 2006). More detailed discussion on the tsunami threat in the United States can be found in a report by Dunbar and Weaver (2008).

4.2 Background

Several characteristics are unique to tsunami hazards. First, tsunami-risk areas are limited to narrow strips along the shoreline (typically less than a few kilometers from the shoreline). Within the inundation zones, damage and losses are, in general, not uniform: the nearer the shoreline, the higher the tsunami power. Second, because of the propagation, tsunamis could affect entire oceans. Transoceanic tsunamis can cause serious damage in coastal communities far away from the earthquake. Those characteristics are different from other natural hazards such as

[2] The US Geological Survey Earthquake Hazards Program, https://earthquake.usgs.gov/earthquakes/eventpage/official19600522191120_30#executive

[3] The NOAA National Centers for Environmental Information, https://www.ncei.noaa.gov/news/great-alaska-earthquake

[4] All of the death tolls presented in this paragraph are obtained from the NOAA NGDC/WDS Global Historical Tsunami Database, https://ngdc.noaa.gov/hazard/tsu_db.shtml.

earthquakes, river floods, and hurricanes, although rapid, intense flows caused by dam failures could have a similar effect.

Because tsunamis are infrequent and because forewarning of tsunami arrival is possible, the primary mitigation tactic for public safety is evacuation. Table 4.1 shows the characteristics of different types of natural hazards. The forewarning times for river floods, hurricanes, and storm waves are much longer than the available times for 'local' tsunamis; hence evacuation strategies would be different from tsunami cases. Such forewarning for evacuation is impractical for earthquakes.

Tsunami hazards are often classified into two types: "local" tsunami and "distant" tsunami. Local tsunamis are those generated within 100 km of a locality of interest. In the event of a local tsunami, earthquake ground shaking would precede the tsunami inundation, and the lead-time for tsunami warning would be short, a few minutes to an hour. Note that warning of a local tsunami includes the natural cue (ground shaking). Distant tsunamis are those generated far away (more than 1,000 km) from a locality of interest. Therefore, prior to the tsunami arrival, no ground shaking can be felt. The distant tsunami arrives a few to several hours after the remote-source earthquake. Therefore, systematic and official tsunami warnings are possible for the coastal communities through NOAA's existing tsunami warning systems.

Table 4.1: Characteristics of common natural hazards

Hazards	Time Scale	Typical Pressure Head	Forewarning Time
River Flood	days	3 meters	a few days
Hurricane/Storm Surge	hours	5 meters	several days
Storm-Generated Waves	seconds	10 meters	several days
Tsunami	minutes	10 meters	minutes to hours
Earthquake	seconds	N/A	none to seconds

The possibility of forewarning for tsunamis is distinctly different from earthquake hazards. The primary focus of earthquake mitigation is to prevent buildings and infrastructure from collapse, because a majority of earthquake casualties are due to crushing and/or suffocation by structure collapses. On the other hand, tsunamis kill people by drowning. As stated earlier, the 2011 Tohoku tsunami resulted in 15,893 people dead, 2,556 missing, and 6,151 people injured as of December 9, 2016, (National Police Agency, 2016), with 94.5 percent of the total death count is attributed to drowning; only 1.2 percent of fatalities were caused by the earthquake[5] and the rest were by fires, landslides, and disease. Only 3 percent of the deaths were attributed to extensive injuries incurred during the tsunami, while 97 percent of the deaths occurred during the tsunami. The foregoing statistics are for the 2011 Tohoku tsunami. Although similar statistics are anticipated for a similar extraordinary tsunami event, it should be cautioned that the outcomes could be different for a smaller tsunami or an event that occurs near a sparsely populated area.

Tsunamis are infrequent but forewarning is possible; thus, the primary mitigation tactic is evacuation, and most of the efforts have focused on the development of effective warning systems,

[5] Earthquake-Report online, an independent site, http://earthquake-report.com/2011/10/02/japan-tohoku-earthquake-and-tsunami-catdat-41-report-october-2-2011/

inundation mapping, and tsunami awareness (e.g., the National Tsunami Hazard Mitigation Program, 2005). However, an understanding of tsunami effects on buildings and infrastructure is also important. The provision of safe havens in the form of tsunami evacuation buildings may significantly reduce the loss of life in tsunami-prone communities where residents might not have sufficient time to evacuate to higher ground prior to tsunami arrival. This condition would exist, for example, where people live on a wide coastal plain, a long narrow spit, or areas bounded by rivers or canals. The 2011 Tohoku tsunami clearly demonstrated the effectiveness of tsunami evacuation buildings in saving lives: it is noted, however, that not all of the evacuation buildings provided total protection to the people for this extreme tsunami event (due to insufficient building height or elevation).

Destruction of ‘critical’ coastal structures could cause significant increase in casualties, even if residents were evacuated to safe havens. Such critical coastal structures include, for example, nuclear power plants, oil and liquefied natural gas (LNG) storage and refinery facilities, and oil and LNG tankers at terminal berths. Recall that the 1964 Great Alaskan Tsunami caused huge fires at the oil storage tanks in Seward, Alaska. Many significant fires broke out in Japan because of the 2011 Tohoku tsunami. The worst critical structure incident was the meltdown accident at Fukushima Dai-Ichi Nuclear Power Plant. Another important factor is debris. Destruction of buildings and infrastructure by tsunamis create substantial amounts of debris that enhance the tsunami forces resulting in further destruction of structures by impact force. Debris also blocks critical transportation methods (roads, bridges, railroads, and ports and harbors) causing significant delay of rescue personnel and equipment during recovery and hampering efforts to fight fires.

Tsunami impacts on structures are substantially affected by the surroundings. Figure 4.1 shows the town of Onagawa immediately after the 2011 Tohoku Tsunami (approximately 18 hours after). The pattern of damage suggests that the sturdy waterfront buildings (a pair of brown colored buildings in the photo) must have acted as a barrier for smaller buildings behind them. Video footage shows a strong water jet formation in the gap between the two large forward buildings, which destroyed everything in its path. The presence of the sturdy reinforced concrete buildings altered the tsunami flow, which in turn affected the surroundings. It should be noted that the present state of tsunami modeling is not capable of accurately predicting such local effects.

In summary, tsunami hazard characteristics are unique from other natural hazards such as floods, hurricanes, and earthquakes.

- Tsunami risk areas are limited to narrow strips along the shoreline and tsunami strength is not uniform within the inundation zones. Also, tsunami impacts are substantially affected by local surroundings. Because tsunamis propagate, transoceanic tsunamis can cause significant damage including loss of lives, far away from the earthquake source.
- Because tsunamis are infrequent and because forewarning of these events is possible, the primary public safety mitigation tactic is evacuation. Requirements for short-time effective evacuation resemble evacuation from tornados. (Note that such forewarning is impractical for earthquakes.)
- Most deaths from tsunami are due to drowning and the trauma associated from being in the water. For an extraordinarily giant tsunami event (e.g. the 2004 Indian Ocean Tsunami and the 2011 Tohoku Tsunami), the number of injuries is considerably smaller than the number of fatalities.
- For the sake of simplicity, tsunami-induced fires and landslides are not evaluated in the present methodology development.

Figure 4.1: Tsunami destruction pattern in Onagawa, Japan due to the 2011 Tohoku Tsunami.

Note: A pair of sturdy large buildings at the waterfront (arrows) acted like barriers for some of the weaker buildings behind. The gap between the buildings created a jet flow that destroyed the narrow strip of the jet trajectory, and caused a deep scour hole between them.

Throughout this documentation, we will use the following terminologies to identify various tsunami inundation measures (see Figure 4.2):

A. Maximum runup height *R*: the vertical elevation of the most landward penetration of the tsunami with respect to the initial sea level. The locations of the most landward penetration are denoted by *X* (*x, y*).

B. Maximum inundation height (this is also *R*): the vertical elevation of the flood level at the object within the tsunami inundation with respect to the initial sea level.

C. Maximum inundation depth *H*: the maximum local flow depth with respect to the ground level.

Figure 4.2: Definition sketch (elevation and plan views) for Tsunami Inundation Terminologies

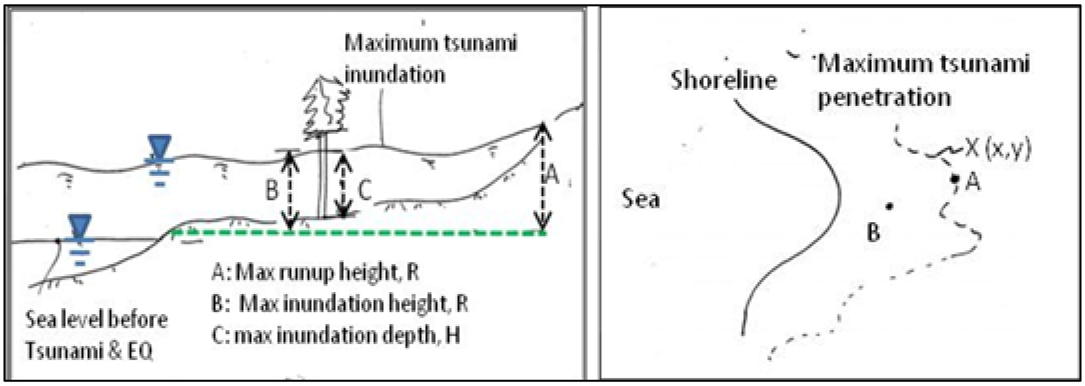

4.3 Description of Tsunami Hydrodynamic Models

Hydrodynamic simulation of tsunamis involves several stages of modeling: 1) tsunami generation, which defines the initial condition; 2) tsunami propagation in the open ocean, continental shelf, and near shore zone; and 3) runup onto the land. Most tsunamis are created by the seafloor deformation caused by co-seismic fault dislocation. Given information on seismic parameters (i.e., earthquake seismic moment, location of the epicenter and the hypocenter, the seismic parameters such as the slip angles: strike, dip, and rake), the resulting seafloor displacement can be calculated based on linear elastic dislocation theory (e.g., Mansinha and Smylie 1971; Okada, 1985).

The prediction of seafloor deformation involves great uncertainties in the seismic parameters as well as inhomogeneity of the seismic fault rupture processes. Typically, the seafloor deformation takes place in a short time and occurs over a large area (approximated 50 ~ 100 km across the fault and 100 ~ 1,000 km along the fault). Because the speed of the fault rupture is much faster (on the order of 1.25 km/sec) than the water-wave speed (~ 0.1 km/sec), tsunami generation can be considered as an instantaneous deformation of the sea surface that is directly translated from the seafloor deformation.

It should be noted, however, that the recent advances in seismic inversion and numerical modeling revealed that the temporal process of the seafloor displacement makes a notable difference in tsunami amplitude (approximately by 20 percent) near the source as in the case of the 2011 Tohoku Tsunami (Takagawa, 2012). Such a large difference may be attributed to the exceptionally deep tsunami source (more than 7,000m deep Japan trench) of the 2011 Tohoku event.

Hydrodynamic simulation for tsunami propagation and runup requires accurate bathymetry and coastal topography data. A typical tsunami wavelength in deep water is on the order of several tens to hundreds of kilometers. Even in a 4,000m deep abyssal plain, the flow induced by tsunami can reach the seafloor; consequently, tsunami propagation and evolution is strongly affected by bottom bathymetry. This is not the case for wind-generated waves, which are typically less than 500m long. Waves having a wavelength less than twice the depth are not affected by the presence of the ocean bottom.

Because of the unique characteristics of tsunamis, analysis requires integrating bathymetry data over the entire ocean basin as well as dry coastal topography information. In other words, the models need data for areas with more than 10,000m deep ocean trenches, 4,000m deep abyssal plains, 200m deep continental shelves, and coastal topography data above sea level.

After a series of tsunami bathymetry-data workshops in Tokyo, Seattle, and Birmingham, UK (Yeh, 1998), bathymetry and coastal topography databases – specifically for tsunami modeling – have been improved significantly by the efforts of NOAA/NGDC (National Geophysical Data Center) and GEBCO (General Bathymetric Chart of the Ocean). The global bathymetry data are now available with a grid size of 1-arc minute: ETOPO-1[6] and GEBCO One Minute Grid[7]. NGDC also developed a 3-arc second coastal relief model for the entire U.S. coast, providing the combined coastal bathymetry and topography data[8]. Note that seamless bathymetry and topography data are critical for inundation modeling. Furthermore**,** NGDC has developed combined near-shore bathymetry and topography data with higher resolution (1-arc-second and 1/3-arc second): NGDC Tsunami Inundation Gridding Project[9]. Those datasets were developed specifically for PMEL's (Pacific Marine Environmental Laboratory) tsunami forecasting modeling effort with the MOST[10] numerical code used for the SIFT[11] operation (see Appendix for more discussion on the SIFT operation).

Required resolution of bathymetry data for tsunami hydrodynamic models depends mainly on the depth. Per the GEBCO Guiding Committee Report 21 (IOC-IHO/GEBCO, 2005), a minimum of 30 grid points per wavelength are needed, as a rule of thumb, for adequate propagation modeling. The same resolution requirement should be applied to resolve the relevant bathymetry features. When the tsunami approaches the shore where the depth is shallow, it may break; then, further refinement of the grid size (say less than 20 m) is required. GEBCO Guiding Committee Report 21 (IOC-IHO/GEBCO, 2005) recommended that the grid spacing for tsunami modeling should be no more than 1 arc-minute (≈ 2 km) in a 4000m deep abyssal plain; 10 arc- second (≈ 300 m) in a 100m deep continental shelf; 3 arc-second (≈ 90m) in 10m deep near-shore waters, and even higher resolution is needed to model flooding and associated velocities accurately.

Although tsunamis contain a wide range of spectral components at the source, most of the energy is contained in the long wave components, and shorter-length (higher frequency) waves are dispersed: note that shorter-length waves propagate slower than the longer ones for gravity-driven waves. For this reason, tsunami propagations are often computed based on the shallow-water-wave theory. The theory comprises the conservation of fluid volume and the conservation of depth-averaged linear momentum with the assumptions of hydrostatic pressure field and uniform horizontal velocities over depth.

---

[6] NOAA National Centers for Environmental Information http://www.ngdc.noaa.gov/mgg/global/global.html

[7] The General Bathymetric Chart of the Oceans (GEBCO) http://www.gebco.net/data_and_products/gridded_bathymetry_data/

[8] NOAA National Centers for Environmental Information http://www.ngdc.noaa.gov/mgg/coastal/coastal.html

[9] NOAA National Centers for Environmental Information http://www.ngdc.noaa.gov/mgg/inundation/

[10] The MOST (Method of Splitting Tsunami) is NOAA's standard numerical simulation code capable of simulating tsunami evolution: earthquake, transoceanic propagation, and inundation of dry land.

[11] SIFT (Short-term Inundation Forecasting for Tsunamis) system is the numerical estimate of amplitude, travel time, and additional tsunami properties using an inundation model constrained by real-time tsunami observations.

Typical formulations of the theory can be expressed respectively as:

$$\frac{\partial h}{\partial t} + \nabla \cdot (h\vec{u}) = 0$$
$$\left(\frac{\partial}{\partial t} + \vec{u} \cdot \nabla\right)\vec{u} + g\nabla h + \gamma \frac{g|\vec{u}|\vec{u}}{h^{4/3}} = g\nabla d$$

Where $\vec{u}$ depth-averaged water velocity, *h* is the water depth, *d* is the water depth from the referenced datum (e.g., the quiescent water level), and γ is the friction coefficient. The resulting model is nondispersive in frequency so that the propagation of wave energy (e.g., the group celerity) is independent of wave number (or wavelength). The use of shallow-water-wave theory can be justified because tsunamis from co-seismic sources are very long (on the order of 100 km or more) and the ocean depth is relatively shallow (on the order of 4 km in the abyssal plain). If the earthquake happened in a depth *h* of 4 km and the generated tsunami wavelength *L* were 100 km, then the measure of frequency dispersion is $\mu^2 = (h/L)^2 = 0.0016$, which is very small and tsunami propagation can be reasonably approximated by the shallow-water-wave theory. In addition, the nonlinearity effect is not prominent for tsunamis propagating in deep oceans. Typically, the tsunami amplitude in ‘deep’ water is less than a meter. For tsunami amplitude, say *a* = 1m in a depth *h* of 4 km, the nonlinearity can be measured by $\varepsilon = a/h = 0.00025$, which is very small. Therefore, linear shallow-water-wave theory with large spatial discretization (say, the grid size being more than 1 minute = 2 km) should work adequately for the propagation computation in deep oceans (Yeh et al., 1996).

When the tsunami reaches the continental slope, a portion of incident tsunami energy could reflect back to the ‘deep’ ocean, depending on how abrupt the depth change is. When the tsunami intrudes onto the continental shelf, the amplitude increases due to the shoaling effect; hence nonlinearity effect (i.e., measured by the ratio of wave amplitude to the depth) becomes important. This is because the tsunami’s kinetic energy (velocity) that is uniformly distributed throughout the ‘deep-water’ depth is squeezed into the shallower depth on the continental shelf, causing the conversion of some portion of kinetic energy to potential energy (wave height).

As the tsunami reaches the continental shelf, the dispersion effect – measured with $\mu^2 = (h/L)^2$ – could become important depending on the length of the incoming tsunami and the width of the continental shelf. When the continental shelf is sufficiently wide in comparison with the tsunami wavelength, a single pulse of the incoming tsunami could be transformed to a series of shorter waves by the dispersion effect. However, when the continental shelf is narrow relative to the incident tsunami wavelength, there is not sufficient time for dispersion to occur and thus the tsunami reaches the shore with little dispersion. In the former case – when the dispersion effect is important – the model based on the Boussinesq approximation (weakly nonlinear and weakly dispersive model) may be appropriate. On the other hand, in the latter case (the narrow continental shelf), it is appropriate to use fully nonlinear shallow-water-wave theory to model the tsunami propagation towards the shore.

When a tsunami approaches the shore and floods inland, friction effects and turbulence become important, and the tsunami motion becomes intrinsically nonlinear. The model also needs to consider natural and artificial configurations, i.e., buildings, trees, mounds, roads, etc. When the detailed effect of tsunami forces on structures is the focus, then more sophisticated numerical models (e.g., based on 3-D Navier-Stokes – perhaps turbulence – model) may need to be implemented. When the maximum runup is a focus, then such natural and manmade obstacles could be parameterized, for example by assigning proper friction factor values.

The foregoing descriptions of hydrodynamic modeling of tsunami generation, propagation, and runup evidently demonstrate that the problem is complex and multi-scale. It is complex because it involves multi-phase (water, air, solid) interactions in a three-dimensional real-world domain where some fundamentals (e.g., turbulence) remain unsolved. It is multi-scale because the length scale of tsunamis in the ocean is on the order of hundreds of kilometers, while the effects of inundation phenomena must be described at scales of a few meters or less. Hence, at present, even the best tsunami modeling yields substantial errors in prediction, and there is much room for improvement in every aspect of the modeling.

4.4 Tsunami Hazard Analysis

Tsunami Hazard Analysis produces the necessary physical tsunami conditions for a coastal community of interest. The role of Tsunami Hazard Analysis is shown in the overall flow chart in Figure 4.3 (note that for distant events, the earthquake components can be bypassed).

Figure 4.3: Flow chart of tsunami loss estimation methodology

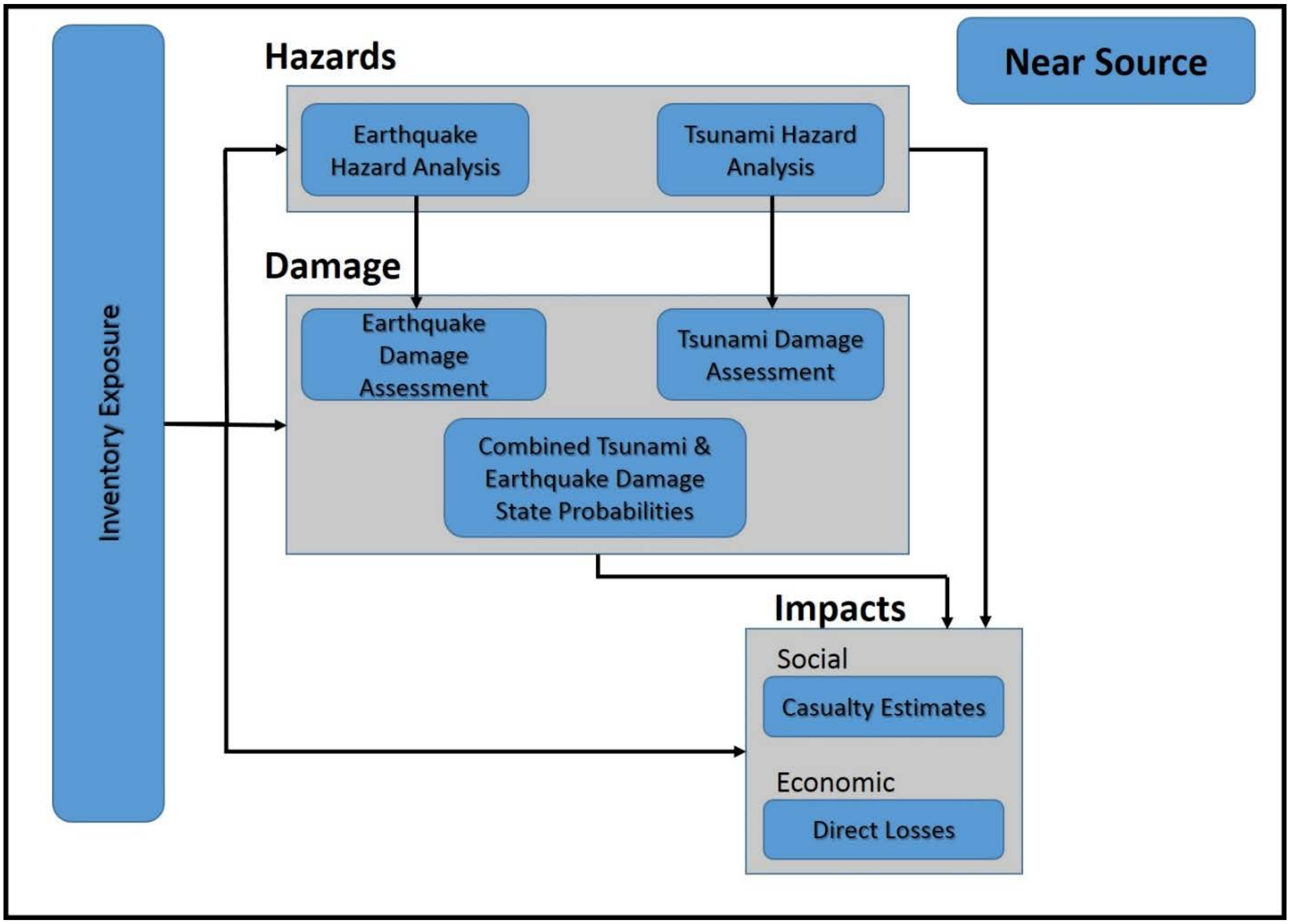

Prediction of tsunami hazard is a formidable task because of the uncertainty involved in the tsunami generation mechanism, ocean bathymetry, and most importantly the occurrence of a tsunamigenic earthquake itself. Given these uncertainties, probabilistic methods rather than deterministic methods are typically used to analyze tsunami hazards. The analysis is an extension of the existing methodology for probabilistic seismic hazard analysis, and involves identifying all possible tsunami sources that could affect a coastal community of interest: see Geist and Parsons (2006). Probabilistic tsunami hazard analysis requires combining tsunami hydrodynamic simulations with the analysis in the field of probabilistic seismic hazard assessment. The resulting database of tsunami simulations is subjected to a statistical analysis that provides the recurrence estimates for tsunami amplitudes that exceed given values.

González et al. (2009) made a detailed probabilistic tsunami hazard assessment for the coastal town of Seaside, Oregon. They used 15 seismic tsunami sources in five Pacific subduction zones: 14 of them are the distant-source events and one is the local-source (Cascadia) event. Each of the seismic events is described with a Poisson distribution model with its recurrence interval. Tsunami inundation in Seaside is then numerically computed for each seismic event. Combining all the events and performing the statistical analysis yields a "hazard curve" i.e., the cumulative distribution function of the exceedance amplitude vs. the annual exceedance probability: see Figure 4.4. A similar methodology was introduced by PG&E (2010) including tsunami events triggered by landslides. Instead of González et al.'s Poissonian model, PG&E assumed that tsunami wave heights are lognormally distributed. Again, the end results are a "hazard curve."

Probabilistic tsunami hazard analysis involves significant computational effort, even for the analysis of one specific coastal community. The analysis itself contains substantial uncertainty because of the lack of sufficient samples (data) to form a proper probability space (see any elementary probability textbook for the concept of a probability space). The most important point to recognize is that the probability is originated from the seismic events that generate tsunamis, while the computation of tsunami propagation and runup itself is deterministic. Considering this, we incorporate probabilistic elements in physical tsunami inundation as a given input parameter to the tsunami hazard analysis. In other words, the users could specify the input tsunami conditions with a given probability, and the probability is evaluated independently of the Hazus methodology. It is anticipated that a systematic probabilistic tsunami database will be developed and become available in the future: for example, PEER (Pacific Earthquake Engineering Research Institute) is currently developing such a database at [http://peer.berkeley.edu/tsunami/.](http://peer.berkeley.edu/tsunami/) The present Hazus methodology developed herein is designed to enable linking with such a forthcoming database.

Figure 4.4: Hazard curve for a representative location offshore Seaside, Oregon (after Gonzalez et al, 2009)

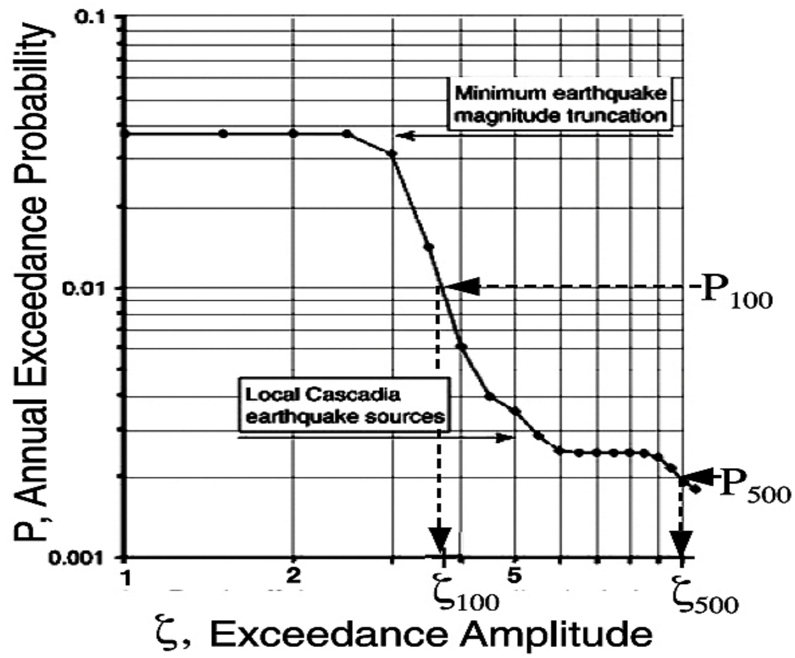

4.5 Input Requirement and Output Information

The Input / Output structure for hazard analysis is depicted in Figure 4.5. The input data and information needed for Tsunami Hazard Analysis identify geographical, geophysical, and seismological conditions for a specified tsunami event. More specifically, the users are asked to provide the following as the input data:

For *Level 1*, input is an expected tsunami runup height *R* for the coastal community, which can be a single measurement for a “quick-look” assessment or can be the runup height as a grid across a region. With a Level 1 analysis, the estimation of velocity is based on an empirical equation that utilizes the maximum runup height and the topography (DEM) as described in Section 4.6. For near-source events, the deformed (post-event) DEM should be used. The location of the tsunami source may be selected from a map of potential tsunami sources provided in the inventory data as shown in Figure 4.6. Note that the height *R* can be the outcome from probabilistic tsunami hazard analysis performed elsewhere. In practice, the tsunami runup height can be the height at the maximum tsunami penetration found in the tsunami inundation/evacuation map for the community (refer to Fig. 4.2). For example, Figure 4.7 shows the inundation map of Cannon Beach, Oregon, that provides two different inundation zones: one for local tsunamis and the other for distant tsunamis. Also shown is the inundation map with a variety of possibilities. Although users can select any runup height *R* and are not constrained by those found in the inundation maps, the runup height *R* could be selected at the maximum elevation within the inundation zone shown in the map. However, the user should define their region based on where the runup height *R* could be reasonably applied. Applying the maximum runup throughout a large study region would result in erroneously high losses.

For *Level 2*, the inputs are grids of the maximum flood depth and maximum velocity. This information can be also probabilistic with the return interval. As discussed in Section 4.8, this methodology is tied closely to the existing NOAA’s SIFT prediction model. Hazus will reduce these inputs to medians as described in Section 4.7 and calculate Momentum Flux by squaring velocity and multiplying by depth.

For *Level 3*, the inputs are grids of Median Inundation Depth (feet) and Median Momentum Flux (ft^3sec^2) directly from the user and no Tsunami Hazard Analysis for damage assessment is performed by Hazus.

Regardless of the level of input, Hazus building damage and loss (Chapter 5) requires both the Median Inundation Depth (feet) (H) for the estimation of nonstructural and content losses, and Median Momentum Flux (ft^3sec^2) (HV^2) for the estimation of structural losses as shown in Figure 4.5.

Figure 4.5: Tsunami Hazard Analysis Input Requirements and Output

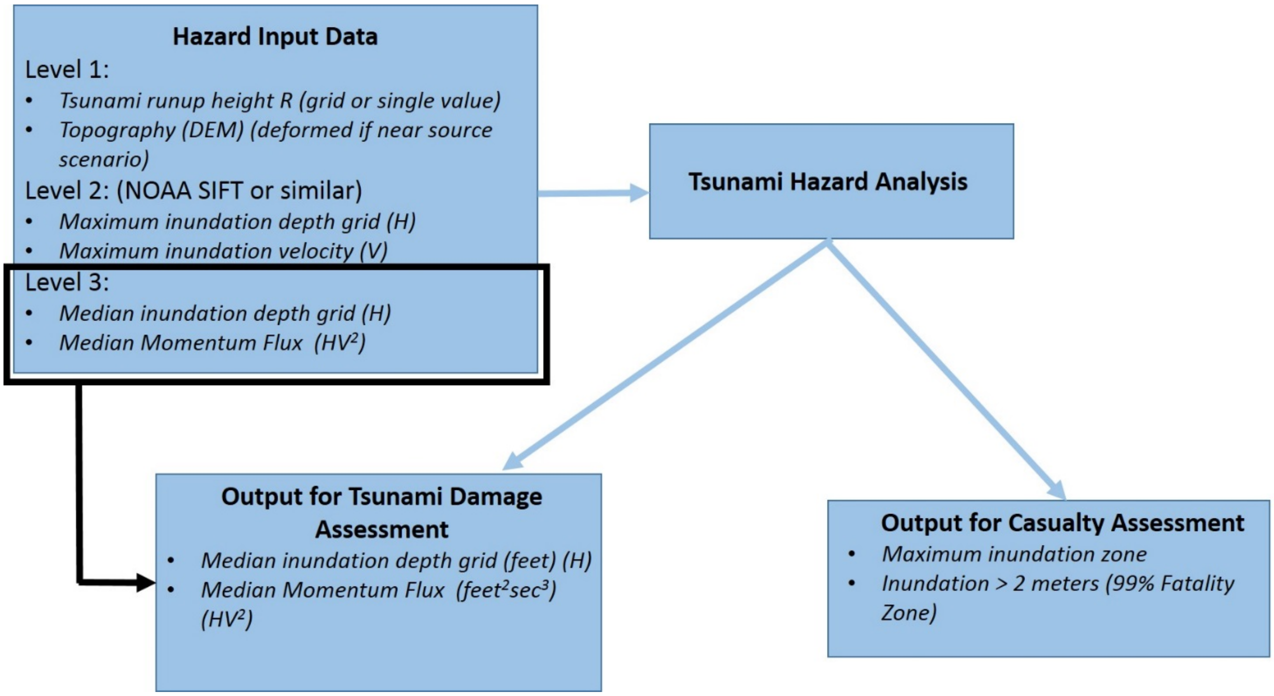

Pre-prepared Data:

- The digital elevation model (or DEM) (*x, y, z*) is required for Level 1 and should consist of the modeled post-event (deformed) topography in the case of near-source events. These are modeled deformations, and can result in several meters of DEM deformation and substantially change the inundation area and potential losses.
- SIFT and other tsunami models have frequently pre-run libraries of scenarios associated with known potential tsunami sources (Figure 4.6).
- For assessing combined earthquake and tsunami losses, it is important to ensure the same source parameters are used for the earthquake loss modeling, as was used to design the tsunami scenario. The Hazus Earthquake Technical and User Guidance manuals outline the source parameter input required for earthquake loss modeling.

Output Data:

Output from Tsunami Hazard Analysis must fulfill the needs for "Tsunami Damage Assessment" and "Casualty Estimates and Debris." These outputs consist of:

- Median of maximum inundation depth H at the structures of interest.
- Median of maximum specific force or momentum flux HV^2 at the structures of interest.

The following outputs are provided by the tsunami hazard analysis or are provided by the user-fed into the Tsunami Impact module, which calculates casualties (see Chapter 6):

- Maximum inundation locations X(x,y) (depth > 0, along the maximum runup contour line)

- Fatality boundary, where depth is greater than 2 meters and fatality rate is modeled as 99 percent
- Arrival time of the leading tsunami, T_0
- Time of max runup, T_{max}
- Time of maximum recession, T_1 (required for future Debris Model)

Note that tsunamis often approach the coast as a series of inundating waves. Therefore, the times of maximum runup and maximum recession may not necessarily occur at the first tsunami inundation. The maximum runup may result from the second, third, or later tsunami inundation, and the maximum recession may not occur in the excursion associated with the maximum runup.

Because the present methodologies of the tsunami loss estimation do not adopt an agent-based modeling for evacuation simulation (see Chapter 6), it is necessary to assume, for the sake of simplicity and conservation, that the times of maximum runup and maximum recession happen at the first tsunami inundation excursion.

Figure 4.6: Locations of potential tsunami source

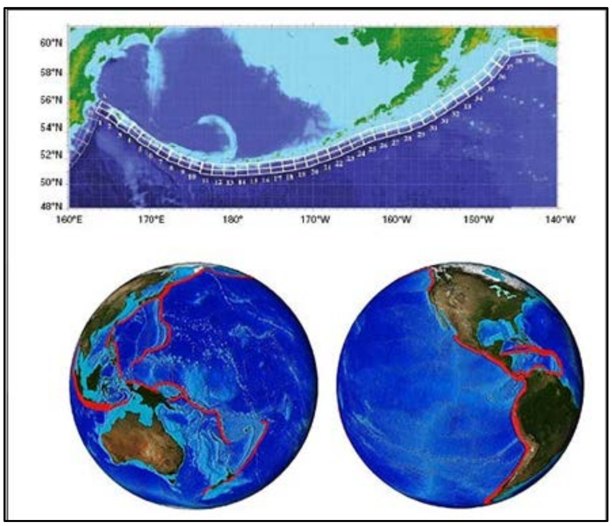

Figure 4.7: A tsunami evacuation map for the town of Cannon Beach, Oregon. (Left: two scenarios, distant and local events. Right: inundation map with inundation zones for distant and local tsunamis.

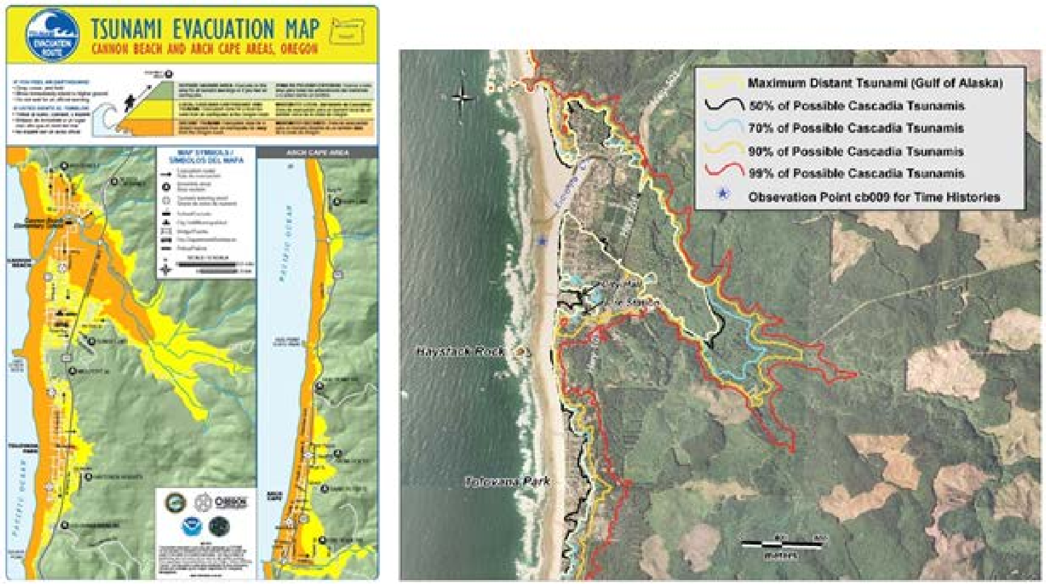

4.6 Estimates without the use of Numerical Model (Level 1 Methodology)

Tsunami Hazard Analysis for Level 1 provides the methodology without the use of numerical simulation model. This provision is necessary because not all areas have both runup height and velocity hazard data required for the Tsunami Damage Loss Model. Hazard data are available from NOAA, as well as State sources:

- Alaska Division of Geological & Geophysical Surveys
- California Geological Survey, California Emergency Management Agency
- University of Hawaii
- Oregon Department of Geology and Mineral Industries
- Washington Department of Natural Resources

NOAA's Forecast Inundation Models have not covered all the U.S. coastal communities: the models are currently available for 75 communities at the NOAA Center for Tsunami Research (http://nctr.pmel.noaa.gov/tsunami-forecast.html). For any of the 75 communities included in the NOAA inundation models, a Level 2 analysis is highly preferred, and the Level 1 methodology at these locations should be used for educational and comparative purposes only. For a given earthquake location, the tsunami arrival time T_0 to a community of interest from the time of earthquake is estimated by:

$$T_0 = \int_l (gh)^{-1/2}\, dl \qquad (4.3)$$

where *h* is the water depth along the propagation path *l* from the tsunami source to the community. Note that travel time maps based on calculated travel times to communities from any ocean location are provided online by the NOAA Centers for Environmental Information (https://maps.ngdc.noaa.gov/viewers/ttt_coastal_locations/).

For a tsunami height *R* given as input, the maximum inundation depths *H* can be estimated by:

$$H(x, y) = R - z(x, y) \tag{4.4}$$

where *z* is the ground elevation at a given location (*x*, *y*) in the community, and the maximum inundation location *X* (*x*, *y*) can be determined along the contour where *z* = *R.*

The Hazus Tsunami Model utilizes raster math, specifically ArcGIS's Spatial Analyst Extension Raster Calculator Geoprocessing tool, to subtract the ground elevation (*z*) DEM from the grid that represent the runup heights (*R*).

Estimating Velocity from Runup (Level 1): It is common that users will have estimated runup depths or heights from tsunami hazard models, evacuation studies, or actual events and ***not*** velocity. Velocity and more specifically Momentum Flux (HV^2) is a required input parameter for all structural losses, while contents and nonstructural losses are based on depth only. The FEMA 2013 methodology proposed an empirical relationship between runup and velocity be used to produce and estimate momentum flux that was available in FEMA P-646: Guidelines for Design of Structures for Vertical Evacuation from Tsunamis.

$$u = fv\sqrt{2gR\left(1 - \frac{z}{R}\right)} \tag{4.5}$$

where f_V is a reduction factor. The reduction factor is needed because Equation 4.5 yields an over- conservative value. The formula is analytic for the runup of a bore (a broken wave of an infinite wavelength propagating into quiescent water) onto a frictionless uniformly sloping beach. Therefore, the runup process results in perfect conversion of the kinetic energy to potential energy (e.g., Ho and Meyer, 1962).

According to laboratory experiments by Yeh et al. (1989), the reduction factor f_V should be less than 0.7. The factor f_V is further adjusted based on the ground roughness in the inundation zone. Analyzing video footage, Fritz et al. (2012) reported the flow speeds near the shoreline of the town of Kesennuma during the 2011 Tohoku Tsunami. They found max $V \approx 6$ m/sec where the maximum runup $R \approx 9$ m. Koshimura (2011) also reported similar data for the town of Onagawa: max $V \approx 7.5$ m/sec where the maximum runup $R \approx 18$ m. Based on these limited data, we use the factor $f_V \approx 0.5$ for the present methodology development: Figure 4.8 demonstrates that factor f_V =0.5 reproduces approximately the flow conditions recorded in Kesennuma and Onagawa.

Figure 4.8: The relation of maximum flow speed Max *V* at the shoreline (z=0) with the maximum runup height *R* based on Equation 4.4 with f_V=0.5

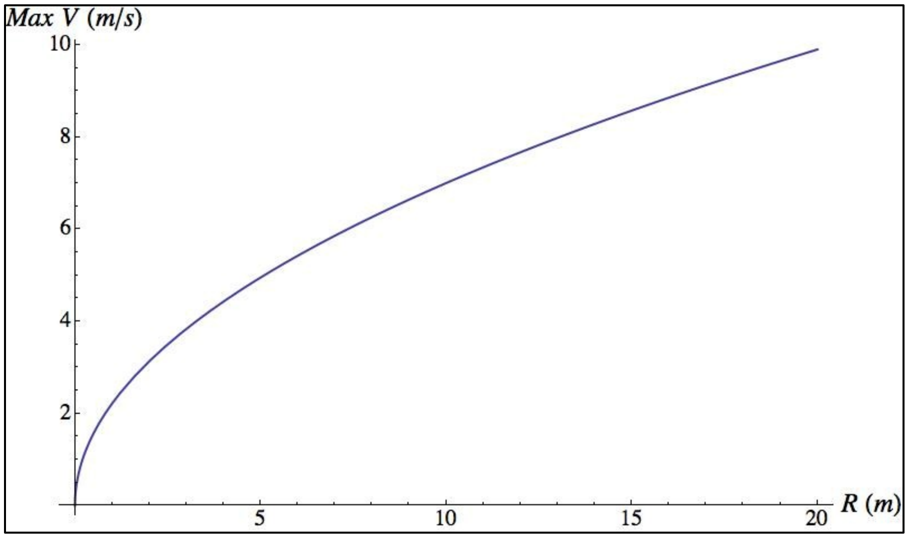

It appears the value of f_V depends not only on the roughness of the runup surface (including the effects of macro roughness such as buildings etc.) but also depends on the ground slope as well as the tsunami source. For a distant tsunami, the waveform tends to become very long: hence the tsunami runup motion is likely a gradual increase in water level (meaning a small value of f_V). On the other hand, a local tsunami often (but not always) creates a leading depression wave that leads to formation of a bore near the shore (Yeh, 2009). Therefore, a relatively large value of f_V can be expected.

However, based on the evaluation in Section 4.6 and new work being done in support of ASCE-7, Harry Yeh, personal communication (2016) recommended the use of a newer ASCE-7 equation, currently proposed for incorporation into tsunami building codes and modifying it to use the maximum runup (*Ra*). Runup is provided by the users runup grid or by the user provided maximum runup value associated with the Level 1 Quick Look feature.

$$u = 0.85\sqrt{gH\left(1 - \frac{z}{Ra}\right)} \qquad (4.6)$$

Where: 0.85 is based on analysis by Patrick Lynette for ASCE, recommended by Ian Robertson, personal communication, 2016, for loss modeling, over 1.0 for tsunami surge and 1.3 for tsunami bore, since both the latter are biased high to ensure conservative design per ASCE 7-16

g = 32.174 ft/s2

H is the depth, in feet, at site of interest

z is surface elevation, in feet, from the DEM at site of interest

R_a is using the maximum runup, in feet, above MSL from each case study grid

Modify H and HV² Maximums to Median Values: The Hazus Tsunami building damage functions are based on median rather than maximum depth and momentum flux values. Following the approach used for the Energy Grade Line Analysis described in Section 4.7, which produces h_{max}, the maximum flow depth, and u_{max}, the maximum flow velocity, at any point along the flow transect for the ASCE 7-16 design provisions, medians are estimated as 2/3 $h_{max}(u_{max})^2$, or 2/3 of the momentum flux assuming both h_{max} and u_{max} occur together and are used to estimate the median flux and depth. The selection of $2/3h_{max}$ to correspond to u_{max} for ASCE was based on numerical modeling and analysis of survivor videos from the Tohoku Tsunami.

Based on the integration of the ASCE methodologies, the sequence of Level 1 computations is summarized in Figure 4.9.

Figure 4.9: Flowchart for Level 1 methodology

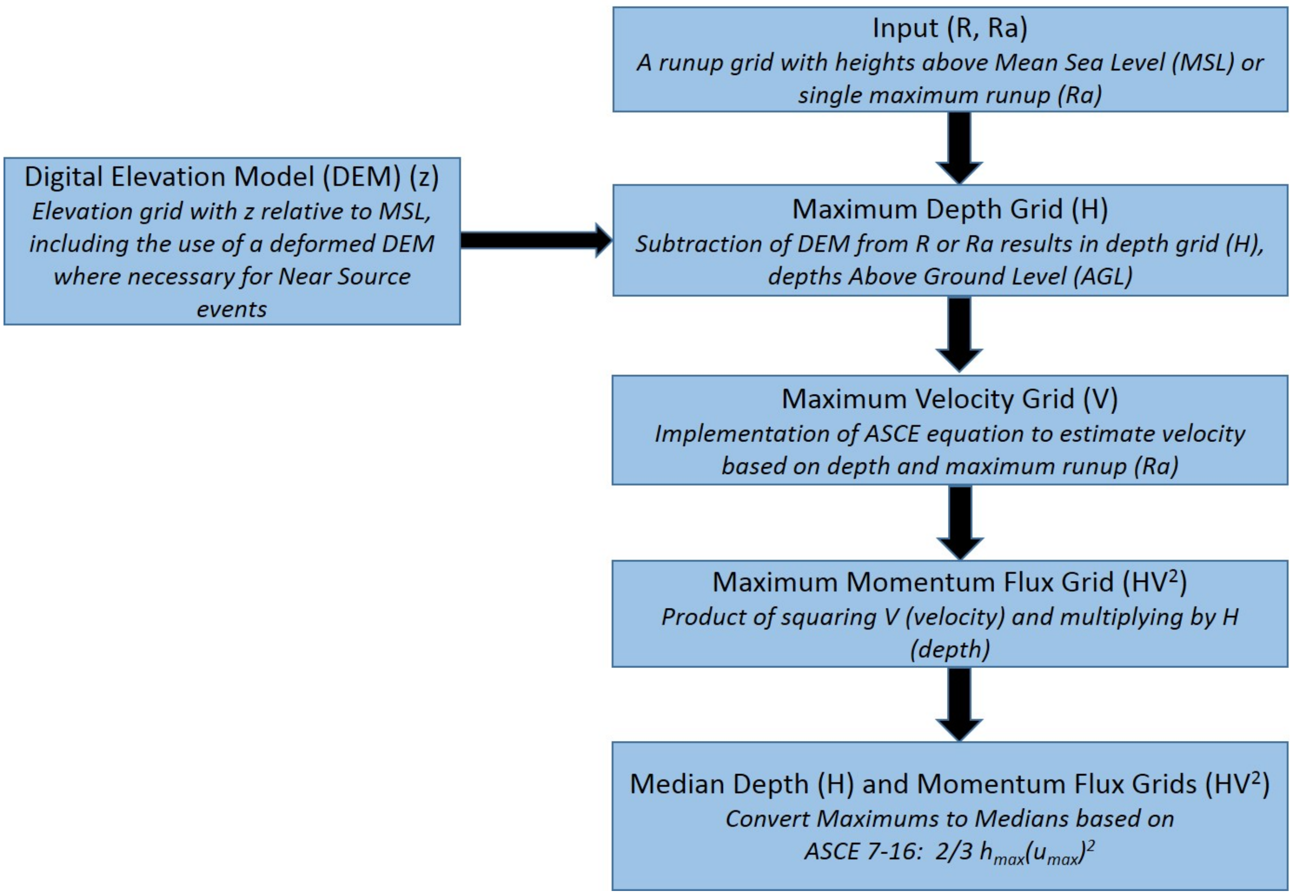

4.7 Evaluation of FEMA P-646 and ASCE Approaches

The FEMA 2013 methodology proposed use of the empirical relationship between runup and velocity that was available in FEMA P-646: Guidelines for Design of Structures for Vertical Evacuation from Tsunamis. To implement the empirical relationship, a reduction factor (*fv*) is used in the equation to prevent overestimation of velocity by reducing flow based on surface roughness and other available factors.

The 2013 methodology further suggests a *fv* value commonly measured in the lab of 0.7 and that two observations during the 2011 Sendai Japan tsunami suggest a value of 0.5 for *fv*. The methodology describes the need to develop a lookup table to assist in assigning this value, however, such values are currently not available. Since the velocity once converted from runup with the empirical equation is squared and then multiplied by depth to estimate the Momentum Flux to be applied to estimate building Damage States, the difference in Damage State and associated losses just by varying between the two values (0.7 and 0.5) suggested in the methodology can almost double the Momentum Flux (Figure 4.10).

Figure 4.10: Influence of *fv* on Momentum Flux

Example Input Runup (ft) (z=5)	Equation 4.4 **(fv=0.5)** Velocity (ft/sec)	Momentum Flux HV2 (ft3/sec2)
15	12.68	1,608.70
16	13.30	1,946.53
17	13.89	2,316.53
18	14.46	2,718.70
19	15.01	3,153.05
20	15.53	3,619.58

Example Input Runup (ft) (z=5)	Equation 4.4 **(fv=0.7)** Velocity (ft/sec)	Momentum Flux HV2 (ft3/sec2)
15	17.76	3,153.05
16	18.62	3,815.19
17	19.45	4,540.39
18	20.25	5,328.66
19	21.01	6,179.98
20	21.75	7,094.37

American Society of Civil Engineers (ASCE) Energy Grade Line Analysis (EGLA):

ASCE also recognized the need to relate runup to velocity and the gap in the available methodologies and developed the EGLA as a method to support new “Tsunami Loads and Effects Design Standards for the United States” (ASCE 7, Chapter 21 and 22) (Chock, 2016). This method recognizes the decay of energy and velocity with distance from the shoreline, as well as the influence of the ground profile (Figure 4.11).

Figure 4.11: ASCE Energy Grade Line Analysis Approach

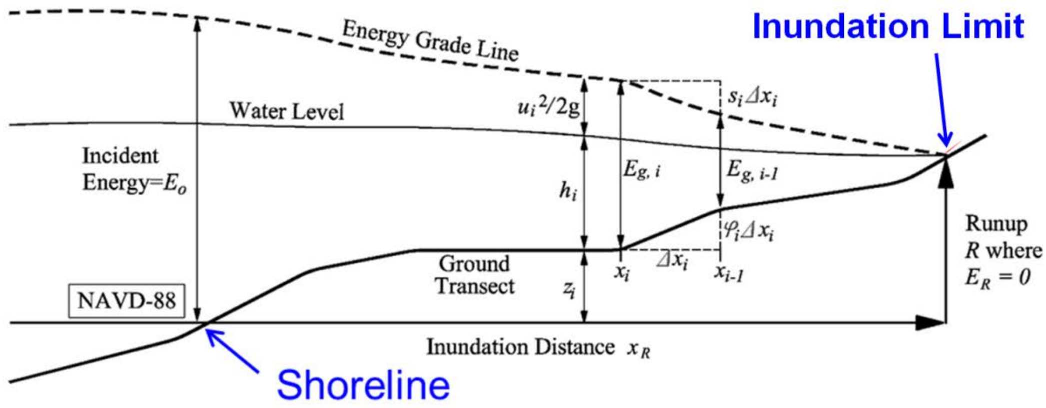

The EGLA methodology has the potential to provide a grid with a range of all possible depths and velocities at each grid based only on the Runup Inundation Limit (Figure 4.12).

Figure 4.12: The EGLA methodology potential grid approach

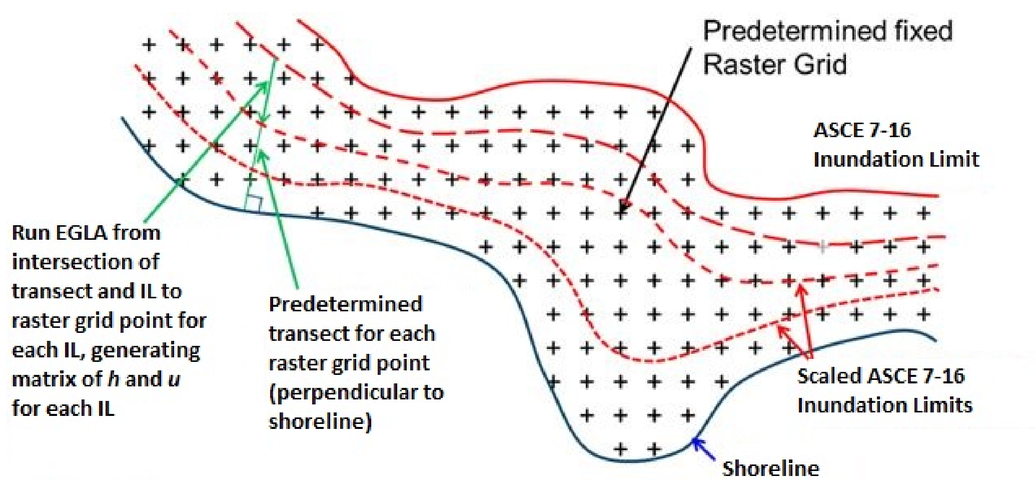

This approach has the benefit of aligning with the Building Code methodology, as well as the ability to reduce the required user input to only the Inundation Limit. However, since the data to support an EGLA grid approach is not yet available, this approach is currently limited to integration in the Level 2 hazard input methodology.

Evaluation of Level 1 Methods to Estimate Velocity from Inundation Grids: Based on the findings from above concerning the P646 method and new work being done in support of ASCE-7, testing of the ASCE-7 equation, modifying it to use the maximum runup (Ra) provided by the users runup grid, was performed. This evaluation summarizes the results comparing the two estimation methods for tsunami velocity against a numerical simulation of tsunami velocity provided by NOAA's SIFT model for five Case Study communities. These empirical equations are intended to provide the capability for Hazus to model potential structural losses when only runup (Level 1) data are available. Numerical modeling provided by SIFT and other tools provides a far more detailed assessment of tsunami velocity for Hazus Level 2 and 3 assessments. Implementing the two equations in ArcGIS's Raster Calculator GeoProcessing tool based on the SIFT grid for the community of Westport, WA based on the Cascadia "L1" scenario:

ASCE Example for Westport: 0.85*SquareRoot(32.174 * "wes_maxdg_ft" * (1 - ("wes_dem_ft" / 71.2847))) (4.7)

P646 Example for Westport: 0.5*SquareRoot(2*32.174 * "wes_maxR_ft" * (1 - ("wes_dem_ft" / 71.2847))) (4.8)

Where:

wes_maxdg_ft is the maximum flow depth grid Above Ground Level (AGL) provided by the SIFT model
wes_maxR_ft is the maximum runup grid relative to Mean Sea Level (MSL) provided by the SIFT model
wes_dem_ft is the deformed post-event topography grid provided by the SIFT model
71.2847 is the maximum runup elevation (Ra) provided by the SIFT model

The SIFT model velocity grid for Westport, WA based on the Cascadia L1 scenario is illustrated in Figure 4.13.

Figure 4.13: SIFT model velocity grid for the Cascadia L1 scenario for Westport, WA

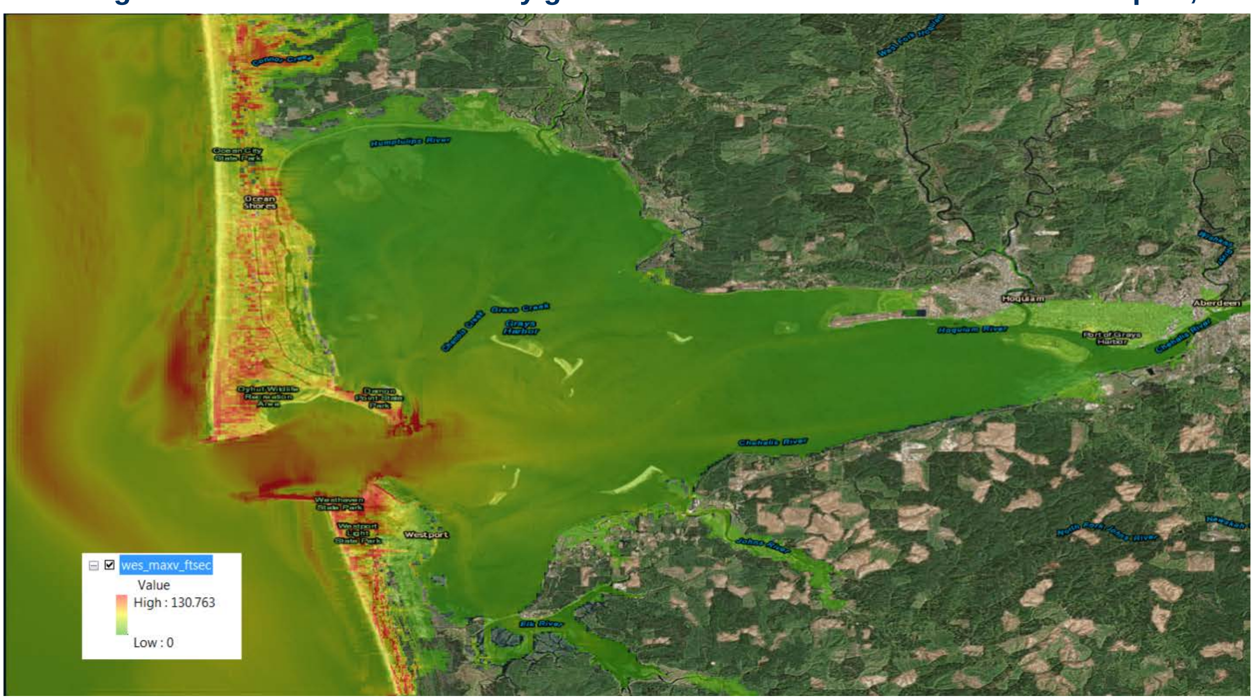

Neither velocity grid estimation method can reflect the detail provided through velocity modeling, however, the velocity grids estimated using the empirical equations are intended to approximate the values providing a Level 1 capability. This will provide loss estimation capability in areas where only the runup information are available. The velocity grid based on the ASCE equation for the Cascadia L1 scenario for Westport, WA is illustrated in Figure 4.14.

Figure 4.14: Velocity grid based on the ASCE equation for the Cascadia L1 scenario for Westport, WA

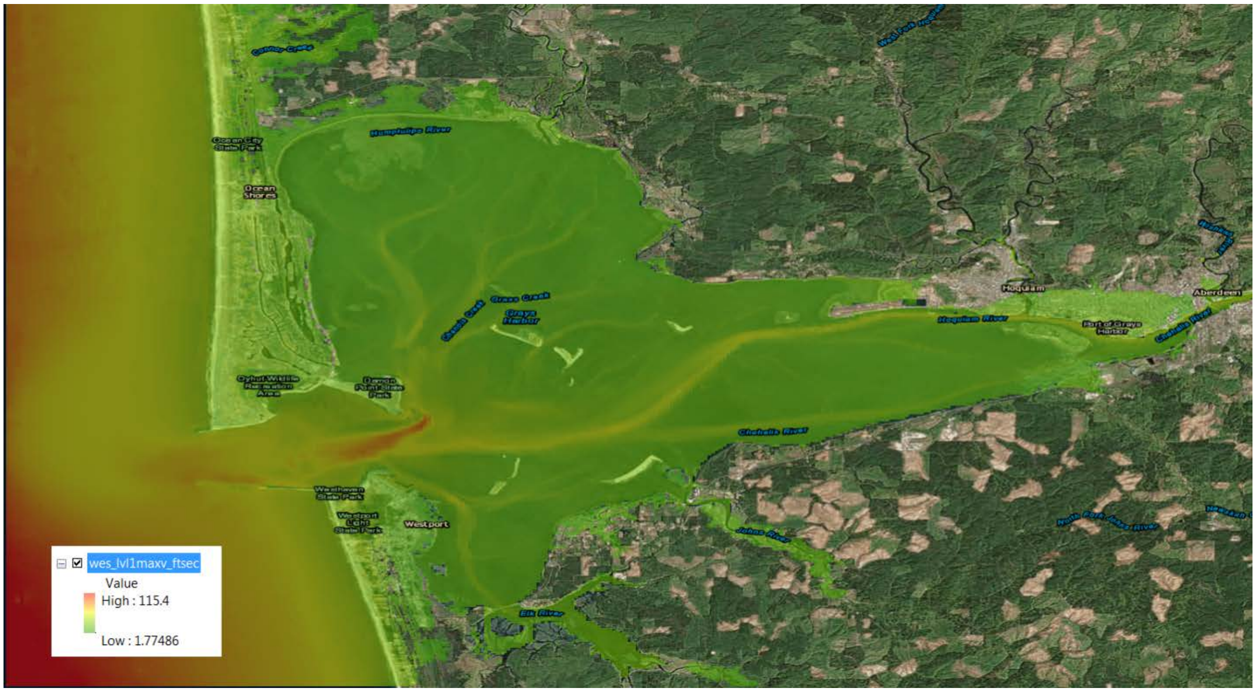

Table 4.2 summarizes the results associated with the two Level 1 equations when comparing with the SIFT output. Difference grids were produced by subtracting the SIFT model maximum velocities from those produced using the ASCE and P646 equations. Further, these grids were masked to include only the on-land inundation areas where the Hazus modeled losses will occur. The cells with italics highlight which of the methods showed the best agreement. A mean of 0 represents good overall agreement, while negatives represent an underestimation of the Level 1 approach as compared to the SIFT model products.

Table 4.2: Results associated with the two Level 1 equations when comparing to SIFT output

ASCE Method		SIFT	ASCE	Difference Grid – Inundation Area (ASCE Lvl1 minus SIFT)			
Case Study	**Rmax (feet)**	**Vmax (ft/sec)**	**Lvl1 Vmax (ft/sec)**	**Mean (ft/sec)**	**Std Dev (ft/sec)**	**Max (ft/sec)**	**Min (ft/sec)**
Kahului, HI	20.6691	22.5277	*20.4363*	*2.53*	3.59	15.11	-16.52
Crescent City, CA	64.3254	42.0679	*36.0605*	*-0.19*	*5.37*	26.86	-25.96
Garibaldi, OR	50.4182	41.3166	*31.5*	*3*	8.56	27.87	-25.46
Homer, AK	10.8768	14.4897	*14.0235*	*7.3*	3.1	12.75	-3.78
Westport, WA	71.2847	99.1494	*37.5062*	*0.23*	*8.43*	34.32	-74.05

P46 Equation Method fv=0.5		SIFT	P646	Difference Grid – Inundation Area (P646 Lvl1 minus SIFT)			
Case Study	**Rmax (feet)**	**Vmax (ft/sec)**	**Lvl Vmax (ft/sec)**	**Mean (ft/sec)**	**Std Dev (ft/sec)**	**Max (ft/sec)**	**Min (ft/sec)**
Kahului, HI	20.6691	22.5277	17.1825	4.86	*2.8*	12.6	-12.43
Crescent City, CA	64.3254	42.0679	30.4499	2.75	6.3	26.48	-24.2
Garibaldi, OR	50.4182	41.3166	26.2744	3.84	*7.65*	22.63	-27.41
Homer, AK	10.8768	14.4897	12.3227	7.31	*1.82*	10.59	-4.5
Westport, WA	71.2847	99.1494	31.3574	1.77	8.39	28.58	-75.76

Figure 4.15 and 4.16 below provide both the Histogram and map illustrating the Difference Grids for the Westport, WA community case study area. Negatives reflect velocity values that are lower in Level 1 approach as compared to SIFT. Agreement appears primarily controlled by depth, where depths are greater, Level 1 techniques overestimate compared to SIFT and where depths are shallow the Level 1 empirical approaches tend to underestimate velocities.

Figure 4.15: Difference Grid Histogram – Westport, WA

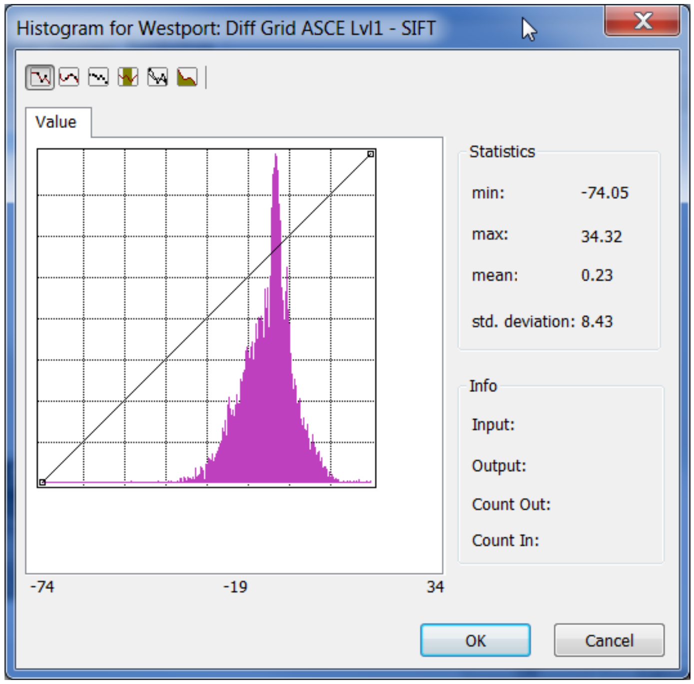

Figure 4.16: Difference Grid Map – Westport, WA

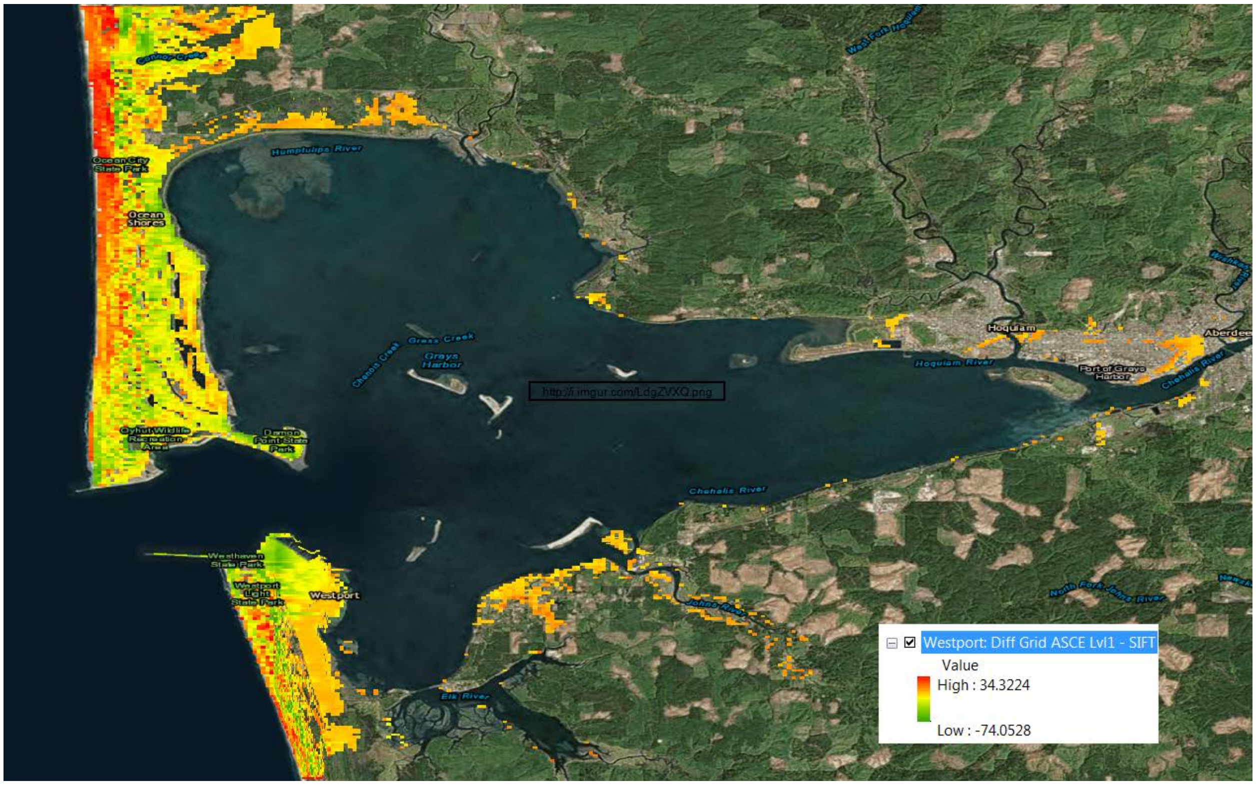

Overall the ASCE method produced maximum velocity values closer to the numeric modeling grid for all scenarios. ASCE also showed better overall agreement for the scenarios with the largest runups and greatest depths (Westport Rmax = 71’ and Crescent City Rmax = 64’). This is especially important since creation of the momentum flux grid requires multiplying these values by depth, amplifying any uncertainty in velocity.

4.8 Numerical Simulation Models (Level 2 and 3 Methodology)

A numerical model is used to obtain the best estimates of the output information and data. Numerical simulations involve modeling the tsunami source, propagation, and runup. There are several numerical codes available for tsunami simulations. Some of the codes are capable of simulating tsunamis in the entire process from earthquake source to runup. For example:

- COMCOT is a model based on nonlinear shallow-water-wave theory (Liu et al., 1994)
- NEOWAVE is a non-hydrostatic model (Yamazaki et al., 2010)
- MOST is based on nonlinear shallow-water-wave theory (NOAA/PMEL’s code)
- SELFE uses a semi-implicit finite-element Eulerian-Lagrangian algorithm (Zhang and Baptista, 2008)
- GeoCLAW is based on a finite volume method with adaptive grid refinement (LeVeque and George, 2007)

Among the available simulation codes, NOAA's SIFT (Short-term Inundation Forecasting for Tsunamis: Gica et al., 2008) appears the most widely available for Level 2 applications since it provides both depth and velocity grids. More importantly, NOAA has already prepared tsunami inundation models – called Forecast Inundation Models – specifically designed and developed for each of the 75 U.S. coastal communities shown in Figure 4.17. NOAA's SIFT operation produces very rapid tsunami predictions with optimized local tsunami runup models: the details of SIFT are described in Section 4.8. With the cooperation of NOAA, Hazus directly utilizes NOAA's SIFT functionality for the *Level 2* methodology, available from the 75 U.S. coastal communities supported under the SIFT program. However, the Level 2 methodology allows the integration of maximum depth and maximum velocity grids from other numeric models. For *Level 3*, the user can decide to use their own and more sophisticated, numerical models providing both median depth and median momentum flux inputs. To date, only Oregon has these files readily available online from Oregon Department of Geology and Mineral Industries (DOGAMI) Open File Reports (http://www.oregongeology.org/pubs/ofr/p-O-13-13.htm).

Figure 4.17: Location and development status of forecast inundation models

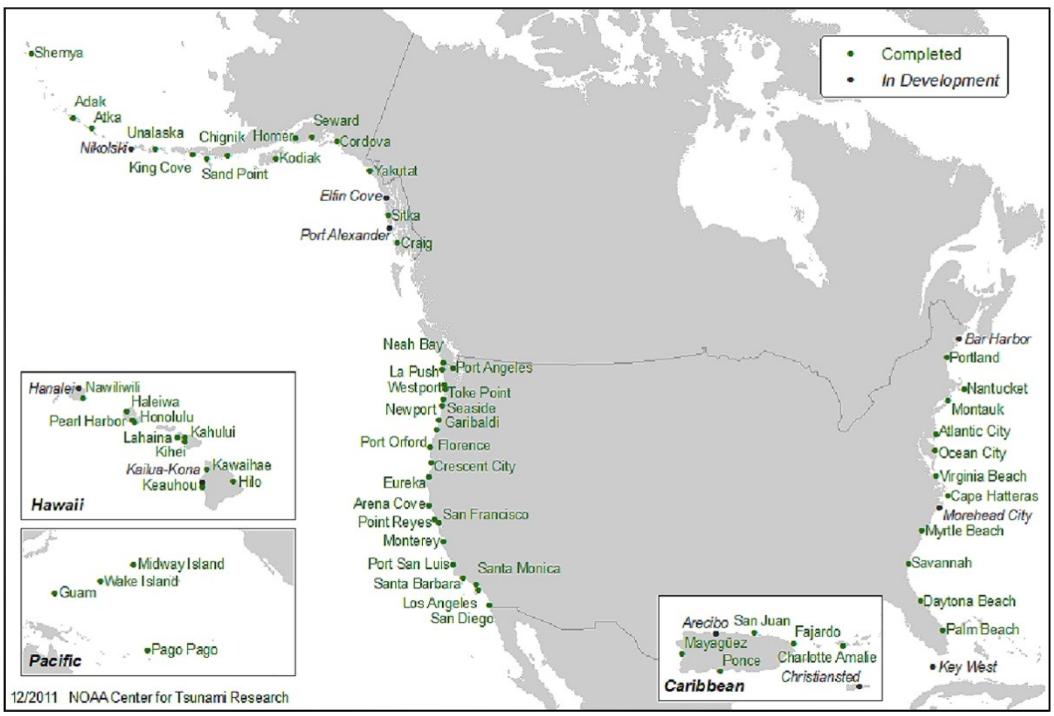

4.9 NOAA's Short-term Inundation Forecasting for Tsunamis (SIFT)

At the NOAA Center for Tsunami Research (NCTR), the standard numerical model for tsunami propagation and runup is called MOST (Method of Splitting Tsunami). The code is based on nonlinear shallow-water-wave theory: see Equation 4.9. In MOST, the spatial dimensions are split so that the original 2D problem is reduced to a sequence of 1-D problems. The resulting formulations are then re-arranged to solve in terms of the Riemann invariants (*r* and *s*) and the eigenvalues λ_r and λ_s:

$$r = u + 2\sqrt{gh};\ s = u - 2\sqrt{gh} \tag{4.9}$$

$$\lambda_{r,s} = u \pm \sqrt{gh} \tag{4.10}$$

This procedure is an application of the classic analytic solution algorithm for a nonlinear hyperbolic equation called the method of characteristics. The numerical code MOST also selects the grid sizes and the time increments so that the physical wave dispersion effects can be modeled utilizing the numerical dispersion that is inherent in the finite difference scheme. MOST can simulate the entire tsunami processes: generation by earthquake, transoceanic propagation, and inundation of dry land.

NOAA has established a comprehensive and efficient system to estimate tsunami inundation, flow velocities, and arrival times for given earthquake information. NOAA called this operation SIFT (Short-term Inundation Forecasting for Tsunamis), which is designed to support a rapid tsunami warning system for the U.S. coasts, and MOST is the foundation for NOAA's SIFT operation. The following is a brief description of SIFT.

With the use of MOST, NOAA had developed what it calls a "propagation database," which is a collection of pre-computed propagation model runs in which tsunamis are generated from selected locations along known and potential earthquake zones (see Figure 4.7 for an example). The database was made for a pre-defined source called a "unit source," which is a tsunami source due to an earthquake with a fault length of 100 km, fault width of 50 km, and a slip value of 1 m, equivalent to the moment magnitude of (M_w) 7.5. A combination of the pre-computed tsunami model runs in the propagation database can provide a quick forecast of the oceanwide propagation of the tsunami as a linear combination of unit sources selected to represent the initial earthquake parameters (epicenter and magnitude). The forecast is updated by improving the linear combination of the source units with more accurate seismic information that had not been available at the initial computation and the tsunami data recorded by the Deep Ocean Assessment of Tsunami (DART) system. Note that the DART buoys are real-time tsunami monitoring systems that are positioned at strategic locations throughout the ocean and play a critical role in tsunami forecasting. The current locations of the buoys are shown in Figure 4.18.

For a given coastal area of interest, tsunami wave height, current speeds, and inundation extent are predicted numerically with the use of the Forecast Inundation Model. First, offshore tsunami waves at any specified location are obtained with a linear combination of the propagation database as described above, and the wave data offshore are used for the tsunami inundation numerical model based on the MOST code, which provides high resolution predictions of tsunami inundation. For a given community of interest, the customized Forecast Inundation Model was developed to achieve the optimal accuracy and an adequate speed of computation.

Currently, NOAA has developed the Forecast Inundation Models for a total of 75 U.S. communities. The list of communities where the Forecast Inundation Models are available is shown in Figure 4.17.

Figure 4.18: Deep Ocean Assessment of Tsunami (DART) and the current deployed DART locations

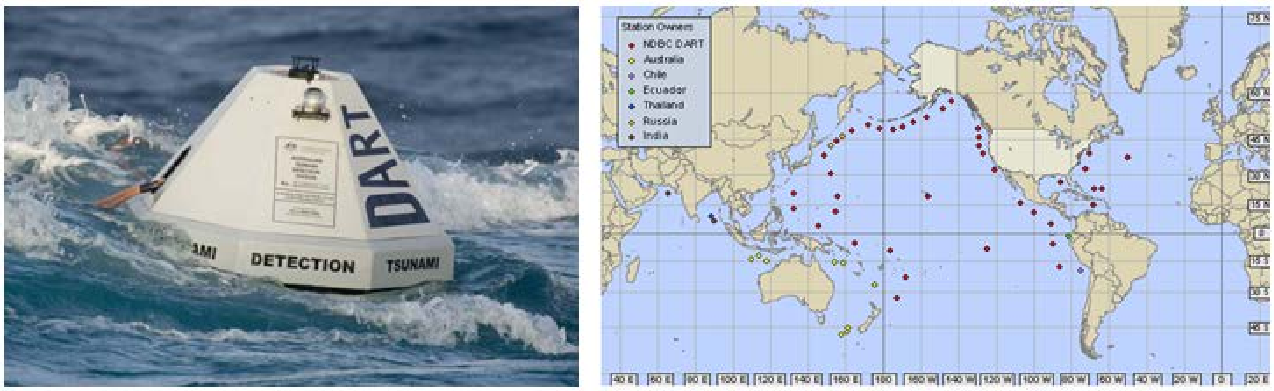

4.10 References

Abe, K, 1995. Estimate of tsunami runup heights from earthquake magnitudes. In: *Tsunami: Progress in Prediction, Disaster Prevention and Warning* (Ed: Tsuchiya, Y, and Shuto, N.) Kluwer Academic Pub. Netherlands, 21-35.

Atwater, B.F., M.R. Satoko, S. Kenji, T. Yoshinobu, U. Kazue, and D.K. Yamaguchi. 2005. *The Orphan Tsunami of 1700: Japanese Clues to a Parent Earthquake in North America*. University of Washington Press, Seattle, Washington.

Borrero, J.C., Legg, M. R. and Synolakis, C. E. (2004). Tsunami Sources in the Southern California Bight, *Geophysical Research Letters*, 28(4) 643-646.

Carrier, G.F., Wu, T.T. and Yeh, H. 2003. Tsunami Runup and Drawdown on a Plane Beach, *Journal of Fluid Mechanics*, 475, 79-99.

Chock, G.Y., 2016, Design for tsunami loads and effects in the ASCE 7-16 standard, Journal of Structural Engineering, 04016093.

Dunbar, P.K. and Weaver, C.S. 2008. *U.S. States and Territories National Tsunami Hazard Assessment: Historical Record and Sources for Waves*. Report to National Tsunami Hazard Mitigation Program, August 2008.

Ewing, L. 2011. *The Tohoku Tsunami of March 11, 2011: a preliminary report on effects to the California coast and planning implications*. A Report to Coastal Commissioners, 40 pp. http://www.coastal.ca.gov/energy/tsunami/CCC_Tohoku_Tsunami_Report.pdf.

FEMA, 2013. *Tsunami Methodology Technical Manual*, 223 pp., Federal Emergency Management Agency, Washington, D.C.

FEMA P646, 2012. Guidelines for Design of Structures for Vertical Evacuation from Tsunamis, Federal Emergency Management Agency, Washington, D.C.

Fritz, H.M., Phillips, D.A., Okayasu, A., Shimozono, T., Liu, H., Mohammed, F., Skanavis, V., Synolakis, C.E., and Takahashi, T. 2012. The 2011 Japan tsunami current velocity measurements from survivor videos at Kesennuma Bay using LiDAR. *Geophy. Res. Lett*., 39, L00G23, doi:10.1029/2011GL050686.

Geist, E.L., 2005, Local Tsunami Hazards in the Pacific Northwest from Cascadia Subduction *Zone Earthquakes*: U.S. Geological Survey Professional Paper 1661-B, 21 p.

Geist, E.L. and Parsons, T. (2006). Probabilistic analysis of tsunami hazards, *Natural Hazards,* 37, 277–314.

Gica, E., Spillane, M.C., Titov, V.V., Chamberlin, C.D. and Newman, J.C. (2008). "Development of the Forecast Propagation Database for NOAA's Short-term Inundation Forecasting for Tsunamis (SIFT)", NOAA Technical Memorandum OAR PMEL-139.

González, F.I., E.L. Geist, B. Jaffe, U. Kanoglu, H.O. Mofjeld, C.E. Synolakis, V.V. Titov, D. Arcas, D. Bellomo, D. Carlton, T. Horning, J. Johnson, J. Newman, T. Parsons, R. Peters, C. Peterson, G. Preist, A. Venturato, J. Weber, F. Wong, and A. Yalciner. 2009. Probabilistic tsunami hazard assessment at Seaside, Oregon, for near- and far-field seismic sources. *Journal of Geophysical Research* 114(C11):C11023.

Ho, D.V. and Meyer, R.E. (1962). Climb of a bore on a beach. Part 1: Uniform beach slope. *J. Fluid Mech.*, 14, 305-318.

IOC-IHO/GEBCO, 2005. Section 5 in the Report on IOC-IHO/GEBCO Guiding Committee XXI *and Sub-Committee on Digital Bathymetry XXI*. Aguascalientes, Mexico.

Johnson, J.M., Satake, K., Holdahl, S.R., and Sauber, J., 1996, The 1964 Prince William Sound earthquake: Joint inversion of tsunami waveforms and geodetic data. *J. Geophys. Res.*, 101, 523 -532.

Koshimura, S. 2011. Field Survey of the 2011 Tsunami Inundation in Tohoku District Towards comprehensive understanding of tsunami disaster. Preliminary Report presented in July 16 2011. The 2011 Tohoku Earthquake Tsunami Joint Survey Group.

LeVeque, R.J. and George, D.L. 2007. High-resolution finite volume methods for the shallow water equations with bathymetry and dry states. In: *Advanced Numerical Models for Simulating Tsunami Waves and Runup*: Proceedings of the Third International Workshop on Long-Wave Runup Models, Catalina, 2004, (Ed: P. L-F. Liu, H. Yeh, C. Synolakis), Advances in Coastal and Ocean Engineering, Vol 10, pp. 43-73, World Scientific, 2007.

Liu, P. L.-F., Cho, Y.-S., Yoon, S.B., and Seo, S.N. 1994. Numerical simulation of the 1960 Chilean tsunami propagation and inundation at Hilo, Hawaii, In: *Recent Development in Tsunami Research* (Ed: M.I. El-Sabh), Kluwer Academic Publisher http://ceeserver.cee.cornell.edu/pll-group/comcot.htm.

Liu, P., Yeh, H., and Synolakis, C. (Editors) 2008. Advanced Numerical Models for Simulating Tsunami Waves and Runup, *Advances in Coastal and Ocean Engineering*, Vol. 10, World Scientific Publishing Co., Singapore. 344 pp.

Mansinha, L. and Smylie, D.E. 1971. The displacement fields of inclined faults. *Bull. Seismol. Soc. Am*. 61, 1433-1440.

National Police Agency, 2016. https://www.npa.go.jp/archive/keibi/biki/higaijokyo_e.pdf.

Okada, Y. 1985. Surface deformation due to shear and tensile faults in a half-space. *Bull. Seismol. Soc. Am.* 75, 1135-1154.

PG&E. 2010. Methodology for probabilistic tsunami hazard analysis: Trial application for the Diablo Canyon Power Plant Site. PEER Workshop on Tsunami Hazard Analyses for Engineering Design Parameters, Berkeley CA, September 2010.

Priest, G.R., Myers III, E.P., Baptista, A.M., Fleuck, P., Wang, K., Kamphaus, R.A., and Peterson, C.D. 1997. *Cascadia Subduction Zone Tsunamis—Hazard mapping at Yaquina Bay, Oregon.* Oregon Department of Geology and Mineral Industries Open-File Report O-97-34, 144 pp.

Priest, G.R., Goldfinger, C., Wang, K., Witter, R.C., Yinglong, Y. and Baptista, A.M., 2009, Tsunami hazard assessment of the northern Oregon coast: a multi-deterministic approach tested at Cannon Beach, Clatsop County, Oregon: Oregon Department of Geology and Mineral Industries Special Paper 41, in press.

Synolakis, C.E., Bernard, E.N., Titov, V.V., Kanoglu, U., and Gonzalez, F. 2007. Standards, criteria, and procedures for NOAA evaluation of tsunami numerical models. NOAA Technical Memorandum OAR PMEL-135.

Takagawa, Y. 2012. Personal communication and manuscript is in preparation.

ten Brink, U.S., Geist, E.L., and Andrews, B.D. (2006). Size distribution of submarine landslides and its implication to tsunami hazard in Puerto Rico. *Geophys. Res. Lett*. 33, L11307.

Yamazaki, Y., Cheung, K.F., and Kowalik, Z. (2010). Depth- integrated, non-hydrostatic model with grid nesting for tsunami generation, propagation and run-up. *International Journal for Numerical Methods in Fluids*, DOI: 10.1002/ftd.2485.

Yamazaki, Y., Kowalik, Z., and Cheng, K.F. 2009 Depth-integrated, non-hydrostatic model for wave breaking and runup. *International Journal of Numerical Methods in Fluids*.

Yeh, H. 1998. Tsunami Researchers Outline Steps for Better Data. *EOS, Trans. Amer. Geophys. Union*, 79, 480 & 484.

Yeh, H. 2006. Maximum fluid forces in the tsunami runup zone, *Journal of Waterway, Port, Coastal, and Ocean Engineering*, 132. 496-500.

Yeh, H. 2007. Design tsunami forces for onshore structures*, J. Disaster Research*, 2. 531-536. Yeh, H. 2009. Tsunami Impacts on Coastlines. In: *The Sea*, Vol. 15 (Ed: E.N. Bernard and A.R. Robinson), Harvard University Press. 333-369.

Yeh, H., Ghazali, A., and Marton, I., 1989. Experimental Study of Bore Runup. *Journal of Fluid Mechanics*, 206, 563-578.

Yeh, H., Liu, P., and Synolakis, C. (Editors) 1996. *Long-Wave Runup Models*, World Scientific Publishing Co., Singapore. 403 pp.

Zhang, Y.-L. and Baptista, A.M. 2008 "SELFE: A semi-implicit Eulerian-Lagrangian finite- element model for cross-scale ocean circulation", *Ocean Modelling*, 21(3-4), 71-96.

5.0 Damage Assessment for Buildings

5.1 Introduction

This chapter describes methods for determining the probability of Moderate, Extensive, and Complete damage to general building stock and user-defined facilities due to tsunami inundation (flood) and tsunami lateral force (flow). The General Building Stock (GBS) in the Hazus Tsunami Model is represented by National Structure Inventory (NSI) points attributed with model building type, occupancy class, and other building inventory characteristics, distributed within the developed portions of census blocks as described in Chapter 3. GBS inventory and loss results are grouped using census blocks for reporting and mapping. User-defined facilities consist of site-specific points that represent structures and include the specific building characteristics required for tsunami damage assessment.

This chapter also describes methods for combining the probability of building damage due to a tsunami with the probability of building damage due to the earthquake that generated the tsunami (i.e., for evaluation of local tsunami damage and loss).

Building damage-state probabilities are used in the evaluation of damage to lifeline buildings (FEMA, 2013, Chapter 6), building-related debris (FEMA, 2013, Chapter 7), displaced households and sheltering needs (FEMA, 2013, Chapter 9), and direct economic losses (Chapter 7). The flow of hazard input from tsunami (Chapter 4) and earthquake damage (from the Earthquake Model), and the damage-state probability output to other current and future damage and loss components of the Hazus Tsunami Model is illustrated in Figure 5.1.

Figure 5.1: Building Damage Module Relationships to Other Components of the Tsunami Loss Estimation Methodology (and the Earthquake Loss Estimate Model)

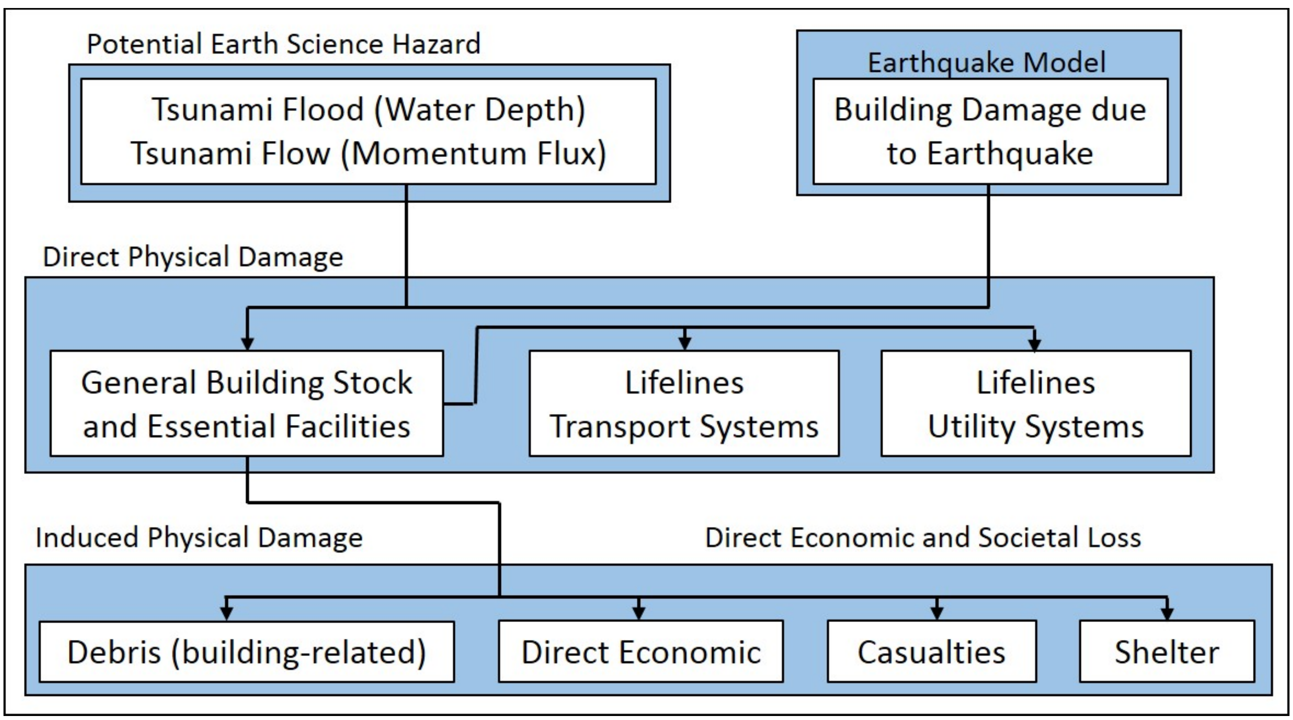

5.1.1 Scope

The scope of this chapter includes development of building damage functions for 36 model building types. Separate sets of damage functions are developed for 1) tsunami "flood" hazard, and 2) tsunami "flow" hazard. Section 5.2 describes each of the 36 model building types.

Building damage functions describe the extent and severity of damage to the 1) structural system (i.e., structural elements supporting gravity loads and resisting lateral loads), 2) nonstructural systems and components (i.e., components of architectural, mechanical, electrical, and plumbing systems), and 3) contents (i.e., furnishings and nonpermanent equipment, etc.). Damage is described by one of three non-nil damage states**:** Moderate, Extensive, and Complete. These damage states are the same as those (of the same name) used by the Earthquake Model to describe the extent and severity of damage due to ground shaking and ground failure. Building damage due to earthquake ground shaking is also described in terms of Slight damage. Slight damage is not required for tsunami, since it is difficult to distinguish from no damage, it is only used for calculation of economic losses and is of no significance to tsunami economic losses. Although the specific cause and manifestation of tsunami damage can be quite different from that of an earthquake, tsunami and earthquake damage states are considered to be the same when they represent a common extent and severity of damage. Section 5.3 describes tsunami damage typical of structural, nonstructural, and contents damage states.

Section 5.4 develops building damage functions for tsunami flood hazard characterized by median values of maximum inundation height (i.e., maximum water depth relative to sea level see Figure 4.2). In this case, damage is assumed to be primarily due to maximum water height (essentially nil water velocity), similar to damage caused by riverine flood, and tsunami flood methods have utilized related information contained in the Hazus Flood Model *Technical Manual* (FEMA, 2011b). The Flood Model estimates dollar losses directly on water depth using experiential dollar loss data available for certain occupancy classes (so-called depth-damage curves). Tsunami flood methods also use water depth, but employ a theoretical approach to estimate inundation damage. When combined with the economic loss functions (Chapter 7), tsunami flood damage functions yield very similar dollar loss results to those of Flood Model for the same model building type (occupancy class) and inundation depth. The theoretical approach of the tsunami flood methods provides a basis to estimate flood-related damage and loss when empirical data are not available for the model building type of interest.

While damage due to tsunami flood primarily affects nonstructural systems and components and contents, lateral forces due to tsunami flow are the primary cause of damage to the building structure, including building collapse (and debris generation). Section 5.5 develops building damage functions for tsunami flow hazard characterized by median values of maximum momentum flux (HV^2). In this case, damage is assumed to be primarily due to lateral forces caused by drag effects and debris carried along by tsunami flow. Tsunami flow methods take an "engineering" approach, drawing from the concepts and criteria of FEMA P646, *Guidelines for Design of Structures for Vertical Evacuation from Tsunamis* (FEMA, 2012), the "pushover" strength of model building types, as provided in the Hazus Earthquake Model *Technical Manual* (FEMA, 2011a), and to lesser degree, Chapter 5 "Flood Loads" of ASCE 7-10 (ASCE, 2010). An "engineering" approach is utilized to parallel on-going tsunami research and Code development work, and to provide a framework for future improvement to building damage functions as the technology progresses. Currently, individual structural element failures due to tsunami hydrodynamic pressures are not explicitly included in the systemic fragility relationships for the model building types.

Section 5.6 develops methods for combining building damage-state probabilities from the different types of hazards considered, including combining tsunami and earthquake damage without "double counting." The end product of these methods is a single set of damage-state probabilities that can be used to evaluate economic and other losses.

5.1.2 Input Requirements and Output Information

Input information and data required to estimate building damage due to tsunami include the following items related to building inventory data, tsunami hazard parameters, and prior earthquake damage (for local tsunami scenario):

Building Inventory Data

1. Model Building Type (MBT) – one of 36 MBTs, including light-frame wood, W1, low-rise reinforced-concrete shear wall, C2L, etc.
2. Height of the first floor above the base of the building (h_F)
3. Height of the base of the building (z) above sea level datum used to define tsunami inundation height (R)
4. Seismic Design Level (e.g., high-code, HC, moderate-code, MC, low-code, LC, pre-code, PC, high-special, HS, moderate-special, MS, or low-special, LS).

Tsunami Hazard Data

1. Median value of maximum inundation height (R) at building location point of interest
2. Median value of maximum momentum flux (hv^2) at building point of interest.

Earthquake Damage Data (from the Earthquake Model)

1. Structural damage-state probabilities
2. Nonstructural drift-sensitive damage-state probabilities
3. Nonstructural acceleration-sensitive damage-state probabilities
4. Contents damage-state probabilities

Typically, model building type and other inventory data are not known for each building of a given census block, and must be inferred on a square footage basis from the inventory of facilities using model building type and occupancy relationships (Chapter 3). The tsunami hazard data may be developed for grids of varying resolution. Thus, while the concepts are developed on a building-specific basis, they are typically applied on a pro rata basis to an aggregated building stock.

Output data developed by the building damage module are estimates of the cumulative probability of being in, or exceeding, each damage-state for hazard parameter (or parameters, if combined) of interest. Discrete damage-state probabilities are created from the cumulative damage probabilities, as described in Section 5.1.3. Discrete damage-state probabilities for model building types and occupancy classes are the outputs of the building damage module. These outputs are used directly as inputs to induced physical damage (debris) and direct economic and societal loss modules, as shown in the flowchart of Figure 5.1.

While the building damage functions are applicable, in theory, to individual buildings, as well as to all buildings of given type, they are more reliable as predictors of damage for large, rather than small, population groups. They should not be considered reliable for prediction of damage to a specific facility without confirmation by a seismic/structural engineering expert using the specific building properties (e.g., pushover strength, etc.).

5.1.3 Form of Damage Functions

Building damage functions are in the form of lognormal fragility curves that relate the probability of being in, or exceeding, a discrete state of damage given the median estimate of the hazard parameter of interest (i.e., median peak inundation height or median peak momentum flux). Figure 5.2 illustrates fragility curves that describe Moderate, Extensive, and Complete structure damage due to tsunami flow (i.e., median peak momentum flux, F), in this case for an older mid-rise reinforced-concrete shear wall building (model building type C2M in Table 5.13)

Figure 5.2: Example fragility curves that describe Moderate, Extensive, and Complete structure damage due to tsunami flow (i.e., median peak momentum flux, F).

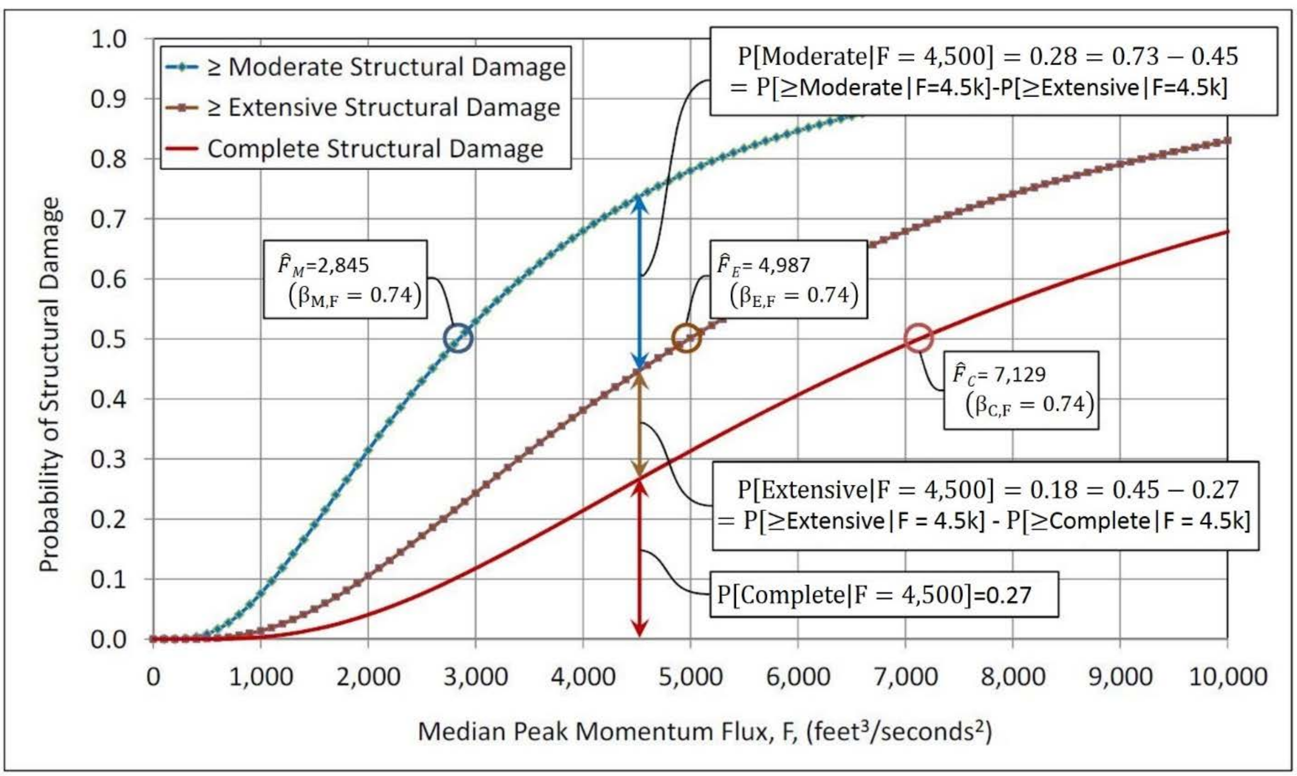

Conceptually, the form of the tsunami building damage functions is the same as the lognormal "fragility" curve format used by the Earthquake Model. Each damage-state curve is defined by the median value and associated variability of the fragility parameter of interest. The variability of these fragility curves has two fundamental components, the variability of the median estimate of the hazard parameter (i.e., uncertainty in demand) and the variability of the median value of the damage state (i.e., uncertainty in capacity) for the hazard of interest. The fragility random variable is expressed in terms of these two sources of uncertainty in Equation 5.1 for damage due to tsunami flood, R_{dsi}, and in Equation 5.2 for damage due to tsunami flow, F_{dsi}, as follows:

$$R_{dsi} = \hat{R}_{dsi}\, \varepsilon_{dsi\backslash R} \varepsilon_R \tag{5.1}$$

$$F_{dsi} = \hat{F}_{dsi} \varepsilon_{dsi\backslash F} \varepsilon_F \tag{5.2}$$

Where: $\hat{R}_{dsi}$ = median value of maximum inundation height associated with damage state, ds_i

$\varepsilon_{\mathrm{dsi|R}}$ = lognormal random "capacity" variable with unit median and logarithmic standard deviation, $\beta_{\mathrm{dsi|R}}$, associated with the uncertainty in the damage state, ds_i, when damage is due to tsunami flood (maximum inundation height)

ε_{R} = lognormal random "demand" variable with unit median and logarithmic standard deviation, β_{R}, associated with the uncertainty in the median estimate of tsunami flood (maximum inundation height)

$\hat{F}_{dsi}$ = median value of maximum momentum flux associated with damage state, ds_i

$\varepsilon_{\mathrm{dsi|F}}$ = lognormal random "capacity" variable with unit median and logarithmic standard deviation, $\beta_{\mathrm{dsi|F}}$, associated with the uncertainty in the damage state, ds_i, when damage is due to tsunami flow (maximum momentum flux)

ε_{F} = lognormal random "demand" variable with unit median and logarithmic standard deviation, β_{F}, associated with the uncertainty in the median estimate of tsunami flow (maximum momentum flux).

Median values of building damage states for damage due to tsunami flood, $\hat{R}_{dsi}$, are developed in Section 5.4 and median values of building damage states for damage due to tsunami flow, $\hat{F}_{dsi}$, are developed in Section 5.5.

In the above formulations, the "capacity" and demand" random variables are assumed to be statistically independent, and total uncertainty may be calculated using Equations (5.3) and (5.4), as follows:

$$\beta_{dsi,R} = \sqrt{\left(\beta_{dsi|R}\right)^2 + (\beta_R)^2} \tag{5.3}$$

$$\beta_{dsi,F} = \sqrt{\left(\beta_{dsi|F}\right)^2 + (\beta_F)^2} \tag{5.4}$$

Where:

$\beta_{dsi,R}$ = logarithmic standard deviation describing the total uncertainty of damage state, ds_i, due to tsunami flood (maximum inundation height)

$\beta_{dsi|R}$ = lognormal standard deviation associated with the uncertainty in the damage state, ds_i, capacity when damage is due to tsunami flood (maximum inundation height)

β_R = logarithmic standard deviation associated with the uncertainty in the median estimate of tsunami flood (maximum inundation height)

$\beta_{dsi,F}$ = logarithmic standard deviation describing the total uncertainty of damage state, ds_i, due to tsunami flow (maximum momentum flux)

$\beta_{dsi|F}$ = logarithmic standard deviation associated with the uncertainty in the damage state, ds_i, capacity when damage is due to tsunami flow (maximum momentum flux)

β_F = logarithmic standard deviation associated with the uncertainty in the median estimate of tsunami flow (maximum momentum flux).

It is important to distinguish the “demand” and “capacity” components of uncertainty, since “demand” uncertainty component used for evaluation of losses due to a deterministic (scenario) tsunami is not required for evaluation of probabilistic losses when using tsunami hazard functions that directly incorporate this uncertainty in the hazard. For evaluation of probabilistic losses with a given deterministic tsunami, values of tsunami hazard uncertainty (β_F and β_R) should be assumed to be nil.

Values of the lognormal standard deviation parameter associated with the uncertainty in the damage state, $\beta_{dsi|R}$, are developed in Section 5.4 and values of the lognormal standard deviation parameter associated with the uncertainty in the damage state, $\beta_{dsi|F}$, are developed in Section 5.5.

The conditional probability of being in, or exceeding, the damage state, ds_i, of interest, is given by Equations (5.5) and (5.6):

$$P[ds_i|R] = \Phi\left[\frac{1}{\beta_{dsi,R}}\ln\left(\frac{R}{\hat{R}_{dsi}}\right)\right] \tag{5.5}$$

$$P[ds_i|F] = \Phi\left[\frac{1}{\beta_{dsi,F}}\ln\left(\frac{F}{\hat{F}_{dsi}}\right)\right] \tag{5.6}$$

The symbol Φ represents the normal distribution in Equations (5.5) and (5.6).

The probability of being in a specific damage state, DS_i, is calculated as difference of the conditional probability of being in, or exceeding, the damage state of interest, ds_i, and the probability of being in, or exceeding, the next, more severe, damage state, ds_{i+1}, as illustrated in Figure 5.2, and as given by Equations 5.7 and 5.8:

$$P[DS_i|R = r] = P[ds_i|R = r] - P[ds_{i+1}|R = r] \tag{5.7}$$

$$P[DS_i|F = f] = P[ds_i|F = f] - P[ds_{i+1}|F = f] \quad (5.8)$$

where the parameters, r and f, represent specific values of the random variables, R and F, respectively, and the values of $P[ds_{i+1}|R = r]$ and $P[ds_{i+1}|F = f]$ are zero when the term DS_i represents the Complete damage state.

5.2 Description of Model Building Types

Table 5.1 lists the 36 model building types of Hazus Tsunami Model height ranges and typical heights. The list is the same as the one presented in Chapter 3.

Table 5.1: Model Building Types, Height Ranges and Typical Heights

No.	Label	Description	Height Range: Name	Height Range: Stories	Typical Height in Stories	Typical Height in Feet
1	W1	Wood, Light Frame (≤ 5,000 sq. ft.)		All	1	14
2	W2	Wood, Greater than 5,000 sq. ft.		All	2	24
3	S1L	Steel Moment Frame	Low-Rise	1-3	2	24
4	S1M	Steel Moment Frame	Mid-Rise	4-7	5	60
5	S1H	Steel Moment Frame	High-Rise	8+	13	156
6	S2L	Steel Braced Frame	Low-Rise	1-3	2	24
7	S2M	Steel Braced Frame	Mid-Rise	4-7	5	60
8	S2H	Steel Braced Frame	High-Rise	8+	13	156
9	S3	Steel Light Frame		All	1	15
10	S4L	Steel Frame with Cast-in-Place Concrete Shear Walls	Low-Rise	1-3	2	24
11	S4M	Steel Frame with Cast-in-Place Concrete Shear Walls	Mid-Rise	4-7	5	60
12	S4H	Steel Frame with Cast-in-Place Concrete Shear Walls	High-Rise	8+	13	156
13	S5L	Steel Frame with Unreinforced Masonry Infill Walls	Low-Rise	1-3	2	24
14	S5M	Steel Frame with Unreinforced Masonry Infill Walls	Mid-Rise	4-7	5	60
15	S5H	Steel Frame with Unreinforced Masonry Infill Walls	High-Rise	8+	13	156

No.	Label	Description	Height Range: Name	Height Range: Stories	Typical Height in Stories	Typical Height in Feet
16	C1L	Concrete Moment Frame	Low-Rise	1-3	2	20
17	C1M	Concrete Moment Frame	Mid-Rise	4-7	5	50
18	C1H	Concrete Moment Frame	High-Rise	8+	12	120
19	C2L	Concrete Shear Walls	Low-Rise	1-3	2	20
20	C2M	Concrete Shear Walls	Mid-Rise	4-7	5	50
21	C2H	Concrete Shear Walls	High-Rise	8+	12	120
22	C3L	Concrete Frame with Unreinforced Masonry Infill Walls	Low-Rise	1-3	2	20
23	C3M	Concrete Frame with Unreinforced Masonry Infill Walls	Mid-Rise	4-7	5	50
24	C3H	Concrete Frame with Unreinforced Masonry Infill Walls	High-Rise	8+	12	120
25	PC1	Precast Concrete Tilt-Up Walls		All	1	15
26	PC2L	Precast Concrete Frames with Concrete Shear Walls	Low-Rise	1-3	2	20
27	PC2M	Precast Concrete Frames with Concrete Shear Walls	Mid-Rise	4-7	5	50
28	PC2H	Precast Concrete Frames with Concrete Shear Walls	High-Rise	8+	12	120
29	RM1L	Reinforced Masonry Bearing Walls with Wood or Metal Deck Diaphragms	Low-Rise	1-3	2	20
30	RM1M	Reinforced Masonry Bearing Walls with Wood or Metal Deck Diaphragms	Mid-Rise	4+	5	50
31	RM2L	Reinforced Masonry Bearing Walls with Precast Concrete Diaphragms	Low-Rise	1-3	2	20
32	RM2M	Reinforced Masonry Bearing Walls with Precast Concrete Diaphragms	Mid-Rise	4-7	5	50
33	RM2H	Reinforced Masonry Bearing Walls with Precast Concrete Diaphragms	High-Rise	8+	12	120
34	URML	Unreinforced Masonry Bearing Walls	Low-Rise	1-2	1	15

No.	Label	Description	Height Range: Name	Height Range: Stories	Typical Height in Stories	Typical Height in Feet
35	URMM	Unreinforced Masonry Bearing Walls	Mid-Rise	3+	3	39
36	MH	Mobile Homes		All	1	12

The model building types of Table 5.1 were originally based on the classification system of FEMA 178, *NEHRP Handbook for the Seismic Evaluation of Existing Buildings* (FEMA, 1992) and may now be found in ASCE 31-03, *Seismic Evaluation of Existing Buildings* (ASCE, 2003). The model building types of the Earthquake Model (and Tsunami Model) expand FEMA 178 and ASCE 31-03 building types to incorporate building height (e.g., low-rise, mid-rise, and high-rise building types), and to also include manufactured housing (mobile homes). General descriptions of the structural system of model building types are found in Chapter 5 of the Earthquake Model *Technical Manual* (and ASCE 31-03).

For evaluation of tsunami inundation, Table 5.2 provides estimates of first-floor heights as a function of foundation type and building age (pre-FIRM and post-FIRM construction). Table 5.3 provides the distribution of foundation types for coastal areas. Coastal foundation data were extracted from a study of erosion by the Heinz Center (Heinz, 2000).   Post-FIRM (feet)

Table 5.2: Default First-Floor Heights above Grade to Top of Finished Floor (from Table 3.14, *Flood Technical Manual,* FEMA 2011b)

Foundation Type	Pre-FIRM (feet)	Post-FIRM (feet) A-Zone	Post-FIRM (feet) V-Zone
Pile (or column)	7	8	8
Pier (or post and beam)	5	6	8
Solid Wall	7	8	8
Basement	4	4	4
Crawl	3	4	4
Fill	2	2	2
Slab	1	1	1

Table 5.3: Distribution of Foundation Types for Coastal Areas (from Tables 3.12 and 3.13, *Flood Technical Manual*, FEMA 2011b)

Foundation Type	Pile	Pier	Solid Wall	Basement	Crawl	Fill	Slab
Pre-Firm Construction – All	7%	7%	1%	2%	46%	0%	37%
Post-Firm Construction – A-Zone (Special Flood Hazard Area)	20%	5%	0%	0%	55%	0%	20%
Post-Firm Construction – V-Zone (Special Flood Hazard Area – High Hazard)	60%	25%	0%	0%	10%	0%	5%

Although these data are not related to a specific model building type, the types of foundations and their frequency of use suggest that they are typical of low-rise, residential construction (e.g., W1 buildings). It may be noted that basements are rarely used for foundations in coastal areas.

5.3 Description of Building Damage States

The discrete states of damage, Moderate, Extensive, and Complete, define damage to the structure, damage to nonstructural systems, and damage to the contents of the model building type of interest. These discrete damage states are intentionally based on the same generic damage states as those of the Earthquake Model to permit combination of damage-state probabilities due to tsunami with damage-state probabilities due to earthquake (e.g., for evaluation of local tsunami damage and loss).

Table 5.4 (adapted from Table 6.1 of the Hazus, *Advanced Engineering Building Module* (AEBM) *Technical Manual* (FEMA, 2002)) summarizes the generic guidelines used to establish median values of structure, nonstructural, and contents damage states for tsunami. These guidelines establish, in an approximate sense, the state of physical damage to the structure, nonstructural systems, and contents, in terms of various types of loss parameters. Like earthquake, nonstructural systems and contents damage states are primarily influenced by economic loss considerations, whereas structure damage states are also influenced by other types of losses, such as shelter (probability of building closure) and debris generation (probability of building collapse). Table shows Damage State and Likely Amount of Damage, Direct Economic Loss, or Building Condition.

Table 5.4: General Guidance Used to Select Building Damage-State Parameters for Tsunami Hazard *(adapted from Table 6.1, Hazus-MH AEBM Technical Manual, FEMA 2002)*

Damage State	Range of Possible Economic Loss Ratios	Probability of Long-Term Building Closure	Probability of Partial or Full Collapse of the Structure	Immediate Post-Event Inspection[1]
Slight[2]	0% - 5%	P = 0	P = 0	Green Tag
Moderate	5% - 25%	P = 0	P = 0	Green Tag
Extensive[3]	25% - 100%	P ≅ 0.5	P ≅ 0[3]	Yellow Tag
Complete[4]	100%	P ≅ 1.0	P > 0[3]	Red Tag

Notes:

[1] Post-event safety inspection “tag” nomenclature is based on the ATC-20 report (ATC, 1987), as revised by the ATC-20-2 report (ATC, 1995), which provides guidance for post-earthquake inspection and classification of buildings damage as “Inspected” (Green Tag), “Restricted Use” (Yellow Tag), or “Unsafe” (Red Tag). Similar post-flood safety inspection “tag” nomenclature is provided in the ATC-45 field manual (ATC, 1994).

[2] Slight damage state is not used for tsunami.

[3] Extensive damage may include local collapse of structural elements and nonstructural components (e.g., out-of-plane failure of walls due to tsunami flow).

[4] Complete structural damage includes: 1) structures that are standing, but a total economic loss, 2) structures that have sustained partial or full collapse, but remain largely in place, and 3) structures that have been “washed away” by tsunami flow.

Conceptually, the same building damage states can occur due to either tsunami flood hazard or tsunami flow hazard. This approach is similar to that of the Earthquake Model which uses the same damage states to represent building damage due to either earthquake ground shaking or earthquake ground failure. A common set of damage states permits separately calculated damage-state probabilities to be combined using appropriate logic (e.g., assumption of statistical independence of the hazards). The notion of hazard independence is supported by tsunami flood damage functions that are based solely on the effects of inundation (i.e., no damage due to tsunami flow) and tsunami flow damage functions that are based solely on the effects of lateral force. It should be noted that depth-damage functions (DDFs) of the Flood Model for coastal areas (i.e., coastal A-Zone and coastal V-Zone areas) incorporate damage due to storm waves as well as inundation and are, therefore, not appropriate for comparison with tsunami "inundation only" flood damage. The DDFs of the Flood Model for A-Zone (low-water velocity) areas are more appropriate for comparison with tsunami "inundation only" building damage functions.

While tsunami damage states are generically the same as those of the Earthquake Model, fewer damage states are required to adequately address tsunami losses. Slight damage is not required for tsunami, since it is difficult to distinguish from no damage, only used for calculation of economic losses and of no significance to tsunami economic losses. Hazus economic loss rates define Slight damage as only two percent of the building's replacement value (and only one percent of contents value), so a large number of buildings in the study region of interest would need to have a large probability of Slight damage to significantly contribute to economic losses. While this can be true for certain earthquake scenarios, tsunami damage tends to be either nil, in areas not exposed to tsunami runup, or likely to be much greater than Slight damage in inundated areas (since even a relatively small depth of water causes more than two percent loss). Along similar lines, Moderate and Extensive states of damage are not used for all model building types and systems. In general, shorter (and lighter) model building types require fewer damage states to reliably calculate tsunami losses.

Table 5.5 summarizes damage states used to characterize tsunami damage to buildings in terms of building system (i.e., structure, nonstructural, and contents), building height (i.e., model building type) and tsunami hazard (i.e., tsunami flood or tsunami flow). Damage to the structural system is assumed to be governed solely by tsunami flow hazard and damage to nonstructural systems and contents (in structures that survive) are assumed to be governed solely by tsunami flood hazard.

Nonstructural systems and contents damage states are based solely on tsunami flood hazard (water depth based on maximum inundation height) assuming that if the building survives tsunami flow effects (e.g., is not washed away or otherwise does not sustain Complete damage to the structure), then damage and related losses to these systems are primarily a function of maximum inundation height. Of course, nonstructural systems and contents are also damaged by tsunami flow, but such damage is assumed to be adequately captured by damage due to inundation (e.g., since nonstructural systems and contents of fully inundated floors are assumed to be a complete loss). Additionally, to the extent that tsunami flow causes Complete damage to the structure, then nonstructural systems and contents are also assumed to have Complete damage. Thus, the probability of Complete structural damage (due to tsunami flow) is an important contributor to building damage and loss, particularly for model building types of shorter, lighter construction (consistent with observations of tsunami damage in past events).

Table 5.5: Summary of Damage States Used to Model Tsunami Damage to Building Systems in Terms of the Type of Hazard and Model Building Types (building height and weight)

Table shows Building Systems Modeled by Damage States[12]

Model Building Type in Terms of Building Height and Weight	Moderate Damage State: based on Tsunami inundation height	Extensive Damage State: based on Tsunami inundation height	Complete Damage State: based on Tsunami inundation height	Moderate Damage State: based on Tsunami momentum flux	Extensive Damage State: based on Tsunami momentum flux	Complete Damage State: based on Tsunami momentum flux
Low-Rise - Light[13]		NSS, CON	NSS, CON			STR
Low-Rise – Other		NSS, CON	NSS, CON		STR	STR
Mid-Rise	NSS, CON	NSS, CON	NSS, CON	STR	STR	STR
High-Rise	NSS, CON	NSS, CON	NSS, CON	STR	STR	STR

Structure damage states are based solely on tsunami flow hazard assuming that the structure of the building is not appreciably damaged unless there is significant tsunami flow velocity. This assumption is consistent with observations of tsunami damage to buildings and Flood Model theory which notes in Section 5.2 of the Flood *Technical Manual*:

> "Unless the floodwaters flow at a high velocity and the structure and the foundation become separated, or the structure is impacted by flood-borne debris, it is unlikely that a building will suffer structural failure in a flood. (Structural failure should be distinguished, however, from suffering substantial damage, wherein the damage due to inundation exceeds 50 percent of the structure's total replacement cost and the building is considered a total loss.) In general, it is expected that the major structural components of a building will survive a flood, but that the structural finishes and contents/inventory may be severely damaged due to inundation."

Table 5.6 provides qualitative descriptions of structure damage states and nonstructural and contents damage states. Subsequent sections of this chapter use these descriptions and other data to establish specific values of damage-state parameters for different model building types.

Conceptually, nonstructural systems and components located on fully "inundated" floors are considered to be ruined (i.e., 100 percent damage), and that only a few feet of water is required to significantly damage contents on a partially inundated floor.

Conceptually, the structure is considered undamaged until lateral forces, due to hydrodynamic loads, including the effects of debris impact, exceed the yield-force capacity of the structural system. Structure damage increases with tsunami force until tsunami flow and debris forces exceed the ultimate-lateral-force capacity of the structural system, and complete failure is assumed to occur. This approach focuses on the global damage to the structure, rather than on failure of

---

[12] Building systems include the structure (STR), nonstructural drift-sensitive (NSD), and nonstructural acceleration sensitive (NSA) systems, collectively identified as nonstructural systems (NSS) in the tsunami model, and building contents (CON).

[13] Low-rise "light" model building types (MBTs) include W1, W2, S3, and MH.

individual elements. As described in Table 5.6, hydrodynamic loads can also cause localized damage to structural elements, including out-of-plane failure of walls, columns, and braces, which could lead to progressive collapse of the building, and tsunami flow can also erode and scour the structure and compromise the foundation, or cause uplift of the building.

Debris strikes are more severely impacting on load-bearing structural elements than on the overall lateral-force-resisting system. While these are important modes of tsunami damage, quantification of building damage due to failure of individual structural elements, possible progressive collapse, and loss of foundation integrity would require detailed structural information that is not available for generic model building types. Rather, tsunami damage functions use estimates of global building strength (which can be inferred from building age, etc.) to relate building damage states to tsunami flow and debris forces.

Table 5.6: Tables Showing Qualitative Descriptions of Building Damage States due to Tsunami Flow and Tsunami Flood

Model Building Type (Height/Weight)	Moderate Structure Damage due to Tsunami Flow	Extensive Structure Damage due to Tsunami Flow	Complete Structure Damage due to Tsunami Flow
Low-Rise – Light MBTs (W1, W2, S3, MH)			A significant portion of structural elements have exceeded their ultimate capacities and/or many critical elements/ connections have failed resulting in dangerous permanent offset, partial collapse, full collapse or building moved off foundation (e.g., “washed away”). Extensive erosion or scour, substantial foundation settlement
Low-Rise - Other		Localized failure of elements at lower floors. Large diagonal cracks in shear walls, failure of steel braces, large flexural cracks/buckling of rebar, buckled flanges and connection failures– large permanent offsets of lower stories. Localized erosion or scour, limited foundation settlement	A significant portion of structural elements have exceeded their ultimate capacities and/or many critical elements/ connections have failed resulting in dangerous permanent offset, partial collapse, full collapse or building moved off foundation (e.g., “washed away”). Extensive erosion or scour, substantial foundation settlement
Mid-Rise - All	Limited, localized damage to elements at lower floors. Diagonal cracks in shear walls, limited yielding of steel braces, cracking and hinging of flexural elements – no or only minor permanent offsets (i.e., less than ½ inch per floor).	Localized failure of elements at lower floors. Large diagonal cracks in shear walls, failure of steel braces, large flexural cracks/buckling of rebar, buckled flanges and connection failures– large permanent offsets of lower stories. Localized erosion or scour, limited foundation settlement	A significant portion of structural elements have exceeded their ultimate capacities and/or many critical elements/connections have failed resulting in dangerous permanent offset, partial collapse, full collapse or building moved off foundation (e.g., “washed away”). Extensive erosion or scour, substantial foundation settlement.

Model Building Type (Height/Weight)	Moderate Structure Damage due to Tsunami Flow	Extensive Structure Damage due to Tsunami Flow	Complete Structure Damage due to Tsunami Flow
High-Rise- All	Limited, localized damage to elements at lower floors. Diagonal cracks in shear walls, limited yielding of steel braces, cracking and hinging of flexural elements – no or only minor permanent offsets (i.e., less than ½ inch per floor).	Localized failure of elements at lower floors. Large diagonal cracks in shear walls, failure of steel braces, large flexural cracks/buckling of rebar, buckled flanges and connection failures– large permanent offsets of lower stories. Localized erosion or scour, limited foundation settlement	A significant portion of structural elements have exceeded their ultimate capacities and/or many critical elements/connections have failed resulting in dangerous permanent offset, partial collapse, full collapse or building moved off foundation (e.g., "washed away"). Extensive erosion or scour, substantial foundation settlement.

Nonstructural Components Ruined by Tsunami Flood (floors fully inundated, unless noted otherwise)

Low-Rise - 1-Story		Floor 1 (1/2 height)	Floor 1
Low-Rise - 2-Story		Floor 1	Floors 1 - 2
Mid-Rise - 5-Story	1st Floor	Floors 1 - 3	Floors 1 - 5
High-Rise - 12-Story	1st Floor Floor	Floors 1 - 6	Floors 1 - 12

Contents Ruined by Tsunami Flood (floors fully inundated, unless noted otherwise)

Low-Rise - 1-Story			Floor 1 (3 feet)
Low-Rise - 2-Story		Floor 1 (3 feet)*	Floors 1 – Floor 2 (3 ft.)
Mid-Rise - 5-Story	Floor 1 (3 feet)	Floors 1 – 2, 3 (3 ft.)	Floors 1 – 4, 5 (3 ft.)
High-Rise - 12-Story	Floor 1 (3 feet)	Floors 1 – 5, 6 (3 ft.)	Floors 1 – 11, 12 (3 ft.)

* 3 ft. designates the depth of water (3 feet) above the 3rd-floor deemed to cause extensive damage to contents of a five-story building

5.4 Building Damage Due to Tsunami Inundation

5.4.1 Scope

This section describes the approach and develops default values of building damage functions due to tsunami flood (water inundation). Default values of the median and logarithmic standard deviation describe the probability of damage to nonstructural systems (NSS) and contents (CON) for each model building type listed in Table 5.1. Tsunami inundation damage is characterized by the Moderate, Extensive, and Complete damage states, identified in Table 5.5 and described in Table 5.6.

5.4.2 Approach

Building damage due to tsunami inundation is assumed to be similar to that caused by other floods that have relatively slow water flow (e.g., riverine flooding). Building damage due to fast moving water flow is treated separately by damage functions that model damage due to hydrodynamic and related loads on the building (Section 5.5).

Damage to nonstructural systems and contents due to tsunami inundation is related directly to the height of the water. Nonstructural systems and contents that are inundated are considered ruined (a total loss) and the damage state (Moderate, Extensive, or Complete) reflects the fraction of the nonstructural systems and contents in the building that are inundated. Consistent with the damage functions of the Flood Model, contents which are primarily floor-supported items are more vulnerable to water depth on a given floor than nonstructural components (which include ceilings, overhead lights, etc., as well as floor supported items. Hence, full-height inundation of a given floor is assumed necessary for 100 percent damage of nonstructural systems on that floor, whereas 3 feet of water on a given floor is assumed sufficient to cause 100 percent damage to building contents on that floor.

Since damage is directly related to water depth, it is important to relate the elevation of building floors to the elevation of tsunami inundation, considering both the height, z, of the building's base above the sea level datum used to characterize tsunami inundation height, and the height of the first floor of the building above its base, h_F. Figure 5.3 illustrates these parameters and their relationship to inundation height at building, R, inundation depth at building, H, and inundation depth relative to the first-floor of the building, H_F.

Figure 5.3: Schematic illustration of the relationship between inundation height at building location (R), inundation depth at building location (H), inundation depth relative to the first-floor (H_F), height of the first-floor above the base of the building (h_F), height of base of building above sea level datum (z), and model building height (h_B) above the first-floor level.

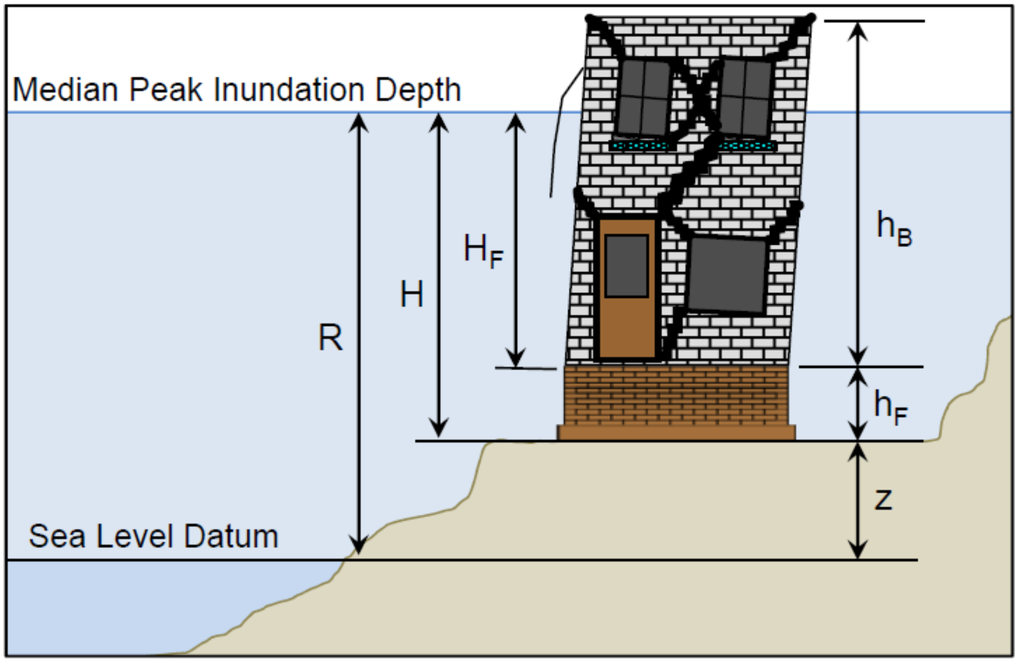

While inundation damage is related to the depth of water in the building (i.e., relative to the elevation of the first-floor that defines model building height), the hazard parameter of interest is inundation height relative to the sea level datum. To properly incorporate uncertainty in the damage state with uncertainty in inundation height, it is necessary that fragility parameters, based on water depth above the first floor, be represented in terms of water height relative to the sea level datum used to define inundation height. These parameters are related by Equation 5.9:

$$R_{dsi} = H_{Fdsi} + h_F + z \quad (5.9)$$

Where: R_{dsi} = Inundation-height-related random variable with median, $\check{R}_{dsi}$, and capacity-related logarithmic standard deviation, $\beta_{dsi|R}$, of damage state i

H_{Fdsi} = Building water depth-related random variable with median, $\hat{H}_{F\,dsi}$, and capacity-related logarithmic standard deviation, $\beta_{dsi|H}$, of damage state i

h_F = Height of first-floor above building base (in feet)

z = Height of building base above sea level datum (in feet).

The height terms, h_F and z, are treated deterministically (i.e., these terms are assumed to be known) and the relationship between the median values of R_{dsi} and HF_{dsi} is given by Equation 5.10

and the relationship between the logarithmic standard values of R_{dsi} and H_{Fdsi} is given by Equation 5.11:

$$R_{dsi} = H_{Fdsi} + h_F + z \tag{5.10}$$

$$\beta_{dsi|R} = ln\left(\frac{z + h_F + e^{\beta_{dsi|H}}\widehat{H}_{Fdsi}}{z + h_F + \widehat{H}_{Fdsi}}\right) \tag{5.11}$$

Where:

R_{dsi}	=	Median value of tsunami inundation height of damage state i (in feet)
H_{Fdsi}	=	Median value of building water depth of damage state i
h_F	=	Height of first-floor above building base (in feet)
z	=	Height of building base above sea level datum (in feet)
$\beta_{dsi\|R}$	=	lognormal standard deviation associated with the uncertainty in the damage state, ds_i, when damage is due to inundation height
$\beta_{dsi\|H}$	=	logarithmic standard deviation associated with the uncertainty in the damage state, ds_i, when damage is due to maximum depth of water in building.

The sum of terms, z + h_F, used to shift median values in Equation 5.10 and to adjust damage- state uncertainty in Equation 5.11, may be observed to have the following effects.

1. For values of z + h_F << $\hat{H}_{F\ dsi}$, damage-state uncertainty remains essentially the same (i.e., no adjustment to uncertainty for damage states with median values much greater than the median inundation height).
2. For values of z + hF >> $\hat{H}_{F\ dsi}$, uncertainty in the median value of the damage state tends to zero and the uncertainty in the hazard (i.e., inundation height) dominates the fragility of buildings whose first-floor elevation is much higher than the median inundation depth of the damage state of interest (e.g., buildings on hills).

5.4.3 Default Values of Damage Function Parameters

Default values of damage function parameters are described in terms of water depth relative to the first floor by the median value of the damage state of interest, $\hat{H}_{F\ dsi}$, and the corresponding measure of damage-state uncertainty, $\beta_{dsi|H}$. As described in previous sections, these parameters must be modified before evaluating building damage due to tsunami inundation, as described by the following three steps.

1. The median value of damage state of interest, $\hat{H}_{F\ dsi}$, is adjusted using Equation 5.0 to represent the median damage in terms of inundation height, $\check{R}_{dsi}$,

2. The value of the logarithmic standard deviation of the damage state of interest, $\beta_{dsi|H}$, is adjusted using Equation 5.11 to represent the uncertainty of the damage state of interest in terms of inundation height, $\beta_{dsi|R}$, and
3. The uncertainty in the damage state of interest, $\beta_{dsi|R}$, is combined with the uncertainty in the inundation height, β_R, using Equation 5-.4 to obtain the total uncertainty of the damage state of interest, $\beta_{dsi,R}$.

The median, $\check{R}_{dsi}$, and the logarithmic standard deviation, $\beta_{dsi,R}$, define the fragility curve of the damage state of interest for building damage due to tsunami inundation.

Table 5.7 summarizes default values of fragility parameters for evaluation of nonstructural system damage states of each model building type, and Table 5.8 summarizes default values of fragility parameters for evaluation of contents damage states of each model building type. Cells in these tables with italics indicate damage states not required to characterize flood-related damage, as described in Table 5.6, for which fragility parameters (median and logarithmic standard deviation values) are set equal to the next, more severe damage state. The basis for the default values fragility parameters is summarized below:

Basis for Default Values of Median Damage

Default values of median damage (i.e., water depth above the first-floor level) are based on the descriptions of damage given in Table 5.6 (depth of water associated with damage states), and the typical values of the building height (and corresponding number of stories) given in Table 5.1. Note: Height values given in Tables 5.1 (and repeated in Table 5.6) represent buildings whose first-floor level is at the base of the building (i.e., $h_F = 0$).

Basis for Default Values of Beta (Logarithmic Standard Deviation)

Default values of Beta (logarithmic standard deviation) are based on the two primary sources of uncertainty in the median values of damage due to tsunami flood, the height of the building and the height at which a particular state of damage is assumed to occur. These two sources of uncertainty are modeled as independent lognormal random variables, and estimates of the uncertainty in the height of the building combined with estimates of the uncertainty in the height of the damage state using the square-root-sum-of-the-squares (SRSS) method.

Table 5.7: Default values of Damage-State Parameters – Median ($\hat{H}_{F\ dsi}$) and Beta (Logarithmic Standard Deviation, $\beta_{dsi|H}$) – for Evaluation of Damage to Nonstructural Systems of Model Building Types due to Tsunami Flood

Model Building Type Name	Model Building Type Height (ft)	Moderate Damage Median (ft)	Moderate Damage Beta	Extensive Damage Median (ft)	Extensive Damage Beta	Complete Damage Median (ft)	Complete Damage Beta
W1	14	*7*	*0.77*	7	0.77	14	0.65
W2	24	*12*	*0.78*	12	0.78	24	0.65
S1L	24	*12*	*0.78*	12	0.78	24	0.65
S1M	60	12	0.62	36	0.33	60	0.35
S1H	156	12	0.65	84	0.35	156	0.36
S2L	24	*12*	*0.78*	12	0.78	24	0.65
S2M	60	12	0.62	36	0.33	60	0.35
S2H	156	12	0.65	84	0.35	156	0.36
S3	15	*7.5*	*0.77*	7.5	0.77	15	0.65
S4L	24	*12*	*0.78*	12	0.78	24	0.65
S4M	60	12	0.62	36	0.33	60	0.35
S4H	156	12	0.65	84	0.35	156	0.36
S5L	24	*12*	*0.78*	12	0.78	24	0.65
S5M	60	12	0.62	36	0.33	60	0.35
S5H	156	12	0.65	84	0.35	156	0.36
C1L	20	*10*	*0.78*	10	0.78	20	0.65
C1M	50	10	0.62	30	0.33	50	0.35
C1H	120	10	0.65	60	0.36	120	0.36
C2L	20	*10*	*0.78*	10	0.78	20	0.65
C2M	50	10	0.62	30	0.33	50	0.35
C2H	120	10	0.65	60	0.36	120	0.36
C3L	20	*10*	*0.78*	10	0.78	20	0.65
C3M	50	10	0.62	30	0.33	50	0.35
C3H	120	10	0.65	60	0.36	120	0.36
PC1	15	*7.5*	*0.77*	7.5	0.77	15	0.65
PC2L	20	*10*	*0.78*	10	0.78	20	0.65
PC2M	50	10	0.62	30	0.33	50	0.35
PC2H	120	10	0.65	60	0.36	120	0.36
RM1L	20	*10*	*0.78*	10	0.78	20	0.65
RM1M	50	10	0.62	30	0.33	50	0.35
RM2L	20	*10*	*0.78*	10	0.78	20	0.65
RM2M	50	10	0.62	30	0.33	50	0.35
RM2H	120	10	0.65	60	0.36	120	0.36
URML	15	*7.5*	*0.77*	7.5	0.77	15	0.65
URMM	36	12	0.65	24	0.43	36	0.49
MH	10	*5*	*0.72*	5	0.72	10	0.59

Table 5.8: Default values of Damage-State Parameters – Median ($\hat{H}_{F\ dsi}$) and Beta (Logarithmic Standard Deviation, $\beta_{dsi|H}$) – for Evaluation of Damage to Contents of Model Building Types due to Tsunami Flood

Model Building Type Name	Model Building Type Height (ft)	Moderate Damage Median (ft)	Moderate Damage Beta	Extensive Damage Median (ft)	Extensive Damage Beta	Complete Damage Median (ft)	Complete Damage Beta
W1	14	*3*	*0.65*	*3*	*0.65*	3	0.65
W2	24	*3*	*0.78*	3	0.78	15	0.65
S1L	24	*3*	*0.78*	3	0.78	15	0.65
S1M	60	3	0.62	27	0.35	51	0.35
S1H	156	3	0.65	75	0.36	147	0.35
S2L	24	*3*	*0.78*	3	0.78	15	0.65
S2M	60	3	0.62	27	0.35	51	0.35
S2H	156	3	0.65	75	0.36	147	0.35
S3	15	*3*	*0.65*	*3*	*0.65*	3	0.65
S4L	24	*3*	*0.78*	3	0.78	15	0.65
S4M	60	3	0.62	27	0.35	51	0.35
S4H	156	3	0.65	75	0.36	147	0.35
S5L	24	*3*	*0.78*	3	0.78	15	0.65
S5M	60	3	0.62	27	0.35	51	0.35
S5H	156	3	0.65	75	0.36	147	0.35
C1L	20	*3*	*0.78*	3	0.78	13	0.65
C1M	50	3	0.62	23	0.35	43	0.35
C1H	120	3	0.65	53	0.36	113	0.35
C2L	20	*3*	*0.78*	3	0.78	13	0.65
C2M	50	3	0.62	23	0.35	43	0.35
C2H	120	3	0.65	53	0.36	113	0.35
C3L	20	*3*	*0.78*	3	0.78	13	0.65
C3M	50	3	0.62	23	0.35	43	0.35
C3H	120	3	0.65	53	0.36	113	0.35
PC1	15	*3*	*0.65*	*3*	*0.65*	3	0.65
PC2L	20	*3*	*0.78*	3	0.78	13	0.65
PC2M	50	3	0.62	23	0.35	43	0.35
PC2H	120	3	0.65	53	0.36	113	0.35
RM1L	20	*3*	*0.78*	3	0.78	13	0.65
RM1M	50	3	0.62	23	0.35	43	0.35
RM2L	20	*3*	*0.78*	3	0.78	13	0.65
RM2M	50	3	0.62	23	0.35	43	0.35
RM2H	120	3	0.65	53	0.36	113	0.35
URML	15	*3*	*0.65*	*3*	*0.65*	3	0.65
URMM	36	3	0.65	15	0.49	27	0.56
MH	10	*3*	*0.59*	*3*	*0.59*	3	0.59

Example Estimate of Flood Damage-State Uncertainty

The two primary sources of uncertainty in the median values of damage due to tsunami flood are 1) the height of the building, and 2) the height at which a particular state of damage is assumed to occur.

Estimates of the uncertainty in the height of the model building type are based on the range of heights that the model building type represents. Since model building types typically represent a relatively large range of heights (i.e., number of stories) the uncertainty in building height is significant. For example, larger wood structures (W2) are nominally two-stories (24 feet) in height, but could be only one-story (12 feet) or as tall as five-stories (60 feet), although heights above three-stories are not common. The range of heights of one-story to three-stories (36 feet) is assumed to roughly represent plus or minus one standard deviation from the median and the corresponding uncertainty in building height is calculated as, ln(36/12)/2, or a beta of about 0.55 due to building height uncertainty.

Estimates of the uncertainty in the height of water associated with the damage state of interest are based on the range of heights that could cause the damage state of interest – typically plus or minus the height of an individual story, or portion thereof for shorter buildings (e.g., one-story and two-story model building types). For example, the Complete damage state of nonstructural systems of a nominal two-story wood (W2) building has a median water depth of 24 feet (building must be fully inundated to have Complete damage), but the height of water that could cause Complete damage is assumed to vary by as much as plus or minus 8 feet (2/3 of story height) or from 16 feet to 32 feet of water, and the corresponding uncertainty in the median is estimated as, ln(32/16)/2, or a beta of about 0.35, assuming this range roughly represents plus or minus one standard deviation from the median.

SRSS combination of the uncertainty in actual building height (0.55) and the uncertainty in the level of water that actually causes Complete damage (0.35) yields a combined uncertainty of about 0.65, the value of beta given in Table 5.7 for Complete damage to nonstructural systems of the W2 model building type. In general, uncertainty is larger for shorter model building types, since the ratio of the range of heights tend to be larger (i.e., variation of a few feet of water is more important to the variation in damage of one-story or two-story buildings than to the variation damage to mid-rise or high-rise buildings).

5.5 Building Damage Functions Due to Tsunami Flow

5.5.1 Overview

This section describes the approach and develops default values of building damage functions due to tsunami flow (lateral force). Default values of the median and logarithmic standard deviation describe the probability of damage to the structure (STR) for each model building type listed in Table 5.1. Tsunami inundation damage is characterized by the Moderate, Extensive, and Complete damage states, identified in Table 5.5 and described in Table 5.6.

5.5.2 Approach

Building damage to the structure due to tsunami flow is assumed to be caused by hydrodynamic forces and debris impact forces. Tsunami flow forces also affect nonstructural components and contents (e.g., walls at the building's perimeter), but nonstructural and contents damage due to tsunami flow is assumed to be encompassed by tsunami flood damage functions (e.g., since walls affected by tsunami flow are also damaged by inundation). Further, and of most significance, nonstructural systems and contents of buildings found to have Complete structure damage due to tsunami flow are assumed to have Complete damage. The assumption of Complete building damage, if the structure sustains Complete damage, is consistent with observed damage due to tsunami (i.e., buildings whose structure failed were either collapsed or washed away).

Development of building damage functions for tsunami flow utilizes an "engineering" approach that is based on the same concepts used for design of structures for tsunami lateral loads, such as those described in the "Guidelines for Design of Structures for Vertical Evacuation from Tsunamis," FEMA P646 (FEMA, 2012). In general, tsunami flow forces create a variety of different loads on structures, including:

1. Hydrostatic forces (i.e., lateral force on walls, etc., due to the pressure of standing water or very low velocity water flow),
2. Buoyant forces (i.e., vertical hydrostatic forces on the structure due to the volume of water displaced by a submerged building, of portion thereof),
3. Hydrodynamic forces (i.e., lateral force on the structure or individual elements due to water flow moving at moderate- or high-velocities),
4. Impulsive forces (i.e., additional lateral force caused by the leading edge of a surge of water impacting a structure, increasing local hydrodynamic loads by as much a factor of 1.5),
5. Debris impact forces (i.e., lateral force from waterborne debris (e.g., floating trees, autos, boats, shipping containers, and debris from other buildings)), and
6. Debris damming forces (i.e., additional lateral force due to the accumulation of debris across the building components resisting hydrodynamic loads).

Few buildings have been designed for tsunami loads, but the design concepts provide a basis for characterizing the strength of model building types in terms of tsunami loads and parameters, namely hydrodynamic loads characterized by momentum flux. In addition to hydrodynamic forces, this approach also incorporates, in an approximate manner, additional lateral force due to debris impact forces.

Damage to the structural system due to hydrodynamic forces is highly dependent on the configuration of the building at lower floor levels. For example, buildings that are open at their base or have perimeter elements that fail either by chance or by design (i.e., breakaway walls) and permit water to flow through the building greatly reduce the hydrodynamic forces on the overall structure. The model building types represent generic configurations defined solely in terms of the number of floors (height) and the total square footage, so the base of the building could be either fully open, partially open, or closed. The tsunami building damage functions assume that each model building type is closed at its base (i.e., does not have breakaway walls, or open areas). Although, windows and doors are likely to allow some water into the building, tsunami flood waters are assumed to flow around the full footprint of the building. This assumption produces maximum hydrodynamic forces on the structure of the building.

Hydrodynamic forces can cause damage to individual structural elements as well as to the overall structural system. In certain cases, failure of individual elements can lead to progressive collapse of the building. Model building types represent generic structural systems defined solely in terms of material, type of construction, and age of construction; insufficient information to evaluate damage to individual structural elements and the likelihood of progressive collapse of the structure. The tsunami building damage functions assume that Complete damage to the structural system due to hydrodynamic forces (and debris impact) occurs before progressive collapse (due to failure of individual structural elements). That is, evaluation of the overall capacity of the structural system is considered a reasonable surrogate for other failure mechanisms that are too complex to evaluate for generic model building types. In addition to hydrodynamic forces, other failure mechanisms include damage to individual structural elements due to hydrostatic forces, impulsive forces, and debris impact forces.

Buoyant forces can cause uplift of smaller buildings when there is a significant difference in the level of water inside and outside of the building, and reduce the effective weight of the building required to resist overturning due to lateral (hydrodynamic) forces. The effect of buoyant forces is most significant for shorter, lighter structures which have less effective weight per unit area at their base. For example, manufactured housing (mobile homes) is particularly susceptible to buoyant forces and would only require about one foot of water above the first-floor level to “float away” (assuming the building was unanchored and water tight).

The tsunami building damage functions assume that Complete damage due to hydrodynamic forces will occur before building uplift can occur due to buoyant forces. It may be noted that the model building types most susceptible to buoyant forces are also the model building types most susceptible to hydrodynamic forces. In the case of a typical (minimally anchored) manufactured housing unit, the median momentum flux of the Complete damage state is only 16 ft^3/sec^2 (Table 5.14), which corresponds to about one foot of water (moving at four feet/second). That is, the unit would be “washed away” by roughly the same depth of water that could cause it to “float away.”

Debris damming forces can increase the effective hydrodynamic forces on the structure due to accumulation of debris across the structural frame. The effects of debris damming are most critical for buildings with an open configuration at their base for which the accumulated debris restricts water flow through the building, but of little or no consequence to buildings that are closed across their base. The tsunami building damage functions ignore the effects of debris damming since they are based on the assumption that the building is fully closed at its base such that water must flow around the full footprint of the building.

Debris impact forces can cause damage to the overall structure (as well as to individual structural elements). Debris impact forces are modeled by a factor, Kd, that increases hydrodynamic forces on the structure to account for the additional lateral forces due to debris impact. Values of the Kd factor greater than 1.0 effectively increase the likelihood of Complete damage to the structure when the building is assumed to be impacted by waterborne debris. Note: Values of the Kd factor less than 1.0 are used to effectively decrease the likelihood of Complete damage to the structure when the building is assumed to be shielded from tsunami flow by other buildings or structures.

The tsunami building damage functions do not explicitly include the effects of erosion and scour which can significantly influence stability and settlement of the shallow foundations, particularly for building sites near the shoreline on unconsolidated sediments. While post-FIRM construction in coastal high hazard areas (V-Zone) are most likely on piles and piers, pre-FIRM construction and post-FIRM construction in the more inland areas typically use shallow foundations (Table 5.3), unless the building is heavy or tall enough to require a deep foundation.

The tsunami building damage functions assume that hydrodynamic loads (including the effects of debris) cause Complete damage to the structural system prior to foundation failure. It may be noted that the model building types most susceptible to erosion and scour (i.e., smaller, older buildings) are also the model building types most susceptible to damage and failure due to hydrodynamic forces. For the most common model building type, W1, typical of older residences, the median momentum flux of the Complete damage state is 247 ft^3/sec^2 (Table 5.14, Pre-Code), which corresponds to about 6.5 feet of water (moving at 6 feet/second).

The tsunami building functions assume that Complete damage to the structural system occurs when hydrodynamic forces (increased for debris impact, or reduced for shielding effects) exceed the lateral force capacity (i.e., pushover) strength of the model building of interest. Estimates of the lateral force capacity of model building types are available from the Earthquake Model, as described in the following sections.

The Earthquake Model is a convenient source of the approximate lateral strength of the structural system of model building types. Lateral strength is an inherent property of the structural system, whether the building is designed for earthquake loads, wind loads, or not designed for lateral loads (even buildings not designed for lateral loads still have inherent lateral strength). The Earthquake Model includes estimates of lateral strength for buildings not designed for earthquake loads (referred to as Pre-Code buildings) as well as those that are designed for earthquake loads.

Lateral force capacity varies with the seismic design level of the structure, which has been deduced from model building data (e.g., location and age), as described in Section 5.4 of the Earthquake Model *Technical Manual* (FEMA, 2011a). The Earthquake Model defines seven seismic design levels encompassing both "common" buildings (e.g., Risk Category II structures, ASCE 7-10) and "special" buildings, such as hospitals and emergency centers (e.g., Risk Category IV structures, ASCE 7-10). Table 5.9 describes these seven seismic design levels in terms of the risk categories and seismic design categories (SDCs) of ASCE 7-10 (ASCE 2010). These relationships apply to buildings designed to current code design requirements).

Table 5.9: Relationship of Hazus Seismic Design Levels and the Risk Categories and Seismic Design Categories (SDCs) of ASCE 7 (ASCE, 2010)

Hazus Seismic Design Level ASCE 7 Seismic Design Criteria Description	Hazus Seismic Design LevelASCE 7 Seismic Design Criteria Symbol	Hazus Seismic Design LevelASCE 7 Seismic Design Criteria Risk Category	Hazus Seismic Design LevelASCE 7 Seismic Design Criteria SDC
High-Code	HC	I - III	D (E)
Moderate-Code	MC	I - III	C
Low-Code	LC	I - III	B
Pre-Code (no seismic design)	PC	I - III	A
Special High-Code	HS	IV	D (F)
Special Moderate-Code	MS	IV	D
Special Low-Code	LS	IV	C

Most buildings were designed and constructed to older vintages of seismic codes (e.g., *Uniform Building Code*) and standards (or not designed for earthquake), and the inventory schemes of Chapter 5 of the Earthquake Model associate the most suitable seismic design level with model building type based on the age and other pertinent inventory data. Table 5.10 provides recommendations for selecting the appropriate seismic design level based on the age of the building and the seismic zone location of the building. Note that these vintage years along with benchmark code adoption information for each tsunami risk State and Territory were used to estimate the seismic design level assignments for the General Building Stock inventory described in Chapter 3.

Table 5.10: Recommended Seismic Design Levels for Existing Buildings without Retrofit

Uniform Building Code	Design Vintage: Post-1975	Design Vintage: 1941 - 1975	Design Vintage: Pre-1941
Zone 4	High-Code	Moderate-Code	Pre-Code[1]
Zone 3	Moderate-Code	Moderate-Code	Pre-Code[1]
Zone 2B	Moderate-Code	Low-Code	Pre-Code[2]
Zone 2A	Low-Code	Low-Code	Pre-Code[2]
Zone 1	Low-Code	Pre-Code[2]	Pre-Code[2]
Zone 0	Pre-Code[2]	Pre-Code[2]	Pre-Code[2]

1. *Assume Moderate-Code design for residential wood-frame buildings (W1).*
2. *Assume Low-Code design for residential wood-frame buildings (W1).*

The Earthquake Model defines the pushover strength (capacity) of model building types in terms of seismic design parameters (e.g., seismic design coefficient C_S) and other related factors, as shown in Figure 5.4. Median values of damage states defined by drift-related criteria are represented by points of peak spectral response located along this curve, as illustrated in Figure 5.4.

Figure 5.4: Example building capacity curve and control points

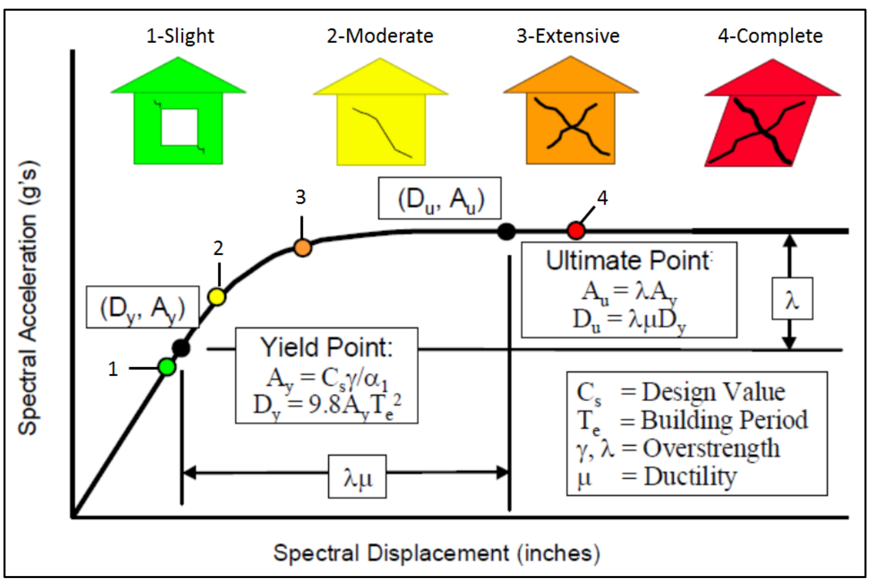

The simple, underlying notion of building damage functions for damage due to tsunami flow is to equate hydrodynamic forces, incorporating the effects of impulsive and debris loads, with the lateral force (pushover) strength of model building types as defined by the properties of capacity curves of the Hazus Earthquake Model. This approach assumes parity in the building damage states which is reasonable, except for collapse.

Earthquake ground motions are vibratory in nature, often intense, but peak forces are typically of short duration (i.e., a few seconds, at most, in a given direction). Hence, buildings can reach their full strength (i.e., reach the plateau of capacity curve in Figure 5.4), but not necessarily displace far enough to collapse before the earthquake force reverses direction. In contrast, peak tsunami flow force is sustained in a given direction for a relatively long period of time (i.e., several minutes), and buildings that have reached their full strength are much more likely to collapse (and possibly be washed away with the flow). Thus, the likelihood of collapse given Complete damage for tsunami flow forces is much higher than that of earthquake.

The lateral force (pushover) strength of a given model building type is defined by the yield capacity and the ultimate capacity, as given by Equations 5.12 and 5.13:

$$F_Y = \propto_1 A_y W \qquad (5.12)$$

$$F_U = \propto_1 A_u W \qquad (5.13)$$

Where:

- F_Y = Initial yield force at base of building (kips or 1,000 pounds-force)
- F_U = Ultimate (pushover) force at base of building (kips)
- α_1 = Modal mass parameter (Table 5.5, Hazus EQ *Technical Manual*)
- A_Y = Spectral acceleration at yield (Table 5.7 Hazus EQ *Technical Manual*)
- A_U = Spectral acceleration at ultimate (Table 5.7 Hazus EQ *Technical Manual*)
- W = Total building seismic design weight (kips)

Lateral shear strength of the structure at the base of the building is assumed to be unaffected by buoyant forces, if any, and W represents the full seismic design weight of the building.

Lateral tsunami flow force, F_{TS}, on a model building type is given by Equation 5.14:

$$F_{TS} = K_d\left(0.5\rho_s C_d B(hv^2)\right) = 0.00219\, K_d B(hv^2) \qquad (5.14)$$

Where:

- F_{TS} = Tsunami force on building (kips)
- K_d = Coefficient used to modify basic hydrodynamic force for lower values of force due to the effects of shielding, etc., and for higher values of force due to the effects of debris impact, etc. (nominal value, K_d = 1.0)
- ρ_S = Fluid density assumed to be 1.1 x 0.064 kips/ft^3 / 32.2 ft/sec^2)

C_d = Drag coefficient (C_d = 2.0, based on FEMA P646 (FEMA, 2012)

B = Plan dimension normal to flow direction (feet)

hv^2 = Median value of maximum momentum flux (ft^3/sec^2)

5.5.3 Default Values of Damage Function Parameters

Default values of damage function parameters are described in terms of maximum momentum flux for the damage state of interest, $\hat{F}_{dsi}$, and the corresponding measure of damage-state uncertainty, $\beta_{dsi|F}$.

Tables 5.11 through 5.17 summarize default values of fragility parameters of each model building type for each of the seven seismic design levels of the Earthquake Model. In these tables, shaded cells indicate damage states not required to characterize flow-related damage, as described in Table 5.6, for which fragility parameters (median and logarithmic standard deviation values) are set equal to the next more severe damage state. The basis for the default values of fragility parameters is summarized below:

Basis for Default Values of Median Damage

Default values of median damage (i.e., maximum momentum flux) are based on the descriptions of damage given in Table 5.6 (for damage to the structure) and the following assumptions:

1. Complete structure damage – Complete damage to the structure occurs when tsunami force is equal to earthquake ultimate force (F_U) capacity of the model building type of interest.
2. Moderate damage – Moderate damage to the structure occurs when tsunami force is equal to earthquake yield force (F_Y) capacity of the model building type of interest.

   Exception: Significant tsunami damage can occur to the foundation and individual structural elements at lower floors of mid-rise and high-rise buildings before the structural system reaches yield. To account for this localized damage, in an approximate manner, Moderate damage (at lower floors) of mid-rise and high-rise buildings is assumed to occur for the same level of tsunami force that causes Extensive damage to low-rise buildings of the same model building type.
3. Extensive structure damage – Extensive damage to the structure occurs when tsunami force is equal to earthquake force corresponding to the average of the yield force and ultimate force, $(F_Y + F_U)/2$, capacities of the model building type of interest.

The above assumptions are used with Equations 5.12, 5.13, and 5.14 to define damage-state medians, as follows:

$$\hat{F}_{dsM} = 457(\propto_1 A_Y W)/(K_d B) \quad (5.15)$$

(5.16)

$$\hat{F}_{dsE} = 457\left(\propto_1 \left(\frac{A_y + A_U}{2}\right)W\right)/(K_d B)$$

$$\hat{F}_{dsC} = 457(\propto_1 A_U W)/(K_d B) \quad (5.17)$$

Where: $\hat{F}_{dsM}$ = Median value of Moderate structure damage due to tsunami flow (ft/sec)

$\hat{F}_{dsE}$ = Median value of Extensive structure damage due to tsunami flow (ft/sec)

$\hat{F}_{dsC}$ = Median value of Complete structure damage due to tsunami flow (ft/sec)

α_1 = Model mass parameter (Table 5.5, Hazus EQ *Technical Manual*)

A_Y = Spectral acceleration at yield (g) (Table 5.7 Hazus EQ *Technical Manual*)

A_U = Spectral acceleration at ultimate (g) (Table 5.7 Hazus EQ *Technical Manual*)

W = Total building seismic design weight (kips), as defined in Table 5.18

K_d = Coefficient modifying basic hydrodynamic force (nominal value, K_d = 1.0)

B = Plan dimension normal to flow direction (feet), as defined in Table 5.18.

Table 5.18 summarizes the assumed values of model building type total seismic design weight (W), total building area, average unit floor weight per square foot (w), and plan dimension (B) used to develop default parameters of tsunami flow building damage functions. Damage-state medians are based on hydrodynamic loads that assume no debris impact and no shielding from other buildings and structures (i.e., K_d = 1.0).

Basis for Default Values of Beta (Logarithmic Standard Deviation)

Default values of Beta (logarithmic standard deviation) are based on the three primary sources of uncertainty in the median values of tsunami flow damage, the uncertainty in building capacity associated with median damage (i.e., $\alpha_1 A_u W$ term), the uncertainty in hydrodynamic loads associated with possible debris impact or conversely, possible shielding from other structures (i.e., the K_d factor), and the uncertainty associated with the plan dimension of the side of the building facing tsunami flow (i.e., the B dimension of the building). These three sources of uncertainty are modeled as independent lognormal random variables, and individual estimates of the uncertainties are combined using square-root-sum-of-the-squares (SRSS) method.

Table 5.11: Default value of Damage-State Parameters-Median (F_{dsi}) and Beta ($\beta_{dsi|F}$) – for Evaluation of Damage to the Structure of High-Code Seismic Design Model Building Types due to Tsunami Flow

MBT Name	Moderate Damage Median (ft^3/s^2)	Moderate Damage Beta	Extensive Damage Median (ft3/s2)	Extensive Damage Beta	Complete Damage Median (ft3/s2)	Complete Damage Beta
W1	494	0.74	494	0.74	494	0.74
W2	1,371	0.73	1,371	0.73	1,371	0.73
S1L	3,913	0.74	3,913	0.74	5,868	0.74
S1M	3,913	0.79	9,656	0.79	15,399	0.79
S1H	3,913	0.79	13,706	0.79	23,500	0.79
S2L	4,407	0.60	4,407	0.60	5,876	0.60
S2M	4,407	0.67	12,491	0.67	20,575	0.67
S2H	4,407	0.67	19,859	0.67	35,311	0.67
S3	823	0.60	823	0.60	823	0.60
S4L	4,583	0.64	4,583	0.64	6,346	0.64
S4M	4,583	0.70	12,574	0.70	20,565	0.70
S4H	4,583	0.70	19,939	0.70	35,295	0.70
S5L	1,170	0.74	1,170	0.74	1,758	0.74
S5M	1,170	0.79	2,724	0.79	4,278	0.79
S5H	1,170	0.80	3,838	0.80	6,505	0.80
C1L	4,696	0.74	4,696	0.74	7,041	0.74
C1M	4,696	0.79	13,755	0.79	22,813	0.79
C1H	4,696	0.79	14,399	0.79	24,102	0.79
C2L	6,170	0.67	6,170	0.67	8,814	0.67
C2M	6,170	0.73	17,360	0.73	28,551	0.73
C2H	6,170	0.73	25,720	0.73	45,270	0.73
C3L	1,170	0.74	1,170	0.74	1,758	0.74
C3M	1,170	0.79	3,259	0.79	5,347	0.79
C3H	1,170	0.80	3,588	0.80	6,005	0.80
PC1	2,350	0.60	2,350	0.60	2,350	0.60
PC2L	5,288	0.60	5,288	0.60	7,051	0.60
PC2M	5,288	0.67	14,075	0.67	22,861	0.67
PC2H	5,288	0.67	20,752	0.67	36,216	0.67
RM1L	5,872	0.60	5,872	0.60	7,829	0.60
RM1M	5,872	0.67	16,648	0.67	27,423	0.67
RM2L	7,046	0.60	7,046	0.60	9,395	0.60
RM2M	7,046	0.67	18,758	0.67	30,470	0.67
RM2H	7,046	0.67	27,656	0.67	48,265	0.67
URML	506	0.66	506	0.66	506	0.66
URMM	506	0.67	1,884	0.67	3,261	0.67
MH	33	0.60	33	0.60	33	0.60

Table 5.12: Default values of Damage-State Parameters – Median (F_{dsi}) and Beta ($\beta_{dsi|F}$) – for Evaluation of Damage to the Structure of Moderate-Code Seismic Design Model Building Types due to Tsunami Flow

MBT Name	Moderate Damage: Median (ft^3/s^2)	Moderate Damage: Beta	Extensive Damage: Median (ft^3/s^2)	Extensive Damage: Beta	Complete Damage: Median (ft^3/s^2)	Complete Damage: Beta
W1	370	0.74	370	0.74	370	0.74
W2	686	0.73	686	0.73	686	0.73
S1L	1,959	0.74	1,959	0.74	2,938	0.74
S1M	1,959	0.79	4,829	0.79	7,700	0.79
S1H	1,959	0.79	6,874	0.79	11,790	0.79
S2L	2,203	0.60	2,203	0.60	2,938	0.60
S2M	2,203	0.67	6,238	0.67	10,272	0.67
S2H	2,203	0.67	9,929	0.67	17,655	0.67
S3	411	0.60	411	0.60	411	0.60
S4L	2,292	0.64	2,292	0.64	3,173	0.64
S4M	2,292	0.70	6,287	0.70	10,283	0.70
S4H	2,292	0.70	9,950	0.70	17,609	0.70
S5L	1,170	0.74	1,170	0.74	1,758	0.74
S5M	1,170	0.79	2,724	0.79	4,278	0.79
S5H	1,170	0.80	3,838	0.80	6,505	0.80
C1L	2,350	0.74	2,350	0.74	3,525	0.74
C1M	2,350	0.79	6,879	0.79	11,407	0.79
C1H	2,350	0.79	7,221	0.79	12,092	0.79
C2L	3,085	0.67	3,085	0.67	4,407	0.67
C2M	3,085	0.73	8,689	0.73	14,293	0.73
C2H	3,085	0.73	12,842	0.73	22,600	0.73
C3L	1,170	0.74	1,170	0.74	1,758	0.74
C3M	1,170	0.79	3,259	0.79	5,347	0.79
C3H	1,170	0.80	3,588	0.80	6,005	0.80
PC1	1,175	0.60	1,175	0.60	1,175	0.60
PC2L	2,644	0.60	2,644	0.60	3,525	0.60
PC2M	2,644	0.67	7,029	0.67	11,414	0.67
PC2H	2,644	0.67	10,376	0.67	18,108	0.67
RM1L	2,938	0.60	2,938	0.60	3,915	0.60

MBT Name	Moderate Damage: Median (ft^3/s^2)	Moderate Damage: Beta	Extensive Damage: Median (ft^3/s^2)	Extensive Damage: Beta	Complete Damage: Median (ft^3/s^2)	Complete Damage: Beta
RM1M	2,938	0.67	8,317	0.67	13,696	0.67
RM2L	3,525	0.60	3,525	0.60	4,698	0.60
RM2M	3,525	0.67	9,372	0.67	15,218	0.67
RM2H	3,525	0.67	13,811	0.67	24,097	0.67
URML	506	0.66	506	0.66	506	0.66
URMM	506	0.67	1,884	0.67	3,261	0.67
MH	33	0.60	33	0.60	33	0.60

Table 5.13: Default values of Damage-State Parameters – Median (F_{dsi}) and Beta ($\beta_{dsi|F}$) – for Evaluation of Damage to the Structure of Low-Code Seismic Design Model Building Types due to Tsunami Flow

MBT Name	Moderate Damage: Median (ft^3/s^2)	Moderate Damage: Beta	Extensive Damage: Median (ft^3/s^2)	Extensive Damage: Beta	Complete Damage: Median (ft^3/s^2)	Complete Damage: Beta
W1	247	0.74	247	0.74	247	0.74
W2	343	0.73	343	0.73	343	0.73
S1L	975	0.74	975	0.74	1,465	0.74
S1M	975	0.79	2,413	0.79	3,850	0.79
S1H	975	0.80	3,415	0.80	5,855	0.80
S2L	1,102	0.60	1,102	0.60	1,469	0.60
S2M	1,102	0.67	3,127	0.67	5,152	0.67
S2H	1,102	0.67	4,965	0.67	8,828	0.67
S3	206	0.60	206	0.60	206	0.60
S4L	1,146	0.64	1,146	0.64	1,586	0.64
S4M	1,146	0.70	3,144	0.70	5,141	0.70
S4H	1,146	0.70	4,975	0.70	8,805	0.70
S5L	1,170	0.74	1,170	0.74	1,758	0.74
S5M	1,170	0.79	2,724	0.79	4,278	0.79
S5H	1,170	0.80	3,838	0.80	6,505	0.80
C1L	1,170	0.74	1,170	0.74	1,758	0.74
C1M	1,170	0.79	3,259	0.79	5,347	0.79
C1H	1,170	0.80	3,588	0.80	6,005	0.80

MBT Name	Moderate Damage: Median (ft^3/s^2)	Moderate Damage: Beta	Extensive Damage: Median (ft^3/s^2)	Extensive Damage: Beta	Complete Damage: Median (ft^3/s^2)	Complete Damage: Beta
C2L	1,542	0.67	1,542	0.67	2,203	0.67
C2M	1,542	0.74	4,336	0.74	7,129	0.74
C2H	1,542	0.74	6,439	0.74	11,335	0.74
C3L	1,170	0.74	1,170	0.74	1,758	0.74
C3M	1,170	0.79	3,259	0.79	5,347	0.79
C3H	1,170	0.80	3,588	0.80	6,005	0.80
PC1	588	0.60	588	0.60	588	0.60
PC2L	1,322	0.60	1,322	0.60	1,763	0.60
PC2M	1,322	0.67	3,523	0.67	5,724	0.67
PC2H	1,322	0.67	5,188	0.67	9,054	0.67
RM1L	1,469	0.60	1,469	0.60	1,961	0.60
RM1M	1,469	0.67	4,159	0.67	6,848	0.67
RM2L	1,763	0.60	1,763	0.60	2,353	0.60
RM2M	1,763	0.67	4,686	0.67	7,609	0.67
RM2H	1,763	0.67	6,906	0.67	12,048	0.67
URML	506	0.66	506	0.66	506	0.66
URMM	506	0.67	1,884	0.67	3,261	0.67
MH	33	0.60	33	0.60	33	0.60

Table 5.14: Default values of Damage-State Parameters-Median (F_{dsi}) and Beta ($\beta_{dsi|F}$) – for Evaluation of Damage to the Structure of Pre-Code Seismic Design Model Building Types due to Tsunami Flow

MBT Name	Moderate Damage: Median (ft^3/s^2)	Moderate Damage: Beta	Extensive Damage: Median (ft3/s2)	Extensive Damage: Beta	Complete Damage: Median (ft3/s2)	Complete Damage: Beta
W1	247	0.74	247	0.74	247	0.74
W2	343	0.73	343	0.73	343	0.73
S1L	975	0.74	975	0.74	1,465	0.74
S1M	975	0.79	2,413	0.79	3,850	0.79
S1H	975	0.80	3,415	0.80	5,855	0.80

MBT Name	Moderate Damage: Median (ft^3/s^2)	Moderate Damage: Beta	Extensive Damage: Median (ft3/s2)	Extensive Damage: Beta	Complete Damage: Median (ft3/s2)	Complete Damage: Beta
S2L	1,102	0.60	1,102	0.60	1,469	0.60
S2M	1,102	0.67	3,127	0.67	5,152	0.67
S2H	1,102	0.67	4,965	0.67	8,828	0.67
S3	206	0.60	206	0.60	206	0.60
S4L	1,146	0.64	1,146	0.64	1,586	0.64
S4M	1,146	0.70	3,144	0.70	5,141	0.70
S4H	1,146	0.70	4,975	0.70	8,805	0.70
S5L	1,170	0.74	1,170	0.74	1,758	0.74
S5M	1,170	0.79	2,724	0.79	4,278	0.79
S5H	1,170	0.80	3,838	0.80	6,505	0.80
C1L	1,170	0.74	1,170	0.74	1,758	0.74
C1M	1,170	0.79	3,259	0.79	5,347	0.79
C1H	1,170	0.80	3,588	0.80	6,005	0.80
C2L	1,542	0.67	1,542	0.67	2,203	0.67
C2M	1,542	0.74	4,336	0.74	7,129	0.74
C2H	1,542	0.74	6,439	0.74	11,335	0.74
C3L	1,170	0.74	1,170	0.74	1,758	0.74
C3M	1,170	0.79	3,259	0.79	5,347	0.79
C3H	1,170	0.80	3,588	0.80	6,005	0.80
PC1	588	0.60	588	0.60	588	0.60
PC2L	1,322	0.60	1,322	0.60	1,763	0.60
PC2M	1,322	0.67	3,523	0.67	5,724	0.67
PC2H	1,322	0.67	5,188	0.67	9,054	0.67
RM1L	1,469	0.60	1,469	0.60	1,961	0.60
RM1M	1,469	0.67	4,159	0.67	6,848	0.67
RM2L	1,763	0.60	1,763	0.60	2,353	0.60
RM2M	1,763	0.67	4,686	0.67	7,609	0.67
RM2H	1,763	0.67	6,906	0.67	12,048	0.67
URML	506	0.66	506	0.66	506	0.66
URMM	506	0.67	1,884	0.67	3,261	0.67
MH	16	0.60	16	0.60	16	0.60

Table 5.15: Default values of Damage-State Parameters – Median (F_{dsi}) and Beta ($\beta_{dsi|F}$) for Evaluation of Damage to the Structure of Special High-Code Seismic Design Model Building Types due to Tsunami Flow

MBT Name	Moderate Damage: Median (ft^3/s^2)	Moderate Damage: Beta	Extensive Damage: Median (ft3/s2)	Extensive Damage: Beta	Complete Damage: Median (ft3/s2)	Complete Damage: Beta
W1	740	0.74	740	0.74	740	0.74
W2	2,057	0.73	2,057	0.73	2,057	0.73
S1L	5,872	0.74	5,872	0.74	8,806	0.74
S1M	5,872	0.79	14,485	0.79	23,099	0.79
S1H	5,872	0.79	20,581	0.79	35,290	0.79
S2L	6,610	0.60	6,610	0.60	8,814	0.60
S2M	6,610	0.67	18,729	0.67	30,848	0.67
S2H	6,610	0.67	29,788	0.67	52,966	0.67
S3	1,234	0.60	1,234	0.60	1,234	0.60
S4L	6,875	0.64	6,875	0.64	9,519	0.64
S4M	6,875	0.70	18,861	0.70	30,848	0.70
S4H	6,875	0.70	29,890	0.70	52,905	0.70
S5L	1,763	0.73	1,763	0.73	2,642	0.73
S5M	1,763	0.79	4,099	0.79	6,435	0.79
S5H	1,763	0.79	5,783	0.79	9,803	0.79
C1L	7,046	0.74	7,046	0.74	10,567	0.74
C1M	7,046	0.80	20,651	0.80	34,257	0.80
C1H	7,046	0.79	21,620	0.79	36,194	0.79
C2L	9,254	0.67	9,254	0.67	13,220	0.67
C2M	9,254	0.73	26,049	0.73	42,844	0.73
C2H	9,254	0.73	38,562	0.73	67,870	0.73
C3L	1,763	0.73	1,763	0.73	2,642	0.73
C3M	1,763	0.79	4,892	0.79	8,020	0.79
C3H	1,763	0.79	5,406	0.79	9,049	0.79
PC1	3,525	0.60	3,525	0.60	3,525	0.60
PC2L	7,932	0.60	7,932	0.60	10,576	0.60
PC2M	7,932	0.67	21,104	0.67	34,275	0.67
PC2H	7,932	0.67	31,128	0.67	54,325	0.67
RM1L	8,814	0.60	8,814	0.60	11,751	0.60

MBT Name	Moderate Damage: Median (ft^3/s^2)	Moderate Damage: Beta	Extensive Damage: Median (ft3/s2)	Extensive Damage: Beta	Complete Damage: Median (ft3/s2)	Complete Damage: Beta
RM1M	8,814	0.67	24,967	0.67	41,120	0.67
RM2L	10,576	0.60	10,576	0.60	14,102	0.60
RM2M	10,576	0.67	28,132	0.67	45,689	0.67
RM2H	10,576	0.67	41,469	0.67	72,361	0.67
URML	759	0.66	759	0.66	759	0.66
URMM	759	0.67	2,825	0.67	4,892	0.67
MH	49	0.60	49	0.60	49	0.60

Table 5.16: Default values of Damage-State Parameters – Median (F_{dsi}) and Beta ($\beta_{dsi|F}$) – for Evaluation of Damage to the Structure of Special Moderate-Code Seismic Design Model Building Types due to Tsunami Flow

MBT Name	Moderate Damage Median (ft^3/s^2)	Moderate Damage Beta	Extensive Damage Median (ft^3/s^2)	Extensive Damage Beta	Complete Damage Median (ft^3/s^2)	Complete Damage Beta
W1	555	0.74	555	0.74	555	0.74
W2	1,028	0.73	1,028	0.73	1,028	0.73
S1L	2,934	0.74	2,934	0.74	4,403	0.74
S1M	2,934	0.79	7,242	0.79	11,549	0.79
S1H	2,934	0.80	10,289	0.80	17,645	0.80
S2L	3,305	0.60	3,305	0.60	4,407	0.60
S2M	3,305	0.67	9,364	0.67	15,424	0.67
S2H	3,305	0.67	14,894	0.67	26,483	0.67
S3	617	0.60	617	0.60	617	0.60
S4L	3,437	0.64	3,437	0.64	4,759	0.64
S4M	3,437	0.70	9,431	0.70	15,424	0.70
S4H	3,437	0.70	14,964	0.70	26,491	0.70
S5L	2,115	0.60	2,115	0.60	2,820	0.60
S5M	2,115	0.67	5,628	0.67	9,140	0.67
S5H	2,115	0.79	14,413	0.79	26,711	0.79
C1L	1,105	0.73	1,105	0.73	1,655	0.73
C1M	1,105	0.79	2,437	0.79	3,770	0.79

MBT Name	Moderate Damage Median (ft^3/s^2)	Moderate Damage Beta	Extensive Damage Median (ft^3/s^2)	Extensive Damage Beta	Complete Damage Median (ft^3/s^2)	Complete Damage Beta
C1H	1,105	0.80	9,601	0.80	18,097	0.80
C2L	4,627	0.67	4,627	0.67	6,610	0.67
C2M	4,627	0.73	13,025	0.73	21,422	0.73
C2H	4,627	0.74	19,281	0.74	33,935	0.74
C3L	1,763	0.73	1,763	0.73	2,642	0.73
C3M	1,763	0.79	4,892	0.79	8,020	0.79
C3H	1,763	0.79	5,406	0.79	9,049	0.79
PC1	1,763	0.60	1,763	0.60	1,763	0.60
PC2L	3,966	0.60	3,966	0.60	5,288	0.60
PC2M	3,966	0.67	10,552	0.67	17,138	0.67
PC2H	3,966	0.67	15,564	0.67	27,162	0.67
RM1L	4,407	0.60	4,407	0.60	5,876	0.60
RM1M	4,407	0.67	12,491	0.67	20,575	0.67
RM2L	5,288	0.60	5,288	0.60	7,051	0.60
RM2M	5,288	0.67	14,075	0.67	22,861	0.67
RM2H	5,288	0.67	20,752	0.67	36,216	0.67
URML	759	0.66	759	0.66	759	0.66
URMM	759	0.67	2,825	0.67	4,892	0.67
MH	49	0.60	49	0.60	49	0.60

Table 5.17: Default values of Damage-State Parameters – Median (F_{dsi}) and Beta ($\beta_{dsi|F}$) – for Evaluation of Damage to the Structure of Special Low-Code Seismic Design Model Building Types due to Tsunami Flow

MBTName	Moderate Damage: Median (ft^3/s^2)	Moderate Damage: Beta	Extensive Damage: Median (ft3/s2)	Extensive Damage: Beta	Complete Damage: Median (ft3/s2)	Complete Damage: Beta
W1	370	0.74	370	0.74	370	0.74
W2	514	0.73	514	0.73	514	0.73
S1L	1,469	0.73	1,469	0.73	2,201	0.73
S1M	1,469	0.79	3,630	0.79	5,791	0.79
S1H	1,469	0.79	5,146	0.79	8,822	0.79
S2L	1,653	0.60	1,653	0.60	2,203	0.60

MBTName	Moderate Damage: Median (ft^3/s^2)	Moderate Damage: Beta	Extensive Damage: Median (ft3/s2)	Extensive Damage: Beta	Complete Damage: Median (ft3/s2)	Complete Damage: Beta
S2M	1,653	0.67	4,682	0.67	7,712	0.67
S2H	1,653	0.67	7,430	0.67	13,207	0.67
S3	308	0.60	308	0.60	308	0.60
S4L	1,719	0.64	1,719	0.64	2,380	0.64
S4M	1,719	0.70	4,715	0.70	7,712	0.70
S4H	1,719	0.70	7,463	0.70	13,207	0.70
S5L	1,763	0.73	1,763	0.73	2,642	0.73
S5M	1,763	0.79	4,099	0.79	6,435	0.79
S5H	1,763	0.79	5,783	0.79	9,803	0.79
C1L	1,763	0.73	1,763	0.73	2,642	0.73
C1M	1,763	0.79	4,892	0.79	8,020	0.79
C1H	1,763	0.79	5,406	0.79	9,049	0.79
C2L	2,314	0.67	2,314	0.67	3,305	0.67
C2M	2,314	0.74	6,521	0.74	10,728	0.74
C2H	2,314	0.74	9,641	0.74	16,967	0.74
C3L	1,763	0.73	1,763	0.73	2,642	0.73
C3M	1,763	0.79	4,892	0.79	8,020	0.79
C3H	1,763	0.79	5,406	0.79	9,049	0.79
PC1	881	0.60	881	0.60	881	0.60
PC2L	1,983	0.60	1,983	0.60	2,644	0.60
PC2M	1,983	0.67	5,276	0.67	8,569	0.67
PC2H	1,983	0.67	7,764	0.67	13,545	0.67
RM1L	2,203	0.60	2,203	0.60	2,938	0.60
RM1M	2,203	0.67	6,238	0.67	10,272	0.67
RM2L	2,644	0.60	2,644	0.60	3,525	0.60
RM2M	2,644	0.67	7,029	0.67	11,414	0.67
RM2H	2,644	0.67	10,376	0.67	18,108	0.67
URML	759	0.66	759	0.66	759	0.66
URMM	759	0.67	2,825	0.67	4,892	0.67
MH	49	0.60	49	0.60	49	0.60

Table 5.18: Assumed Values of Total Seismic Design Weight (W), Total Building Area, Average Unit Weight per Square Foot (w) and Plan Dimension (B) of Model Building Types used to Develop Default Values of Damage-State Parameters of Tsunami Flow Damage Functions

MBT Name	No. of Floors	Area (sf)	w (psf)	W (kips)	B (feet)
W1	1	1,600	30	48	40
W2	2	5,000	40	200	50
S1L	2	10,000	150	1,500	70
S1M	5	50,000	180	9,000	100
S1H	13	130,000	180	23,400	100
S2L	2	10,000	150	1,500	70
S2M	5	50,000	180	9,000	100
S2H	13	130,000	180	23,400	100
S3	1	2,500	60	150	50
S4L	2	10,000	180	1,800	70
S4M	5	50,000	200	10,000	100
S4H	13	130,000	200	26,000	100
S5L	2	10,000	180	1,800	70
S5M	5	50,000	200	10,000	100
S5H	13	130,000	200	26,000	100
C1L	2	10,000	180	1,800	70
C1M	5	50,000	200	10,000	100
C1H	12	120,000	200	24,000	100
C2L	2	10,000	180	1,800	70
C2M	5	50,000	200	10,000	100
C2H	12	120,000	200	24,000	100
C3L	2	10,000	180	1,800	70
C3M	5	50,000	200	10,000	100
C3H	12	120,000	200	24,000	100
PC1	1	40,000	100	4,000	200
PC2L	2	10,000	180	1,800	70
PC2M	5	50,000	200	10,000	100
PC2H	12	120,000	200	24,000	100
RM1L	2	10,000	180	1,800	70
RM1M	5	50,000	200	10,000	100

MBT Name	No. of Floors	Area (sf)	w (psf)	W (kips)	B (feet)
RM2L	2	10,000	180	1,800	70
RM2M	5	50,000	200	10,000	100
RM2H	12	120,000	200	24,000	100
URML	1	10,000	180	1,800	70
URMM	3	30,000	200	6,000	100
MH	1	600	20	12	50

Example Estimate of Tsunami Flow Damage-State Uncertainty

The three primary sources of uncertainty in the median values of damage due to tsunami flow are 1) the uncertainty in building capacity, as defined by "pushover" strength of the building's structure, 2) the uncertainty in hydrodynamic loads due to debris impact and shielding effects, and 3) the uncertainty in the plan dimension of the side of the building that faces tsunami flow.

An estimate of the uncertainty in building capacity is based on the range of building strengths that the model building type could possibly have. In this case, uncertainty in model building type strength is estimated by the range of yield and ultimate strengths. For example, the larger wood (W2) model building type designed for high-code seismic forces has yield strength of 60 kips and an ultimate strength of 150 kips. This range of strengths is assumed to represent two standard deviations and the corresponding uncertainty in building strength is calculated as, ln(150/60)/2, or a beta of about 0.46 due to uncertainty in building strength capacity.

An estimate of the uncertainty in hydrodynamic loads due to possible debris impact (which would increase hydrodynamic forces) and possible shielding of the building (which would decrease hydrodynamic forces) are based on the range of K_d values that encompass these possibilities. For example, the larger wood (W2) model building type has K_d values that are assumed to be as large as 2.0 (assumed maximum increase due to potential debris impact) to as small as 0.5 (assumed maximum reduction due to potential shielding of other structures). This broad range of K_d values is assumed to represent plus or minus two standard deviations from the median and the corresponding uncertainty in demand is estimated as, ln(2.0/0.5)/4, or a beta of about 0.35.

An estimate of the uncertainty in the plan dimension (B) that defines the length of the side of the building that faces tsunami flow, is based on the range of plan dimensions that the building could reasonably have. For example, the larger wood (W2) model building type (which has a nominal plan dimension of 50 feet), is assumed to have a plan dimension that could be as small as 30 feet, or as large as 75 feet. This range of plan dimensions is assumed to represent plus or minus one standard deviation from the median and the corresponding uncertainty in demand is estimated as, ln(75/30)/2, or a beta of about 0.46.

SRSS combination of the uncertainty in building capacity (0.46), the uncertainty in the K_d factor (0.35), and the uncertainty in plan dimension, B, defining the length of the side of the building facing tsunami flow (0.46) yields a total uncertainty of about 0.73, the value of beta given in Table 5.11 for Complete damage to nonstructural systems of the W2 model building type.

5.6 Optimizing Damage-State Probability Calculations

To rapidly estimate damage-state probabilities, both the flood inundation depth and flood flow are represented by index values where the median values intersect the site of interest. For flood depth, index values (1-198) are assigned to building points in 0.25 foot increments from a depth of 0 to 14 feet and then by one foot increments from 14 to 156 feet of flood depth. Likewise, flux index values (1-120) are assigned based on 50 ft^3/s^2 increments from 0 to 2,000 ft^3/s^2 and by 1,000 ft^3/s^2 increments from 2,000 to 82,000 ft^3/s^2. Depths and flows greater than these ranges will be assigned the highest index value, however, complete damage to all building types are presumed at these levels.

5.7 Evaluating Combined Earthquake and Tsunami Damages

5.7.1 Overview

This section describes the concepts and “Boolean logic” rules used to combine the probability of a given building damage state due to tsunami with probability of the same building damage state due to earthquake. Formulas based on these concepts and rules are summarized in the next section. It should be noted that tsunami damage-state probabilities due to flood need not be combined with those due to tsunami flow, since tsunami flood and flow damage states are mutually exclusive (i.e., tsunami flood only affects nonstructural systems and contents, tsunami flow only affects the structure).

Tsunami building damage states are combined with earthquake building damage states assuming that the damage states are statistically independent, except as noted below:

1. Probability of Complete Damage – The probability of Complete damage also includes the joint probability of Extensive Damage due to tsunami and Extensive damage due to earthquake based on the assumption that Extensive damage due to tsunami occurring to a building that already has Extensive damage due to earthquake would result in Complete damage to the building. This concept applies to structure, as well as nonstructural and contents damage states.
2. Probability of Extensive or greater Damage – The probability of at least Extensive damage also includes the joint probability of Moderate Damage due to tsunami and Moderate damage due to earthquake based on the assumption that Moderate damage due to tsunami occurring to a building that already has Moderate damage due to earthquake would result in Extensive damage to the building. This concept applies to structure, as well as nonstructural and contents damage states.
3. Probability of Nonstructural and Contents Damage due to Complete Structure Damage – The probability of nonstructural and contents damage also includes the probability of Complete structure damage, $P[C_{STR}|EQ+TS]$, based on the assumption that nonstructural systems and contents are completely damaged in a building that sustains Complete damage to the structural system. This concept applies to all nonstructural and contents damage states.

5.7.2 Formulas for Combining Damage-State Probabilities - Earthquake with Tsunami

This section summarizes the formulas for calculating the combined probability of Complete (C), Extensive (E), Moderate (M), and Slight (S) damage states for building damage due to tsunami (TS) and building damage due to earthquake (EQ). Formulas are provided for the structure (STR), nonstructural drift-sensitive systems (NSD), nonstructural acceleration-sensitive systems (NSA), and building contents (CON), recognizing that tsunami damage to nonstructural systems (NSS) does not distinguish between drift-sensitive and accelerations sensitive components.

Formulas for calculating combined probabilities of damage to the structure (STR) due to earthquake and tsunami (EQ+TS) hazards are given by Equations 5.18 through 5.21 for Complete (C_{STR}), Extensive (E_{STR}), Moderate (M_{STR}), and Slight (S_{STR}) structure damage states:

$$P[C_{STR}|EQ+TS] = P[C_{STR}|EQ] + P[C_{STR}|TS] - P[C_{STR}|EQ]\,P[C_{STR}|TS] + (P[\geq E_{STR}|EQ] - P[C_{STR}|EQ])\,(P[\geq E_{STR}|TS] - P[C_{STR}|TS]) \quad (5.18)$$

$$P[\geq E_{STR}|EQ+TS] = P[\geq E_{STR}|EQ] + P[\geq E_{STR}|TS] - P[\geq E_{STR}|EQ]\,P[\geq E_{STR}|TS] + (P[\geq M_{STR}|EQ] - P[\geq E_{STR}|EQ])(P[\geq M_{STR}|TS] - P[\geq E_{STR}|TS]) \quad (5.19)$$

$$P[\geq M_{STR}|EQ+TS] = P[\geq M_{STR}|EQ] + P[\geq M_{STR}|TS] - P[\geq M_{STR}|EQ]\,P[\geq M_{STR}|TS] \quad (5.20)$$

$$P[\geq S_{STR}|EQ+TS] = P[\geq S_{STR}|EQ] + P[\geq M_{STR}|TS] - P[\geq S_{STR}|EQ]\,P[\geq M_{STR}|TS] \quad (5.21)$$

Formulas for calculating combined probabilities of damage to nonstructural drift-sensitive (NSD) systems due to earthquake and tsunami (E+T) hazards are given by Equations 5.22 through 5.25 for Complete (C_{NSD}), Extensive (E_{NSD}), Moderate (M_{NSD}) and Slight (S_{NSD}) nonstructural drift- sensitive damage states:

$$P[C_{NSD}|EQ+TS] = P[C_{STR}|EQ+TS] + (1 - P(C_{STR}|EQ+TS)(P[C_{NSD}|EQ] + P[C_{NSS}|TS] - P[C_{NSD}|EQ]\,P[C_{NSS}|TS] + (P[\geq E_{NSD}|EQ] - P[C_{NSD}|EQ]\,P[\geq E_{NSS}|TS]) - P[C_{NSS}|TS]) \quad (5.22)$$

$$P[\geq E_{NSD}|EQ+TS] = P[C_{STR}|EQ+TS] + (1 - P(C_{STR}|EQ+TS)(P[\geq E_{NSD}|EQ] + P[E_{NSS}|TS] - P[\geq E_{NSD}|EQ]P[\geq E_{NSS}|TS] + P[M_{NSD}|EQ] - P[\geq E_{NSD}|EQ])P[\geq M_{NSS}|TS] - P[\geq E_{NSS}|TS]) \quad (5.23)$$

$$P[\geq M_{NSD}|EQ+TS] = P[C_{STR}|EQ+TS] + (1 - P[C_{STR}|EQ+TS])(P[\geq M_{NSD}|EQ] + P[\geq M_{NSS}|TS] - P[\geq M_{NSD}|EQ]\,P[\geq M_{NSS}|TS]) \quad (5.24)$$

$$P[\geq S_{NSD}|EQ + TS] = P[C_{STR}|EQ + TS] + (1 - P[C_{STR}|EQ + TS])(P[\geq S_{NSD}|EQ] + P[\geq M_{NSD}|TS] - P[\geq S_{NSD}|EQ]\,P[\geq M_{NSD}|TS])$$

Formulas for calculating combined probabilities of damage to nonstructural acceleration-sensitive (NSA) systems due to earthquake and tsunami (E+T) hazards are given by Equations 5.26 through 5.29 for Complete (C_{NSA}), Extensive (E_{NSA}), Moderate (M_{NSA}), and Slight (S_{NSA}) nonstructural acceleration-sensitive damage states:

$$P[C_{NSA}|EQ + TS] = P[C_{STR}|EQ + TS] + (1 - P[C_{STR}|EQ + TS])\big(P[C_{NSA}|EQ] + P[C_{NSS}|TS] - P[C_{NSA}|EQ]\,P[C_{NSS}|TS] + (P[\geq E_{NSA}|EQ] - P[C_{NSA}|EQ])(P[\geq E_{NSS}|TS] - P[C_{NSS}|TS])\big) \quad (5.26)$$

$$P[\geq E_{NSA}|EQ + TS] = P[C_{STR}|EQ + TS] + (1 - P[C_{STR}|EQ + TS])\big(P[\geq E_{NSA}|EQ] + P[\geq E_{NSS}|TS] - P[\geq E_{NSA}|EQ]\,P[\geq E_{NSS}|TS] + (P[\geq M_{NSA}|EQ] - P[\geq E_{NSA}|EQ])(P[\geq M_{NSS}|TS] - P[E_{NSS}|TS])\big) \quad (5.27)$$

$$P[\geq M_{NSA}|EQ + TS] = P[C_{STR}|EQ + TS] + (1 - P[C_{STR}|EQ + TS])(P[\geq M_{NSA}|EQ] + P[\geq M_{NSS}|TS] - P[\geq M_{NSA}|EQ]\,P[\geq M_{NSS}|TS]) \quad (5.28)$$

$$P[\geq S_{NSA}|EQ + TS] = P[C_{STR}|EQ + TS] + (1 - P[C_{STR}|EQ + TS])(P[\geq S_{NSA}|EQ] + P[\geq M_{NSA}|TS] - P[\geq S_{NSA}|EQ]\,P[\geq M_{NSS}|TS]) \quad (5.29)$$

Formulas for calculating combined probabilities of damage to building contents (CON) due to earthquake and tsunami (E+T) hazards are given by Equations 5.30 – 5.33 for Complete (C_{CON}), Extensive (E_{CON}), Moderate (M_{CON}), and Slight (S_{CON}) contents damage states:

$$P[C_{CON}|EQ + TS] = P[C_{STR}|EQ + TS] + (1 - P[C_{STR}|EQ + TS])\big(P[C_{CON}|EQ] + P[C_{CON}|TS] - P[C_{CON}|EQ]\,P[C_{CON}|TS] + (P[\geq E_{CON}|EQ] - P[C_{CON}|EQ])(P[\geq E_{CON}|TS] - P[C_{CON}|TS])\big) \quad (5.30)$$

$$P[\geq E_{CON}|EQ + TS] = P[C_{STR}|EQ + TS] + (1 - P[C_{STR}|EQ + TS])\big(P[\geq E_{CON}|EQ] + P[\geq E_{CON}|TS] - P[\geq E_{CON}|EQ]\,P[\geq E_{CON}|TS] + (P[\geq M_{CON}|EQ] - P[\geq E_{CON}|EQ])(P[\geq M_{CON}|TS] - P[\geq E_{CON}|TS])\big) \quad (5.31)$$

$$P[\geq M_{CON}|EQ + TS] = P[C_{STR}|EQ + TS] + (1 - P[C_{STR}|EQ + TS])(P[\geq M_{CON}|EQ] + P[\geq M_{CON}|TS] - P[\geq M_{CON}|EQ]\,P[\geq M_{CON}|TS])] \quad (5.32)$$

$$P[\geq S_{CON}|EQ + TS] = P[C_{STR}|EQ + TS] + (1 - P[C_{STR}|EQ + TS])(P[\geq S_{CON}|EQ] + P[\geq M_{CON}|TS] - P[\geq S_{CON}|EQ]\,P[\geq M_{CON}|TS]) \quad (5.33)$$

The equations above describe the cumulative probabilities (i.e., probability of greater than or equal to the damage state of interest). Note, the “cumulative” probability of Complete damage is also the probability of the Complete damage state, since it is the most severe state of damage. The discrete probabilities of other damage states are calculated as the difference in the probability of the damage state of interest and the next more severe damage state, as given by Equations 5.34 through 5.36 for Extensive (E_{STR}), Moderate (M_{STR}), and Slight (S_{STR}) structure damage states:

$$P[E_{STR}|EQ + TS] = P[\geq E_{STR}|EQ + TS] - P[C_{STR}|EQ + TS] \quad (5.34)$$

$$P[M_{STR}|EQ + TS] = P[\geq M_{STR}|EQ + TS] - P[\geq E_{STR}|EQ + TS] \quad (5.35)$$

$$P[S_{STR}|EQ + TS] = P[\geq S_{STR}|EQ\_TS] - P[\geq M_{STR}|EQ + TS] \quad (5.36)$$

Discrete damage-state probabilities of nonstructural drift-sensitive systems, nonstructural acceleration-sensitive systems, and building contents are calculated in the same manner as that of the above equations for the structure.

5.8 References

ASCE, 2003. *Seismic Evaluation of Existing Buildings*. American Society of Civil Engineers Standard ASCE/SEI 31-03. (Reston, VA: ASCE).

ASCE, 2010. Minimum Design Loads for Buildings and Other Structures. American Society of Civil Engineers Standard ASCE/SEI 7-10. (Reston, VA: ASCE).

ASCE, 2012. Tohoku Japan Tsunami of March 11, 2011 – Performance of Structures, ASCE Monograph, American Society of Civil Engineers Standard. (Reston, VA: ASCE).

ATC, 1989. “Procedures for Post-earthquake Safety Evaluation of Buildings,” ATC-20 Report, Applied Technology Council (ATC). (Redwood City, CA: ATC).

ATC, 1994. “Field manual: safety evaluation of buildings after windstorms and floods,” ATC-45, Applied Technology Council ATC). (Redwood City, CA: ATC).

ATC, 1995. “Addendum to the ATC-20 Procedures for Post-earthquake Safety Evaluation of Buildings,” ATC-20-2, Applied Technology Council ATC). (Redwood City, CA: ATC).

Davis, Stuart A., "Business Depth-Damage Analysis Procedures," Water Resources Support Center, Institute for Water Resources, USACE Research Report 85-R-5.

EERI, 2011. "The Tohoku, Japan, Tsunami of March 1, 2011: Effects on Structures," Earthquake Engineering Research Institute (EERI) Special Earthquake Report, Learning From Earthquakes – September 2011, (Oakland, CA: EERI).

FEMA, 1992*. NEHRP Handbook for the Seismic Evaluation of Existing Buildings*. Federal Emergency Management Agency, FEMA 178. (Washington, D.C.: FEMA).

FEMA, 2002. *Earthquake Loss Estimation Methodology, HAZUS99-MR1, Advanced Engineering Building Module, Technical and User's Manual*, prepared by National Institute of Building Sciences (NIBS) for the Federal Emergency Management Agency. (Washington, D.C.: NIBS).

FEMA, 2004. *Guidelines and Specification for Flood Hazard Mapping*, Section D.4, "Coastal Flooding Analyses and Mapping Pacific Coast," Federal Emergency Management Agency (FEMA), November 2004 (FEMA, Washington, D.C.).

FEMA, 2011a. *Multi-hazard Loss Estimation Methodology: Earthquake Model, HAZUS-MH MR4 Technical Manual*, prepared by the National Institute of Building Sciences (NIBS) for the Federal Emergency Management Agency. (Washington, D.C.: NIBS).

FEMA, 2011b. Multi-hazard Loss Estimation Methodology: Flood Model, HAZUS-MH MR4 *Technical Manual*, prepared by the National Institute of Building Sciences (NIBS) for the Federal Emergency Management Agency. (Washington, D.C.: NIBS).

FEMA, 2012. Guidelines for Design of Structures for Vertical Evacuation from Tsunamis, FEMA P646, April 2012, Federal Emergency Management Agency. (Washington, D.C: FEMA).

FEMA, 2013. *Tsunami Methodology Technical Manual*, 223 pp., Federal Emergency Management Agency, Washington, D.C.

Gokon, Hidemeomi, and Shunichi Koshimura, 2012. "Mapping of Building Damage of the 2011 Tohoku Earthquake Tsunami in Miyagi Prefecture," Coastal Engineering Committee, Japan Society of Civil Engineers, Coastal Engineering Journal, Vol. 54, No. 1, March 24, 2012, (World Scientific Publishing Company: www.worldscientific.com).

Jones, Christopher P., 2011. "Large Building Flood Damage Functions," (white paper), August 31, 2010, revised June 22, 2011.

Jones, C., 2004. "Supporting Documentation for D.4.9.2.1 High Velocity Flow VE Zone," discussion of supporting documentation for FEMA Guidelines and Specification for Flood Hazard Mapping, Section D.4, C. Jones 12-08-04, (private communication).

Koshimura, Shuniche (Tohoku University), Yuichi Namegaya (AIST), Hideaki Yanagisawa (TEPCO), "Tsunami Fragility - A new measure to identify tsunami damage," Journal of Disaster Research, 2009.

MLIT, 2011. Press release, Ministry of Land, Infrastructure, Transport and Tourism (MLIT), 2011 (in Japanese).

Murty, C.V.R., Durgesh C. Rai, Sudhir K. Jain, Hemant B. Kaushik, Goutam Mondal, and Suresh R. Dash, 2006. "Performance of Structures in the Andaman and Nicobar Islands (India) during the December 2004 Great Sumatra Earthquake and Indian Ocean Tsunami," Earthquake Spectra, Volume 22, No. S3, June 2006 (Oakland, CA: EERI).

Reese, Stefan, Brendon A. Bradley, Jochen Bind, Graeme Smart, William Power, James Sturman, 2011. "Empirical building fragilities from observed damage in the 2009 South Pacific tsunami," Earth-Science Reviews, Elsevier (National Institute of Water and Atmospheric Research).

Reese, S., W. J. Cousins, W. L. Power, N. G. Palmer, I. G. Tejakusuma, and S. Nurgrahadi, 2007. "Tsunami vulnerability of buildings and people in South Java – field observation after the July 2006 Java tsunami," Nat Hazards and Earth System Sciences, 7, 573-589, October 15, 2007, (Copernicus Publications).

Robertson, I.N., Carden, L., Riggs, H.R., Yim, S., Young, Y.L., Paczkowski, K. and Witt, D., "Reconnaissance following the September 29, 2009 tsunami in Samoa," University of Hawaii, Research Report UHM/CEE/10-01.

Ruangrassamee, Anat, Hideaki Yanagisawa, Piyawat Foytong, Panitan Lukkunaprasit, Shunichi Koshimura, and Fumihiko Imamura, 2006. "Investigation of Tsunami-Induced Damage and Fragility of Buildings in Thailand after the December 2004 Indian Ocean Tsunami," Earthquake Spectra, Volume 22, No. S3, June 2006 (Oakland, CA: EERI).

Saatcioglu, Murat, Ahmed Ghobarah, Ioan Nistor, 2006. "Performance of Structures in Indonesia during the December 2004 Great Sumatra Earthquake and Indian Ocean Tsunami," *Earthquake Spectra*, Volume 22, No. S3, June 2006 (Oakland, CA: EERI).

Suppasri, A. S, Koshimura, F. Imamura, 2011. "Developing tsunami fragility curves based on satellite remote sensing and the numerical modeling of the 2004 Indian Ocean tsunami in Thailand," *Natural Hazards Earth System Sciences*, 11, 173-189, January 20, 2011.

Suppasri, Anawat, Erick Mas, Shunichi Koshimura, Kentaro Imai, Kenji Harada, FumihikoImahura, 2012. "Developing Tsunami Fragility Curves from the Surveyed Data of the 2011 Great East Japan Tsunami in Sendai and Ishinomaki Plains," Coastal Engineering Committee, Japan Society of Civil Engineers, *Coastal Engineering Journal*, Vol. 54, No. 1, March 24, 2012, (World Scientific Publishing Company: www.worldscientific.com).

The Heinz Center, 2000. *Evaluation of Erosion Hazards*, The H. John Heinz III Center for Science, Economics and the Environment. (Washington, D.C.).

Tinti, S., R. Tonini, L. Bressan, A. Armigliato, A. Gargi, R. Guillande, N. Valencia and S.Scheer, 2011. "Handbook of Tsunami Hazard and Damage Scenarios," SCHEMA Project, *JRC Scientific and Technical Reports*, EUR 24691 EN, 2011 (Joint Research Centre, Institute for the Protection and Security of the Citizen, Bologna, Italy).

6.0 Casualty Estimation

6.1 Introduction

This chapter describes the methodology used to estimate casualty losses in the Hazus Tsunami Model. Casualty losses are provided by two measures: 1) the travel time for people to evacuate tsunami danger zones (called *evacuation travel time* in this model), and 2) the number of casualties for a given tsunami event. The evacuation travel time provides information on how long it could take for people to safely reach higher ground. This information is useful for identifying tsunami-risk areas within the coastal community. The evacuation travel time is determined once the location of a safe haven is identified without consideration of tsunami arrival times. On the other hand, consideration of the timing of tsunami warning and arrival times must be evaluated when calculating casualties.

Among many natural hazards, human losses caused by tsunamis are especially difficult to estimate. In the event of an earthquake, human losses directly relate to the extent of damage to buildings and infrastructure, which is strongly correlated with the earthquake magnitude and built environment. With little or no forewarning time from an earthquake for evacuation, a majority of casualties result from crushing or suffocation associated with structure collapse. In contrast, there is lead-time for prediction of a tsunami after detecting a seismic signal, possibly allowing for an effective warning and evacuation period. The lead-time can range from a few minutes for a local source to ten or more hours for a distant source. Tsunami warning lead-times are shorter than those of some other natural hazards such as volcanic eruptions, hurricanes, and river floods.

Suppasri et al. (2011) compiled data on fatality rate (fatality rate is the ratio of the number of people killed to the total population in the inundation area) for many historical tsunami events in Japan including the 2011 Tohoku Tsunami, as well as the 2004 Indian Ocean Tsunami in India, Thailand, and Indonesia, the 2006 Java Tsunami, and the 2010 Mentawai Tsunami. Observations from their analysis reveal that the tsunami's flow condition (represented by maximum runup heights) is not the controlling factor determining the fatality rate. Consider, for example, the 0.015 percent fatality rate data point at a 2.5m tsunami runup height.

At a similar runup height (3 ~ 3.5 m), a data point exists showing the fatality rate at about 50 percent, an increase by more than three orders of magnitude. Another example is a comparison of nearly 100 percent fatality rate at the 5m tsunami runup height with the 0.06 percent fatality rate at the tsunami runup height of 31m. Evidently, tsunami runup height alone is not a good indicator when estimating fatality rate. The figure shows one important point, however, which is that the tsunami fatality rate diminishes when the maximum tsunami "height" is less than 1.5 m. Note that tsunami runup "height" is the elevation from the sea level; the actual inundation "depth" at a location of interest is usually smaller than the "height:" see the definition sketch in Chapter 4, Figure 4.2 for the difference between "depth" and "height."

In the same paper, Suppasri et al. (2011) demonstrated better correlation between fatality rate and housing damage rate than the correlation between fatality rate and tsunami runup height. This trend makes sense because humans dwell in houses. Nonetheless, their results are for a specific tsunami event (the 2011 Tohoku Tsunami) in a specific locality (Miyagi Prefecture). Careful examination for each tsunami event presented in their research indicates such a correlation cannot be used for the prediction of a fatality rate in a different locality caused by a different tsunami event.

It is believed that critical factors for determining tsunami impacts on humans are a) prior knowledge and/or experience with tsunamis, b) effective education motivating people to evacuate in a timely manner, and c) effective tsunami warning systems. Age and its associated *mobility capacity* is also another critical factor. Therefore, temporal and spatial information about the tsunami runup are crucial. For example, warnings with more accurate tsunami information are possible when the tsunami arrival occurs a long time after the earthquake. Thus, a distant tsunami may have fewer casualties when compared with a similar tsunami from a local source. A shorter evacuation distance to a safe haven results in a better chance of survival.

Human behaviors and actions under strained conditions are difficult to predict. Nonetheless, one of the most systematic and logical methodologies for casualty estimation for a given tsunami scenario is agent-based modeling (Wood and Schmidtlein, 2011). In agent-based modeling, a system is modeled as a collection of autonomous decision-making entities called agents. Agents can be each evacuee or a group of evacuees. An individual agent evaluates the situation and makes decisions based on a set of rules. Agent-based simulations for tsunamis have been performed in the past, for the town of Owase, Japan (Katada et al. 2006), for Long Beach Peninsula, Washington (Yeh et al., 2009), and for the town of Cannon Beach, Oregon (Yeh and Karon, 2011). However, agent-based modeling requires detailed spatiotemporal data of tsunami inundation processes, in addition to geospatial data such as road networks, locations, and operations of warning transmissions (e.g., TV, radios, loud speakers, and mobile warning vehicles), and demographic data. Also needed is social information for how people respond to the warning and interact with other evacuees (including tourists), and how people are killed and injured (casualty modeling). For Level 1 and Level 2 methodologies, the “concept” of agent- based modeling is implemented in a simplified manner. For Level 3 analysis, results from agent-based simulation models could be used instead, although this option is not fully implemented in the current methodology. This implementation includes a Level 1 methodology utilizing a “roads only” network approach and a Level 2 methodology using the travel time output from the USGS Pedestrian Evacuation Analyst (version EvacAnalystInstaller_20141023) is implemented: (https://geography.wr.usgs.gov/science/vulnerability/tools.html).

The Casualty Losses module estimates the evacuee travel times and statistics of the fatality and injury counts, and their spatial distribution for a community of interest. As shown in the tsunami loss estimation flow chart in Figure 6.1 (note that for distant events, the earthquake components can be bypassed), data of tsunami inundation processes are provided by the Tsunami Hazard Analysis module, and the Damage Assessment unit provides the effects of earthquake damage on human losses. It must be emphasized that the methodology presented here is as rational as possible even though the outcomes are strongly determined by human decision making and behaviors. Unlike physical laws governed in fluid flows and structural behaviors, human behaviors are not controlled by clear laws, but must be estimated by their tendencies (both based on empirical data and hypotheses).

> *Because of the unavoidable uncertainties, we design the methodology such that the users are allowed to make their own judgment calls for the characterization of a community and human behaviors of the residents and visitors.*

Because of the complexity, only pedestrian evacuation is considered and possibilities of other evacuation means such as automobiles, bikes, boats, etc. are excluded. In addition, the model includes the possibility of evacuation to tall and tsunami-resistant buildings, by using modified hazard zones or the USGS tool.

Figure 6.1: Flow chart of tsunami loss estimation methodology

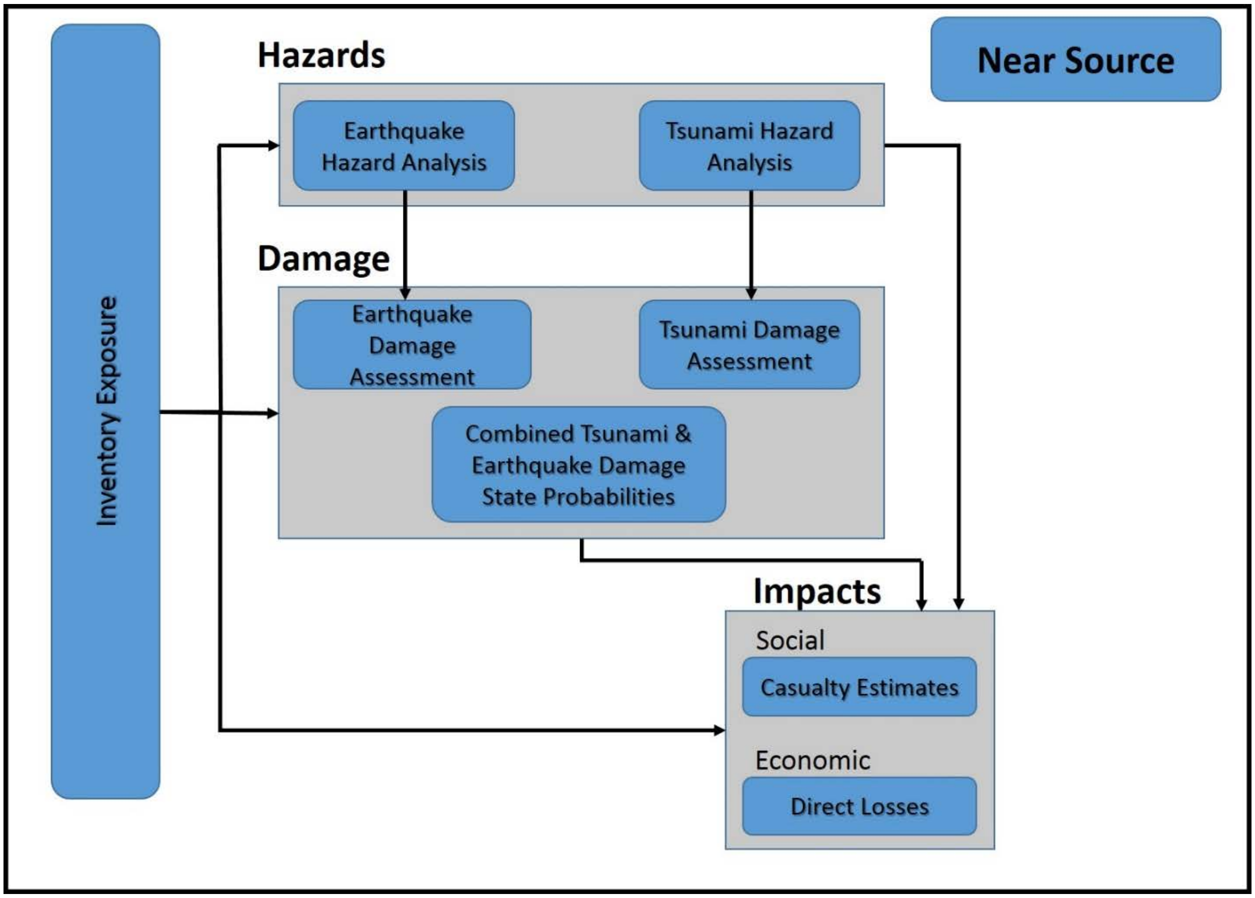

6.2 Input Requirement and Output Information

Input information and data include the following items for a given tsunami event from Tsunami Hazard Analysis (Chapter 4), combined earthquake and tsunami damage assessment (Chapter 5), and those prepared for this module. The input/output diagram is shown in Figure 6.2.

Input data from User & Tsunami Hazard Analysis:

- Maximum inundation locations X(x,y) (depth > 0, along the maximum runup contour line)
- Fatality boundary, where depth is greater than 2 meters and fatality rate is modeled as 99 percent
- Arrival time of the leading tsunami, T_0
- Time of max runup, T_{max}
- Warning time, T_{warn}, after earthquake: this includes a natural cue (ground shaking, $T_{warn} = 0$) for a local tsunami

Figure 6.2: Flow chart of tsunami loss estimation methodology

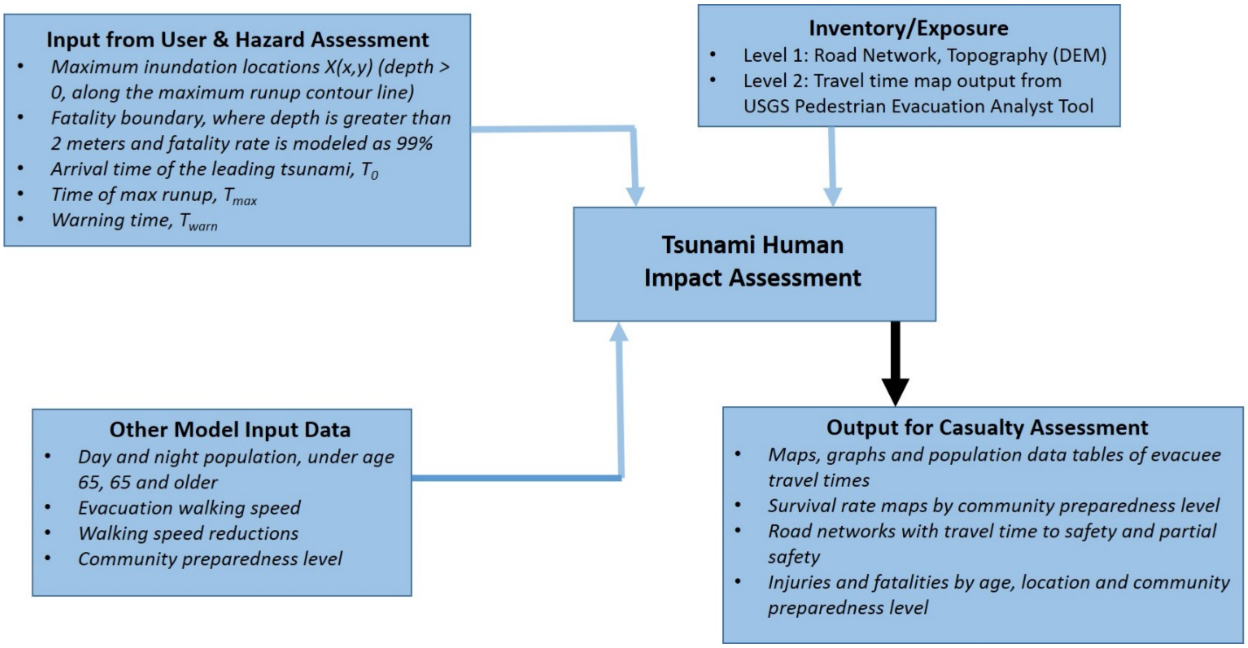

<u>Levels of Analysis</u>

Level 1: The Hazus Level 1 casualty analysis integrates methodology from the USGS Pedestrian Evacuation Analyst, however, uses a “roads only” approach for evacuation. This approach helps ensure evacuation routing is not inadvertently placed across flooded or otherwise impassable areas, however, it may not be the fastest route to safety if across land routes are available. The Level 1 methodology calculates the path-distance using both a DEM and road-network provided by the user and applies the walking speeds selected by the user (Table 6.1). The model includes optional external download links for the U.S. Census TIGER road network and the USGS National Elevation Datasets or users can provide their own datasets.

Level 2: The Hazus Level 2 casualty analysis directly integrates the travel time map outputs from the USGS Pedestrian Evacuation Analyst. Both the travel time to safety (depth ≤ 0), T_{travel}, and travel time to partial safety (depth ≤ 2 meters), T^*_{travel}, are required as inputs for the Level 2 analysis. The Hazus interface with the USGS tool provides the capability to:

- Preprocess hazard zone and validate the safe zones to ensure slivers or erroneous areas determined as “safe” are removed.
- Utilize the entire Land-Cover, validating impassable areas, rather than just road network, to ensure the fastest least-cost routes are incorporated.
- Incorporate vertical evacuation structures into the analysis, including the ability to evaluate mitigation strategies (casualty reduction) associated with proposed structures.
- Validate population summaries and incorporate seasonal populations, such as beach goers and cruise ship populations into impacted blocks.

Input data prepared for this module:

- Population data are included with the National Structure Inventory (NSI) data as discussed in Chapter 3. These data include day and night population estimates for each structure, as well as estimates of under age 65, and 65 and older populations. These populations are distributed based on census block level Longitudinal Employer and Household Data (LEHD) to specific Hazus occupancy types, except for school's data that are based on a national dataset from Oak Ridge National Labs (ORNL) that include the numbers of students, teachers, and staff for each facility that are used directly for peak day populations (see Chapter 3 for details). Although the population data and loss results are summarized by census block, only the NSI point populations that are impacted by tsunami inundation are included in the casualty assessment.
- Community preparedness levels: Good, Fair, and Poor. The grades can be determined based, for example, on the condition of shore-protection structures, emergency loud speakers, preparation of evacuation routes and signs, community's risk management level, and/or the education level for tsunami awareness. The users may attempt to specify "good" for a tsunami-ready community designated by National Weather Service (http://www.tsunamiready.noaa.gov/).

Input data considerations from Earthquake Damage Assessment:

- The functionality status of evacuation routes / bridges from the Hazus Earthquake Model output can be used as input to adjust walking speed reductions (Table 6.2), remove roadway segments in Level 1 or might be defined as impassable areas in the Level 2 analysis in the Hazus Tsunami Model.
- The casualties resulting from the earthquake could be considered in further reducing walking speeds because of rendering aid to the injured or for those directly injured by the earthquake.

Output Data

Output data are the graphical presentation of evacuee travel time and the statistics on the numbers of casualties (both fatalities and injuries). The casualty map shows both the total numbers and their spatial distributions. The results include:

- Day and night evacuee populations.
- Under age 65, 65 and over evacuee populations.
- Travel time to safety and partial safety for under age 65, and 65 and over populations.
- Survival rates for under age 65, and 65 and over populations for each community preparedness level
- Day and night injuries for under age 65, and 65 and over populations for each community preparedness level
- Day and night fatalities for under age 65, and 65 and over populations for each community preparedness level

Table 6.1: Pedestrian Walking Speeds (USGS Pedestrian Evacuation Analyst, meters per second)

Pedestrian Travel Speeds	(meters/second)
Slow walk	1.10
Fast walk	1.52
Slow run	1.79
Fast run	3.85

Table 6.2: Walking Speed Reduction Factors

Under 65	65 and Older
1.00	0.80

6.3 Methodology for Casualty Estimates

To avoid double-counting casualties, the number of casualties caused by the preceding earthquake in each population block are first estimated and provided separately. The methodology does not address a combined casualty model including the likelihood that earthquake injuries would likely increase tsunami casualties since evacuation would be made more difficult. Population in each block depends on time of day and season; population patterns would be different between daytime and nighttime, and the presence of tourists. Casualty also depends on the vulnerability of people – age and gender (see for example, Doocy et al., 2007, 2009; Guha-Sapir et al., 2006; MacDonald, 2005; Nuemayer and Plümper, 2007; Prater et al., 2007; Yeh, 2010): this factor is included through evacuation walking speeds and reduction factors (Tables 6.1 and 6.2). Drowning criteria based on physiology and tsunami dynamics (force balance) are not considered in the present methodology, although such criteria are often used in agent-based models used in Level 3.

As discussed earlier, earthquake casualty is directly related to earthquake intensity and building vulnerability because the severity of shaking determines whether buildings are collapsed or severely damaged, and the building collapse and damage kill and injure people. The strength of tsunamis (e.g. measured by tsunami runup height) is, however, not a good indicator for predicting casualty rates. The important factors are prior knowledge and experience with tsunamis (i.e., education) as well as timely and effective notification via tsunami warning systems. Consequently, temporal information on tsunami inundation (although no detailed flow depths and velocities are used here) is essential for estimating casualties. Table 6.3 summarizes the temporal parameters and Figure 6.3 provides a flow chart of the Tsunami Casualty Model.

Table 6.3: Casualty Model Parameters

Casualty Parameter	Description
T_{travel}	Provided by T_{travel} time view summarized by census block, using USGS Pedestrian Evacuation Analyst tool based on under age 65 walking speeds and reduced for age 65 and older (0.80), summary view for population totals and travel time to safety in minutes is provided by analysis
T^{*}_{travel}	Provided by T^{*}_{travel} time view summarized by census block, using USGS Pedestrian Evacuation Analyst tool based on under age 65 walking speeds to the area of partial safety (depth 0-2 meter) and reduced for 65 and older (0.80), summary view for population totals and travel time to partial safety in minutes. This should always be less than or equal to T_{travel}.
T_O (arrival time) Minutes	Estimated from Tsunami Travel Time maps for distant tsunamis, and ***estimated by user*** for local tsunamis
T_{MAX} (time to max runup) Minutes	***Estimated by user***, with a default value populated based on T_O plus 5 minutes, this always needs to be equal to or larger than T_O
T_W (warning time) Time to Issue Warning in Minutes	***Estimated by user,*** defaults for distant (40 minutes) and local (10 minutes), *note provided to user to use 0 when warning cue is provided by earthquake ground shaking*, all user parameters are summarized before launching analysis and included in reporting. This may not be greater than T_O.
C_{PREP}	Community Preparedness Level (Good, Fair or Poor) grading, defaults are 0.2, 0.6 and 1.0, respectively, and provided in an editable Analysis Parameter table (e.g. NWS TsunamiReady may be used for Good)
C_{STD}	Community Preparedness Level (Good, Fair or Poor) proportionality constant (termed “betas” for consistency with Hazus methodology), defaults are 0.3, 0.5 and 0.8, respectively, and provided in an editable Analysis Parameter table (e.g. NWS TsunamiReady may be used for Good)
T_{PREP}	Estimate in minutes for community to react to warning. Based on $C_{PREP}(T_O – T_W)$
T_{CRIT}	Difference between the evacuation time and the time available to evacuate. Calculated from $T_{CRIT} = (T_{MAX} – T_W) – (T_{PREP} + T_{travel})$, 50% of population reaches safety at $T_{crit} = 0$.
Day or Night	Defines the starting population distribution as peak day or night. Both day and night results are provided.

Figure 6.3: Flow chart of tsunami loss estimation methodology

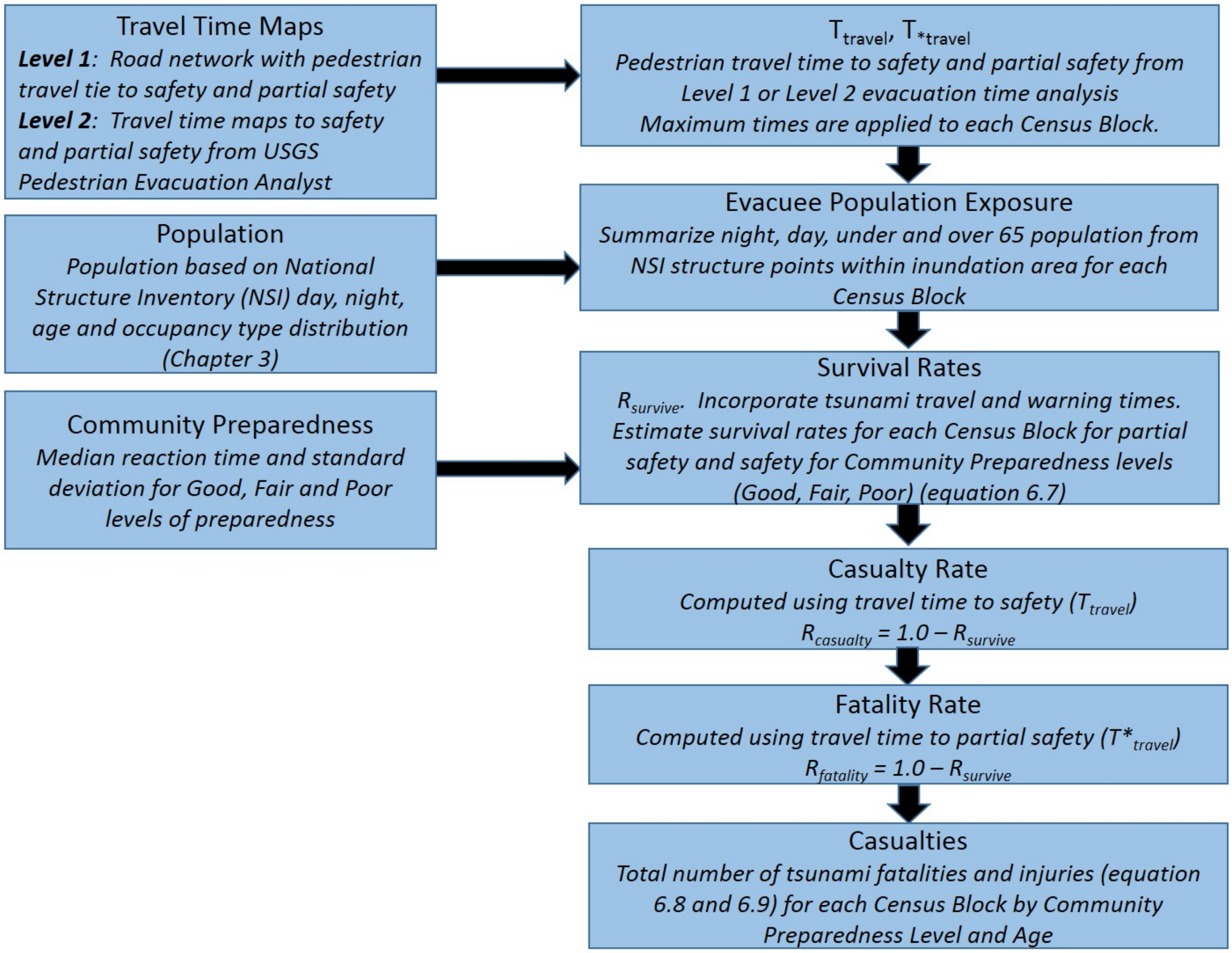

First, we determine the critical time T_{crit}, which represents the time difference between the evacuation time and the available time to evacuate:

$$T_{crit} = T_{available} - T_{evacuation} \text{ or more specifically,}$$

$$T_{crit} = (T_{max} - T_w) - (T_{prep} + T_{travel}) \qquad (6.1)$$

Note that the FEMA (2013) methodology provided a special case formula for when the tsunami arrival at the shore is the evacuation cue, when tsunami warning is not issued or issued after its arrival, however, by requiring that the user-provided warning time is less than or equal to the tsunami travel time, Tw ≤ To, (Table 6.3) the special case was not required.

If the evacuation travel time represents the median time for a given evacuee population, then, more than half of the population would travel beyond the inundation zone and thus be unharmed when the critical time $T_{crit} > 0$. When $T_{crit} < 0$, less than half would be unharmed, and when T_{crit} = 0, then it is a 50/50 situation (50 percent of the evacuee population would reach the area beyond the maximum penetration of the tsunami).

It is important to recognize that when people receive tsunami warnings (either official warnings or natural cues), not everyone starts to evacuate at once: this is due to individuals' preparation behaviors, communication among their families and neighbors, and other various personal decision-making processes. The timing to initiate evacuation is the primary reason why the evacuee pack spreads out from the initial population block. Assuming evacuees' population spread is skewed and is kept in the positive time ($t > 0$), we model the evacuees' initial distribution to be lognormal. It is pointed out that the choice of lognormal distribution is merely for convenience to form a skewed and 'smooth' distribution function of the evacuee population in $t > 0$. While the log function could imply some nonlinear effect of self-interactions, its physical justification is weak. With this caveat, the lognormal probability density function in terms of time t can be written as:

$$P(t) = \frac{1}{s\sqrt{2\pi}t} \mathrm{Exp}(-(\ln t - M)^2/2s^2) \quad (6.2)$$

And the cumulative distribution function:

$$D(t) = \frac{1}{2}\left[1 + erf\left((ln\, t - M)/s\sqrt{2}\right)\right] \quad (6.3)$$

Where erf (*) is the error function, the parameters s and M are related to the mean μ, the variance σ^2 and the mode of the variable t:

$$\mu = Exp\left(M + \frac{s^2}{2}\right); \sigma^2 = Exp(s^2 + 2M)(Exp(s^2) - 1);$$
$$\mathrm{mode} = \mathrm{Exp}(\mathrm{M} - \mathrm{s}^2); \mathrm{median} = \mathrm{Exp}(\mathrm{M}) \quad (6.4)$$

In the Casualty Losses module, we set the evacuation preparation time T_{prep} at the mode of the lognormal distribution, which means that the parameter T_{prep} represent the most probable initial time for people to evacuate.

Because neither adequate empirical data nor reliable models for the behavior of humans to tsunami hazards are available, it is necessary to estimate the parameters by judgment. Nevertheless, we believe that the methodologies in Hazus must be as rational as possible including the consideration of several key elements described below. With the methodology framework in place, we believe that the development of human behavior modeling will be able to be incorporated in the future.

We assume that people tend to act quickly in a short interval of time by responding to a warning for a local tsunami (including severe ground shaking). On the other hand, their response spans a long period for a distant tsunami when they are told that the tsunami will not arrive for several hours. Therefore, we model peoples response time to warnings as proportional to the time difference between the warning time and the tsunami arrival time. Hence, the standard deviation, σ (the square root of the variance σ^2 in (6.4)) for the lognormal distribution is estimated as:

$$\sigma = C_{std}\,(T_0 - T_w) \tag{6.5}$$

The proportionality constant ("*betas*") C_{std} = 0.3, 0.5, and 0.8 result in possible spreads in the evacuee distributions for the three community preparedness levels: good, fair, or poor for which Hazus provides results.

The value of the warning effectiveness and preparation time T_{prep} is not specified but pre-assigned based on one of three grades of community preparedness. Recall that T_{prep} represents the most 'probable' time (i.e., mode) for people to initiate evacuation after a tsunami warning is received (including the natural cue: ground shaking). The mode of the evacuation initiation can be modified by the user and is set at the preparation time T_{prep}:

$$mode = T_{prep} = C_{prep}(T_0 - T_w) \tag{6.6}$$

in which we use C_{prep} = 0.2, 0.6, and 1 for the three grades of community preparedness (see Table 6.4). Users may modify these parameters based on warning effectiveness and preparation time T_{prep} for the community, or as an option, users could mix the preparedness level results for each Census Block in the community. Note the values of C_{std} were modified slightly from FEMA (2013) based on performance testing summarized in Tables 6.5 and 6.6 below. In addition, the case where tsunami travel time is less than warning time, $T_o < T_w$, was removed by requiring $T_w \leq T_o$.

Figure 6.4 shows the resulting probability density function for the time to initiate evacuation with various values of C_{std} for both typical local-tsunami and distant-tsunami cases. The resulting distribution appears realistic, but can be fine-tuned when better information is obtained. Also note that each distribution function in the figure represents the spread due to response to the warning only: effects of the pedestrian traveling process are not included, since that is provided directly from the USGS methodology.

Table 6.4: Default parameters to determine the initial evacuee spread based on their response to the warning

Community Preparedness Level	Parameter to determine evacuation initiation time C_{prep} (equation 6.6)	Parameter for the deviation of evacuation initiation C_{std}, which determines the spread (equation 6.5)
Good	0.2	0.3
Fair	0.6	0.5
Poor	1	0.8

Figure 6.4: Probability density functions of the population ratio for lognormal distribution with the different values of spread (Good, Fair, Poor).

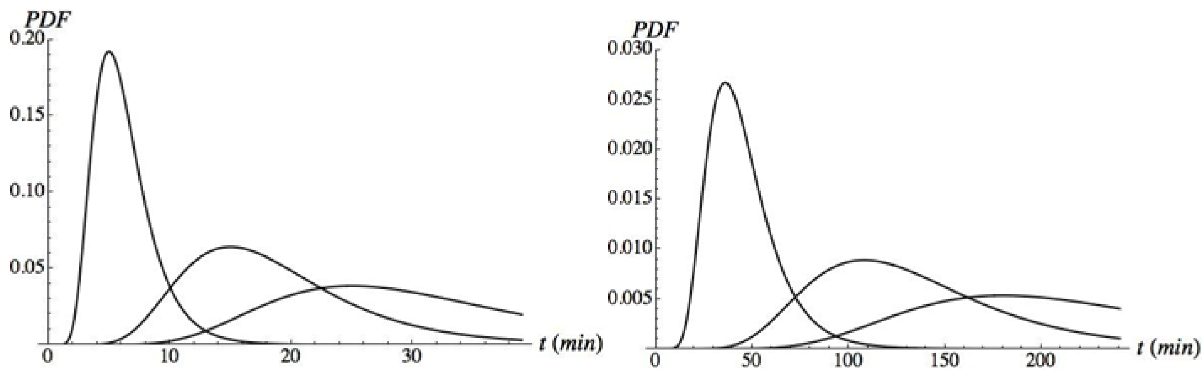

Left) for a typical local tsunami event: tsunami arrival time T0 = 25 min., time of maximum inundation Tmax = 30 min., and tsunami warning time Tw = 0 (the same time as the earthquake). Right) for a typical distant tsunami event: T0 = 250 min., Tmax = 255 min., and Tw = 70 min. The three lines in each plot represent the grades of the preparedness of the coastal communities: the narrower distribution corresponds to a better-prepared community.

The survival rate $R_{survive}$ is the value of the cumulative distribution at $t = T_{med} + T_{crit}$. The basis of this methodology implements a lognormal cumulative distribution to estimate the survival rate probabilities that can be implemented in a spreadsheet function and utilized as fast running SQL update statements in the Hazus program as follows:

$$R_{SURVIVE} = NORMDIST(LN(T_{PREP} + T_{CRIT}),LN(T_{PREP}),(C_{STD}), 1 \qquad (6.7)$$

Where 1 represents the cumulative distribution function, yielding the casualty rate determined by $R_{causalty}$ =1.0 – $R_{survive}$. The spreadsheet implementation allowed for the computation of thousands of examples based on various tsunami travel and warning times (including T_w = 0 where the ground shaking provides cue), as well as evacuation time combinations for each community preparedness level. Table 6.5 illustrates a summary of results, $R_{survive}$, for potential near-source events, while Table 6.6 provides a summary of results for distant-source events.

Table 6.5: Sampling of Survival Rates Based on Methodology – Near Source

Time in Minutes: Tsunami Travel	Time in Minutes: Max Inundation Extent	Time in Minutes: Issue Warning	Time in Minutes: Pedestrian Evacuation	Community Reaction Time: Tprep Good	Community Reaction Time: Tprep Fair	Community Reaction Time: Tprep Poor	Survival Rates Based on Community Preparedness Levels: Good	Survival Rates Based on Community Preparedness Levels: Fair	Survival Rates Based on Community Preparedness Levels: Poor
0	5	0	0	0	0	0	0%	0%	0%
5	10	5	3	0	0	0	0%	0%	0%
10	15	0	10	2	6	10	99.89%	35.77%	19.31%
15	20	0	15	3	9	15	95.57%	11.99%	8.48%
20	25	0	30	4	12	20	0%	0%	0%
25	30	0	15	5	15	25	99.99%	50.00%	26.16%
30	35	0	30	6	18	30	27.17%	0.52%	1.26%
35	40	10	15	5	15	25	99.99%	50.00%	26.16%
40	45	10	30	6	18	30	27.17%	0.52%	1.26%
45	50	10	15	7	21	35	100%	63.63%	33.70%
50	55	10	30	8	24	40	98.19%	17.36%	11.01%
55	60	10	15	9	27	45	100%	69.81%	37.67%

Table 6.6: Sampling of Survival Rates Based on Methodology – Distant Source

Tsunami Travel Time in Minutes	Max Inundation Extent Time in Minutes	Issue Warning Time in Minutes	Pedestrian Evacuation Time in Minutes	Tprep Good: Community Reaction Time	Tprep Fair: Community Reaction Time	Tprep Poor: Community Reaction Time	Survival Rates based on Community Preparedness Level: Good	Survival Rates based on Community Preparedness Level: Fair	Survival Rates based on Community Preparedness Level: Poor
60	65	10	60	10	30	50	0%	0%	0%
80	85	20	15	12	36	60	100%	74.44%	40.99%
100	105	20	60	16	48	80	93.16%	9.60%	7.30%
120	125	20	15	20	60	100	100%	79.13%	44.76%
140	145	20	60	24	72	120	99.96%	41.90%	22.17%
160	165	20	15	28	84	140	100%	80.88%	46.31%
180	185	40	60	28	84	140	99.99%	50.94%	26.64%
200	205	40	15	32	96	160	100%	81.40%	46.79%
220	225	40	60	36	108	180	100%	61.50%	32.43%
240	245	40	15	40	120	200	100%	82.10%	47.44%
260	265	40	60	44	132	220	100%	67.23%	35.96%
280	285	40	15	48	144	240	100%	82.55%	47.88%

These tables represent reasonable survival rates that follow the logic described throughout this chapter regarding critical time and community preparedness levels. One rare exception is that for very low survival rates, the poorly prepared community may have a slighter higher rate (1.26 percent vs 0.52 percent, Lines 7 and 9, Table 6.5) than the fair community. This is attributed to the relative high standard deviation and wide distribution function associated with poor and is not expected to have a significant impact on casualty results.

The number of casualties consists of the numbers of injuries and fatalities. To distinguish a fatality from an injury, we set a criterion in terms of the inundation depth: we assume that 99 percent of people would be killed if they were caught in a depth of more than 2m. With the Evacuation Travel Time for fatality T^*_{travel} (to the boundary of the 2m depth), the foregoing calculations are repeated to obtain the fatality rate $R_{fatality}$. Here we assume the injury rate decreases linearly from 99 percent to nil from the point of 2m inundation depth toward the maximum inundation $X(x, y)$. This logic is illustrated in Figure 6.5

Total number of casualties for a given population block j can then be calculated by: $N_j \times R_{casualty}$, where N_j is the number of people in the population block j summarized from the population in structures that are in the inundation areas. Then, the number of fatalities for the population block j can be calculated by:

$$NF_j = N_j \times \left(0.99\, R_{fatality} + {}^{1}/_{2}\left(R_{casualty} - 0.99\, R_{fatality}\right)\right) \tag{6.8}$$

And the number of injuries is:

$$NI_j = {}^{1}/_{2}\, N_j\left(R_{casualty} - 0.99\, R_{fatality}\right) = N_j \times R_{casualty} - NF_j \tag{6.9}$$

Note that these equations are repeated for under age 65, 65 and over, as well as each community preparedness level. It should be emphasized that the foregoing estimate excludes potential survivors who have evacuated to tall, sturdy buildings.

Total numbers of fatalities and injuries for this community are the summations $\sum_j NF_j$ and $\sum_j NI_j$ respectively.

Figure 6.5: A sketch illustrates the logic to determine fatality and injury

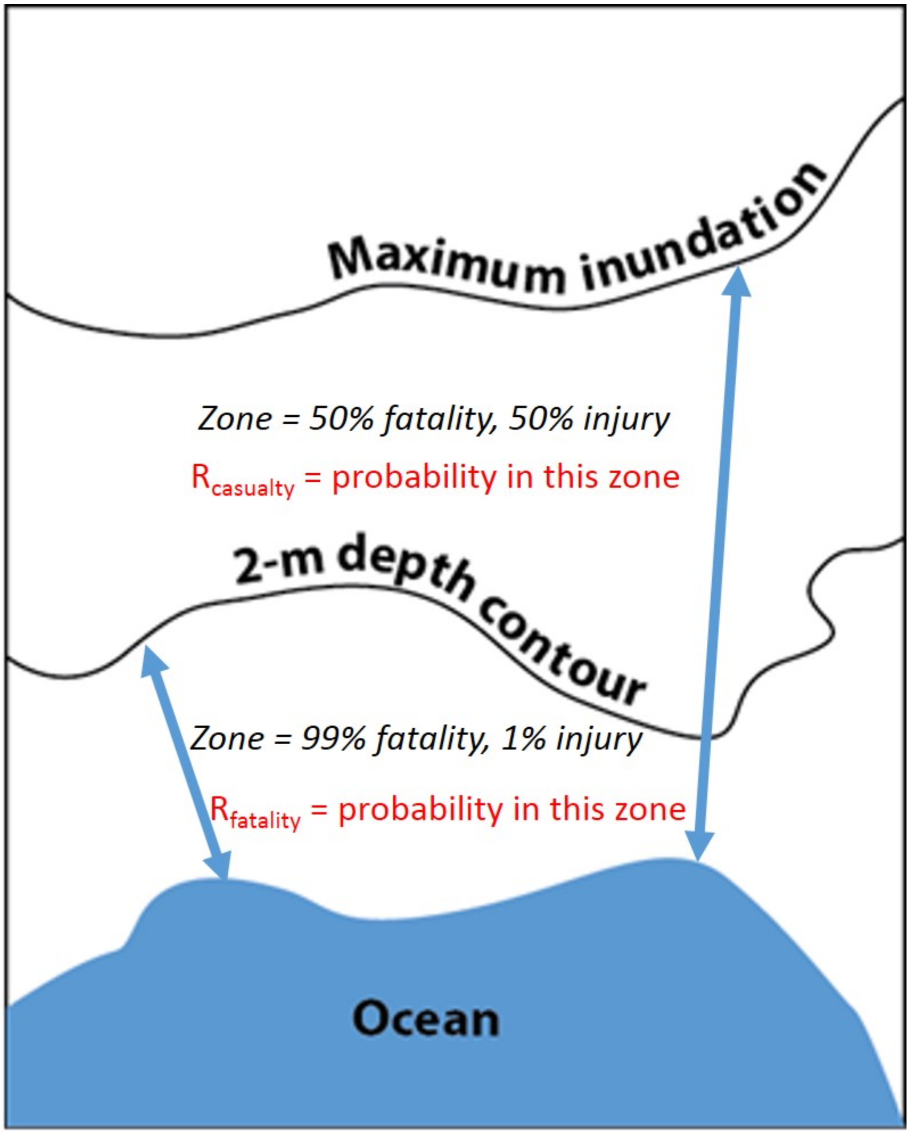

The FEMA (2013) example case with the conditions of preparation time T_{prep} = 10 min.; tsunami arrival time T_0 = 25 min.; time at maximum inundation T_{max} = 30 min.; tsunami warning time T_w = 0 (essentially immediately upon occurrence of the earthquake); evacuee travel time T_{travel} = 18 min. using the $R_{survive}$ probability equation 6.7, yields a rate of 64.2 percent for the fair preparedness level community example. Consequently, the resulting casualty rate is 100 – 64.2 = 35.8 percent. If we assume the Evacuation Travel Time T^*_{travel} to an inundation depth of 2.0m was 17 min. instead of 18 min, then equation 6.7 yields 70.0 percent. Therefore, the probability of a 99 percent fatality rate would be 30.0 percent. For a given population block with 193 people, Equation 6.10 yields the estimated number of fatalities:

$$(193) \times \{0.99\ (0.300) + \tfrac{1}{2}\ (0.358 - 0.99\ (0.300))\} = 57 \text{ people} \qquad (6.10)$$

and Equation 6.11 the number of injuries:

$$(193) \times (0.358) - (57) = 12 \text{ people} \tag{6.11}$$

This compares well to the FEMA (2013) analysis of 56 fatalities and 13 injuries for this example case.

6.4 Future Enhancements

A future Level 3 analysis could use results from agent-based simulation models, although this option is not included for the present methodology development. Agent-based modeling for tsunami events has been performed in the past for the town of Owase, Japan (Katada et al. 2006), for Long Beach Peninsula, Washington (Yeh et al. 2009), and for the town of Cannon Beach, Oregon (Yeh and Karon, 2011).

The FEMA (2013), as well as Yeh (2014), methodology recognizes that once people begin evacuating to a safe haven, they further disperse due to age and demographic factors incorporating a standard deviation, σ_{walk}., that is included in the final cumulative distribution function. However, the method was modified to leverage the evacuee travel times that are directly provided from the USGS Pedestrian Evacuation Analysts GIS-based approach. We also recognized that the community preparedness level based methodology has a larger influence on the survival rate methodology. This potential dispersion of evacuees as a result of deviation in the walking speed assumptions could be incorporated in the future.

In addition, a methodology could be developed to better combine earthquake and tsunami casualties. On one hand, calculating these separately can result in an overestimation, however, fatality rates for earthquakes are exceptionally smaller than for those exposed to tsunami inundation. Therefore, it seems more likely that the casualties caused by the earthquake could lead to additional tsunami casualties by slowing evacuation because of those directly injured or those rendering aid to the injured.

6.5 References

Doocy, S., Robinson, C., Moodie, C., and Burnham, G. (2009). "Tsunami-Related Injury in Aceh Province, Indonesia." *Global Public Health*, 4(2), 205-214.

Doocy, S., Rofi, A., Moodie, C., Spring, E., Bradley, S., and Burnham, G. (2007). "Tsunami Mortality in Aceh Province, Indonesia." *Bulletin of the World Health Organization*, 85, 273-278.

Eubanks, J. (1994). Pedestrian Accident Reconstruction, Tucson: Lawyers & Judges Publishing, 281 pp.

Guha-Sapir, D., Parry, L.V., Degomme, O., Joshi, P.C., and Saulina Arnold, J.P. (2006). “Risk factor for mortality and injury: Post-tsunami epidemiological findings from Tamil Nadu. Centre for Research on the Epidemiology of Disaster,” Catholic University of Louvain, Brussels, Belgium, 48pp.

Highway Capacity Manual, 2010. Transportation Research Board, National Research Council, 1650pp.

JICE (Japan Institute of Construction Engineering) 2011:

http://www.jice.or.jp/sinsai/sinsai_detail.php?id=2743

Katada, T., Kuwasawa, N., Yeh, H., and Pancake, C. 2006. Integrated simulation of tsunami hazards, Proc. *8th National Conference on Earthquake Engineering*, San Francisco.

Kuhn, Randall. 2009. Tsunami and conflict in Sri Lanka. A report to U.N. Project on the Economics of Disaster Risk Reduction:

https://www.gfdrr.org/sites/gfdrr/files/Kuhn_Tsunami%26Conflict.pdf

MacDonald R. (2005). "How Women Were Affected by the Tsunami: A Perspective from Oxfam." *PLoS Medicine*, 2 (6), 474 – 475.

Nuemayer, E., and Plümper, T. (2007). "The Gendered Nature of Natural Disasters: The Impact of Catastrophic Events on the Gender Gap in Life Expectancy, 1981 – 2002" Annals of the American Association of Geographers, 97 (3), 551 - 566.

Prater, C., Peacock, W.G., Grover, H., and Arlikatti, S. (2007). Personal communication, Texas A&M University.

Suppasri, A., Koshimura, S., Imai, K., Mas, E., Gokon, H., Muhari, A., and Imamura, F. 2012. Damage characteristics and field survey of the 2011 Great East Japan Tsunami in Miyagi Prefecture. *Costal Engineering Journal*, 54(1), DOI: 10.1142/S0578563412500052

Tobler W (1993) Three presentations on geographical analysis and modeling—non-isotropic geographic modeling. Speculations on the geometry of geography; and global spatial analysis. UCSB. National Center for Geographic Information and Analysis Technical Report 93-1. Available at: http://ncgia.ucsb.edu/technical-reports/PDF/93-1.pdf

Wood, N.J., Schmidtlein, M.C. 2011. Anisotropic path modeling to assess pedestrian-evacuation potential from Cascadia-related tsunamis in the US Pacific Northwest. *Natural Hazards*, DOI 10.1007/s11069-011-9994-2

Yeh, H. 2014. Tsunami Hazard and Casualty Estimation Model: 10th U.S. National Congress on Earthquake Engineering, 11 pp.

Yeh, H. 2010. Gender and age factors in tsunami casualties, *Natural Hazards Review*, 11 (1), 29-34

Yeh, H., Fiez, T., and Karon, J. 2009. *A Comprehensive Tsunami Simulator for Long Beach Peninsula. Phase-1: Framework Development*. Washington State Military Department, 27 pp.

Yeh, H. and Karon, J. 2011. *Comprehensive Tsunami Simulator for Cannon Beach*, Oregon. Report to the City of Cannon Beach

7.0 Direct Economic Losses

7.1 Introduction

This chapter describes the conversion of damage-state information, developed in previous modules, into estimates of dollar loss.

The methodology provides estimates of the structural and nonstructural repair costs caused by building damage and the associated loss of building contents and business inventory. Building damage can also cause additional losses by restricting the building's ability to function properly. To account for this, business interruption, including rental income losses are estimated. These losses are calculated from the building damage estimates by use of methods described later. The methodology flowchart highlighting the Direct Economic Loss component is shown in Figure 7.1.

Figure 7.1: Direct Economic Losses Relationship to other Components of the Tsunami Loss Estimate Methodology

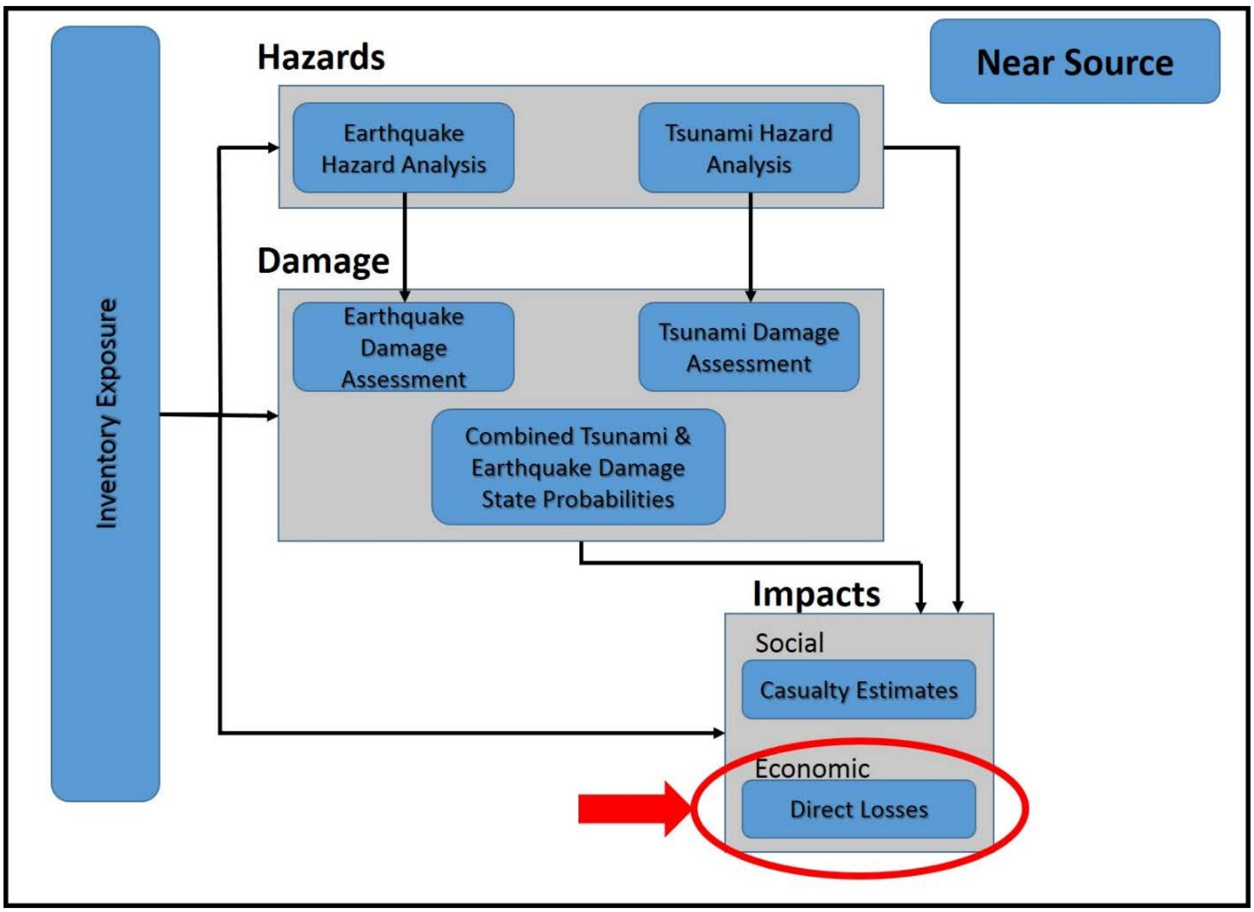

7.2 Scope

This chapter provides descriptions of the methodologies, the derivation of default data, and explanatory tables for a number of direct economic loss items, derived from estimates of building and lifeline damage. For building-related items, methods for calculating the following dollar losses are provided:

- Building Repair and Replacement Costs
- Building Contents Losses
- Building Inventory Losses

To enable time-dependent losses to be calculated, default values are provided for:

- Building Recovery Time and Loss of Function (business interruption) time

Procedures for calculating the following time-dependent losses are provided:

- Relocation Expenses
- Proprietor's Income and Wage Losses
- Rental Income Losses

7.3 Input Requirements

Input data for direct economic losses consists of building damage estimates from the direct physical damage module. The damage estimates are in the form of probabilities of being in each damage state, for each structural type or occupancy class. The building classification system is discussed in Chapter 3. Damage states are discussed in detail in Chapter 5. Damage-state probabilities are provided from the direct physical damage module for both structural and nonstructural damage. These damage-state probabilities are then converted to monetary losses using inventory information and economic data. For Default Data Analysis (Level 1) values, the buildings are classified into three broad occupancy/use-related categories: residential, commercial/institutional, and industrial. These categories are used to determine the non-structural element make-up of the buildings and the nature and value of their contents. Building replacement cost data is provided for each of the 33 occupancy classes presented in Chapter 3.

7.4 Building Repair and Replacement Costs

To establish dollar loss estimates, the damage-state probabilities must be converted to dollar loss equivalents. Losses will be due to both structural and nonstructural damage. For a given occupancy and damage state, building repair, and replacement costs are estimated as the product of the floor area of each building type within the given occupancy, the probability of the building type being in the given damage state, and repair costs of the building type per square foot for the given damage state, summed over all building types within the occupancy.

For structural damage, losses are calculated as follows:

$$\mathrm{CS_{ds,i}} = \mathrm{BRC_i} * \sum_{i=1}^{33} \mathrm{PMBTSTR_{ds,i}} * \mathrm{RCS_{ds,i}} \tag{7.1}$$

$$\mathrm{CS_i} = \sum_{ds=2}^{5} \mathrm{CS_{ds,i}} \tag{7.2}$$

where:

$CS_{ds,i}$	= cost of structural damage (repair and replacement costs) for damage state ds and occupancy i
BRC_i	= building replacement cost of occupancy i
$PMBTSTR_{ds,I}$	= probability of occupancy being in structural damage state ds, see Chapter 5
$RCS_{ds,I}$	= structural repair and replacement ratio for occupancy i in damage state ds, Table 7.1

The structural repair cost ratio for structural damage for each damage state and occupancy is shown in Table 7.2. Note that damage state "none" (ds = 1) does not contribute to the calculation of the cost of structural damage and thus the summation in Equation 7.2 is from ds = 2 to ds = 5. In addition, when the tsunami model is run without the earthquake model, the Slight damage state is not used for tsunami.

A similar calculation is performed for nonstructural damage. Nonstructural damage does not include the damage to contents such as furniture and computers; content loss is accounted for separately.

Nonstructural damage costs are calculated as follows:

$$\mathrm{CNS_{ds,i}} = \mathrm{BRC_i} * \mathrm{PONS_{ds,i}} * \mathrm{RC_{ds,i}} \tag{7.3}$$

$$\mathrm{CNS_i} = \sum_{ds=2}^{5} \mathrm{CNS_{ds,i}} \tag{7.4}$$

Where:

$CNS_{ds,i}$	= cost of nonstructural damage (repair and replacement costs) for damage state ds and occupancy i

CNS_i	= cost of nonstructural damage (repair and replacement costs) for occupancy i
BRC_i	= building replacement cost of occupancy i
$PONS_{ds,i}$	= probability of occupancy i being in nonstructural damage state ds,
$RC_{ds,i}$	= nonstructural repair and replacement ratio for occupancy i in damage state ds (Table 7.2)

The repair cost ratios for nonstructural damage for each damage state are shown in Tables 7.2. The total cost of building damage (CBD_i) for occupancy class i is the sum of the structural and nonstructural damage.

$$\mathrm{CBD_i} = \mathrm{CS_i} + \mathrm{CNS_i} \tag{7.5}$$

Finally, to determine the total cost of building damage (CBD), Equation 7.5 must be summed over all the occupancy classes.

$$\mathrm{CBD} = \sum_{\mathrm{i}} \mathrm{CBD_i} \tag{7.6}$$

The following tables are from the Hazus Earthquake Model *Technical Manual* – Tables 15.2 through 15.4.

Table 7.1: Structural Repair Cost Ratios (% of building replacement cost)

No.	Label	Occupancy Class	Structural Damage State: **Slight**	Structural Damage State: **Moderate**	Structural Damage State: **Extensive**	Structural Damage State: **Complete**
1	RES1	**Residential:** Single Family Dwelling	0.5	2.3	11.7	23.4
2	RES2	**Residential:** Mobile Home	0.4	2.4	7.3	24.4
3-8	RES3a-f	**Residential:** Multi Family Dwelling	0.3	1.4	6.9	13.8
9	RES4	**Residential:** Temporary Lodging	0.2	1.4	6.8	13.6
10	RES5	**Residential:** Institutional Dormitory	0.4	1.9	9.4	18.8
11	RES6	**Residential:** Nursing Home	0.4	1.8	9.2	18.4
12	COM1	**Commercial:** Retail Trade	0.6	2.9	14.7	29.4
13	COM2	**Commercial:** Wholesale Trade	0.6	3.2	16.2	32.4
14	COM3	**Commercial:** Personal and Repair Services	0.3	1.6	8.1	16.2
15	COM4	**Commercial:** Professional/Technical/ Business Services	0.4	1.9	9.6	19.2
16	COM5	**Commercial:** Banks/Financial Institutions	0.3	1.4	6.9	13.8
17	COM6	**Commercial:** Hospital	0.2	1.4	7.0	14.0
18	COM7	**Commercial:** Medical Office/Clinic	0.3	1.4	7.2	14.4
19	COM8	**Commercial:** Entertainment & Recreation	0.2	1.0	5.0	10.0
20	COM9	**Commercial:** Theaters	0.3	1.2	6.1	12.2
21	COM10	**Commercial:** Parking	1.3	6.1	30.4	60.9
22	IND1	**Industrial:** Heavy	0.4	1.6	7.8	15.7
23	IND2	**Industrial:** Light	0.4	1.6	7.8	15.7
24	IND3	**Industrial:** Food/Drugs/Chemicals	0.4	1.6	7.8	15.7
25	IND4	**Industrial:** Metals/Minerals Processing	0.4	1.6	7.8	15.7
26	IND5	**Industrial:** High Technology	0.4	1.6	7.8	15.7
27	IND6	**Industrial:** Construction	0.4	1.6	7.8	15.7
28	AGR1	**Agriculture:** Agriculture	0.8	4.6	23.1	46.2
29	REL1	**Religion/Non-Profit:** Church/Membership Organization	0.3	2.0	9.9	19.8
30	GOV1	**Government:** General Services	0.3	1.8	9.0	17.9
31	GOV2	**Government:** Emergency Response	0.3	1.5	7.7	15.3
32	EDU1	**Education:** Schools/Libraries	0.4	1.9	9.5	18.9
33	EDU2	**Education:** Colleges/Universities	0.2	1.1	5.5	11.0

Note that the values in the last column (corresponding rows) of Tables 7.1 and 7.2 must sum to 100 since the complete damage state implies that the structure must be replaced. The replacement value of the structure is the sum of the structural and nonstructural components.

Table 7.2: Nonstructural Repair Costs (% of building replacement cost)

No.	Label	Occupancy Class	Nonstructural Damage State: **Slight**	Nonstructural Damage State: **Moderate**	Nonstructural Damage State: **Extensive**	Nonstructural Damage State: **Complete**
1	RES1	**Residential:** Single Family Dwelling	1.5	7.7	33	76.6
2	RES2	**Residential:** Mobile Home	1.6	7.6	30.2	75.6
3-8	RES3a-f	**Residential:** Multi Family Dwelling	1.7	8.6	34.4	86.2
9	RES4	**Residential:** Temporary Lodging	1.8	8.6	34.6	86.4
10	RES5	**Residential:** Institutional Dormitory	1.6	8.1	32.4	81.2
11	RES6	**Residential:** Nursing Home	1.6	8.2	32.6	81.6
12	COM1	**Commercial:** Retail Trade	1.4	7.1	26.7	70.6
13	COM2	**Commercial:** Wholesale Trade	1.4	6.8	25.6	67.6
14	COM3	**Commercial:** Personal and Repair Services	1.7	8.4	31.9	83.8
15	COM4	**Commercial:** Professional/Technical/ Business Services	1.6	8.1	30.8	80.8
16	COM5	**Commercial:** Banks/Financial Institutions	1.7	8.6	32.7	86.2
17	COM6	**Commercial:** Hospital	1.8	8.6	32.8	86
18	COM7	**Commercial:** Medical Office/Clinic	1.7	8.6	32.5	85.6
19	COM8	**Commercial:** Entertainment & Recreation	1.8	9	34.1	90
20	COM9	**Commercial:** Theaters	1.7	8.8	33.4	87.8
21	COM10	**Commercial:** Parking	0.7	3.9	15.2	39.1
22	IND1	**Industrial:** Heavy	1.6	8.4	27.7	84.3
23	IND2	**Industrial:** Light	1.6	8.4	27.7	84.3
24	IND3	**Industrial:** Food/Drugs/Chemicals	1.6	8.4	27.7	84.3
25	IND4	**Industrial:** Metals/Minerals Processing	1.6	8.4	27.7	84.3
26	IND5	**Industrial:** High Technology	1.6	8.4	27.7	84.3
27	IND6	**Industrial:** Construction	1.6	8.4	27.7	84.3

No.	Label	Occupancy Class	Nonstructural Damage State: **Slight**	Nonstructural Damage State: **Moderate**	Nonstructural Damage State: **Extensive**	Nonstructural Damage State: **Complete**
28	AGR1	**Agriculture:** Agriculture	0.8	5.4	17.6	53.8
29	REL1	**Religion/Nonprofit:** Church/Membership Organization	1.7	8	30.6	80.2
30	GOV1	**Government:** General Services	1.7	8.2	31.2	82.1
31	GOV2	**Government:** Emergency Response	1.7	8.5	32.2	84.7
32	EDU1	**Education:** Schools/Libraries	1.6	8.1	34	81.1
33	EDU2	**Education:** Colleges/Universities	1.8	8.9	38.7	89

7.5 Other Costs

Building Contents

Building contents are defined as furniture, equipment that is not integral with the structure, computers, and other supplies. Contents do not include inventory or nonstructural components such as lighting, ceilings, mechanical and electrical equipment, and other fixtures.

The cost of contents damage is calculated as follows:

$$\mathrm{CCD_i = CRV_i * \sum_{ds=2}^{5} CD_{ds,i} * PMBTNS_{ds,i}} \quad (7.7)$$

Where:

CCD_i = cost of contents damage for occupancy i

CRV_i = contents replacement value for occupancy i

$CD_{ds,I}$ = contents damage ratio for occupancy i in damage state ds (Table 7.3)

$PMBTNS_{ds,I}$ = the probability of occupancy i being in content damage state ds

Unlike earthquake, the contents damage ratios in Table 7.3 assume that at the complete damage state for a tsunami that contents are not salvageable. The earthquake model assumes a 50% salvage rate for contents in a completely damaged structure.

Table 7.3: Contents Damage Ratios (% of contents replacement cost)

No.	Label	Occupancy Class	Nonstructural Damage State: **Slight**	Nonstructural Damage State: **Moderate**	Nonstructural Damage State: **Extensive**	Nonstructural Damage State: **Complete**
1	RES1	**Residential:** Single Family Dwelling	1	5	25	100
2	RES2	**Residential:** Mobile Home	1	5	25	100
3-8	RES3a-f	**Residential:** Multi Family Dwelling	1	5	25	100
9	RES4	**Residential:** Temporary Lodging	1	5	25	100
10	RES5	**Residential:** Institutional Dormitory	1	5	25	100
11	RES6	**Residential:** Nursing Home	1	5	25	100
12	COM1	**Commercial:** Retail Trade	1	5	25	100
13	COM2	**Commercial:** Wholesale Trade	1	5	25	100
14	COM3	**Commercial:** Personal and Repair Services	1	5	25	100
15	COM4	**Commercial:** Professional/Technical/ Business Services	1	5	25	100
16	COM5	**Commercial:** Banks/Financial Institutions	1	5	25	100
17	COM6	**Commercial:** Hospital	1	5	25	100
18	COM7	**Commercial:** Medical Office/Clinic	1	5	25	100
19	COM8	**Commercial:** Entertainment & Recreation	1	5	25	100
20	COM9	**Commercial:** Theaters	1	5	25	100
21	COM10	**Commercial:** Parking	1	5	25	100
22	IND1	**Industrial:** Heavy	1	5	25	100
23	IND2	**Industrial:** Light	1	5	25	100
24	IND3	**Industrial:** Food/Drugs/Chemicals	1	5	25	100
25	IND4	**Industrial:** Metals/Minerals Processing	1	5	25	100
26	IND5	**Industrial:** High Technology	1	5	25	100
27	IND6	**Industrial:** Construction	1	5	25	100
28	AGR1	**Agriculture:** Agriculture	1	5	25	100
29	REL1	**Religion/Nonprofit:** Church/Membership Organization	1	5	25	100

No.	Label	Occupancy Class	Nonstructural Damage State: **Slight**	Nonstructural Damage State: **Moderate**	Nonstructural Damage State: **Extensive**	Nonstructural Damage State: **Complete**
30	GOV1	**Government:** General Services	1	5	25	100
31	GOV2	**Government:** Emergency Response	1	5	25	100
32	EDU1	**Education:** Schools/Libraries	1	5	25	100
33	EDU2	**Education:** Colleges/Universities	1	5	25	100

<u>Business Inventory Losses</u>

Business inventories vary considerably with occupancy. For example, the value of inventory for a high-tech manufacturing facility would be very different from that of a retail store. Thus, it is assumed for this model that business inventory for each occupancy class is based on annual gross sales. Since losses to business inventory most likely occur from water damage to either the inundated stacks of inventory or from earthquake shaking collapsing inventory (for a local earthquake event), it is assumed, as it was with building contents, that nonstructural damage is a good indicator of losses to business inventory. As with structural and non-structural losses, the slight damage state is not considered for tsunami-only damages. Business inventory losses then become the product of the total inventory value (floor area times the percent of gross sales or production per square foot) of buildings of a given occupancy in each damage state, the percent loss to the inventory, and the probability of given damage states. The business inventory losses are given by the following expressions.

$$\mathrm{INV_i} = \mathrm{FA_i} * \mathrm{SALES_i} * \mathrm{BI_i} * \sum_{i=22}^{28} \mathrm{INV_i} \tag{7.8}$$

$$\mathrm{INV} = \mathrm{INV_{12}} + \mathrm{INV_{13}} + \sum_{i=22}^{28} \mathrm{INV_i} \tag{7.9}$$

Where:

INV_i	= value of inventory losses for occupancy i
INV	= total value of inventory losses (only occupancies 12, 13 and 22-28 would have inventories, so the summation includes only these occupancies)
FA_i	= floor area of occupancy group i (in square feet)
$SALES_i$	= annual gross sales or production ($ per square foot) for occupancy i (see Table 7.4)
BI_i	= business inventory as a percentage of annual gross sales for occupancy i (see Table 7.4)

$PONS_{ds,i}$	probability of occupancy i being in nonstructural damage state ds
$INVD_{ds,i}$	percent inventory damage for occupancy i in damage state ds

Table 7.4: Business Inventory Parameters

SOccupID	Occupancy	Annual Sales ($ per sq. ft)	Bus. Inv. (% annual sales)	% Slight Dmg.	% Moderate Dmg.	% Extensive Dmg.	% Complete* Dmg.
28	AGR1	$148.00	8	1	5	25	50
12	COM1	$53.00	13	1	5	25	50
13	COM2	$77.00	10	1	5	25	50
22	IND1	$713.00	5	1	5	25	50
23	IND2	$226.00	4	1	5	25	50
24	IND3	$697.00	5	1	5	25	50
25	IND4	$656.00	3	1	5	25	50
26	IND5	$437.00	4	1	5	25	50
27	IND6	$768.00	2	1	5	25	50

**some salvage of inventory is assumed at the complete damage state*

Loss of Income and Wage Loss

Business activity generates several types of income. First is income associated with capital, or property ownership. Business generates profits, and a portion of this is paid out to individuals (as well as to pension funds and other businesses) as dividends, while another portion, retained earnings, is invested back into the enterprise. Businesses also make interest payments to banks and bondholders for loans. They pay rental income on property and make royalty payments for the use of tangible assets. Those in business for themselves, or in partnerships, generate a category called proprietary income, one portion of which reflects their profits and the other that reflects an imputed salary (e.g., the case of lawyers or dentists). Finally, the biggest category of income generated/paid is associated with labor. In most urban regions of the U.S., wage and salary income comprises more than 75 percent of total personal income payments.

Income losses occur when building damage disrupts economic activity. Income losses are the product of floor area, income realized per square foot and the expected days of loss of function for each damage state. Proprietor's income losses are expressed as follows:

$$\mathrm{YLOS_i} = (1 - \mathrm{RF_i}) * \mathrm{FA_i} * \mathrm{INC_i} * \sum_{ds=2}^{5} \mathrm{POSTR_{ds,i}} * \mathrm{LOF_{ds}} \qquad (7.10)$$

Where:

$YLOS_i$	= income losses for occupancy class i
FA_i	= floor area of occupancy class i (in square feet)
INCi	= income per day (per square foot) for occupancy class i (see Table 7.5)
$POSTR_{dsi}$	= probability of occupancy i being in structural damage state ds
LOF_{ds}	= loss of function time for damage state ds
RF_i	= income recapture factor for occupancy i (see Table 7.6)

The business-related losses can be recouped to some extent by working overtime after the event and this is shown in the recapture factor. For example, a factory that is closed for six weeks due to directly-caused structural damage or indirectly-caused shortage of supplies may work extra shifts in the weeks or months following its reopening. It is necessary that there be a demand for its output (including inventory buildup), but this is likely to be the case as undamaged firms try to overcome input shortages, other firms that were temporarily closed try to make-up their lost production as well, and firms outside the region press for resumption of export sales to them.

Wage losses are calculated using the same equation by substituting wages per square foot per day for income (Table 7.5) and replacing the income recapture factor with the wage recapture factor (Table 7.6).

Table 7.5: Capital Income and Wages

Occupancy	Net Income (sqft/day)	Net Income (sqft/year)	Wage (sqft/day)	Employees* per sqft	Output (sqft/day)
AGR1	$0.266	$97.160	$0.105	0.004	0.993
COM1	$0.070	$25.621	$0.245	0.004	0.519
COM10	$-	$-	$-	0	0
COM2	$0.115	$42.019	$0.302	0.002	0.674
COM3	$0.152	$55.363	$0.357	0.004	0.795
COM4	$1.195	$436.237	$0.424	0.004	1.162
COM5	$1.364	$497.797	$0.692	0.006	3.771
COM6	$0.190	$69.203	$0.446	0.005	0.993
COM7	$0.379	$138.407	$0.893	0.01	1.987
COM8	$0.695	$253.823	$0.553	0.007	1.253
COM9	$0.228	$83.044	$0.536	0.006	1.193
EDU1	$0.190	$69.203	$0.446	0.005	3.85
EDU2	$0.379	$138.407	$0.893	0.01	5.851
GOV1	$0.125	$45.468	$3.427	0.025	0.795
GOV2	$-	$-	$5.209	0.038	0.913
IND1	$0.288	$105.016	$0.476	0.003	2.014
IND2	$0.288	$105.016	$0.476	0.003	2.014
IND3	$0.384	$140.021	$0.637	0.004	2.685
IND4	$0.872	$318.147	$0.492	0.003	2.13
IND5	$0.575	$210.032	$0.954	0.006	4.026
IND6	$0.281	$102.383	$0.516	0.005	1.995
REL1	$0.152	$55.363	$0.357	0.004	1.987
RES1	$-	$-	$-	0	0
RES2	$-	$-	$-	0	0
RES3A	$-	$-	$-	0	0
RES3B	$-	$-	$-	0	0
RES3C	$-	$-	$-	0	0
RES3D	$-	$-	$-	0	0
RES3E	$-	$-	$-	0	0
RES3F	$-	$-	$-	0	0
RES4	$0.114	$41.522	$0.267	0.003	0.596
RES5	$-	$-	$-	0	0
RES6	$0.190	$69.203	$0.446	0.005	0.993

*for details concerning the capture of employment data, please see the U.S. Bureau of Labor and Statistics: http://www.bls.gov/cew/cewbultn15.htm#Employement

Table 7.6: Recapture Factors

Occupancy	Wage Recapture (%)	Employment Recapture (%)	Income Recapture (%)	Output Recapture (%)
RES1	0	0	0	0
RES2	0	0	0	0
RES3a-f	0	0	0	0
RES4	0.60	0.60	0.60	0.60
RES5	0.60	0.60	0.60	0.60
RES6	0.60	0.60	0.60	0.60
COM1	0.87	0.87	0.87	0.87
COM2	0.87	0.87	0.87	0.87
COM3	0.51	0.51	0.51	0.51
COM4	0.90	0.90	0.90	0.90
COM5	0.90	0.90	0.90	0.90
COM6	0.60	0.60	0.60	0.60
COM7	0.60	0.60	0.60	0.60
COM8	0.60	0.60	0.60	0.60
COM9	0.60	0.60	0.60	0.60
COM10	0.60	0.60	0.60	0.60
IND1	0.98	0.98	0.98	0.98
IND2	0.98	0.98	0.98	0.98
IND3	0.98	0.98	0.98	0.98
IND4	0.98	0.98	0.98	0.98
IND5	0.98	0.98	0.98	0.98
IND6	0.95	0.95	0.95	0.95
AGR1	0.75	0.75	0.75	0.75
REL1	0.60	0.60	0.60	0.60
GOV1	0.80	0.80	0.80	0.80
GOV2	0	0	0	0
EDU1	0.60	0.60	0.60	0.60
EDU2	0.60	0.60	0.60	0.60

Obviously, this ability to “recapture” production will differ across industries. It will be high for those that produce durable output and lower for those that produce perishables or “spot” products (examples of the latter being utility sales to residential customers, hotel services, entertainment). Even some durable manufacturing enterprises would seem to have severe recapture limits because they already work three shifts per day; however, work on weekends, excess capacity, and temporary production facilities all can be used to make up lost sales.

Table 7.6 presents a set of recapture factors for the economic sectors used in the direct loss module. They are deemed appropriate for business disruptions lasting up to three months. As lost production becomes larger, it is increasingly difficult to recapture it for both demand-side and supply-side reasons. For more advanced studies, users may choose to adjust recapture factors downward for longer disruptions (see *Hazus Tsunami Model User Guidance* for the location of these table for editing).

Rental Income Losses

Rental income losses are the product of floor area, rental rates per sq. ft., and the expected days of loss of function for each damage state. Rental income losses include residential, commercial, and industrial properties. It is assumed that a renter will pay full rent if the property is in the damage state none or slight. Thus, rental income losses are calculated only for damage states 3, 4, and 5. It should be noted that rental income is based upon the percentage of floor area in occupancy i that is being rented (1 - $\%OO_i$).

$$RY_i = (1 - \%OO_i) * FA_i * RENT_i * \sum_{ds=3}^{5} POSTR_{ds,i} * RT_{ds} \qquad (7.11)$$

Where:

RY_i	= rental income losses for occupancy
$\%OO_i$	= percent owner occupied for occupancy i (see Table 7.7)
FA_i	= floor area of occupancy group i (in square feet)
$RENT_i$	= rental cost ($\$/ft^2/day$) for occupancy (see Table 7.8)
$POSTR_{ds,I}$	= probability of occupancy i being in structural damage state ds
RT_{ds}	= recovery time for damage state ds

Rental rates vary widely with region and depend on local economic conditions including vacancy rate, the desirability of the neighborhood, and the desirability of the buildings. Regional and city rental rates are published annually by various real estate information services. The percentage rates given for owner occupancy are judgmentally based. For a given study region, census data will provide a more accurate measure for residential numbers.

Table 7.7: Percentage Owner Occupied

Occupancy	% Owner Occupied
AGR1	95
COM1	55
COM10	25
COM2	55
COM3	55
COM4	55
COM5	75
COM6	95
COM7	65
COM8	55
COM9	45
EDU1	95
EDU2	90
GOV1	70
GOV2	95
IND1	75
IND2	75
IND3	75
IND4	75
IND5	55
IND6	85
REL1	90
RES1	75
RES2	85
RES3A	35
RES3B	35
RES3C	35
RES3D	35
RES3E	35
RES3F	35
RES4	0
RES5	0
RES6	0

Table 7.8: Rental and Disruption Costs

Occupancy	Rental Costs (sqft/day)	Rental Costs (sqft/month)	Disruption Costs (sqft/month)
AGR1	$0.03	$0.79	$0.79
COM1	$0.04	$1.34	$1.26
COM10	$0.01	$0.39	$-
COM2	$0.02	$0.55	$1.10
COM3	$0.05	$1.57	$1.10
COM4	$0.05	$1.57	$1.10
COM5	$0.07	$1.96	$1.10
COM6	$0.05	$1.57	$1.57
COM7	$0.05	$1.57	$1.57
COM8	$0.07	$1.96	$-
COM9	$0.07	$1.96	$-
EDU1	$0.04	$1.18	$1.10
EDU2	$0.05	$1.57	$1.10
GOV1	$0.05	$1.57	$1.10
GOV2	$0.05	$1.57	$1.10
IND1	$0.01	$0.24	$-
IND2	$0.01	$0.31	$1.10
IND3	$0.01	$0.31	$1.10
IND4	$0.01	$0.24	$1.10
IND5	$0.01	$0.39	$1.10
IND6	$0.01	$0.16	$1.10
REL1	$0.04	$1.18	$1.10
RES1	$0.03	$0.79	$0.94
RES2	$0.02	$0.55	$0.94
RES3A	$0.02	$0.71	$0.94
RES3B	$0.02	$0.71	$0.94
RES3C	$0.02	$0.71	$0.94
RES3D	$0.02	$0.71	$0.94
RES3E	$0.02	$0.71	$0.94
RES3F	$0.02	$0.71	$0.94
RES4	$0.08	$2.36	$0.94
RES5	$0.02	$0.47	$0.94
RES6	$0.03	$0.86	$0.94

Relocation Costs

Relocation costs may be incurred when the level of building damage is such that the building or portions of the building are unusable while repairs are being made. While relocation costs may include a number of expenses, in this model, only the following components are considered: disruption costs that include the cost of shifting and transferring, and the rental of temporary space. It should be noted that the burden of relocation expenses are not expected to be borne by the renter. Instead it is assumed that the building owners will incur the expense of moving their tenants to a new location. It should also be noted that a renter who has been displaced from a property due to earthquake damage would cease to pay rent to the owner of the damaged property and only pay rent to the new landlord. Therefore, the renter has no new rental expenses. It is assumed that the owner of the damaged property will pay the disruption costs for his renter. If the damaged property is owner-occupied, then the owner will have to pay for disruption costs in addition to the cost of rent while he is repairing his building.

It is assumed in this model that it is unlikely that an occupant will relocate if a building is in the damage states none or slight. The exceptions are some government or emergency response services that need to be operational immediately after an earthquake. However, these are considered to contribute very little to the total relocation expenses for a region and are ignored. Finally, it is assumed that entertainment, theaters, parking facilities, and heavy industry (COM8, COM10, IND1) will not relocate to new facilities. Instead they will resume operation when their facilities have been repaired or replaced. Relocation expenses are then a function of the floor area, the rental costs per day per square foot, a disruption cost, the expected days of loss of function for each damage state, the type of occupancy, and the damage state itself. These are given by the following expression.

$$\mathrm{REL_i} = \mathrm{FA_i} * \begin{bmatrix} (1 - \%OO_i) * \sum_{ds=3}^{5} \left(POSTR_{ds,i} * DC_i\right) + \\ \%OO_i * \sum_{ds=3}^{5} \left(POSTR_{ds,i} * (DC_i + RENT_i * RT_{ds})\right) \end{bmatrix} \tag{7-12}$$

where:

REL_i	= relocation costs for occupancy class i (i = 1-18 and 23-33) FA_i floor area of occupancy class i (in square feet)
FA_i	= floor area of occupancy class i (in square feet)
$POSTR_{ds,i}$	= probability of occupancy class i being in structural damage state ds
DC_i	= disruption costs for occupancy i (\$/ft^2, see Table 7.8)
RT_{ds}	= recovery time for damage state ds (see Table 7.10)
%OO	= percent owner-occupied for occupancy i (see Table 7.7)
$RENT_i$	= rental cost (\$/ft^2/day) for occupancy i (see Table 7.8)

Loss of Function

The damage-state descriptions provide a basis for establishing loss of function and repair time. We distinguish between loss of function and repair time. Here loss of function is the time that a facility is not capable of conducting business. This, in general, will be shorter than repair time because business will rent alternative space while repairs and construction are being completed. The time to repair a damaged building can be divided into two parts: construction and clean-up time, and time to obtain financing, permits, and complete design. For the lower damage states, the construction time will be close to the real repair time. At the higher damage levels, a number of additional tasks must be undertaken that typically will considerably increase the actual repair time. These tasks, which may vary considerably in scope and time between individual projects, include:

- Decision-making (related to business of institutional constraints, plans, financial status, etc.)
- Negotiation with FEMA (for public and nonprofit), SBA, etc.
- Negotiation with insurance company, if insured
- Obtain financing
- Contract negotiation with design firm(s)
- Detailed inspections and recommendations
- Preparation of contract documents
- Obtain building and other permits
- Bid/negotiate construction contract
- Start-up and occupancy activities after construction completion

Building repair and clean-up times are presented in Table 7.9. These times represent estimates of the median time for actual cleanup and repair, or construction. These estimates provide the basis of the values presented in Table 7.10 that are extended to account for delays in decision making, financing, inspection, etc., as outlined above, and represent estimates of the median time for recovery of building functions used by Hazus.

Table 7.9: Building Repair and Cleanup Times (Days)

Occupancy	None Repair Time	Moderate Repair Time	Extensive Repair Time	Complete Repair Time
AGR1	0	10	30	60
COM1	0	30	90	180
COM10	0	20	80	160
COM2	0	30	90	180
COM3	0	30	90	180
COM4	0	30	120	240
COM5	0	30	90	180
COM6	0	45	180	360
COM7	0	45	180	240
COM8	0	30	90	180
COM9	0	30	120	240
EDU1	0	30	120	240
EDU2	0	45	180	360
GOV1	0	30	120	240
GOV2	0	20	90	180
IND1	0	30	120	240
IND2	0	30	120	240
IND3	0	30	120	240
IND4	0	30	120	240
IND5	0	45	180	360
IND6	0	20	80	160
REL1	0	30	120	240
RES1	0	30	90	180
RES2	0	10	30	60
RES3A	0	30	120	240
RES3B	0	30	120	240
RES3C	0	30	120	240
RES3D	0	30	120	240
RES3E	0	30	120	240
RES3F	0	30	120	240
RES4	0	30	120	240
RES5	0	30	120	240
RES6	0	30	120	240

Table 7.10: Building Recovery Time (Days)

Occupancy	None Repair Time	Moderate Recovery Time	Extensive Recovery Time	Complete Recovery Time
AGR1	0	20	60	120
COM1	0	90	270	360
COM10	0	60	180	360
COM2	0	90	270	360
COM3	0	90	270	360
COM4	0	90	360	480
COM5	0	90	180	360
COM6	0	135	540	720
COM7	0	135	270	540
COM8	0	90	180	360
COM9	0	90	180	360
EDU1	0	90	360	480
EDU2	0	120	480	960
GOV1	0	90	360	480
GOV2	0	60	270	360
IND1	0	90	240	360
IND2	0	90	240	360
IND3	0	90	240	360
IND4	0	90	240	360
IND5	0	135	360	540
IND6	0	60	160	320
REL1	0	120	480	960
RES1	0	120	360	720
RES2	0	20	120	240
RES3A	0	120	480	960
RES3B	0	120	480	960
RES3C	0	120	480	960
RES3D	0	120	480	960
RES3E	0	120	480	960
RES3F	0	120	480	960
RES4	0	90	360	480
RES5	0	90	360	480
RES6	0	120	480	960

Repair times differ for similar damage states depending on building occupancy: thus simpler and smaller buildings will take less time to repair than more complex, heavily serviced, or larger buildings. It has also been noted that large, well-financed corporations can sometimes accelerate the repair time compared to normal construction procedures.

However, establishment of a more realistic repair time does not translate directly into business or service interruption. For some businesses, building repair time is largely irrelevant, because these businesses can rent alternative space or use spare industrial/commercial capacity elsewhere. These factors are reflected in Table 7.11, which provides multipliers to be applied to the values in Table 7.10 to arrive at estimates of business interruption for economic purposes. The factors in Tables 7.9, 7.10, and 7.11 are judgmentally derived, using ATC-13, Table 9.11 as a starting point.

The times resulting from the application of the Table 7.11 multipliers to the times shown in Table 7.10 represent median values for the probability of business or service interruption. For none and slight damage, the time loss is assumed to be short, with cleanup by staff, but work can resume while slight repairs are done. For most commercial and industrial businesses that suffer moderate or extensive damage, the business interruption time is shown as short on the assumption that these concerns will find alternate ways of continuing their activities. The values in Table 7.11 also reflect the fact that a proportion of business will suffer longer outages or even fail completely. Church and Membership Organizations generally find temporary accommodation quickly, and government offices also resume operating almost at once. It is assumed that hospitals and medical offices can continue operating, perhaps with some temporary rearrangement and departmental relocation if necessary, after moderate damage, but with extensive damage their loss of function time is also assumed to be equal to the total time for repair.

For other businesses and facilities, the interruption time is assumed to be equal to, or approaching, the total time for repair. This applies to residential, entertainment, theaters, parking, and religious facilities whose revenue or continued service, is dependent on the existence and continued operation of the facility.

The modifiers from Table 7.11 are multiplied by extended building construction times as follows:

$$LOF_{ds} = BCT_{ds} * MOD_{ds} \tag{7.13}$$

where:

LOF_{ds} = loss of function for damage state ds

BCT_{ds} = extended building construction and clean up time for damage state ds (see Table 7.10)

MOD_{ds} = construction time modifiers for damage state ds (see Table 7.11)

Table 7.11: Construction Time Modifiers

Occupancy	None Construction Time	Moderate Construction Time	Extensive Construction Time	Complete Construction Time
AGR1	0	0.05	0.1	0.2
COM1	0.5	0.1	0.3	0.4
COM10	0.1	1	1	1
COM2	0.5	0.2	0.3	0.4
COM3	0.5	0.2	0.3	0.4
COM4	0.5	0.1	0.2	0.3
COM5	0.5	0.05	0.03	0.03
COM6	0.5	0.5	0.5	0.5
COM7	0.5	0.5	0.5	0.5
COM8	0.5	1	1	1
COM9	0.5	1	1	1
EDU1	0.5	0.02	0.05	0.05
EDU2	0.5	0.02	0.03	0.03
GOV1	0.5	0.02	0.03	0.03
GOV2	0.5	0.02	0.03	0.03
IND1	0.5	1	1	1
IND2	0.5	0.2	0.3	0.4
IND3	0.5	0.2	0.3	0.4
IND4	0.5	0.2	0.3	0.4
IND5	0.5	0.2	0.3	0.4
IND6	0.5	0.2	0.3	0.4
REL1	1	0.05	0.03	0.03
RES1	0	0.5	1	1
RES2	0	0.5	1	1
RES3A	0	0.5	1	1
RES3B	0	0.5	1	1
RES3C	0	0.5	1	1
RES3D	0	0.5	1	1
RES3E	0	0.5	1	1
RES3F	0	0.5	1	1
RES4	0	0.5	1	1
RES5	0	0.5	1	1
RES6	0	0.5	1	1

7.6 References

Applied Technology Council (1985). Earthquake Damage Evaluation Data for California, ATC-13, Applied Technology Council, Redwood City, CA.

Hazus Earthquake *Technical Manual*

G&E Engineering Systems, Inc., May 1994, "NIBS Earthquake Loss Estimation Methods, Technical Manual, Transportation and Utility Systems".

Jackson, P.L., Editor, Means Square Foot Costs, (1994), R.S. Means Company, Inc., Kingston, MA.

Phipps, M., et. all, 1992, Degenkolb Report on Effects of Loma Prieta Earthquake on Industry.

8.0 Evaluation of Building Damage

This section incorporates information from the FEMA (2013) Chapter 5 evaluation of the building damage functions, including comparison to building damage ratios from previous events. FEMA (2013) Chapter 5 evaluated Hazus tsunami building damage fragility curves and corresponding economic loss ratio curves for tsunami (assuming nil earthquake damage and loss), and compares estimated values of the loss ratio with observations of building damage from recent tsunamis. The loss ratio is defined as the cost of building damage repair or replacement divided by the full replacement value of the building or subsystem of interest. Estimated values of the loss ratio are compared to observed damage since the loss ratio represents the combined effects of damage to the structural system (due to flow) and nonstructural and contents damage (due to flood). Observations of building damage typically mix structural and nonstructural damage in the same damage state (i.e., structural damage is not clearly distinguished from nonstructural damage), making it difficult to compare individual estimates of structural, nonstructural, and contents damage with observed damage.

Estimated values of the loss ratio are expressed in terms of the depth of water above the base of the building (H) since this is the hazard parameter commonly used by post-tsunami investigations to report and evaluate observed damage to buildings. As described in FEMA (2013), building damage functions define the probability of structure damage in terms of tsunami flow (momentum flux). Equation 6.6 of FEMA P646 (FEMA 2012) was used to convert structure damage expressed in terms of momentum flux to structure damage expressed in terms of water depth (H). Equation 6.6 defines momentum flux in terms of inundation height (R) and an assumed height of the building above sea level datum (z), where H = R – z (see Figure 5.3). The examples of this section assume the value of z to be 20 feet (above sea level datum) and use values of R without the 1.3 increase suggested by FEMA P646 for design. Note: Estimated probabilities of structure damage and associated values of the loss ratio expressed in terms of water depth, H, could be significantly different, if the relationship between momentum flux and water depth is substantially different from that of Equation 6.6 of FEMA P646.

Loss ratio calculations are based on the methods and economic loss rates of Chapter 7. Economic loss rates are 100 percent economic loss for Complete damage, 50 percent economic loss for Extensive damage and 10 percent economic loss for Moderate damage. These rates apply to the structure, nonstructural systems, and contents of the building. Total building economic loss is based on the assumption that the structure represents 17 percent, the nonstructural systems represent 50 percent, and contents represent 33 percent of total model building replacement value (i.e., replacement value including all contents). These fractions of total building replacement value are generally representative of residential and commercial buildings.

8.1 Example Building Damage Loss Curves

Figures 8.1 through 8.3 show the probability of damage to the structural system, nonstructural systems, and contents, and Figure 8.4 shows the associated loss ratio curves for older, Pre-Code (PC) one-story wood buildings (W1). Similarly, Figures 8.5 through 8.7 show the probability of damage to the structural system, nonstructural systems, and contents, and Figure 8.8 shows the associated loss ratio curves for older, Pre-Code (PC) five-story concrete buildings (C2M). For both model building types, the height of the first-floor above the base of the buildings (h_F) is assumed to be 3 feet, corresponding to a height of 23 feet above sea level datum ($z + h_F$).

Figure 8.1: Example fragility curves - probability of structural system damage due to tsunami flow (expressed in terms of median peak inundation depth) – older 1 story wood buildings (W1 – PC)

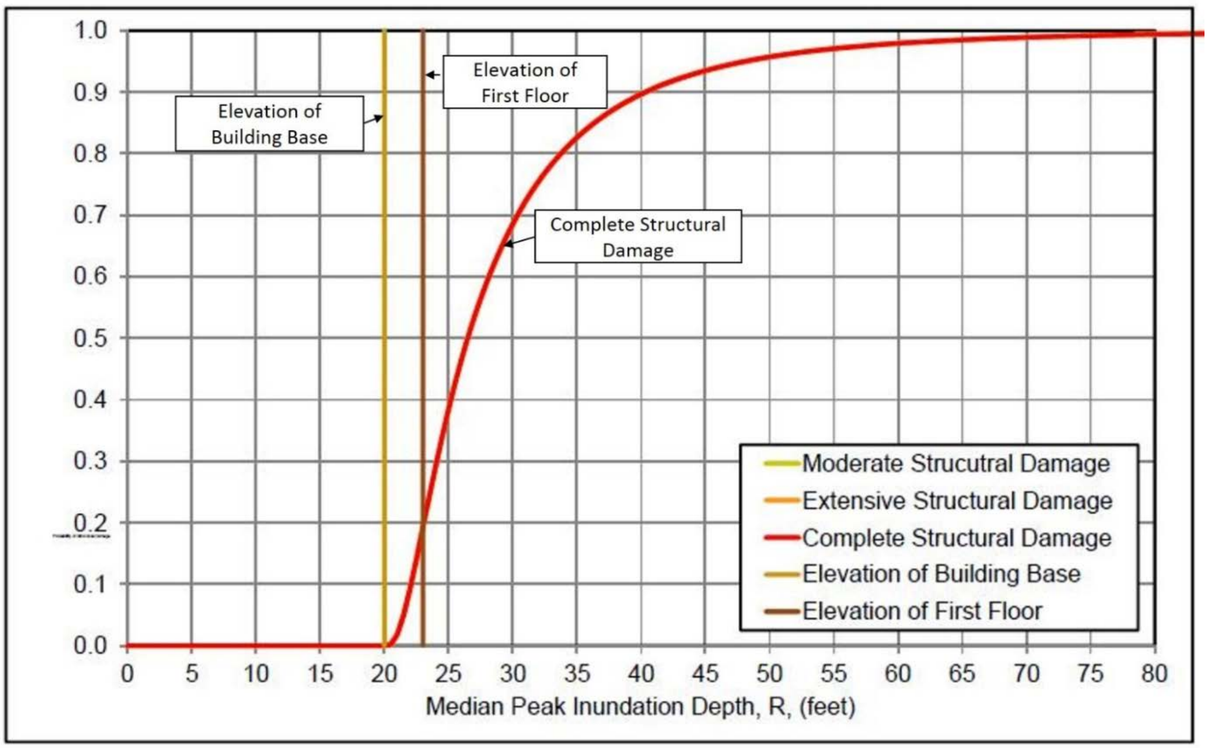

Figure 8.2: Example fragility curves - probability of nonstructural damage due to tsunami flood - older 1-story wood buildings (W1 – PC)

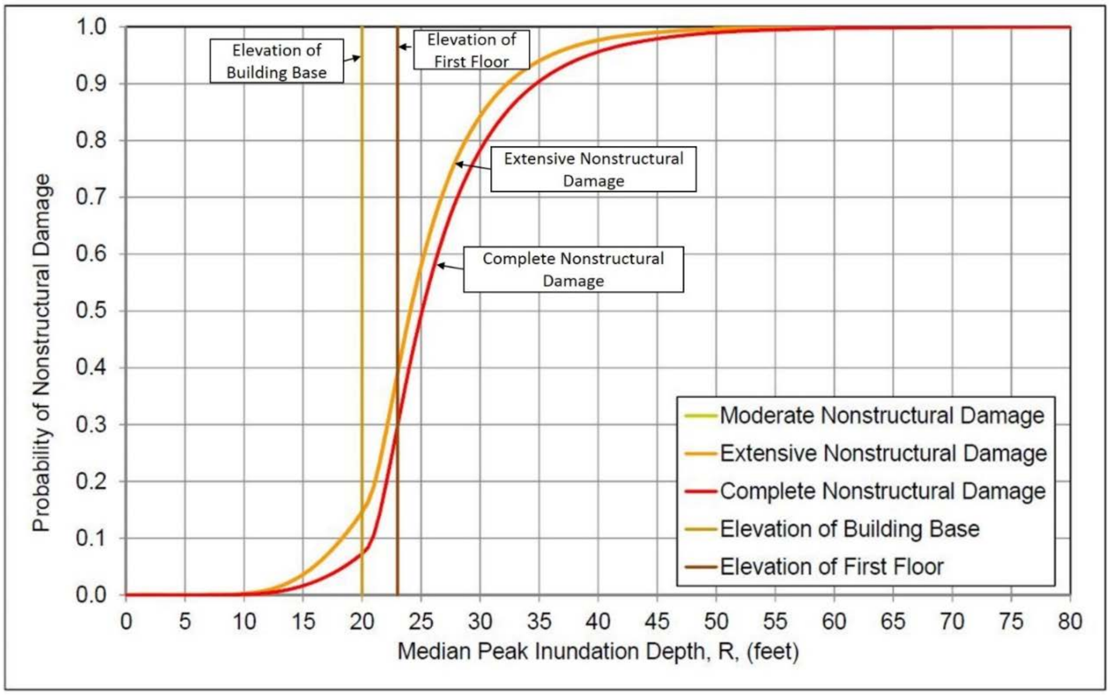

Figure 8.3: Example fragility curves - probability of contents damage due to tsunami flood – older 1-story wood buildings (W1 – PC)

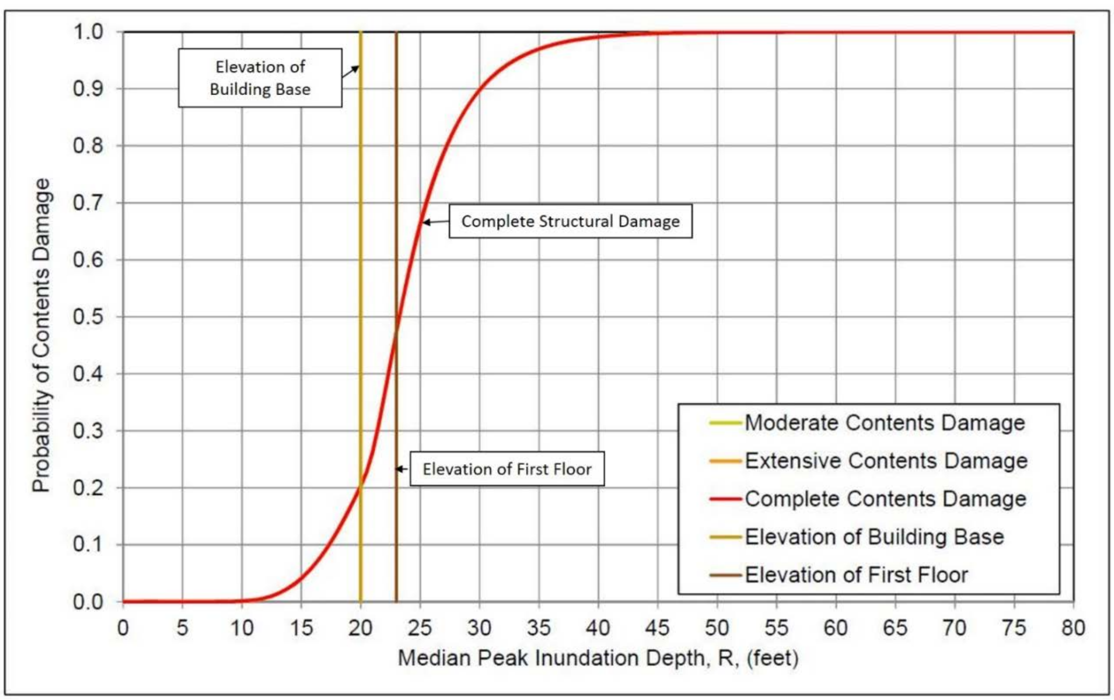

Figure 8.4: Example loss ratio curves – total building, structural system, nonstructural systems and contents - older 1-story wood buildings (W1 – PC)

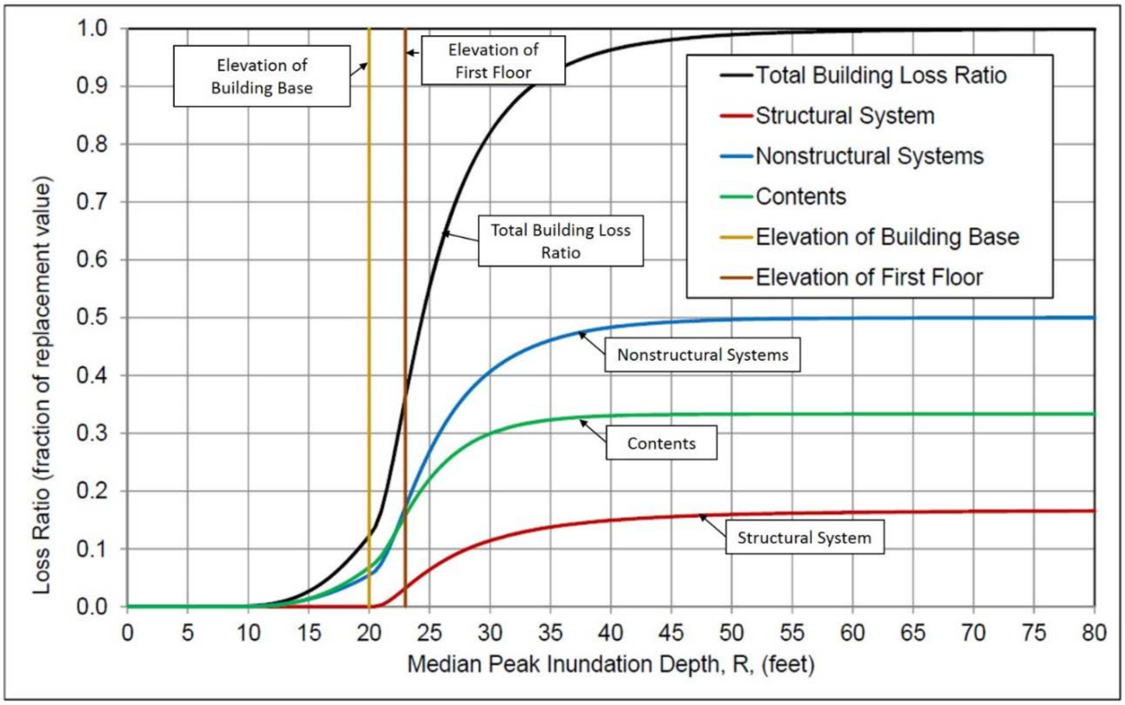

Figure 8.5: Example fragility curves - probability of structural system damage due to tsunami flow (expressed in terms of median peak inundation depth) – Older 5 story concrete buildings (C2M – PC). Note: These fragility curves are derived from momentum flux-based fragility curves shown in Figure 5.2.

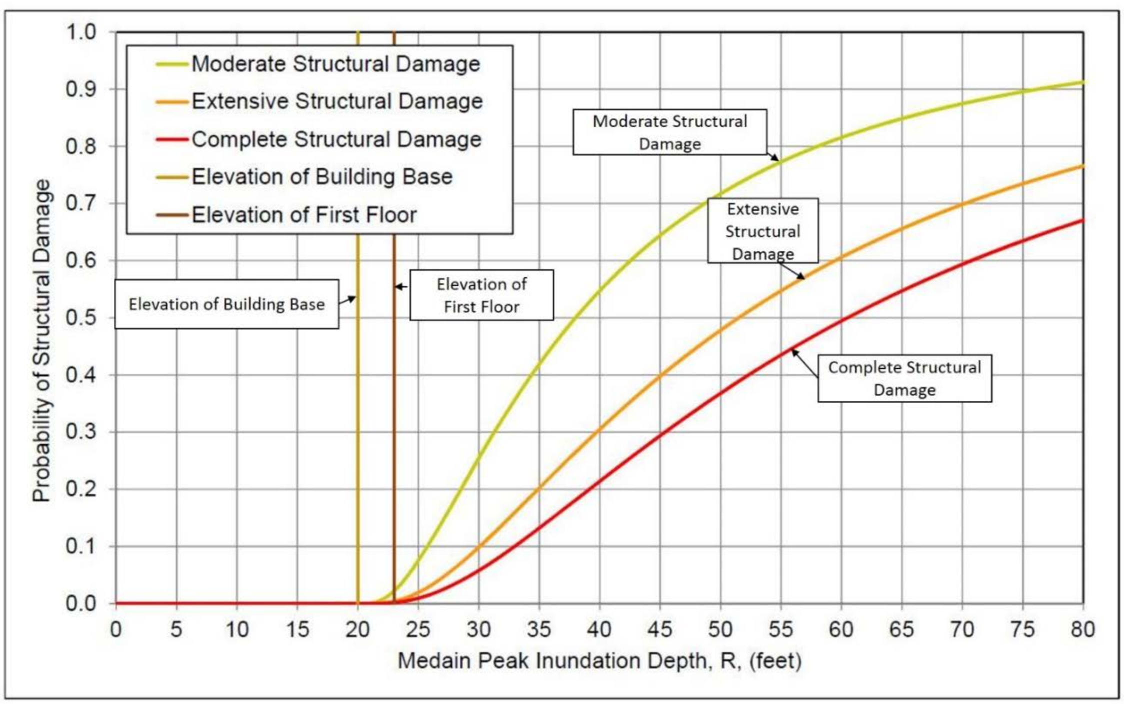

Figure 8.6: Example fragility curves - probability of nonstructural damage due to tsunami flood - older 5-story concrete buildings (C2M – PC)

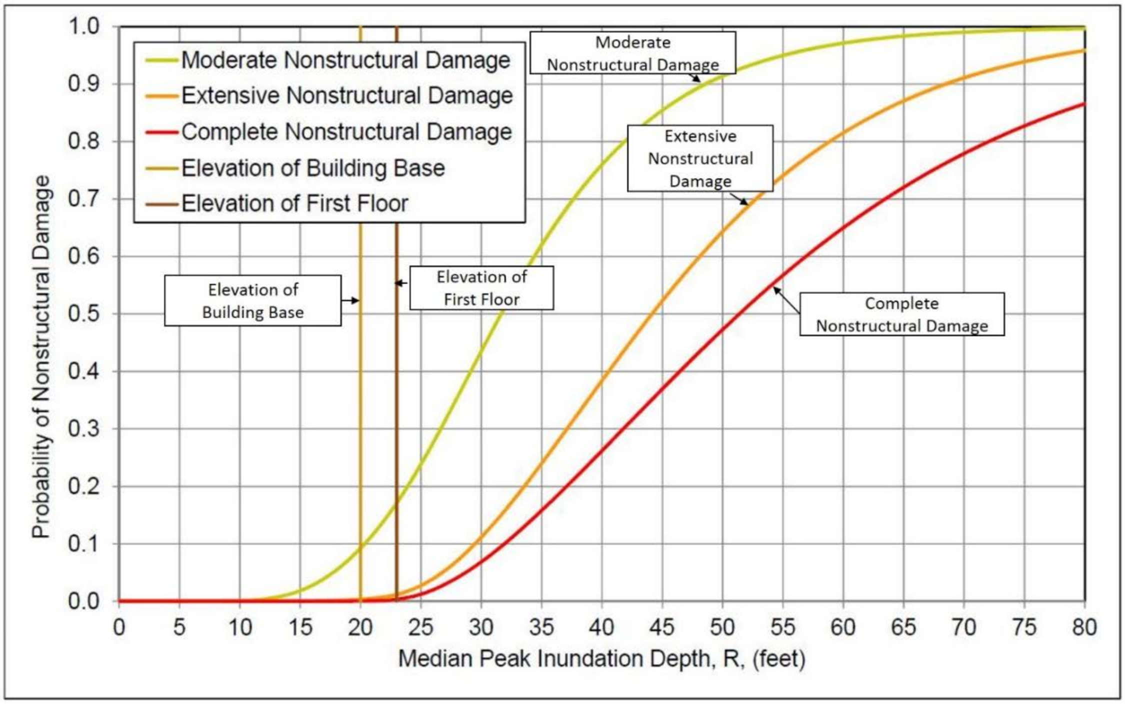

Figure 8.7: Example fragility curves - probability of contents damage due to tsunami flood – older 5-story concrete buildings (C2M – PC)

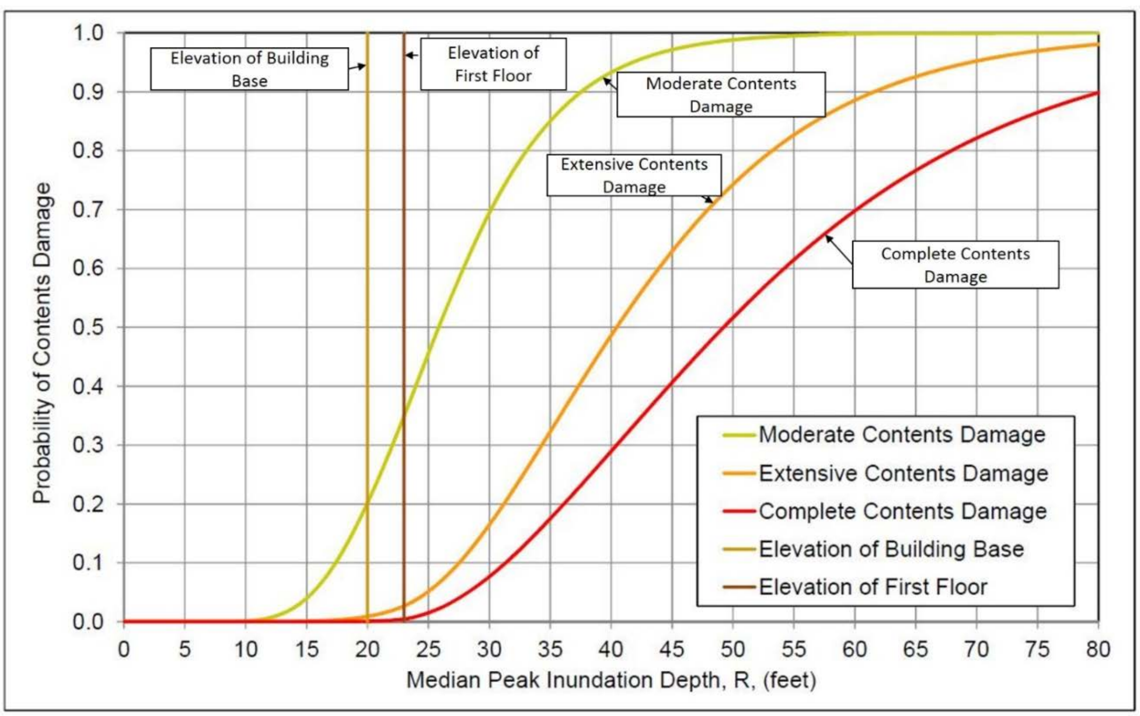

Figure 8.8: Example loss ratio curves – total building, structural system, nonstructural systems and contents - older 2-story concrete buildings (C2L – PC)

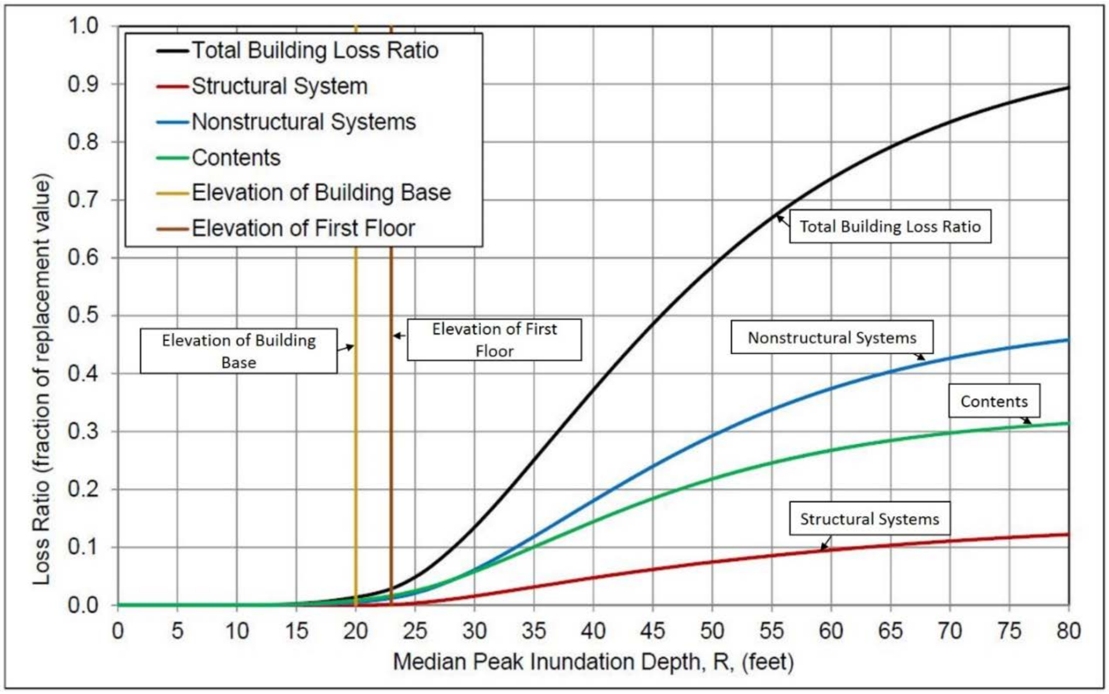

In Figures 8.1 through 8.3, fragility curves for Moderate damage and, in some cases, Extensive damage are not visible since they have the same properties as the next, more severe damage state (e.g., these curves are hidden by the Complete structural damage fragility curve in Figure 8.1). When Moderate or Extensive states are not required for the calculation of damage, their fragility values are, by definition, the same as those of the next, more severe damage state. In all cases, Slight damage is not shown since it is not used for calculation of tsunami damage and losses (i.e., presumed to have the same properties as Moderate damage).

In Figures 8.2, 8.3, 8.6, and 8.7, the probabilities of nonstructural and contents damage incorporate the probability of Complete structural damage, in accordance with the logic and formulas of Chapter 5 The probability of Complete structure damage can significantly increase the probability of damage to nonstructural systems and contents of shorter buildings. For example, the nonstructural damage curves of one-story wood buildings, shown in Figure 8.2, emulate the shape of the Complete structural damage shown in Figure 8.1 (for depths of water above the base of the building).

Nonstructural and contents fragility curves shown in Figures 8.2, 8.3, 8.6, and 8.7 incorporate flood-related hazard uncertainty assumed to be β_R = 0.3, in accordance with Equation 5.3 and structural fragility curves (prior to conversion from momentum flux to water depth) incorporate flow-related hazard uncertainty assumed to be β_F = 0.5, in accordance with Equation 5.4. The effect of incorporating hazard uncertainty is to modestly flatten fragility and loss curves and to accentuate non-zero estimates of nonstructural and contents damage and associated losses for median estimates of inundation depth at or less than the elevation of first-floor (i.e., values of $R \le 23$ feet, in these figures). As discussed in Chapter 5, non-zero probabilities of damage and loss reflect the inherent uncertainty in the depth of water, that is water depth could be higher (or lower) than the estimate of the median value of inundation depth at the building of interest. Incorporation of hazard uncertainty is appropriate for estimation of damage and loss in future "scenario" earthquakes, but would not be appropriate for estimation of damage and loss observed in past tsunamis for which water depths are reasonably well known.

Tables 8.1 through 8.6 summarize the depths of water above the base of the building corresponding to loss ratios of 15 percent (15% LR), 50 percent (50% LR), and 85 percent (85% LR). In all cases, the base of the building is assumed to be 20 feet above sea level datum (z = 20 feet). In each table, the three loss ratios are provided for two lateral strength conditions of the model building types; 1) building strength corresponding to modern (High-Code) construction in a high seismic region, and 2) building strength corresponding to older (Pre-Code) construction. Note: Model building types (and depths) shown with italics indicate older model building types not permitted for use as modern construction.

The three loss ratios range of tsunami consequences that range from significant economic loss (15% LR), but likely limited structural failures, to extreme economic loss (85% LR) and likely structure failure. Since the loss ratio curves are inherently probabilistic, they never reach 100 percent loss (see for example Figure 5.8). For all intents and purposes, 85 percent LR represents complete loss of the building, at least partial collapse, and should be considered comparable to post-event observations of tsunami damage characterized as "partial failure" or "collapse".

Table 8.1: Water depths (H), in feet, corresponding to loss ratios (LRs) of 15%, 50% and 85% for model building types with first-floors above grade (h_F = 3 ft.), not impacted by debris (K_d = 1.0) and incorporating hazard uncertainty (β_F = 0.5 and β_R = 0.3)*

Model Building Type	Modern High-Code Buildings 15% LR	Modern High-Code Buildings 50% LR	Modern High-Code Buildings 85% LR	Model Building Type	Older Pre-Code Buildings 15% LR	Older Pre-Code Buildings 50% LR	Older Pre-Code Buildings 85% LR
MH	0	1	2.5	MH	0	0.5	2
W1	0.5	5.5	14	W1	0.5	4	11
URML	*1*	*6*	*14.5*	S3	0.5	4	9.5
S3	1	7	17	W2	1.5	5.5	14.5
PC1	1	9.5	23.5	URML	1	6	14.5
W2	2.5	10	24.5	PC1	1	6.5	14.5
C3L	*2*	*10*	*24.5*	S1L	2.5	10	24
S5L	*2.5*	*10.5*	*26*	C1L	2	10	24.5
C1L	2.5	14	36	C3L	2	10	24.5
S1L	3	15	37	S2L	2.5	10.5	23.5
C2L	2.5	15	38.5	S4L	2.5	10.5	24.5
PC2L	2.5	15	36.5	S5L	2.5	10.5	26
RM1L	2.5	15	37.5	PC2L	2.5	10.5	24
S2L	3	15.5	37	C2L	2.5	11	26
S4L	3	15.5	38	RM1L	2.5	11	25
RM2L	2.5	15.5	39.5	RM2L	2.5	11.5	26.5
URMM	*6.5*	*17*	*36.5*	URMM	6.5	17	36.5
S5M	*9*	*23*	*49.5*	S1M	8.5	22	48
C3M	*9*	*23*	*48.5*	S5M	9	23	49.5
C3H	*10.5*	*30*	*70.5*	C1M	9	23	48.5
S5H	*11.5*	*33*	*80.5*	C3M	9	23	48.5
C1M	13.5	33	68	PC2M	10.5	24.5	48.5
S1M	14	33.5	68.5	S2M	10.5	25	51
PC2M	14.5	34	68	S4M	10.5	25	51
C2M	14.5	34.5	71	C2M	10.5	25.5	52
RM1M	15	35	70.5	RM1M	11	25.5	51
RM2M	15	35.5	72	RM2M	11	26.5	52.5
S2M	16	36.5	72.5	C1H	10.5	30	70.5
S4M	15.5	36.5	72.5	C3H	10.5	30	70.5
C1H	19	50.5	107.5	S1H	11	31	76.5
S1H	20	56	121.5	S5H	11.5	33	80.5
PC2H	24	58	117	PC2H	14	36.5	77.5
C2H	23.5	59	121.5	S2H	14.5	38	84.5
RM2H	24.5	60	121	S4H	14	38	85.5
S4H	25.5	65	132.5	C2H	14.5	39	85
S2H	26	65.5	131.5	RM2H	16	40.5	85

* *Note: Building types with italics show model building types that are not permitted for high-code seismic design. These are shown in table to highlight their relative ranking and damageability.*

Table 8.2: Water depths (H), in feet, corresponding to loss ratios (LRs) of 15%, 50% and 85% for model building types with first-floors above grade (h_F = 3 ft.), impacted by debris (K_d = 2.0) and incorporating hazard uncertainty (β_F = 0.5 and β_R = 0.3)

Model Building Type	Modern High-Code Buildings 15% LR	Modern High-Code Buildings 50% LR	Modern High-Code Buildings 85% LR	Model Building Type	Older Pre-Code Buildings 15% LR	Older Pre-Code Buildings 50% LR	Older Pre-Code Buildings 85% LR
MH	0	0.5	2	MH	0	0	1
W1	0.5	4	11	W1	0.5	2.5	7.5
URML	*0.5*	*4.5*	*10.5*	S3	0.5	2.5	6
S3	1	5.5	12.5	W2	1	4	10
W2	2	7.5	19	PC1	0.5	4.5	11
C3L	*2*	*8*	*19.5*	URML	0.5	4.5	10.5
PC1	1	8	19	S1L	2	7.5	19
S5L	*2*	*8.5*	*20.5*	S2L	2	8	18.5
C1L	2.5	12	30	S4L	2	8	19
S1L	3	12.5	30	C1L	2	8	19.5
S2L	3	13	30	C3L	2	8	19.5
S4L	3	13	31	S5L	2	8.5	20.5
C2L	2.5	13	32	PC2L	2	8.5	19
PC2L	2.5	13	30	RM1L	2	8.5	19.5
RM1L	2.5	13	31	C2L	2	9	20.5
RM2L	2.5	13.5	32.5	RM2L	2	9	21
URMM	*5*	*13.5*	*29*	URMM	5	13.5	29
S5M	*6.5*	*17.5*	*40*	S1M	6	16.5	38.5
C3M	*7*	*18.5*	*40*	S5M	6.5	17.5	40
C3H	*8*	*22*	*55*	C1M	7	18.5	40
S5H	*8*	*23.5*	*60.5*	C3M	7	18.5	40
S1M	11	28	58.5	S2M	8	19	41
C1M	11.5	28.5	58.5	S4M	7.5	19	41
PC2M	12.5	29.5	58	PC2M	8	19	39.5
C2M	12.5	30.5	61.5	C2M	8	20.5	43
RM1M	13	30.5	60.5	RM1M	8.5	20.5	41.5
S2M	13.5	31	61.5	RM2M	9	21	43.5
S4M	13	31	61.5	S1H	7.5	22	57.5
RM2M	13.5	31	62	C1H	8	22	55
C1H	14.5	40	88.5	C3H	8	22	55
S1H	15	42.5	98	S5H	8	23.5	60.5

Model Building Type	Modern High-Code Buildings 15% LR	Modern High-Code Buildings 50% LR	Modern High-Code Buildings 85% LR	Model Building Type	Older Pre-Code Buildings 15% LR	Older Pre-Code Buildings 50% LR	Older Pre-Code Buildings 85% LR
PC2H	19	47	96.5	PC2H	10.5	27	60
C2H	19.5	50	104	S2H	10.5	27.5	63.5
S2H	19.5	51	107.5	S4H	10	27.5	64.5
S4H	19	51	108.5	C2H	11	29.5	67.5
RM2H	21	51.5	104.5	RM2H	12	31	67.5

Table 8.3: Water depths (H), in feet, loss ratios (LRs) of 15%, 50% and 85% for model building types with first-floors above grade (h_F = 3 ft.), not impacted by debris (K_d = 1.0) and ignoring hazard uncertainty (β_F = 0.0 and β_R = 0.0)

Model Building Type	Modern High-Code Buildings 15% LR	Modern High-Code Buildings 50% LR	Modern High-Code Buildings 85% LR	Model Building Type	Older Pre-Code Buildings 15% LR	Older Pre-Code Buildings 50% LR	Older Pre-Code Buildings 85% LR
MH	0.5	1	2.5	MH	0.5	0.5	1.5
W1	3	6	12.5	W1	2	5	9.5
URML	*3*	*6.5*	*12.5*	S3	2.5	5	8.5
S3	3.5	7.5	15	W2	2.5	6.5	13
PC1	4	9	21.5	URML	3	6.5	12.5
W2	4.5	10.5	22.5	PC1	3.5	7	13
C3L	*4.5*	*10.5*	*22.5*	S1L	4.5	10.5	22.5
S5L	*4.5*	*11.5*	*24*	C1L	4.5	10.5	22.5
C1L	5	14.5	33	C3L	4.5	10.5	22.5
C2L	5	15	35.5	S2L	5	11	22
S1L	5	15.5	34.5	S4L	5	11.5	23
PC2L	5	15.5	34	S5L	4.5	11.5	24
RM1L	5	15.5	34.5	C2L	4.5	11.5	24
RM2L	5	15.5	36.5	PC2L	4.5	11.5	22.5
S2L	5.5	16.5	34.5	RM1L	5	11.5	23
S4L	5.5	16.5	35.5	RM2L	5	12.5	24.5

Table 8.4: Water depths (H), in feet, loss ratios (LRs) of 15%, 50% and 85% for model building types with first-floors at grade (h_F = 0 ft.), impacted by debris (K_d = 2.0) and ignoring hazard uncertainty (β_F = 0.0 and β_R = 0.0)

Model Building Type	Modern High-Code Buildings 15% LR	Modern High-Code Buildings 50% LR	Modern High-Code Buildings 85% LR	Model Building Type	Older Pre-Code Buildings 15% LR	Older Pre-Code Buildings 50% LR	Older Pre-Code Buildings 85% LR
MH	0.5	1	2.5	MH	0	0.5	1.5
W1	1	4.5	11.5	W1	1	3.5	8.5
URML	*1*	*5*	*12*	S3	1	4	8
S3	1	6	14	URML	1	5	12
PC1	1	7	20.5	W2	1.5	5.5	12.5
W2	2.5	9.5	21.5	PC1	1	5.5	12
C3L	*2*	*9.5*	*21.5*	S1L	2.5	9.5	21.5
S5L	*2.5*	*10*	*23*	C1L	2	9.5	21.5
C1L	2	12.5	31.5	C3L	2	9.5	21.5
C2L	2	13	34	S2L	2.5	10	21
PC2L	2	13	32.5	S5L	2.5	10	23
RM1L	2	13	33.5	C2L	2	10	23
RM2L	2	13	35	PC2L	2	10	21
S1L	2.5	13.5	33	RM1L	2	10	22
S2L	2.5	14.5	33.5	S4L	2.5	10.5	22
S4L	2.5	14.5	34	RM2L	2	11	23.5

Table 8.5: Water depths (H), in feet, loss ratios (LRs) of 15%, 50% and 85% for model building types with first-floors above grade (h_F = 3 ft.), impacted by debris (K_d = 2.0) and ignoring hazard uncertainty (β_F = 0.0 and β_R = 0.0)

Model Building Type	Modern High-Code Buildings 15% LR	Modern High-Code Buildings 50% LR	Modern High-Code Buildings 85%LR	Model Building Type	Older Pre-Code Buildings 15% LR	Older Pre-Code Buildings 50% LR	Older Pre-Code Buildings 85% LR
MH	0.5	0.5	1.5	MH	0	0	0.5
W1	2	5	9.5	S3	1.5	3	5.5
URML	*2.5*	*5*	*9.5*	W1	1.5	3.5	6.5
S3	3	6	11	W2	1.5	4	9
W2	3.5	8	17.5	URML	2.5	5	9.5
PC1	4	8	17	PC1	2.5	5.5	9.5
C3L	*3.5*	*8.5*	*18*	S1L	3.5	8.5	17.5
S5L	*4*	*9*	*19*	S2L	4	8.5	16.5
C1L	4.5	12.5	27.5	C1L	3.5	8.5	18
S1L	5	13	28	C3L	3.5	8.5	18
C2L	5	13.5	29.5	S4L	4	9	17.5
PC2L	5	13.5	27.5	S5L	4	9	19
S2L	5	14	28	PC2L	4	9	17.5
S4L	5	14	28.5	C2L	4	9.5	19
RM1L	5	14	28.5	RM1L	4	9.5	18
RM2L	5	14.5	30	RM2L	4.5	10	19.5

Table 8.6: Water depths (H), in feet, loss ratios (LRs) of 15%, 50% and 85% for model building types with first-floors at grade (h_F = 0 ft.), impacted by debris (K_d = 2.0) and ignoring hazard uncertainty (β_F = 0.0 and β_R = 0.0)

Model Building Type	Modern High-Code Buildings 15% LR	Modern High-Code Buildings 50% LR	Modern High-Code Buildings 85% LR	Model Building Type	Older Pre-Code Buildings 15% LR	Older Pre-Code Buildings 50% LR	Older Pre-Code Buildings 85% LR
MH	0	0.5	1.5	MH	0	0	0.5
W1	1	3.5	8.5	W1	0.5	2.5	6
URML	*1*	*4*	*8.5*	S3	1	2.5	5
S3	1	4.5	10.5	W2	1	3.5	8.5
PC1	1	6	16	PC1	1	4	9
W2	2	7.5	16.5	URML	1	4	8.5
C3L	*2*	*7.5*	*17*	S1L	2	7.5	16.5
S5L	*2*	*8*	*18*	C1L	2	7.5	17
C1L	2	11	26	C3L	2	7.5	17
S1L	2.5	11.5	27	S2L	2.5	8	16
PC2L	2	11.5	26.5	S4L	2.5	8	16.5
C2L	2	12	28	S5L	2	8	18
RM1L	2	12	27.5	PC2L	2	8	16.5
S2L	2.5	12.5	27	C2L	2	8.5	18
S4L	2.5	12.5	27.5	RM1L	2	8.5	17
RM2L	2	12.5	28.5	RM2L	2	9	18.5

Values of water depth given in Table 8.1 represent model building types with the first floor located at three feet above the base of building (h_F), assume no debris impact or shielding effects (K_d = 1.0 and incorporate hazard uncertainty (β_F = 0.5 and β_R = 0.3), representing building properties that would be appropriate for evaluation of building damage due to a tsunami scenario. Water depths in Table 8.2 represent the same building conditions, expect that they also include a nominal amount of debris impact (K_d = 2.0), illustrating the potential significance of debris impact on building damage and resulting losses.

Trends in the water depths shown in Tables 8.1 and 8.2 are consistent with qualitative observations of tsunami damage. Taller buildings (i.e., mid-rise and high-rise model building types) can have significant damage and economic loss (to lower floors), but are unlikely to have extensive structural damage or fail (unless tsunami inundation height is very large). It should be noted that the cost of repair of a high-rise building with a 15 percent LR (limited damage) is about twice the cost of replacement of a low-rise building with an 85% percent LR, since the high-rise building is more than 10 times larger and more valuable than the low-rise building.

Tables 8.3 through 8.6 provide water depths for low-rise buildings based on hazard and building properties deemed to best represent observations of building damage due to tsunami. Only low-rise model building types are included in these tables, since low-rise buildings are the most vulnerable building types and observed damage is generally not available for taller buildings. In each of these tables, the hazard uncertainty is assumed to be nil for comparison with observed damage for which the water depth is assumed to be reasonably well known.

Tables 8.3 and 8.4 provide values of the water-depth assuming no debris impact which is possible, but unlikely for most buildings observed to have sustained significant damage in recent tsunamis. Table 8.3 assumes that the first floor of model building types is three feet above grade (i.e., above the base of the building). Table 8.4 assumes that the first floor of model building types is at grade. Actual height of the first floor of buildings damaged by a tsunami is typically not reported, but likely to be somewhere between 0 feet (slab-on-grade construction) and three feet above grade (buildings with a crawl space). The height of the first floor is most important for water depths associated with a 15 percent LR, since smaller loss ratios are primarily due to damage to nonstructural components and contents. The height of the first floor is less important to water depths associated with an 85 percent LR, since larger losses are influenced by structural failure which is not dependent on first-floor height (i.e., force due to momentum flux is not a function of h_F). In general, the difference in water depths associated with 85% LR is not more than one foot for the same model building type with the first floor three feet above grade and with the first floor at grade.

Tables 8.5 and 8.6 provide values of the water depth assuming additional force on the structure due to a nominal amount of debris impact ($K_d = 2.0$). The effects of even a nominal amount of debris impact are significant for the lighter, low-rise structures. It is not possible to know the specific type and amount of debris, if any, which contributed to the observed building damage in past tsunamis. However, photos and videos tend to support the notion that it is more likely, than not, that debris impact contributed to observed building damage and loss, and likewise estimates of damage and loss to lighter buildings (W1 and W2) should include the effects of debris, even if very approximately.

8.2 Comparison of Estimated Building Loss and Observed Building Damage

Table 8.7 compares water depths based on tsunami building damage functions (estimated damage) with water depths of observed damage to buildings due to recent tsunamis (Section 8.3). Comparisons are made for Hazus model building types for which observed tsunami damage is available for comparable types of construction. The model building types include, light-frame wood and timber construction (W1 and W2), low-rise unreinforced masonry (URML), low-rise reinforced-concrete moment frames (C1L), low-rise reinforced-concrete shear walls (C2L), low-rise reinforced-concrete moment frames with masonry infill (C3L), and low- rise steel frames with cast-in-place concrete shear walls (S4L).

Estimated damage to the structure, nonstructural systems, and contents is characterized by water depths corresponding to an 85 percent loss ratio (i.e., damage requiring repair or replacement cost equal to 85 percent of the value of the building and contents). Loss ratio, rather than actual damage-state fragility, is used in these comparisons with observed damage since it combines structural and nonstructural (and contents) damage that better represents observed damage states (which typically combine structural and nonstructural damage). Water depths corresponding to 85 percent loss are taken from Table 8.5 for lighter buildings (W1 and W2) which reflect some nominal amount of damage due to debris impact, and from Table 8.3 for other (heavier) buildings less susceptible to debris impact damage. Water depths are reported for both High-Code and Pre-Code model building strengths. In general, Pre-Code strength is the more appropriate of the two strengths for comparison with observed buildings damage.

Table 8.7: Comparison of water depths, in feet, representing estimated damage corresponding to an 85 percent loss ratio and observed damage representing initiation of "Partial Failure" of buildings in the 2004 Indian Ocean tsunami, and median "Collapse" damage to buildings in the 2009 Samoa and 2011 Tohoku tsunamis

Model Building Type: Name	Model Building Type: No. of Stories	Estimated Damage–High-Code Strength: 85 Percent Loss Ratio (Tables 8.3 and 8.5)	Estimated Damage–Pre-Code Strength: 85 Percent Loss Ratio (Tables 8.3 and 8.5)	Observed Damage: 2004 Indian Ocean SCHEMA Handbook (Tinti et al., 2010)	Observed Damage: 2009 Samoa Tsunami (Reese et al., 2011)	Observed Damage: 2011 Tohoku Tsunami (Suppasri et al., 2012)
W1	1	9.5	6.5	8.5	5.3	
W1	1&2					13.5
W2	2	17.5	9.0			15.9
URML	1		12.5	13.0	8.2	
C1L	2	33.0	22.5	22.0		
C2L	2	35.5	24.0		24.0	
C3L	2		22.5	19.5		
S4L	2	35.5	23.0	31.0		

Water depths of observed damage are available from the SCHEMA Handbook based largely on observations of building damage in Banda Aceh (Thailand) after the 2004 Indian Ocean Tsunami (Tinti et al. 2011) and from post-event surveys and evaluations of buildings damaged in American Samoa and Samoa due to the 2009 South Pacific (Samoa) tsunami (Reese et al. 2011) and in the Miyagi and Fukushima prefectures of Japan due to the 2011 Tohoku tsunami (Suppasri et al. 2012), as summarized in Section 8.3. Water depths are based on the damage state of each of the three sources that is deemed to best represent extreme damage corresponding to an 85 percent loss ratio. For all intents and purposes, 85 percent loss ratio represents full building loss, and likely partial or full building collapse. Accordingly, water depths were selected that correspond to the initiation of "Partial Failure" (Table 8.8), and the median values of "Collapse" damage fragility (Tables 8.9 and 8.10). Note: Median values represent the hazard level for which 50 percent of the buildings would be expected to have collapsed.

As shown in Table 8.7, water depths corresponding to an 85 percent loss ratio (estimated damage) compare well with water depths of extreme (collapse) damage observed in recent tsunamis (observed damage). Note: Shaded cells indicate the preferred strength level for comparison of water depths of estimated building damage with observed building damage. All estimated water depths are rounded to the nearest one-half foot.

Wood Model Building Types (W1 and W2). The 6.5-foot water depth estimated for the single-story light frame wood (W1) model building type with Pre-Code strength falls within the 5.3-foot to 8.5-foot range of water depths of observed failure and collapse of wood buildings in Banda Aceh and American Samoa/Samoa. The 9-foot (Pre-Code strength) and 17.5-foot (High-Code strength) water depths of the W2 model building type bound the 15.9-foot water depth of observed collapse damage to mixed-use Japanese buildings. Similarly, the 9.5-foot (W1) and 17.5-foot (W2) water depths of wood buildings with High-Code strength bound the 13.5-foot water depth of observed collapse damage to one-story and two-story wooden Japanese residences.

Unreinforced Masonry Model Building Type (URML). The 12.5-foot water depth estimated for the single-story unreinforced masonry (URML) model building type falls within the 8.2-foot to 13-foot range of water depths of observed failure and collapse of unreinforced masonry buildings in Banda Aceh and American Samoa/Samoa.

Reinforced-Concrete Model Building Types (C1L, C2L and C3L). The 22.5-foot to 24-foot range of water depths estimated for low-rise reinforced concrete moment frame (C1L), shear wall (C2L) and frame with infill (C3L) model building types with Pre-Code strength is essentially the same as the 19.5-foot to 24-foot range of water depths of observed failure and collapse of concrete buildings in Banda Aceh and American Samoa/Samoa.

Steel Frame with Concrete Shear Wall Model Building Type (S4L). The 23-foot (Pre-Code strength) to 35.5-foot (High-Code strength) range of water depths estimated for the low-rise steel frame with concrete shear wall model building type bounds the 31-foot water depth of observed failure of similar construction in Banda Aceh

8.3 Observed Building Damage Due to Tsunami – Post-Event Surveys

8.3.1 Introduction

Post-event surveys have generated a considerable amount of information on the observed performance of buildings in recent tsunamis, and in some cases, researchers have developed damage functions (e.g., fragility curves) from observed damage. This section provides an overview of observed tsunami damage to buildings and a summary of derived fragility data, when such is available.

Observations of tsunami damage provide a valuable basis for a “sanity check” of the tsunami flood and flow building damage functions, but in general cannot be used directly to calibrate fragility parameters of the Hazus Tsunami Model, for the reasons discussed below.

1. Combined Flood and Flow Damage. Observed damage typically represents the combined effects of tsunami flood and tsunami flow, and cannot be compared directly with Hazus functions that define either building damage due solely to flood or building damage due solely to flow. Further, most damaged buildings are smaller, shorter structures (e.g., one- and two-story residences) for which Complete damage to the structure is dominated by tsunami force (flow effects), although observed damage to these buildings is typically expressed in terms of maximum depth of water, rather than maximum momentum flux (the hazard parameter used by the Hazus Tsunami Model to estimate damage to the structure due to tsunami flow).
2. Maximum Water Depth. The depth of tsunami inundation over a large affected region can only be estimated approximately, and typically does not account for subtle, but important differences in the height of water affecting individual buildings due to likely differences in the base and/or first-floor elevation of individual buildings. The elevation of the base and first floor are key parameters of the Hazus tsunami building damage functions.

3. Type of Construction. Damage data are only available for buildings located outside the United States for which building design and construction may differ substantially from United States practice. The structural system (even if known) may not correspond to one of the Hazus model building types and local building code requirements for lateral force design are likely not the same as those of the United States (which are used to define the lateral strength of Hazus model building types).
4. Damage States. Different research studies have typically used different damage-state definitions to develop fragility curves from observed data, all of which are to some degree different from the damage states of Hazus. In general, damage states of fragility curves based on observed data by others tend to mix damage to the structure with damage to nonstructural systems and contents, and express damage in terms of loss ratio (i.e., dollar loss as a fraction of replacement value). Whereas, Hazus defines damage states separately for the structure, nonstructural systems, and the contents of the building in terms of the physical condition of each these building systems (e.g., Table 5.6).

The above points are made to avoid comparing Hazus damage "apples" with observed damage "oranges," not to suggest that actual observed damage (and loss) data should not be used to validate Hazus building damage functions for tsunami. Rather, to the extent applicable and to the degree of precision warranted by the data, the Hazus building damage functions should (and in general do) emulate actual observations of tsunami damage to buildings.

8.3.2 Overview of Observed Building Damage in Recent Tsunamis

This section provides annotated summaries of papers and reports containing pertinent tsunami hazard and building damage data of the 2004 Indian Ocean Tsunami (Suppasri et al. 2011, Saatcioglu et al. 2006, Murty et al. 2006, Ruangrassamee et al. 2006 and Tinti et al., 2011), the 2006 Java tsunami (Reese et al. 2007), the 2009 South Pacific (Samoa) tsunami (Robertson et al. 2010, Reese et al. 2011), and the 2011 Tohoku tsunami (EERI 2011, MLIT 2011, Gokon et al., 2012, Suppasri et al., 2012).

2004 Indian Ocean Tsunami

Suppasri, A. S, Koshimura, F. Imamura, 2011. "Developing tsunami fragility curves based on satellite remote sensing and the numerical modeling of the 2004 Indian Ocean tsunami in Thailand," Natural Hazards Earth System Sciences, 11, 173-189, January 20, 2011.

> This paper summarizes development of tsunami fragility curves based on high-resolution satellite images of building damage in Thailand taken before and after the 2004 Indian Ocean Tsunami of December 26, 2004. Building damage is based on the number of buildings that have lost roofs (i.e., destroyed buildings) relative to the number of buildings in the area of interest, expressed as a function of estimated water depth, velocity, and hydrodynamic force, where values of these different hazard parameters were developed by a numerical model. Fragility curves are developed for three (undefined) damage states of RC structures, and for "structural destruction" of RC and "mixed" construction. The damage state corresponding to destruction of RC structures (height undefined) is shown as having a median inundation depth of about 5m (and about 2m for "mixed" construction).

Saatcioglu, Murat, Ahmed Ghobarah, Ioan Nistor, 2006. “Performance of Structures in Indonesia during the December 2004 Great Sumatra Earthquake and Indian Ocean Tsunami,” Earthquake Spectra, Volume 22, No. S3, June 2006 (Oakland, CA: EERI).

> This paper summarizes reconnaissance conducted in Indonesia to investigate the effects of the December 26, 2004 earthquake and tsunami on buildings, bridges, and other physical infrastructure. The damaging effects of the tsunami were most pronounced in unreinforced masonry walls, nonengineered reinforced-concrete buildings, and low-rise timber-framed buildings. In some cases, engineered structures that survived tsunami forces showed evidence of extensive damage due to seismic forces. The majority of the seismic damage was attributed to poor design and detailing of nonductile buildings

Murty, C.V.R., Durgesh C. Rai, Sudhir K. Jain, Hemant B. Kaushik, Goutam Mondal, and Suresh R. Dash, 2006. “Performance of Structures in the Andaman and Nicobar Islands (India) during the December 2004 Great Sumatra Earthquake and Indian Ocean Tsunami,” Earthquake Spectra, Volume 22, No. S3, June 2006 (Oakland, CA: EERI).

> This paper describes damage sustained by buildings and structures in the Andaman and Nicobar Islands area due to the earthquake and tsunami of December 26, 2004. On some islands, damage was predominantly tsunami-related, while on others damage was primarily due to earthquake forces.

Ruangrassamee, Anat, Hideaki Yanagisawa, Piyawat Foytong, Panitan Lukkunaprasit, Shunichi Koshimura, and Fumihiko Imamura, 2006. “Investigation of Tsunami-Induced Damage and Fragility of Buildings in Thailand after the December 2004 Indian Ocean Tsunami,” Earthquake Spectra, Volume 22, No. S3, June 2006 (Oakland, CA: EERI).

> This paper describes damage to civil engineering structures, including buildings, along the west coast of southern Thailand due to the earthquake and tsunami of December 26, 2004. A database of 94 damaged reinforced-concrete buildings was developed and used to evaluate the relationship between the damage level measured by one of four structure damage states (no damage, secondary member damage, primary member damage, and collapse) and the distance of the building from the shoreline and inundation height (above the first floor).

Tinti, S., R. Tonini, L. Bressan, A. Armigliato, A. Gargi, R. Guillande, N. Valencia and S. Scheer, 2011. Handbook of Tsunami Hazard and Damage Scenarios, SCHEMA Project, JRC Scientific and Technical Reports, EUR 24691 EN, 2011 (Joint Research Centre, Institute for the Protection and Security of the Citizen, Bologna, Italy).

> This research report documents the results of the SCHEMA (Scenarios for Hazard-induced Emergencies Management) Project that illustrate the concepts and methods for producing tsunami scenarios, including damage functions and matrices for a number of common European building types. The report defines building types on the basis of their resistance capacity, five damage levels ranging from Light Damage to Collapse, and provides a range of flow depths for each damage level and building type derived from empirical field observations collected after the December 26, 2004 tsunami.

2006 Java Tsunami

Reese, S., W. J. Cousins, W. L. Power, N. G. Palmer, I. G. Tejakusuma, and S. Nurgrahadi, 2007. “Tsunami vulnerability of buildings and people in South Java – field observation after the July 2006 Java tsunami,” Nat Hazards and Earth System Sciences, 7, 573-589, October 15, 2007, (Copernicus Publications).

This paper describes the work of a reconnaissance team of New Zealand and Indonesian scientists who investigated the South Java area affected by the tsunami of July 17, 2006. The paper contains data acquired to calibrate models used to estimate tsunami inundation, casualty rates and damage levels. Damage ratios are estimated as a function of water depth (above floor) for four types of construction: 1) timber/bamboo, 2) brick traditional, 3) brick traditional with RC-columns, and 4) RC-frame with brick infill walls, distinguishing between “exposed” buildings, and buildings “shielded” by other buildings.

Damage ratios, defined as the (cost of repair)/(cost to replace) were derived from damage due to foundation and floor (15 percent of total cost), walls (50 percent), roof and ceiling (15 percent), and fittings and services (20 percent). At a water depth of 2 m, buildings made of timber and traditional brick (one-story) had 70 percent to 100 percent loss, buildings made of traditional brick with RC columns had approximate 50 percent loss, when exposed, and 20 percent loss when shielded and buildings made of RC columns had low loss. Due to the relative valuation of building systems of this paper, these loss ratios reflect damage primarily to structural elements.

2009 South Pacific (Samoa) Tsunami

Robertson, I.N., Carden, L., Riggs, H.R., Yim, S., Young, Y.L., Paczkowski, K. and Witt, D., “Reconnaissance following the September 29, 2009 tsunami in Samoa," University of Hawaii, Research Report UHM/CEE/10-01.

This report documents the work of a reconnaissance team from the University of Hawaii that investigated damage to coastal structures and buildings on Tutuila Island, American Samoa, and Upolu, Samoa due to the September 29, 2009 tsunami. The report provides descriptions and photos of typical damage to engineered and nonengineered buildings (as well as other infrastructure). The results of the survey indicate that most timber and masonry residential structures subjected to tsunami loads suffered significant damage or complete destruction. Engineered structures such as commercial buildings, schools, and churches (which are often built slightly elevated above the surrounding land) generally performed much better structurally than neighboring residential buildings.

Reese, Stefan, Brendon A. Bradley, Jochen Bind, Graeme Smart, William Power, James Sturman, 2011. "Empirical building fragilities from observed damage in the 2009 South Pacific tsunami," Earth-Science Reviews, Elsevier (National Institute of Water and Atmospheric Research).

This paper summarizes the work of a multi-disciplinary reconnaissance team that collected damage data and developed empirical fragility functions for buildings of coastal city sites in American Samoa and Samoa affected by the September 29, 2009 tsunami. Fragility functions were developed for a variety of building classes, including wood (timber) residences, masonry, and reinforced-concrete (RC) structures, including the

effects of “shielding” and “entrained debris.” Fragility functions are developed solely on the basis of observed water depth due to the paucity of velocity or other hazard data.

2011 Tohoku Tsunami

EERI, 2011. "The Tohoku, Japan, Tsunami of March 1, 2011: Effects on Structures," EERI Special Earthquake Report, Learning from Earthquakes – September 2011, (EERI: Oakland, CA).

This special earthquake report of Earthquake Engineering Research Institute (EERI) summarizes the work of the multi-disciplinary reconnaissance team of the American Society of Civil Engineers (ASCE) accompanied by Japanese researchers and practitioners who visited over 45 towns and cities of the Tohoku coastline affected by the 2011 Tsunami. The report includes photos and descriptions of typical damage to buildings and other structures. A more detailed report of observations and findings is being published as an ASCE monograph (ASCE, 2012).

MLIT, 2011. Press Release, Ministry of Land, Infrastructure, Transport and Tourism (MLIT), 2011 (in Japanese).

Press release issued by the Japan Ministry of Land, Infrastructure, Transport and Tourism (MLIT) that summarizes inundation depth and building damage data (and other data) for coastal areas affected by 2011 Tohoku tsunami.

Gokon, Hidemeomi, and Shunichi Koshimura, 2012. “Mapping of Building Damage of the 2011 Tohoku Earthquake Tsunami in Miyagi Prefecture,” Coastal Engineering Committee, Japan Society of Civil Engineers, Coastal Engineering Journal, Vol. 54, No. 1, March 24, 2012, (World Scientific Publishing Company: www.worldscientific.com).

This paper describes tsunami building damage for the cities of the Miyagi Prefectures affected by the 2011 Tsunami obtained from pre-event and post-event aerial photos. Buildings without roofs are classified as “Washed-away;” buildings with roofs are classified as “Surviving.” The study found 47,655 (29.4 percent) of the 162,015 buildings in Miyagi Prefecture exposed to inundation to be Washed-away, noting that approximately one-half of the exposed buildings in the prefecture (82,754) are classified by the National Police Agency as “devastated.”

Suppasri, Anawat, Erick Mas, Shunichi Koshimura, Kentaro Imai, Kenji Harada, Fumihiko Imahura, 2012. “Developing Tsunami Fragility Curves from the Surveyed Data of the 2011 Great East Japan Tsunami in Sendai and Ishinomaki Plains,” Coastal Engineering Committee, Japan Society of Civil Engineers, Coastal Engineering Journal, Vol. 54, No. 1, March 24, 2012, (World Scientific Publishing Company: www.worldscientific.com).

This paper describes field surveys of inundation depth and associated damage to buildings at 10 locations in the Miyagi and Fukushima prefectures affected by the March 11, 2011 Tsunami. Building damage was classified as either Flood only, Minor, Moderate, Major or Complete. Of the 189 buildings surveyed, 150 were wood residences, typically one-story and two-story houses. Of the 150 wood residences, 57 houses (38 percent) had flood-only damage, 27 houses (18 percent) had Minor damage, 38 houses (25 percent) had Moderate damage, 11 houses (7 percent) had Major damage and 17 houses (12 percent) had Complete damage. The paper develops

fragility functions of these damage states as a function of inundation depth, and compares representative inundation depths of these damage functions with representative inundation depths of building damage due to the 2004 Indian Ocean Tsunami (Ruangrassamee et al. 2006, Suppasri et al., 2011) and the 2006 Java tsunami (Reese et al., 2007). These comparisons found that damage to wood houses surveyed in Miyagi prefecture after the 2011 tsunami to be associated with inundation depths that were roughly twice the inundation depths of previous tsunamis for comparable damage to wood residences. These findings are consistent with the observation that Japanese residential wood construction damaged in the 2011 Tohoku tsunami is generally much better built than the wood residences damaged in the 2004 Indian Ocean, 2006 Java and 2009 Samoa tsunamis.

8.3.3 Building Damage Functions Derived from Observed Data

This section summarizes properties of building damage functions, including fragility curves, derived from observed damage due to the 2004 Indian Ocean Tsunami (Tinti et al. 2011), the 2009 South Pacific (Samoa) tsunami (Reese et al. 2011), and the 2011 Tohoku tsunami (Suppasri et al. 2012).

2004 Indian Ocean Tsunami

The "Handbook of Tsunami Hazard and Damage Scenarios," of the SCHEMA Project (Tinti et al. 2011) defines 11 building types, primarily residential and common coastal buildings, on the basis of their resistance capacity, as follows (from Table 4 of the SCHEMA handbook):

A. Light construction of wood, timber, clay (A1) and rudimentary shelters (A2)
B. Unreinforced masonry – plain brick, etc., (B1) and wooden timber/clay materials (B2)
C. Unreinforced concrete/masonry – brick infill (C1), lava stone blocks/clay bricks (C2)
D. Unreinforced concrete – larger residential/commercial (D)
E. Reinforced concrete (RC)/steel frame – Up to 3 stories (E1), over 3 stories (E2)
F. Other – Harbor, industrial, and hangar buildings (F) and
G. Other – Administrative, historical and religion buildings (G).

For comparison with Hazus model building types:

“A1” is most like Hazus W1, Pre-Code strength, buildings

“B1” is most like Hazus URML buildings

“C1” is most like Hazus C3L, Pre-Code strength, buildings

“D” is most like Hazus C1L, Pre-Code strength, buildings

“E1” is most like Hazus S4L, Pre-Code strength, buildings (although strength could be higher).

Table 5 of the SCHEMA handbook defines five damage levels, as follows:

Light Damage No structural damage, minor nonstructural damage

Important Damage	No structural damage, failure/collapse of nonstructural walls
Heavy Damage	Structural damage that could affect building stability
Partial Failure	Partial collapse, integrity of structure compromised
Collapse	Complete collapse (washed away)

For comparison with Hazus building damage functions:

“Important Damage” is most like Extensive/Complete nonstructural damage

“Heavy Damage” is most like Hazus Extensive structural damage

“Partial Failure” and “Collapse” are most like Hazus Complete structural damage.

Table 8.8 (*from Table 6 of the SCHEMA handbook*) shows the range of water depths associated with each damage level for building classes A, B, C, D and E1. The range of water depths shown in Table 5.7 are based on damage functions derived (by the SCHEMA project) from empirical field observations collected in Banda Aceh after the December 26, 2004 tsunami.

Table 8.8: Summary of the Ranges of Water Depths Associated with Defined Damage Levels and Building Types based on Empirical Field Observations Collected in Banda Aceh after 2004 Indian Ocean Tsunami (from Table 6, Tinti et al. 2011)

Building Type	Water Depth Range (in feet) by Damage Level Light	Water Depth Range (in feet) by Damage Level Important	Water Depth Range (in feet) by Damage Level Heavy	Water Depth Range (in feet) by Damage Level Partial Failure	Water Depth Range (in feet) by Damage Level Collapse
Light Construction (A)	0 - 6	6 - 7	7 - 8.5	8.5 – 12.5	> 12.5
Unreinforced Masonry (B)	0 - 6.5	6.5 – 10	10 - 13	13 – 16.5	> 16.5
Unreinforced Concrete (C)	0 - 8	8 - 13	13 – 19.5	19.5 – 27	> 27
Unreinforced Concrete (D)	0 - 6.5	6.5 - 15	15 – 22	22 -30	> 30
RC/Steel Frame (E1)	0 - 10	10 - 20	20 - 31	31 - 41	> 41

2009 South Pacific (Samoa) Tsunami

The research paper, "Empirical building fragilities from observed damage in the 2009 South Pacific tsunami," (Reese, 2010) provides fragility data for masonry, concrete and wood residential construction.

For comparison with Hazus model building types:

“Masonry Residential” is most like Hazus URML buildings

“Reinforced-Concrete Residential” is most like Hazus C2L, Pre-Code strength, buildings

“Timber (Wood) Residential” is most like Hazus W1, Pre-Code strength, buildings.

Table 4 of the subject paper defines the following five damage states:

Light	Nonstructural damage only
Minor	Significant nonstructural, minor structural damage
Moderate	Significant structural and nonstructural damage
Severe	Irreparable structural damage (100 percent loss)
Collapse	Complete structural damage

For comparison with Hazus building damage functions:

“Minor” damage is most like Hazus Extensive nonstructural damage

“Moderate” damage is most like Hazus Extensive structural and nonstructural damage

“Severe” and “Complete” damage are most like Hazus Complete structure damage.

Table 8.9 summarizes median and standard deviation values of lognormal fragility curves fit to empirical depth-damage data from the 2009 South Pacific tsunami (from Table 6, Reese et al. 2011). Note. Residential masonry buildings are subdivided into groups representing shielded and unshielded conditions and groups with and without the effects of debris impact damage.

Table 8.9: Summary of the Median Water Depths (and logarithmic standard deviations) associated with Defined Damage States and Building Types based on Empirical Depth-Damage Data Collected in America Samoa and Samoa after the 2009 South Pacific Tsunami (from Table 6, Reese et al. 2011)

Building Type	Median Water Depth (in feet) by Damage State (and logarithmic standard deviations): Light	Median Water Depth (in feet) by Damage State (and logarithmic standard deviations): Minor	Median Water Depth (in feet) by Damage State (and logarithmic standard deviations): Moderate	Median Water Depth (in feet) by Damage State (and logarithmic standard deviations): Severe	Median Water Depth (in feet) by Damage State (and logarithmic standard deviations): Collapse
Generic	1.0 (0.43)	1.6 (0.49)	4.0 (0.58)	6.0 (0.62)	9.1 (0.55)
Masonry Residential	1.0 (0.46)	1.5 (0.40)	4.2 (0.35)	6.1 (0.41)	8.2 (0.40)
Shielded - Masonry Residential			4.5 (0.37)	10.2 (0.49)	12.8 (0.56)
Unshielded - Masonry Residential			3.8 (0.36)	4.7 (0.40)	7.4 (0.42)
Debris - Masonry Residential			3.0 (0.36)	4.7 (0.32)	
No Debris - Masonry Residential			4.5 (0.32)	6.4 (0.40)	
Reinforced-Concrete Residential			4.5 (0.56)	11.3 (0.54)	24 (0.93)
Timber (Wood) Residential			3.8 (0.38)	4.1 (0.40)	5.3 (0.28)

2011 Tohoku Tsunami

The paper "Developing Tsunami Fragility Curves from the Surveyed Data of the 2011 Great East Japan Tsunami in Sendai and Ishinomaki Plains" (Suppasri et al. 2012) provides fragility data for wood residences and mixed-used occupancies.

For comparison with Hazus model building types:

"Wooden House" (one-story) is most like Hazus W1, Moderate-Code strength, buildings

"Wooden House" (two-story) is most like Hazus W2, Moderate-Code strength, buildings

"Mixed-Use" is most like Hazus W2, Moderate-Code strength, buildings.

Table 2 of the subject paper defines the following five damage states:

Flood Only	No structural damage
Minor	Window is damaged, but no damage on wall
Moderate	Window and one part of wall are damaged

Major	Window and large part of wall are damaged
Collapse	Window, wall and column are damaged

For comparison with Hazus building damage functions:

"Major" damage is most like Hazus Extensive or Complete (W1) nonstructural damage

"Collapse" damage is most like Hazus Complete structural damage.

Table 8.10 summarizes median and standard deviation values of lognormal fragility curves fit to empirical depth-damage data from the 2011 Tohoku tsunami (from Table 4, Suppasri et al. 2012).

Table 8.10: Summary of the Median Water Depths (and logarithmic standard deviations) associated with Defined Damage States and Building Types based on Empirical Depth-Damage Data Collected at 10 locations in Miyagi and Fukushima Prefectures affected by the 2011 Tohoku Tsunami (from Table 4, Suppasri et al. 2011)

Building Type	Median Water Depth (in feet) by Damage State (and associated logarithmic standard deviation): Flood only	Median Water Depth (in feet) by Damage State (and associated logarithmic standard deviation): Minor	Median Water Depth (in feet) by Damage State (and associated logarithmic standard deviation): Moderate	Median Water Depth (in feet) by Damage State (and associated logarithmic standard deviation): Major	Median Water Depth (in feet) by Damage State (and associated logarithmic standard deviation): Collapse
Wooden House (1-story and 2-story, typical)	NA	7.8 (0.26)	9.3 (0.23)	12.3 (0.22)	13.5 (0.24)
Mixed-Type	NA	7.8 (0.32)	10.2 (0.32)	14.0 (0.29)	15.9 (0.29)

8.3.4 Summary of Observed Damage

The damage ranges and fragility data based on observed damage show a wide variation building performance which cannot be explained solely on the basis of differences in the definitions of damage states and/or differences in building construction of the different regions. For example, based largely on buildings damaged in Banda Aceh by the 2004 Indian Ocean Tsunami, the SCHEMA Handbook (Tinti et al. 2011) shows over 12.5 feet of water is required to collapse light wood and timber construction (Table 8.8). In contrast, Reese et al. (2010) shows a median collapse depth of only 5.3 feet for timber (wood) residences damaged in the 2009 South Pacific (Samoa) tsunami (Table 8.9). Finally, Suppasri et al. (2012) shows a median collapse depth of 13.5 feet for Japanese wooden houses damaged in the 2011 Tohoku tsunami (Table 8.10). Arguably, Japanese residences are better built, on average, than similar types of wood buildings damaged in Banda Aceh and Samoa (and America Samoa), so higher water levels would be expected for collapse of Japanese residences.

One possible explanation for the wide variation in water depths observed to have caused collapse of similar types of wood construction is the likely difference in the hydrodynamic force (momentum flux) on the buildings in the areas affected by the three events. That is, the flow velocity of the water at the depth associated with collapse was likely not the same for the areas affected by each of the three tsunamis, and if substantially different could affect collapse performance of buildings characterized solely by inundation depth. The relatively low median values of collapse and other damage states of buildings in Samoa and America Samoa (Table 8.9) suggest that the water velocities in the areas where buildings were surveyed was likely greater, on average, than the water velocities in the areas of Banda Aceh (Thailand) surveyed after the 2004 Indian Ocean Tsunami, and the areas of the Miyagi and Fukushima prefectures of Japan surveyed after the 2011 Tohoku tsunamis.

Although limited to one event, detailed evaluations of damage to unreinforced masonry buildings in the 2009 Samoa tsunami show the potential benefits of shielding provided by other building and structures, and the potential detrimental effects of debris impact. Shielding greatly reduced the likelihood of "Severe" damage (approximately a factor of 2 decrease in the median height of water depth for this damage state) and debris impact increased the likelihood of "Severe" damage (approximately a factor of 1.5 increase in the median height of water depth for this damage state).

Finally, while the observations of building damage in recent tsunamis provide a basis for a "sanity check" of Hazus building damage functions, they are not suitable for direct "calibration" of building fragility parameters and methods since:

i. they have defined different damage states from those of Hazus (which tend to mix structural and nonstructural damage together),

ii. only characterize damage in terms of water depth (rather than also considering momentum flux), and

iii. only apply to a limited number of Hazus model building types.

8.4 References

ASCE, 2003. *Seismic Evaluation of Existing Buildings*. American Society of Civil Engineers Standard ASCE/SEI 31-03. (Reston, VA: ASCE).

ASCE, 2010. *Minimum Design Loads for Buildings and Other Structures*. American Society of Civil Engineers Standard ASCE/SEI 7-10. (Reston, VA: ASCE).

ASCE, 2012. *Tohoku Japan Tsunami of March 11, 2011 – Performance of Structures*, ASCE Monograph, American Society of Civil Engineers Standard. (Reston, VA: ASCE).

ATC, 1989. "Procedures for Post-earthquake Safety Evaluation of Buildings," ATC-20 Report, Applied Technology Council (ATC). (Redwood City, CA: ATC).

ATC, 1994. "Field manual: safety evaluation of buildings after windstorms and floods," ATC-45, Applied Technology Council ATC). (Redwood City, CA: ATC).

ATC, 1995. "Addendum to the ATC-20 Procedures for Post-earthquake Safety Evaluation of Buildings," ATC-20-2, Applied Technology Council ATC). (Redwood City, CA: ATC).

Davis, Stuart A., "Business Depth-Damage Analysis Procedures," Water Resources Support Center, Institute for Water Resources, USACE Research Report 85-R-5.

EERI, 2011. "The Tohoku, Japan, Tsunami of March 1, 2011: Effects on Structures," Earthquake Engineering Research Institute (EERI) Special Earthquake Report, Learning From Earthquakes – September 2011, (Oakland, CA: EERI).

FEMA, 1992. *NEHRP Handbook for the Seismic Evaluation of Existing Buildings*. Federal Emergency Management Agency, FEMA 178. (Washington, D.C.: FEMA).

FEMA, 2002. *Earthquake Loss Estimation Methodology, HAZUS99-MR1, Advanced Engineering Building Module, Technical and User's Manual*, prepared by National Institute of Building Sciences (NIBS) for the Federal Emergency Management Agency. (Washington, D.C.: NIBS).

FEMA, 2004. *Guidelines and Specification for Flood Hazard Mapping*, Section D.4, "Coastal Flooding Analyses and Mapping Pacific Coast," Federal Emergency Management Agency (FEMA), November 2004 (FEMA, Washington, D.C.).

FEMA, 2012. *Guidelines for Design of Structures for Vertical Evacuation from Tsunamis*, FEMA P646, April 2012, Federal Emergency Management Agency. (Washington, D.C: FEMA).

FEMA, 2011a. *Multi-hazard Loss Estimation Methodology: Earthquake Model, HAZUS-MH MR4 Technical Manual*, prepared by the National Institute of Building Sciences (NIBS) for the Federal Emergency Management Agency. (Washington, D.C.: NIBS).

FEMA, 2011b. *Multi-hazard Loss Estimation Methodology: Flood Model, HAZUS-MH MR4 Technical Manual*, prepared by the National Institute of Building Sciences (NIBS) for the Federal Emergency Management Agency. (Washington, D.C.: NIBS).

Gokon, Hidemeomi, and Shunichi Koshimura, 2012. "Mapping of Building Damage of the 2011 Tohoku Earthquake Tsunami in Miyagi Prefecture," Coastal Engineering Committee, Japan Society of Civil Engineers, *Coastal Engineering Journal*, Vol. 54, No. 1, March 24, 2012, (World Scientific Publishing Company: www.worldscientific.com).

Jones, Christopher P., 2011. "Large Building Flood Damage Functions," (white paper), August 31, 2010, revised June 22, 2011.

Jones, C., 2004. "Supporting Documentation for D.4.9.2.1 High Velocity Flow VE Zone," discussion of supporting documentation for FEMA *Guidelines and Specification for Flood Hazard Mapping*, Section D.4, C. Jones 12-08-04, (private communication).

Koshimura, Shuniche (Tohoku University), Yuichi Namegaya (AIST), Hideaki Yanagisawa (TEPCO), "Tsunami Fragility - A new measure to identify tsunami damage," *Journal of Disaster Research*, 2009.

MLIT, 2011. Press release, Ministry of Land, Infrastructure, Transport and Tourism (MLIT), 2011 (in Japanese).

Murty, C.V.R., Durgesh C. Rai, Sudhir K. Jain, Hemant B. Kaushik, Goutam Mondal, and Suresh R. Dash, 2006. "Performance of Structures in the Andaman and Nicobar Islands (India) during the December 2004 Great Sumatra Earthquake and Indian Ocean Tsunami," *Earthquake Spectra*, Volume 22, No. S3, June 2006 (Oakland, CA: EERI).

Reese, Stefan, Brendon A. Bradley, Jochen Bind, Graeme Smart, William Power, James Sturman, 2011. "Empirical building fragilities from observed damage in the 2009 South

Pacific tsunami," *Earth-Science Reviews*, Elsevier (National Institute of Water and Atmospheric Research).

Reese, S., W. J. Cousins, W. L. Power, N. G. Palmer, I. G. Tejakusuma, and S. Nurgrahadi, 2007. “Tsunami vulnerability of buildings and people in South Java – field observation after the July 2006 Java tsunami,” Nat Hazards and Earth System Sciences, 7, 573-589, October 15, 2007, (Copernicus Publications).

Robertson, I.N., Carden, L., Riggs, H.R., Yim, S., Young, Y.L., Paczkowski, K. and Witt, D., "Reconnaissance following the September 29, 2009 tsunami in Samoa," University of Hawaii, Research Report UHM/CEE/10-01.

Ruangrassamee, Anat, Hideaki Yanagisawa, Piyawat Foytong, Panitan Lukkunaprasit, Shunichi Koshimura, and Fumihiko Imamura, 2006. “Investigation of Tsunami-Induced Damage and Fragility of Buildings in Thailand after the December 2004 Indian Ocean Tsunami,” *Earthquake Spectra*, Volume 22, No. S3, June 2006 (Oakland, CA: EERI).

Saatcioglu, Murat, Ahmed Ghobarah, Ioan Nistor, 2006. “Performance of Structures in Indonesia during the December 2004 Great Sumatra Earthquake and Indian Ocean Tsunami,” *Earthquake Spectra*, Volume 22, No. S3, June 2006 (Oakland, CA: EERI).

Suppasri, A. S, Koshimura, F. Imamura, 2011. "Developing tsunami fragility curves based on satellite remote sensing and the numerical modeling of the 2004 Indian Ocean tsunami in Thailand," *Natural Hazards Earth System Sciences*, 11, 173-189, January 20, 2011.

Suppasri, Anawat, Erick Mas, Shunichi Koshimura, Kentaro Imai, Kenji Harada, Fumihiko Imahura, 2012. “Developing Tsunami Fragility Curves from the Surveyed Data of the 2011 Great East Japan Tsunami in Sendai and Ishinomaki Plains,” Coastal Engineering Committee, Japan Society of Civil Engineers, *Coastal Engineering Journal*, Vol. 54, No. 1, March 24, 2012, (World Scientific Publishing Company: www.worldscientific.com).

The Heinz Center, 2000. *Evaluation of Erosion Hazards*, The H. John Heinz III Center for Science, Economics and the Environment. (Washington, D.C.).

Tinti, S., R. Tonini, L. Bressan, A. Armigliato, A. Gargi, R. Guillande, N. Valencia and S. Scheer, 2011. "Handbook of Tsunami Hazard and Damage Scenarios," SCHEMA Project, *JRC Scientific and Technical Reports*, EUR 24691 EN, 2011 (Joint Research Centre, Institute for the Protection and Security of the Citizen, Bologna, Italy